Secondary resource directive

Characterisation of mining waste in central and western Bergslagen, Sweden

Patrick Casey, Cecilia Brolin, Lena Persson, Daniel Sopher,
Virginie Leroux & Stefan Persson

January 2024

SGU-rapport 2024:02

SGU Geological Survey of Sweden

Cover photo: Open pit mine at Wigströmsgruvan.
Photo: Patrick Casey

Author: Patrick Casey, Cecilia Brolin, Lena Persson, Daniel Sopher,
Virginie Leroux & Stefan Persson

Reviewed by: Magnus Ripa & Mehrdad Bastani
Head of unit: Ildikó Antal Lundin

Editor: Lina Rönnåsen

Geological Survey of Sweden
Box 670, 751 28 Uppsala, Sweden
phone: 018-17 90 00
e-mail: sgu@sgu.se

CONTENTS

ABSTRACT

In 2021, the Geological Survey of Sweden (Sveriges geologiska undersökning, SGU) together with the Swedish Environmental Protection Agency received a governmental directive to work to increase the possibilities for sustainable extraction of metals and minerals from secondary resources (N2021/01038). The work is intended to contribute to the transition to a more circular and resource-efficient economy. The directive in its entirety was reported to the government in February 2023 (SGU RR 2023:01).

As part of the directive, SGU has documented, sampled, and characterised mining waste (waste rock and tailings) at closed Swedish mines to estimate the quantities of metals and minerals. Metallurgical slag and burnt alum shale were also investigated. Secondary resources from mining waste can possibly contribute to the supply of the critical raw materials needed in the ongoing energy transition.

A total of 70 locations was sampled by SGU during 2021 and 2022, with altogether 1,067 samples. A series of reports present background information and available data for each of these locations, as well as the results from the new investigations.

This report covers a subset of the investigated locations within the directive, from western and central Bergslagen in Sweden. Sampling was conducted at eleven locations at the mine sites of Hällefors, Stollberg, Kaveltorp, Ljusnarsberg, Grängesberg, Blötberget, Ställberg, Bastkärn, Mossgruvan, Yxsjöberg and Wigström.

Results showed many of the mines contained waste with high levels of critical raw materials, including base metals, rare earth elements and elements such as tungsten and beryllium. These results can assist in the determination of the potential to recover these raw materials from mining waste and in guiding classification of resources according to the United Nations Framework Classification of mineral resources.

Reporting of critical raw materials is given in tables, which also provide levels of other resources of economic interest. Estimates of remaining resources using geophysical methods to determine the volume was conducted on tailings repositories and used to calculate tonnage of remaining material.

SAMMANFATTNING

År 2021 fick Sveriges geologiska undersökning (SGU) tillsammans med Naturvårdsverket i regeringsuppdrag att arbeta för ökade möjligheter till hållbar utvinning av metaller och mineral ur sekundära resurser (N2021/01038). Arbetet är tänkt att bidra till omställningen till en mer cirkulär och resurseffektiv ekonomi. Uppdraget i sin helhet redovisades till regeringen i februari 2023 (SGU RR 2023:01).

Som en del av uppdraget har SGU dokumenterat, provtagit och karakteriserat gruvavfall (varphögar och sandmagasin) vid nedlagda svenska gruvor för att bedöma mängden metaller och mineral. Även metallurgiskt slagg samt rödfyr, som är en rest av bränd alunskiffer, har undersökts. Sekundära resurser från gruvavfall kan möjligen bidra till försörjningen av de kritiska råvaror som behövs i den pågående energiomställningen.

Inom uppdraget har totalt 70 platser provtagits under 2021 och 2022, med sammanlagt 1 067 prover. I en serie rapporter presenteras förutom resultaten från de nya undersökningarna även bakgrundsinformation och tillgängliga data för respektive undersökt plats.

Denna rapport tar upp en delmängd av de undersökta platserna inom uppdraget, från västra och centrala Bergslagen. Provtagningen utfördes på elva platser vid gruvorna Hällefors, Stollberg, Kaveltorp, Ljusnarsberg, Grängesberg, Blötberget, Ställberg, Bastkärn, Mossgruvan, Yxsjöberg och Wigström.

Kritiska råvaror är allt viktigare i dagens samhälle eftersom högteknologiska lösningar kräver andra metaller än de tidigare basmetallerna. Dessa råvaror klassificeras som *kritiska* baserat på deras ekonomiska betydelse för EU:s industri och en hög risk för avbrott i produktionen eller tillgången av dem (EU Commission 2020). De sällsynta jordartsmetallerna spelar till exempel en viktig roll i elbilar och i magneter till turbiner i vindkraftverk. Idag importerar EU nästan 30 procent av alla kritiska råvaror som produceras i världen, men producerar bara 3 procent av dem.

Inom projektet har olika geofysiska metoder använts på olika typer av sandmagasin vilket har lett till ett unikt underlag för att utvärdera lämpligheten för olika metoder under olika förutsättningar. De metoder som har testats och utvärderats är elektrisk resistivitets tomografi (ERT), inducerad polarisation (IP), dragen transient elektromagnetisk (eng. *towed transient electromagnetics*, tTEM) och radiomagnetotellurik (RMT). Sandmagasinen har varierat gällande ursprungsmaterial (typ av mineralisering), vattenmättnadsgrad, kornstorlek och inte minst tillgänglighet för olika mätmetoder. Begränsning av anrikningssanden har på huvuddelen av sandmagasinen kunnat identifierats utifrån de geofysiska mätningarna. Det finns indikationer på att IP-metoden kan användas som en direkt eller indirekt metod för att kartlägga områden med förhöjda halter av metaller inom sandmagasinen.

För att få en bättre förståelse för den sekundära resursen är det viktigt att ha en bra karakterisering av den primär resursen från vilken gruvavfallet skapades. Som en del av det här projektet har därför ytterligare undersökningar av berggrunden i anslutning till flera områden med sekundära resurser utförts. Syftet med dessa undersökningar var att skapa bättre geologiskt och geofysiskt underlag runt dessa objekt för att där det är möjligt skapa modeller eller uppdaterade geologiska kartor. Som en del av undersökningarna utfördes nya geologiska observationer och provtagning av bergarter och gråberg. Fysikaliska egenskaper i form av magnetisk susceptibilitet och remanens samt densitet mättes vid SGU:s petrofysiska laboratorium i Uppsala. Nya markbaserade geofysiska mätningar utfördes också vid flera objekt för att undersöka den primära mineraliseringen.

Resultat

De elva områden som provtagits i västra Bergslagen representerar tre olika mineraliseringstyper: sulfidmalmer (Hällefors, Stollberg, Kaveltorp, Ljusnarsberg), järnoxidmalmer (Grängesberg, Blötberget, Ställberg, Bastkärn, Mossgruvan) och volframskarnmalmer (Yxsjöberg, Wigström).

Vid samtliga områden förutom Stollberg provtogs gråberg med minst 15 prover för varje analyserat objekt. Vid Stollberg, Kaveltorp, Grängesberg, Blötberget och Yxsjöberg provtogs även anrikningssand, både ytprover med spade och djupprover med borrutrustning för en mer detaljerad undersökning. På samtliga av dessa sandmagasin förutom Kaveltorp utfördes flera geofysiska mätningar för karakterisering och avgränsning av anrikningssanden. Tredimensionella modeller har tagit fram, och volym och massa för magasinen har beräknats. Dessa resultat tillsammans med analysresultat från provtagning har lett till att potentialen av både kritiska och icke-kritiska metaller och mineral har kunnat beräknas. Områdena med de mest intressanta halterna sammanfattas nedan.

Grängesberg och Blötberget var två av de största gruvorna i västra Bergslagen. Vid dessa har järnmalm brutits sedan 1700-talet. Malmerna består av en järnoxid-apatitmineralisering som liknar den i Kiruna. Provtagningen visade höga halter av fosfat och sällsynta jordartsmetaller i både varp och i sandmagasin. Anrikningssanden i Grängesbergs tre stora sandmagasin beräknas kunna innehålla 21 500 ton sällsynta jordartsmetaller, 156 000 ton fosfor och 2,2 miljoner ton järn. Blötbergets sandmagasin beräknas kunna innehålla ytterligare 5 500 ton sällsynta jordartsmetaller, 30 000 ton fosfor och 500 000 ton järn.

Yxsjöbergs gruva var den största volframproducenten i Sverige. Under gruvans drift deponerades 5,2 miljoner ton anrikningssand i två sandmagasin, av vilka det ena, Morkullstjärnen provtogs. Sanden innehåller förhöjda halter av flera kritiska råvaror, och kan potentiellt innehålla 37 000 ton flusspat, 2000 ton volfram, 1060 ton vismut och 289 ton beryllium. Gråberget i Yxsjöberg innehåller ytterligare 644 ton volfram, 75 ton vismut och 28 ton beryllium.

Stollberg var den största sulfidmalmsgruvan i västra Bergslagen där 2,8 miljoner ton anrikningssand producerades. Analyser visar att Stollbergs sandmagasin potentiellt kan innehålla 13 600 ton zink, 8 500 ton bly, 39 ton antimon och 25 ton silver. Provtagning av gråberg vid de andra sulfidmalmsgruvorna i västra Bergslagen visade i genomsnitt ett innehåll på 1–2 tusen ton bly och zink, samt några hundra ton koppar.

INTRODUCTION

In 2021, the Geological Survey of Sweden (Sveriges geologiska undersökning, SGU) together with the Swedish Environmental Protection Agency received a governmental directive to work to increase the possibilities for sustainable extraction of metals and minerals from secondary resources (N2021/01038). The goal of the sampling and geophysical investigations conducted in this study was to provide a general estimate of potential critical raw materials (CRM) and other minerals of economic interest in the mine waste. In addition, any potential legal and regulatory factors that could hinder investigation and recovery of these materials should be identified. The directive in its entirety was reported to the government in February 2023 (SGU RR 2023:01).

During 2021 and 2022 SGU conducted investigations at several closed Swedish mines to estimate the quantities of metals and minerals. SGU has produced a series of reports which present background information and available data for each site, as well as findings from any new investigations conducted as part of the assignment. This report covers central and western Bergslagen, where a total of 11 former mines were studied (see Fig. 3 in section *Regional geology of Bergslagen*). Each mine was divided into "objects", with an object being defined as a specific type of material sampled, i.e. waste rock heap(s) or tailings repository. Therefore, one study site may have several objects sampled should the site contain both waste rock and tailings. A total of 18 objects were sampled between the 11 mines.

Waste rock (swe: *gråberg*) is the uneconomical fraction of rock removed during the mining process. This material can be composed of the overburden of host rock removed to access the mineralised portion of an ore deposit, material removed in the construction of the mine and access tunnels, to poorly mineralised rock that was not economical for mineral recovery during mine operations. This material is typically deposited near the mine, and can be used later as material for construction such as road or rail ballast, or to back-fill the mine to prevent collapses or as part of efforts to reclaim the mine site and return it to a natural state.

Tailings are the remnants of ore processing and enrichment that are discarded after production. Ore is crushed and the economic fraction is separated from the gangue minerals using various methods depending on the resource to be recovered, such as floatation or magnetic separation methods. No recovery methods can obtain complete recovery of the economic fraction (excepting heap leaching of gold, which can achieve near complete extraction of gold from ore) leaving tailings containing recoverable quantities of economic material. Additionally, minerals that were not of economic interest at the time of extraction may become valuable as new technologies increase demand for these minerals and new extraction methods allow for recovery of the material.

In addition to the estimation of resource potential, this project aims to investigate the geology and geochemistry of the source rocks and mines to further aid in the estimation of resources by identifying CRM mineralogy and their recoverability. This project has studied two of the main mining districts in Sweden: Northern Norrbotten and Bergslagen, with Bergslagen divided between three reports, northern, eastern and southern, and western and central.

The present work builds upon prior studies conducted by Hallberg and Reginiussen (2020; 2019). These studies focused primarily on identification of regions of CRM mineralisation in Sweden and on application of new sampling methodologies for mine waste, including composite sampling of waste rock and tailings. Additionally, these reports looked at the source of the ore mineralisations by drill core scanning and analysis. Applicable data from these previous studies will be included with data acquired in this report.

Calculations of potential resources presented in this report are based on whole rock geochemical analyses and data provided from SGU's MALMdb. SGU's MALMdb is a resource that presents statistics on production at mines within Sweden (https://www.apps.sgu.se/kartvisare/kartvisare-malm-mineral.html). These data rely upon historic reported statistics obtained from mine operators. These estimates include total ore extracted, produced waste rock, and tailings deposited after enrichment. Calculated resource potentials reported herein do not consider post mining activity, such as later removal of material for use as aggregate or ballast, or as backfill in mines. For tailings repositories these estimates of potential resources assume all material is fully accessible and does not consider tailings that are currently below the water level in lakes. In some cases, geophysical data collected from tailings repositories can provide a more accurate estimate of accessibility of resources and will be noted in the discussion. Further evaluation of data presented herein by competent persons as defined by the UNFC (UNFC, 2019) is needed to provide any qualified resource estimations, and as such the resource potential herein should be considered as only a framework for guiding future studies.

CRITICAL RAW MATERIALS

Access to raw materials is an essential part of the supply chain necessary for the production of modern goods. Certain materials are critical to the production of modern technology as well as driving the shift towards a more sustainable economy. These "critical raw materials" (CRM) include materials such as lithium for batteries in electric cars, rare earth elements (REEs) which are used in a wide range of applications from magnets in wind turbines (neodymium) and solar cells, to doping agents (e.g. europium) for phosphors in LCD screens in computers and cell phones. In 2008, the European Commission launched the European Raw Minerals Initiative to improve understanding these materials and identify weak points in the supply chains for these materials. In 2011, the EU released a list of 14 primary resources that it determined to be "Critical Raw Materials" (CRM), with the list expanding to 34 critical and strategic raw materials in 2023 (EU commission, 2023). A key factor for determining a critical resource is supply risk. For many CRMs production is concentrated in one region, and often these resources have the potential to see their supplies restricted due to geopolitical effects. Many of these raw materials are produced by nation-states with political instability or may block access to these materials for use as leverage in international trade or to hinder export of strategic materials for their own purposes. For example, 75% of the world's supply of rare earth elements (REE) are produced in China (Fig. 1). Some CRMs, such as cobalt and tantalum, are "conflict minerals" and are intimately associated with geopolitical instability in Africa and the exploitation of child labour in their production, while the profits from these commodities are known for funding armed conflict. (Opijnen and Oldenziel, 2010).

Europe is heavily reliant on import of critical metals, consuming 25–30% of critical metals produced in the world, while producing only 3% internally (Brown et al., 2016). Identifying sources of these CRMs in the European Union is a step in reaching the goal of securing the supply chain via independent production and decreasing reliance on potentially antagonistic state actors for import of these resources. Additionally, by shifting production to nations with strong environmental and human rights practices, the environmental and human toll of the production of these resources can be limited.

Recently additional focus has been placed on secondary sources of CRMs, so called "secondary raw materials". Secondary raw materials include materials leftover from mine operations, recycling, and industrial waste generated during manufacturing. These secondary resources, especially recycling, are planned to contribute to the circular economy reducing the need for primary sources of CRM. Previous studies such as PROSUM (2017) have studied these secondary waste streams such as mine waste and recycling. By investigating the use of secondary sources of raw material these resources can be secured without the long process and expense of opening a new mine.

Table 1. 2023 list of critical and strategic raw materials (EU Commission, 2023).

Aluminium/Bauxite	Germanium	Phosphorus
Antimony	Hafnium	Scandium
Arsenic	Helium	Silicon metal
Feldspar	Heavy rare earth elements	Strontium
Beryllium	Lithium	Tantalum
Bismuth	Light rare earth elements	Titanium
Boron/Borate	Magnesium	Tungsten
Cobalt	Manganese	Vanadium
Coking coal	Natural graphite	Copper[1]
Feldspar	Niobium	Nickel[1]
Fluorspar	Platinum group metals	
Gallium	Phosphate rock	

[1] Copper and nickel do not meet the CRM thresholds but are included on the CRM list as strategic raw materials.

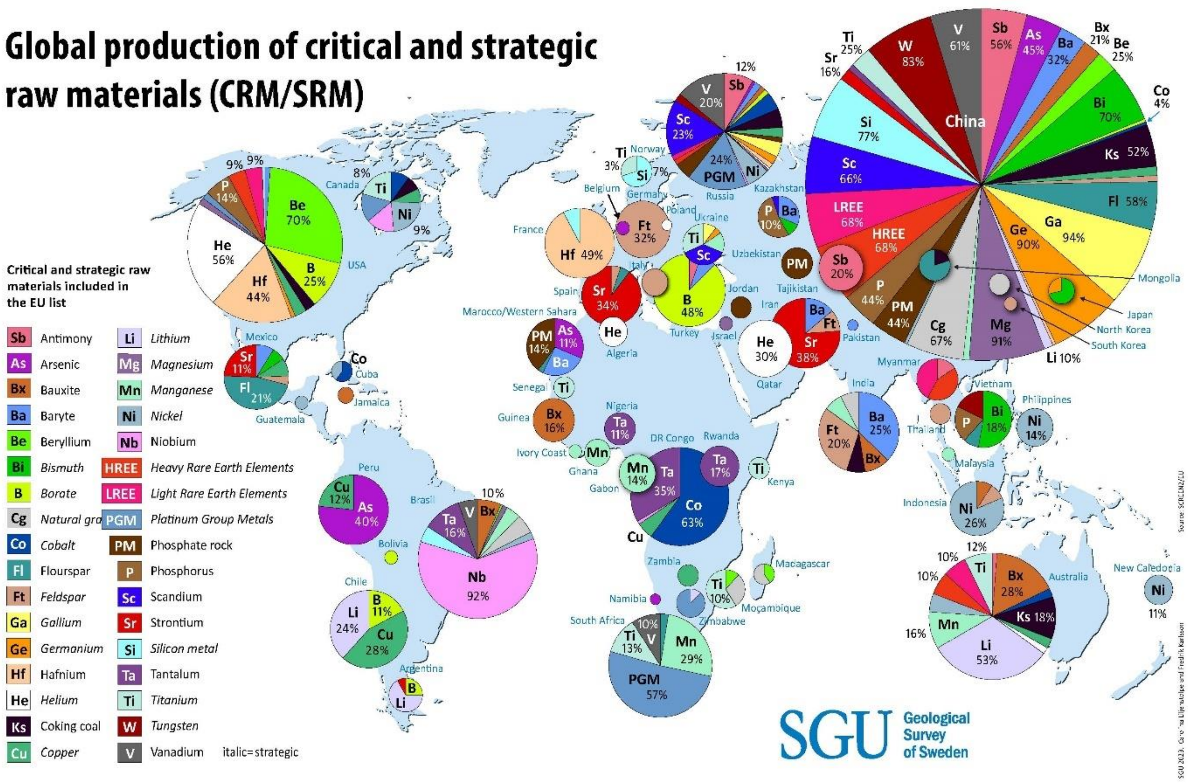

Figure 1. Production statistics of critical and strategic elements in the world.

CRM in Sweden

Sweden has historically been one of the primary metal producers in Europe, with a mining history going back to prehistoric times (SGU, 2020). Mining in Sweden has predominantly occurred throughout central to northern Sweden, including: Bergslagen, in central Sweden, Skellefte district in the mid-north, and Norrbotten in the north of the country (Fig. 2), as well as in the Caledonides in the west. Sweden's mining history has traditionally been focused on Fe and base metals such as Zn, Cu and Pb as well as precious metals such as gold and silver. Mining of other metals now considered to be critical, such as W and cobalt, has occurred in smaller amounts.

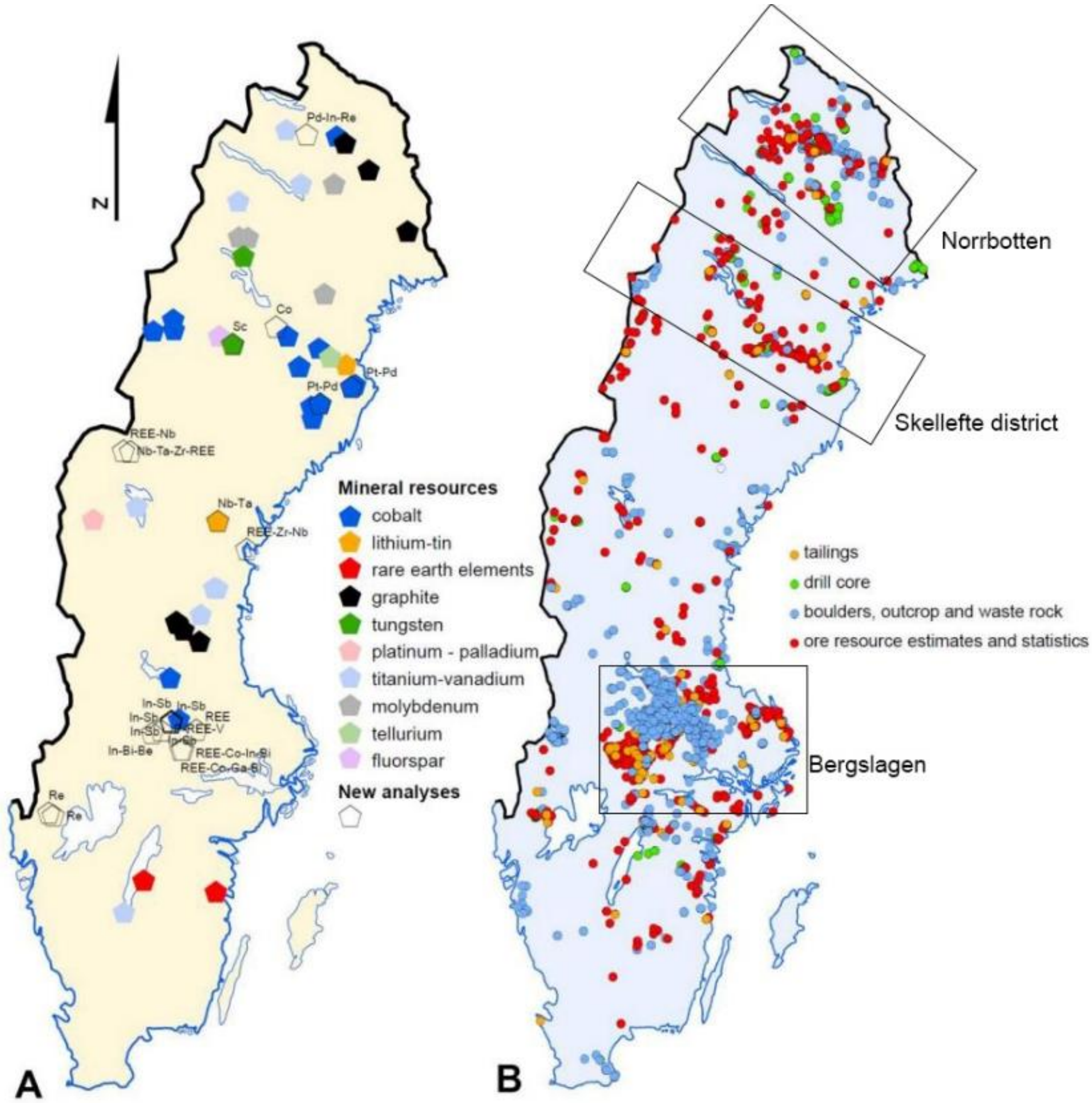

Figure 2. Map of mineral resources in Sweden. **A.** Identified sources of CRM in Sweden. **B.** Locations of data sources in SGU's MALMdb. Modified from Hallberg and Reginiussen (2020).

Other critical metals, such as the rare earth element group also have an intimate history with Sweden. Many of the elements were discovered from the Ytterby quartz and feldspar mine located 20 kilometres northeast of Stockholm, with many REEs taking their name from this small mine, such as yttrium, erbium, terbium, and ytterbium. Cerium and lanthanum were originally discovered and mined commercially at the Bastnäs mines in Västmanland county. At these mines, REE was predominantly a curiosity, and only exploited in small amounts, and often discarded with other uneconomic portions of the mine waste.

Modern mining methods have become efficient at separating the valuable fraction of ore from the waste materials. However, with the long mining history of Sweden, and the changes through even the past decades of which raw materials are used within emerging industries, the large amounts of mining waste of over 3 billion tonnes may provide a viable source of secondary raw materials.

Documentation of mine production statistics throughout its history has allowed for Sweden to be an ideal case for studying the potential recovery of CRMs from mining waste. Waste rock and tailings from historical mine production are abundant in Sweden, and an inventory of these resources is necessary to identify the potential to exploit these resources. SGU has created the mine production statistic database (MALMdb) to make available to the public historic records of ore production, processing, and mine waste produced.

In addition to the critical metals listed in Table 1 above, this report will also present results for other metals of economic interest, including Fe, Sn, Mo; precious metals (Ag, Au, PGM) and base metals that have historically been mined in Sweden (Zn, Cu, Pb).

REGIONAL GEOLOGY OF BERGSLAGEN

The Bergslagen Lithotectonic unit (fig. 3) is composed of three dominant tectonic subdivisions: the Paleoproterozoic greenschist to granulite facies subjected to metamorphism during the Svecokarelian orogeny; post-Svecokarelian rocks in western Bergslagen that were dominantly metamorphosed during the 1.2–0.9 Ga Sveconorwegian orogeny, and Neoproterozoic and later supracrustal rocks (Stephens et al., 2009). Mineralisation predominantly occurred approximately at 1.9 Ga with minor mineralisation events occurring around 1.79 Ga.

The dominant mineralisation in Bergslagen occurred in metavolcanic and metasedimentary supracrustal rocks dating to approximately 1.91–1.89 Ga. The metavolcanic and metasedimentary rocks are predominantly felsic to intermediate with rhyolitic rock dominating (Stephens and Jansson, 2021). The initial production of volcanic rock was explosive in nature, with the basal metavolcanics dominated by pyroclastic flows and airfall deposits as evidenced by lapilli and relict pumice clasts and are interpreted as vent proximal deposits (Allen et al., 1996). Coherent lava flows of felsic to intermediate composition are also found in these lower units. The second stage of deposition of extrusive rocks was likely ash-fall dominated as evidenced by their relict sedimentary features that are better preserved in the lower metamorphic facies rocks of western Bergslagen indicating vent distal deposition (Stephens and Jansson, 2021).

During periods of volcanic quiescence carbonates formed, intercalated with metavolcanic successions and provided an important host for ore mineralisation. These carbonates are predominantly organic in nature produced by stromatolite reefs, demonstrating a rather shallow basin depth (Allen et al., 1996). The presence of stromatolites is a useful indicator of younging direction, and preserved ashfall layers between growth layers of the stromatolites is evidence for continuing minor volcanism during the quiet periods (Stephens and Jansson, 2021). These carbonate units are often dolomitized, though the timing of the dolomitization is often unclear with evidence of regional dolomitization occurring for example in the Sala region (Ripa et al., 2002), and syn-volcanic dolomitization resulting from hydrothermal fluid flow relating to ore formation observed at Garpenberg (Stephens et al., 2009).

Intrusive rocks are the dominant rock type by volume in Bergslagen, in which the supracrustal rocks now form inliers. Three distinct intrusive suites are identified: i) Granitoid-dioritoid-gabbroid (GDG) (1.91–1.87 Ga) which was co-volcanic with the deposition of the supracrustal rocks and formation of most mineralisation, ii) the Granitoid-syenetoid-dioritoid-gabbroid suite (GSDG) (1.9–1.8 Ga) the) and iii) the Granite-pegmatite suite (GP), which terminated at 1.7 Ga (Stephens et al., 2009).

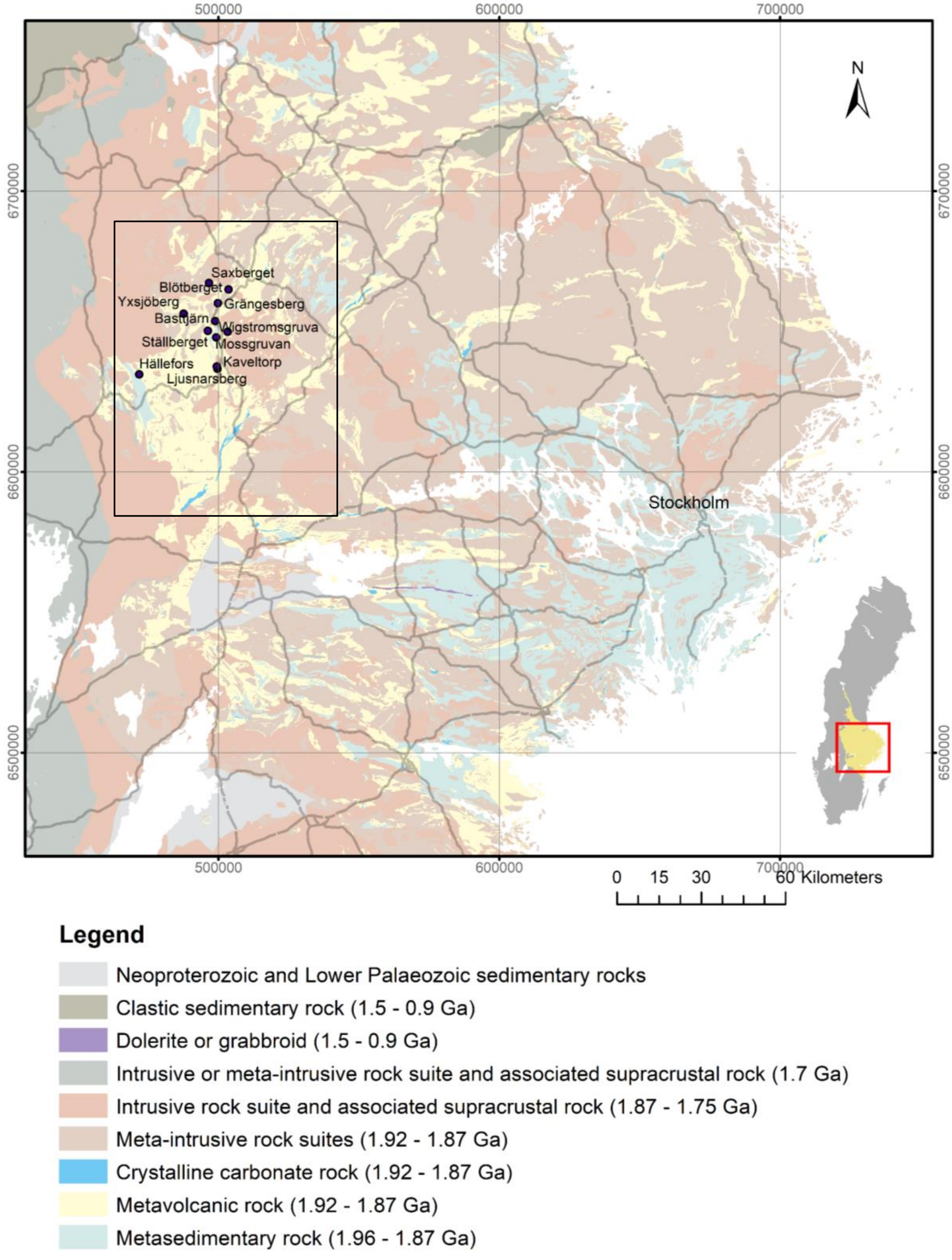

Figure 3. Map showing bedrock of Bergslagen in 1 million scale. Western Bergslagen and the sampled objects are shown in the rectangle.

Hydrothermal alteration is common in Bergslagen, occurring as secondary remobilisation by hydrothermal fluids. Mg, Na, K and calc-silicate (skarn) alteration are the dominant alterations. It should be noted that in this report “skarn” is used as a descriptive term of hydrothermally altered rocks showing typical skarn mineralogy and evidence of Mg±K, Si, or Ca modification, and not indicative of the genetic nature of the rock. Alteration is strong around mineral deposits, with evidence of K and Mg alteration. Magnesium alteration is typically feldspar destructive, replacing feldspar with phyllosilicate minerals (sericitisation).

Metamorphism in Bergslagen occurred shortly after the formation of the supracrustal rocks, ranging from greenschist facies through granulite facies. Amphibolite facies rock dominates throughout most of Bergslagen (Stephens and Jansson, 2021). The lowest metamorphic grades are found in the far west near the boundary with the Sveconorwegian orogeny, and Hällefors is considered the type locality for Bergslagen due to better preservation of original textures (Allen et al., 1996). Recrystallization of the felsic volcanic rocks can prove to make identification of the protolith difficult. Older terminology divides the supracrustal felsic metavolcanics into two types, the “hälleflinta” which underwent greenschist facies metamorphism is an extremely fine-grained rock that has been recrystallized with a texture and fracture that is reminiscent of flint. Leptites are the higher-grade metamorphic equivalent of the hälleflinta, where a higher degree of metamorphic recrystallization has led to a coarser texture.

Ore mineralisation in Bergslagen can be divided into three dominant types, each with subgroups. Most mineralisation was syn-volcanic with some exceptions. Fe mineralisation is the dominant ore in Bergslagen comprising 78% of deposits (Stephens et al., 2009), with magmatic, exhalative, and hydrothermal remineralisation (±Mn) the predominant modes of mineralisation. The largest Fe ore bodies in Bergslagen are magmatic Kiruna-type Fe-oxide-apatite deposits of Grängesberg. Other large Fe mineralisations such as Stråssa are exhalative banded Fe formations, or seafloor skarn carbonate replacement Fe ores associated with sulphide mineralisation such as Ställberg.

Sulphide mineralisation makes up 21% of other mineralisation and two modes of mineralisation occur the sedimentary-ash-siltstone deposits (SAS), such as Zinkgruvan. These ores are stratiform exhalative ores formed on the seafloor by venting of metal and sulphide rich fluids into dense seafloor brines. These ores typically have a large, continuous extent in sheet-like bodies and are dominated by Zn and Pb with subordinate Cu.

The second type of mineralisation is stratabound-volcanic-associated-limestone-skarn deposits (SVALS), such as Garpenberg and Falun. These mineralisations occur as massive to disseminated ore bodies lacking in the continuous extent of the SAS type deposits, occurring instead as lenses of strongly altered carbonate bodies showing skarn type alteration. Within the sulphide mines sampled within this report, SVALS type deposits dominate, such as Kaveltorp and Ljusnarsberg.

The remaining 1% of ore mineralisation types are skarn replacement ores related to the emplacement of the 1.80–1.77 Ga GP suite. These ores include Mo, Bi, and W mineralisations, with the largest found near Yxsjöberg, where the W mineralisation formed in relation to fluid flow from the emplacement of a GP suite body interacting with silicate and carbonate bodies.

Background geophysics

Regional scale maps of geophysical data over the western Bergslagen area are shown in figure 4. The residual magnetic field calculated from airborne measurements collected between 2016 and 2019 is shown (fig. 4A), as well as the residual Bouguer anomaly calculated from ground-based measurements (fig. 4B). Several of the deposits discussed during this report are highlighted on the maps.

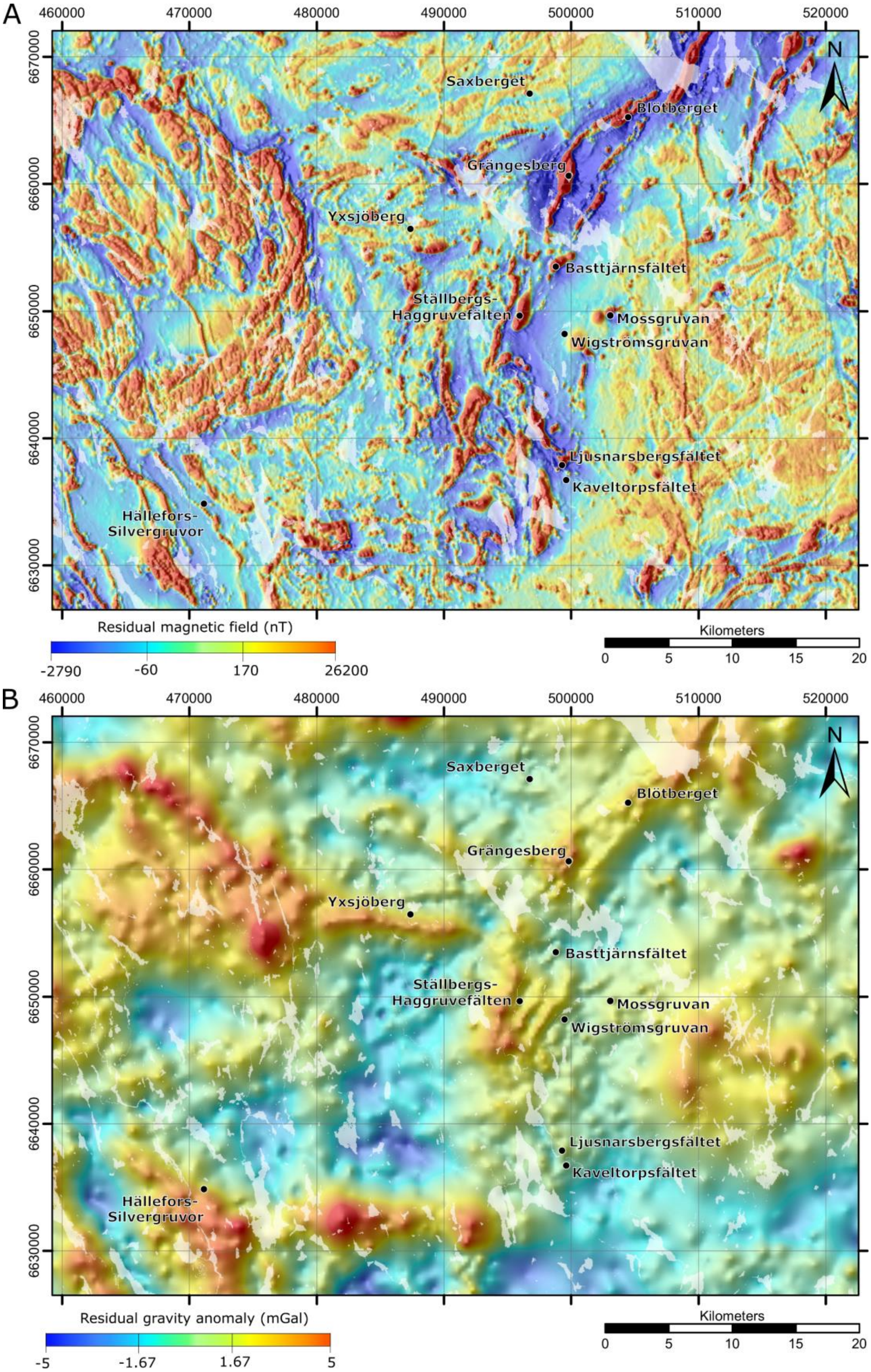

Figure 4. Regional geophysical maps for the Western Bergslagen area. **A**. Map of the residual magnetic field intensity calculated from airborne measurements collected between 2016 and 2019. **B.** Map of the residual Bouguer anomaly calculated using all available gravity measurements in SGU's database.

Perhaps the most notable feature on the residual magnetic field map (fig. 4A) is a series of strong anomalies with an approximately northeast – southwest strike in the central and eastern part of the map. These anomalies correspond to a zone where Fe oxide mineralisation is prevalent within the felsic metavolcanic sequence, often associated with carbonate / calc-silicate rocks (Stephens et al., 2009). Within this mineralised zone, magnetite is often the predominant Fe-oxide mineral, which leads to high magnetic susceptibilities (Magnusson and Lundqvist, 1933; Magnusson, 1940). Several of the deposits discussed in this report lie on this series of anomalies, namely, Blötberget, Grängesberg, Basttjärnsfältet, Ställbergsfältet and Ljusnarsbergsfältet, which are documented to include significant amounts of Fe-oxide mineralisation (Magnusson, 1940). The densities of this zone of carbonate / calc-silicate rocks and associated mineralisation are also typically higher than the surrounding felsic volcanic and granitic rocks (Stephens et al., 2009). Hence, a positive gravity anomaly in figure 4B is also linked to this zone. The strong magnetic anomaly about 10 km to the east of the Hällefors silvergruvor is also caused by iron Fe-oxide mineralisation and carbonate / calc-silicate rocks. However, the strong positive gravity anomaly in this area is likely to be associated with the presence of mafic rocks as well as Fe-mineralisation (fig. 3).

In contrast to the Fe oxide deposits, strong, regional scale magnetic anomalies are not observed at the predominantly sulphide or W/Mo bearing deposits, for example at Yxsjöberg, Wigströmsgruvan, Kaveltorpsfältet, Saxberget and Hällefors Silvergruvor. However, the occurrence of magnetite together with sulphide mineralisation, leads to small magnetic anomalies at Kaveltorpsfältet, Saxberget as well as some of the deposits at Hällefors Silvergruvor (Magnusson, 1940; Sundius et al., 1966; Vivallo and Rickard, 1990).

A region with a relatively strong positive residual magnetic anomaly can be observed on the western side of the map in Figure 4A. This corresponds to a region of predominantly intrusive granitic to syenitic rocks, 1.81–1.78 Ma, which can have relatively high magnetic susceptibilities. This is somewhat atypical when considering the other granitic rocks in Bergslagen, which normally have relatively low magnetic susceptibilities. A positive gravity anomaly also occurs along the edge of this region of intrusive rocks and extends close to the Yxsjöberg deposit. This anomaly is interpreted to be associated with intrusive mafic rocks, which are more extensive at depth than mapped at the surface. Elsewhere in Figure 4, regions with relatively low residual magnetic and gravity anomaly values typically correspond to areas dominated by felsic volcanic and intrusive rocks. These include the area to the southeast of Kaveltorpsfältet and Grängesberg, the area to the west of Saxberget and the area between Ställbergsfältet and Hällefors silvergruvor. More detail about the geophysical response and available data for each of the deposits discussed in this report are provided later.

METHODS

Composite samples

A composite sample of waste rock is a random sampling of approximately 2–5 kg of rock from a waste rock pile. The sampling methodology for waste rock in this project was developed by Sädbom and Bäckström (2018) in conjunction with a previous project investigating critical metals in Bergslagen. The first step in composite sampling is to divide the waste rock into various subdivisions based on the properties of the waste rock piles. This work can be done in advance of fieldwork using historic data from the mine, as well as aerial photos and LiDAR data. These subdivisions can be based on morphology, i.e. steep piles, flat piles, average size of material, amount of vegetation et cetera. Also important to make note of is the levels of mineralisation observed within the samples. As metal prices fluctuate during operations of the mine some mineralised material may not be economical to process during times of low metal prices. However, this material is removed to access more richly mineralised material and can be stored in separate piles for recovery should rises in metal prices make the material economical to process. These potential variations in mineral content in waste rock heaps can affect the apparent concentrations of CRM in waste rock, with the sampling of a single richly mineralised waste rock pile creating a "nugget effect". Thus, to dilute the potential effect of sampling favouring richly mineralised piles, a minimum of 15 composite samples are collected from all mine waste to ensure an accurate reflection of the contents of the mine site as a whole. Sädbom and Bäckström (2018) demonstrated with moving average analysis that after a minimum 15 samples the data trends became consistent enough to rely upon the data, negating any nugget effect caused by richly mineralised waste rock piles.

Once the object has been divided, the sampling area is described according to morphology, size of material, and vegetation, as well as any other important information such as proximity to former loading or sorting areas and then sampled. Only waste rock heaps where waste rock is exposed should be sampled to avoid digging beneath vegetation and topsoil. Samples are then collected by randomly selecting between 40 and 50 blocks and hammering off chips between 2–7 cm in size. To ensure randomness sampled blocks should be selected "blindly" to prevent geologist induced bias. Therefore, selection of blocks sampled in this study were chosen via "blind hammer fall" where a geologic hammer was allowed to fall at random, and the rock it struck was then sampled. Also used was the "step method", where between 510 steps were taken across the waste rock, and the rock directly underfoot on the final step was sampled. An ideal weight of a composite sample was between 2–5 kg, the large sample size aiding in further dilution the nugget effect, where even a small number of richly mineralised rock chips could increase apparent concentrations of elements of interest.

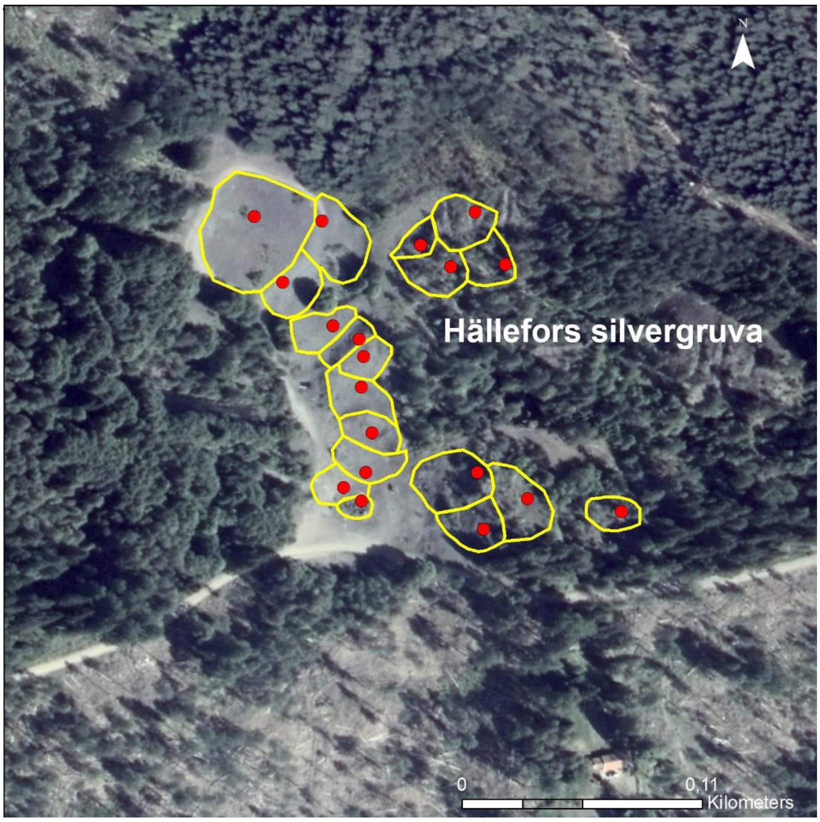

Figure 5. Example of division of the waste rock at Hällefors silvergruva into 19 objects for sampling.

Collected rock chips were then examined and categorized roughly by their composition and recorded. Examples of typical categories in western Bergslagen for the collected chips were felsic metavolcanic, skarn, mineralised (sulphide/Fe), granite and carbonate. In addition to the composite samples of waste rock several individual samples were collected of each of the dominant types of lithology in the waste rock heaps for petrophysical analysis, and a richly mineralised sample of each type of mineralisation was collected for whole rock geochemical analysis and thin section microscopy.

Sources of error

The avoidance of waste rock that is covered by topsoil or heavy vegetation as outlined in the methodology leads to a potential source of error in the total estimates of CRMs provided for some objects and should be considered when interpreting resource estimates. This is due to a sampling bias weighted towards the exclusion of waste rock that had a chemistry preferential to, or at the very least not hostile to the growth of vegetation. This bias can be expected particularly in mines with sulphide mineralisation that have been abandoned for long periods of time. Low-sulphur waste rock, such as the felsic volcanic host rock may be more agreeable to the growth of vegetation and formation of soils than high-sulphur waste rock that produces an inhospitable environment for plant life.

Indeed, observations at Ljusnarsberg indicated that overgrown waste rock heaps were dominated by the felsic volcanic host rock, while exposed heaps suitable for sampling by the above methodology showed strong sulphide weathering. This may lead to an overrepresentation of sulphide rich samples as these were the most available and accessible for sampling at these waste heaps. Therefore, at some objects where sampling methodology may bias results toward overrepresentation of richly mineralised samples it will be noted that estimates of potential mineral resources may be overstated.

Sampling of tailings

Surface sampling

To obtain a rough picture of elements of interest and their concentrations contained in each tailing repository, samples were taken from shallow depth by hand sampling. At each sampling site the coordinates and morphology of the area was recorded, including vegetation. Using a shovel, the upper layer of oxidized tailings was removed to ensure sampling was conducted at a depth where weathering had not affected the tailings. Using an Edelman auger, 5–10 samples of approximately 1–2 kg were collected from depths between 0.5 and 1 metre. The collected material was then photographed and field observations of colour, size of the material, and moisture content were recorded.

At the laboratory, samples were air or vacuum dried at room temperature. Heat was avoided in the drying process to avoid any potential changes in the mineral makeup of the samples which may have affected concentrations of elements released during digestion. Approximately 400 grams of material were then sent to an outside laboratory for geochemical characterisation. After drying, bulk density measurements were carried out. One decilitre (dl) of dry material was weighed and recalculated to tonnes per m^3.

Geophysical methods for investigations of tailings

Geophysical investigations were performed on a selection of the mine tailings: Morkulltjärnen in Yxsjöberg, Jan-Mattsdammen, Svandammen and Hötjärnen in the Grängesberg area, as well as the tailings from Stollberg and Blötberget. The aim was to investigate the petrophysical properties of tailings, both regarding its surroundings, between different geological settings and to compare different depositional material. One main goal was to determine the thickness of the tailings to model the volume of the deposits and calculate tonnage.

The assumption is that the tailings material has different petrophysical characteristics compared to its surroundings and is distinguishable by geophysical measurements. A secondary hypothesis is that variations within the material's petrophysical properties may also be identifiable by geophysical methods. To be able to link the geophysical signature from the measurements with petrophysical, geochemical and mineral characteristics, drillings were conducted in conjunction to the measured profiles in all investigated areas.

Several different geophysical methods were tested and evaluated, and a comprehensive description of the various methods, survey design and results will be presented in a separate publication (Bastani et al. 2024, in prep.) The main methods in focus were electrical resistivity tomography (ERT) and induced polarisation (IP) which is conducted simultaneously with the same instrument (Fig. 6). Other methods used at the tailings were radio magnetotelluric (RMT) and towed transient electromagnetic (tTEM).

The ERT-method is a direct measurement of the grounds resistance to conduct electrical current. An array of electrodes is inserted in the ground along a profile and electrical current is transmitted. Different electrodes act as current and potential during a predesigned measurement scheme, giving information along the profile and at depth. IP measurements are done simultaneously as the ERT-measurement but with somewhat adjusted acquisition parameters. IP-measurements are based on different material having different IP-effect, put simply the ability of the material to act as a capacitor. This effect results in a delay time for charges to build up (and decay?) when the current is switched on (or off).

Figure 6. ERT and IP measurement at the Hötjärnen tailings deposit in Grängesberg. Photo: Cecilia Brolin.

Transient electromagnetics (TEM) is a geophysical technique where the induced electric and magnetic fields caused by transient pulses are measured. As a result, the electrical resistivity distribution of the ground can be determined. The tTEM (towed transient electromagnetic) system (Auken et al., 2018) consists of a transmitter and receiver coil, which are towed behind an all-terrain vehicle (ATV). The RMT method makes use of the signal in the frequency range 10–250 kHz from distant radio transmitters. The ratio between the horizontal electric and magnetic field components for each frequency is directly related to the electrical resistivity distribution of the ground. The signal at the lower frequencies penetrates deeper into the ground and the variation of resistivity with depth can then be determined. The EnviroMT system, developed at Uppsala University, was used in this study (Bastani, 2001).

See Bastani et al. (2024, in prep.) for a more detailed description of all geophysical methods used within this project. In this report only the main conclusions and characteristics from the geophysical measurements in each investigated area will be presented.

At each tailings repository several profiles were measured with the aim to cover the area as much as possible. Due to differences in accessibility, topography, and size of the areas, the number of profiles and the location of these were adjusted for each tailings deposit. Different methods also have different ease of access and thereby different distributions within each area.

Drilling

Drilling of tailings repositories was undertaken at Kaveltorp, Grängesberg, Yxsjöberg, Blötberget and Stollberg with the goal of characterising the geochemistry of tailings at depth. Drilling locations were chosen based on concentration of CRMs as well as distinctive differences in composition of tailings and their properties as shown by the geophysical surveys. An initial probing was conducted at each hole to determine the depth to till or bedrock. Samples were taken every metre, photographed, and where possible multiple samples were taken for each metre where there were stark visual differences in the tailings including colour or grain size.

The sampling method of the tailings depended upon the properties of the tailings at the drill site and could change during drilling at each hole, with different methods illustrated in figure 7. In ideal tailings, i.e. moist, but not saturated, well compacted sand, a borehole was sampled with a 1 metre sampler with a 40 mm diameter equipped with a core cutter and catcher. This allowed sampling at 1 metre intervals and kept the integrity of the sample for the identification of structures within the sediment. Below the water table sampling could become more difficult as the high water content of the tailings led to a more fluid like behaviour in the tailings, and the sample could flow out of the core cutter. Additionally, waterlogged tailings led to the collapse of the borehole, which would lead to the sampler capturing sediments from above the targeted layer. Therefore, in waterlogged tailings a 100 by 20 cm wide screw was used to capture the sample. This method unfortunately introduces the possibility of contamination into the sample, as the core is exposed. During withdrawal from the borehole the captured sediment is in contact with the sides of the borehole and can pick up tailings from the layers above. To reduce this contamination the outer 2–3 cm of the sampled material is scraped away, and only the innermost material sampled. This method provided several litres of material, which allows for dilution of any remaining contamination by the volume of material.

Upon return to the laboratory, samples were processed with the same methods as used in the surface sampling campaign and sent away for analysis.

Figure 7. A. Tailings repository at Grängesberg. **B.** Sample taken with screw with outer part of the core removed to reduce contamination. **C.** Core sample taken with 40 mm sampler. Photos: Patrick Casey.

Geochemical analysis

Geochemical analysis of all samples was conducted by ALS laboratories. Sample preparation including weighing and crushing took place at ALS Piteå, Sweden. Samples were initially crushed to approximately 2 mm, and the samples were subsequently split and pulverized to <75 µm fractions for analysis at ALS Galway, Ireland. Three SGU internal standards were analysed with each batch of samples to ensure the accuracy and reproducibility of the results. A total of 61 major and trace elements were analysed. Major elements were analysed using ICP-AES after acid digestion. Trace elements were analysed using lithium borate fusion prior to acid digestion and ICP-MS. Aqua regia and 4 acid digestion with ICP-MS analysis was used for trace elements with low concentrations. Ore minerals that exceed detection limit of standard analyses (typically 10,000 ppm) were analysed again using ore-grade methods with higher detection limits. Many elements are analysed multiple times using several analysis methodologies, and data in this report are presented using SGU's preferred analysis methodology. For a complete list of elements analysed and their preferred analytical methodology, see appendix 1: Sample Digestion and Analytical Methods.

Data from analyses are presented in table and chart form. Scatterplots and line charts were created in Microsoft Excel™ and spiderplots presenting REE concentrations were created using GCDkit software (Janoušek et al., 2006).

Thin sections

Polished thin sections were made of richly mineralised samples collected from each mine. Where bedrock mapping was conducted, thin sections were also made to identify structures and to classify rock type. Thin sections were analysed using optical microscopy using transmitted and reflected light.

Further analysis of thin sections for identification of difficult to identify mineral phases as well as analysis of trace components of the minerals analysis was carried out using an FEI Quanta650 scanning electron microscope (SEM) as well as back scatter electron (BSE) at the Swedish Museum of Natural History. Elemental composition of minerals was obtained using an Oxford Instruments electron dispersal spectrometer (EDS) with an 80 mm^2 detector and a 25 to 45 second analysis time. Elements greater in atomic number than Li were analysed except for Be, due to the Be X-ray window used in the instrument. Spectra were analysed and compositions calculated with Aztec software by Oxford Instruments. Detection limits for trace elements were typically around 0.5%.

Geophysical methods for mapping

At some of the locations in this study additional observations and measurements were performed with the aim of improving the understanding of the bedrock and primary mineralisation coupled to the secondary waste deposits. As part of this work additional ground magnetic and very low frequency (VLF) measurements were performed using a GEM GSMV-19 instrument (which also records the position information using GPS). These ground geophysical measurements were collected either as individual profiles or over an area to characterise features of interest in the bedrock. Additional ground gravity measurements were also collected using a Scintrex CG-5 instrument. Position data for the gravity measurements were collected using a GNSS instrument from Topcon and corrected using network RTK from SWEPOS. In addition, bedrock samples were collected for subsequent measurements of magnetic susceptibility, density and remnant magnetization in SGU's petrophysics laboratory. Measurements of magnetic susceptibility were also performed at outcrops in the field using a handheld SM20 susceptibility meter.

At various points in this report we show maps of the available geophysical data for the different focus areas. For the gravity measurements the so called "residual anomaly" is often shown. This is generated by first interpolating the Bouguer anomaly data, which is then upward continued. The residual anomaly is generated by subtracting the upward continued version of the Bouguer anomaly from the original interpolated Bouguer anomaly. This has the effect of removing the lower frequency features from the map. A similar process is used to generate the residual anomaly for the airborne magnetic measurements. Here the total magnetic field intensity data is first interpolated, after reduction to the magnetic pole. An upward continued version of the magnetic field intensity data is then subtracted from the original magnetic field intensity to generate the residual anomaly. The parameters for upward continuation and grid size used for the different areas varies depending on the data which is available. However, the gravity and magnetic data are typically upward continued by 3km and 1km, respectively, when generating the residual maps.

TUNGSTEN DEPOSITS

Yxsjöberg

Background

Yxsjöberg (6656471/487368), 13 km southwest of Grängesberg in Örebro county (fig. 8), represents the single largest exploited deposit of W in Sweden. Originally mined as a copper deposit in the 19th century; tungsten and fluorite were mined during the periods 1918–1920, 1935–1963, and 1969–1989. Tungsten from Yxsjöberg occurs in the form of scheelite with minor wolframite in skarn mineralisation dated to 1798 ± 2 Ma during the waning phase of the Svecokarelian orogeny (Romer and Öhlander, 1994). Mineralisation occurred in skarn altered carbonate bodies hosted in the supracrustal metavolcanic rocks typical to Bergslagen. Three mines were in operation, Finngruvan, Kvarnåsen and Nävergruvan, which produced ore with a concentration of 0.24–0.32 w% W, 0.16% w% Cu, and 5.0 % fluorite (Rothelius, 1957). Approximately 5.3 million tonnes of ore were mined at Yxsjöberg between 1938 and 1989 (table 2), with supplementing ore coming from W deposits at Wigströmsgruvan and Sandudden.

Ore was processed on site at the dressing plant at Yxsjöberg, where approximately 5.2 million tonnes of tailings were deposited in the tailings ponds Morkulltjärnen and Smaltjärnen. Smaltjärnen is the older of the two, with deposition of tailings beginning in 1897 and ending in 1963. Morkulltjärnen was used as a tailings repository starting in 1969 through the end of production at Yxsjöberg in 1989. Tungsten ore was processed starting in 1918 using gravity separation and roasting methods, which produced an approximately 50% recovery of W. In the in 1977 the flotation method was introduced at Yxsjöberg, which increased the recovery of W to 75% (Hällström et al., 2018).

The tailings repository at Smaltjärnen has received attention for the potential to affect groundwater due to high concentrations of elements that pose health hazards, including Be and W. Ground water measurements near Yxsjöberg have shown the highest recorded levels of Be observed in groundwater at 5 mg/L (Hällström et al., 2018) and tungsten, which has been identified as a contaminant of concern by the United States Environmental Protection Agency is also present in high levels in routine groundwater measurements taken by the local municipal government. Remediation through reprocessing of the tailings has been suggested as a means of removing contaminants from the area (Hällström et al., 2018).

Smaltjärnen has been well sampled during investigations by Luleå Technical University (LTU) in conjunction with the REMinE-project to examine the potential for re-mining of the tailings for W and as such the analyses presented here represent only samples collected by SGU from the Morkulltjärnen repository. For further information on the Smaltjärnen tailings and the REMinE project see Hällström et al. (2018) and Mulenshi et al. (2019).

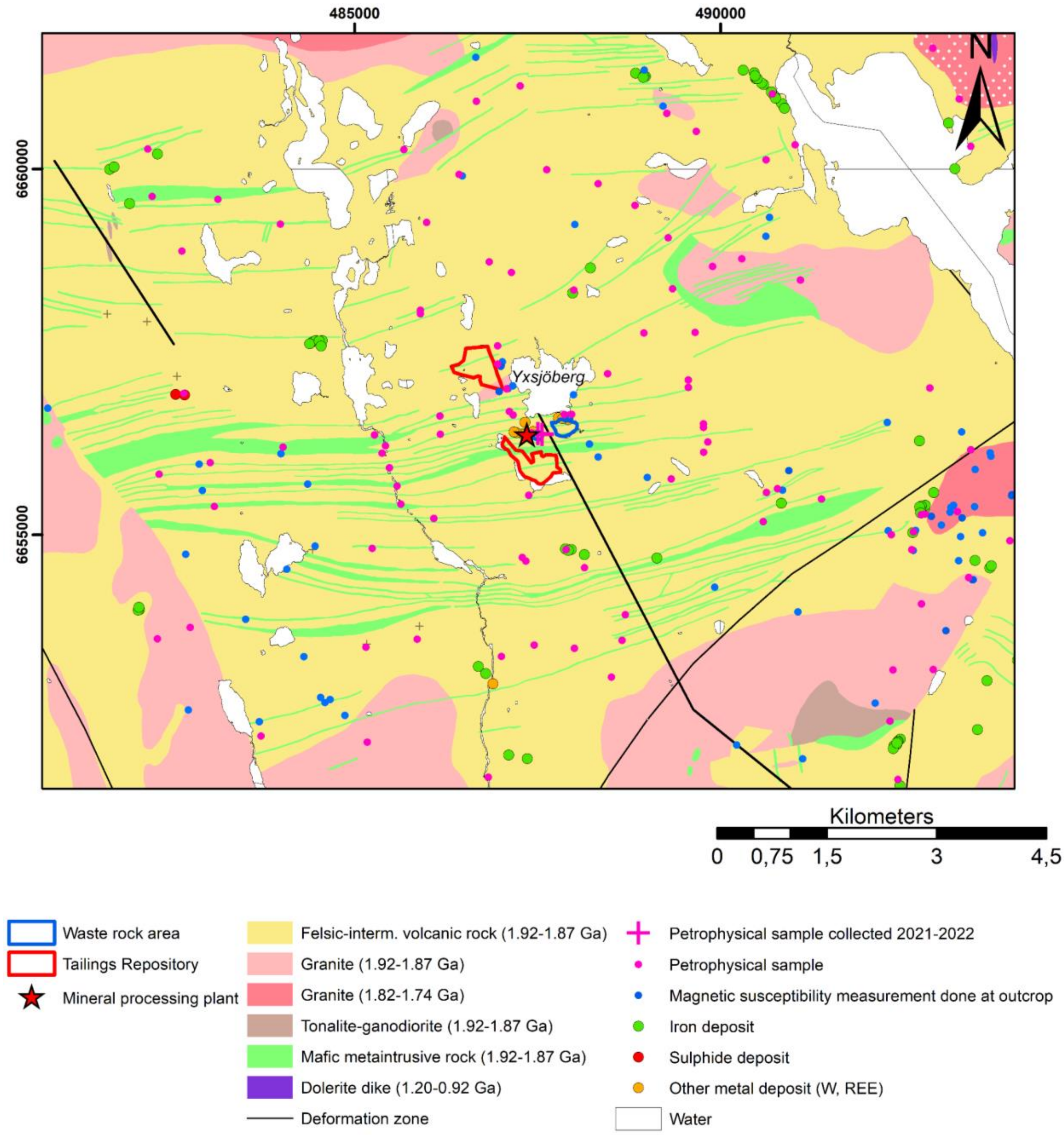

Figure 8. Bedrock map of the Yxsjöberg mine and its surroundings.

Table 2. Production statistics from Yxsjöberg.

	Total (Mt)	W (%)	Cu (%)	CaF_2 (%)
Mined Ore	4.94	0.26	0.16	5.88
Processed in dressing plant	5.32			
Tailings	5.24			
Waste rock	0.64			

Available geophysical data

Airborne data (magnetic, VLF, gamma spectrometry)

The oldest airborne data for the area around Yxsjöberg were collected by SGU in 1972, where only magnetic and natural gamma measurements were made. In 1979, LKAB collected additional airborne data over a region to the west of Yxsjöberg. The acquisition parameters for this dataset were the same as those for the data collected in 1972 (table 3), with the addition of VLF (1 transmitter) measurements. The most modern airborne data over the Yxsjöberg area were collected by SGU between 2016 and 2019. As part of these new measurements magnetic, natural gamma and VLF (2 transmitters) measurements were made. Details of the different airborne surveys over the area around Yxsjöberg can be seen in table 3.

Figure 9 shows a map of the residual magnetic field intensity over the area around Yxsjöberg, calculated from airborne data collected between 2016 and 2019. A number of positive magnetic anomalies can be seen on the map in the area surrounding Yxsjöberg. These anomalies appear to be predominantly associated with Fe oxide mineralisation which occur within skarn / calc-silicate rocks. These skarn rocks are in turn located with the sequence of felsic volcanic rocks which constitute most of the bedrock mapped in this area (fig. 8). Mafic rocks occur within an east-west dike system which cross cuts the older rocks of the study area. These mafic rocks do not appear to have a notably higher magnetic susceptibility than the surrounding felsic metavolcanic rocks and hence, do not appear to give rise to any significant anomalies in figure 9. Regions lacking in anomalies often correspond to areas with granitic rock types. A small magnetic anomaly can be observed at the location of the Yxsjöberg deposit. This is consistent with petrophysical measurements of waste rock from Yxsjöberg collected as part of this project, which show that the mineralisation has an extremely higher magnetic susceptibility (229972×10^{-6} SI) than is typical for the surrounding felsic volcanic rocks. Ripa and Antal Lundin (2020) interpret a series of folds within the felsic volcanic sequence based on the vertical derivative of the airborne magnetic data. In their interpretation the mineralisation at Yxsjöberg appears to be located at the intersection between the northern flank of a fold and a deformation zone with a northeast strike.

Table 3. Complete list of the airborne geophysical surveys collected in the area around Yxsjöberg. Unless otherwise stated all data are collected using a small, manned aeroplane.

Year	Organisation	Geophysical methods used	Area (SGU map sheet)	Flight direction (degrees)	Flight line separation (m)	Flight altitude (m)
1972*	SGU	Magnetics, gamma spectrometry	Part of 12E and 12F	East–West (90°)	200	30
1979*	LKAB	Magnetics, gamma spectrometry, VLF (1 transmitter)	Part of 12E (project R66)	East–West (90°)	200	30
2016	SGU	Magnetics, gamma spectrometry, VLF (2 transmitter)	Part of 13F,13G, 12E, 12F, 12G, 12H, 11E, 11F, 11G and 11H	Northwest – Southeast (130°)	200	60
2017	SGU	Magnetics, gamma spectrometry, VLF (2 transmitter)	Part of 12E, 12F, 11E, 11F, 10E and 10F	Northwest – Southeast (130°)	200	60
2019	SGU	Magnetics, gamma spectrometry, VLF (2 transmitter)	Part of 12E	East–West (90°)	200	60

* Not used for producing maps in this report

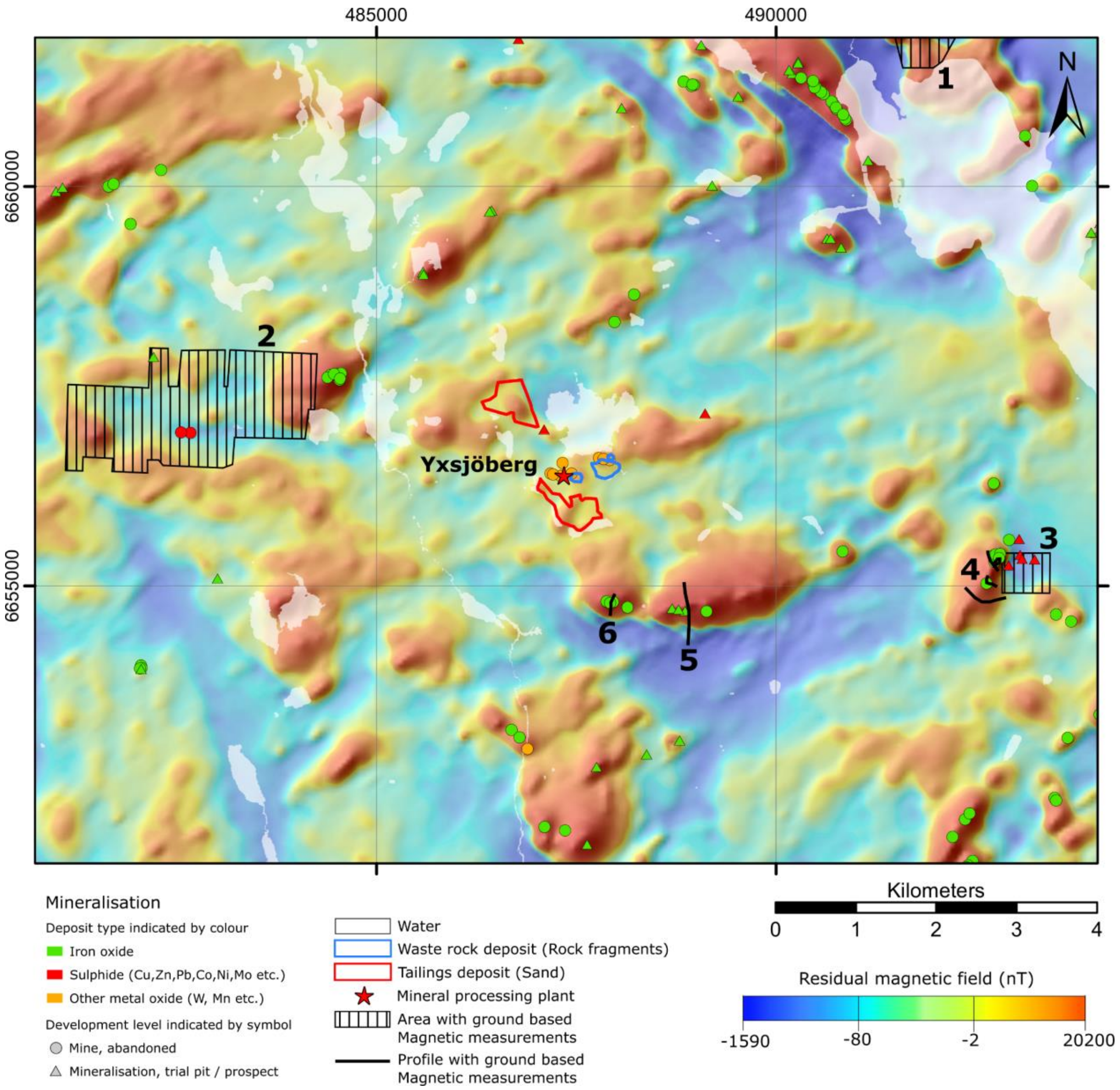

Figure 9. Map of residual magnetic field for the area around Yxsjöberg. The location of ground-based magnetic measurements, listed in table 4 are shown.

Figure 10 shows a map of the apparent resistivity calculated from airborne VLF measurements collected between 2016 and 2019. In this map several of the low resistivity anomalies appear to coincide with areas of low-lying terrain and wetlands as well as powerlines. However, several northeast – southwest striking low resistivity features appear to be present, which could correspond to deformation zones. One of these zones lies to the northeast of Yxsjöberg and another, to the southeast (which intersects the area of ground measurements labelled with a 7).

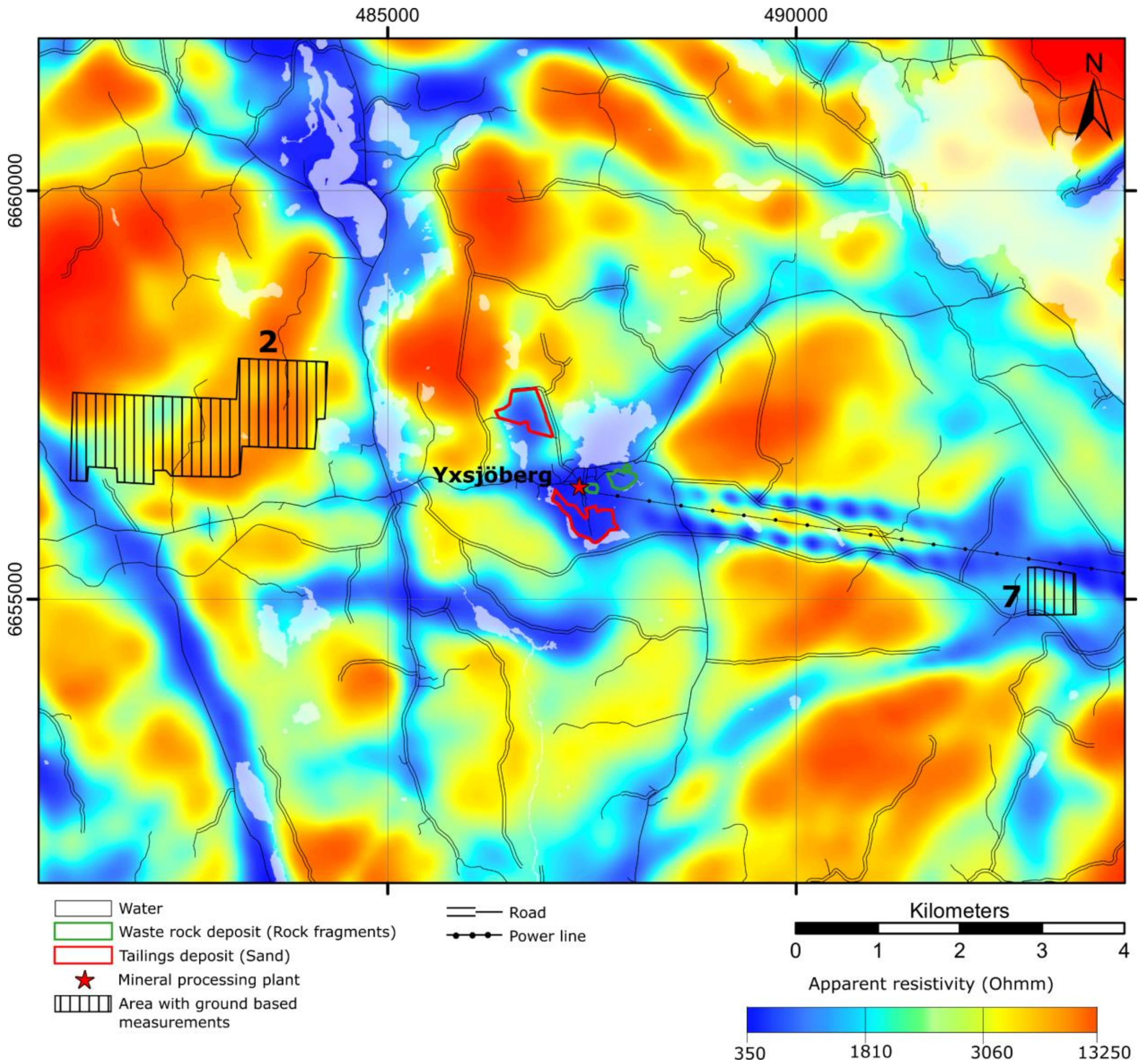

Figure 10. Map of apparent resistivity derived from airborne VLF data collected between 2016 and 2019 for the area around Yxsjöberg. The location of ground-based electromagnetic and IP measurements, listed in table 4 are shown.

Ground-based EM, Magnetic and IP measurements

Several sets of ground-based geophysical measurements are available within SGUs database for the area around Yxsjöberg. The locations of these data are shown in figure 9 and 10 as numbered areas or profiles. Details of the different measurements are summarised in Table 4. These data include several areas where magnetic and slingram measurements have been collected to the northeast and east of Yxsjöberg (areas 1, 3 and 7). These data have recently been digitized by SGU from analogue maps. Between 2006 and 2012 Kopparberg Mineral AB collected magnetic and IP data to the west of Yxsjöberg. In 2017 several ground magnetic profiles were collected by SGU to the southeast of Yxsjöberg as part of ongoing bedrock mapping work (Ripa and Antal Lundin, 2020).

Table 4. Ground-based magnetic, electromagnetic and IP measurements for the area around Yxsjöberg. Numbers correspond to the numbered polygons/lines shown in figure 9 and 10.

Polygon/Line number and name	Method	Year acquired	Responsible	Comments
1. mgtmid1850	Magnetic			Profile spacing of 20 m to 10 m.
2. Pala nr 100	Magnetic and IP	2006–2012	Kopparberg Mineral Exploration AB	Profile spacing of between 25 and 100 m.
3. mgtmid1550	Magnetic	1979		Profile spacing of 20 m.
4. MP17ILA0001 – MP17ILA0005	Magnetic	2017	SGU	Five profiles collected in this area
5. MP17ILA0006	Magnetic	2017	SGU	One profile collected in this area
6. MP17ILA0007	Magnetic	2017	SGU	One profile collected in this area
7. mgtmid4136 and mgtmid4137	Slingram, SR 18kHz	1979		Profile spacing of 40 m to 20 m.

Ground-based gravity

Figure 11 shows a map of the residual gravity anomaly for the area around Yxsjöberg. The density of measurement points is highest in the south-eastern part of the map, where measurements have been recorded every 100–200 metres along roads. Elsewhere in the map the typical distance between measurement points is 1–2 km.

The gravity response in this area is dominated by an approximately east-west striking positive anomaly, parallel to the general strike of the numerous mafic dikes which have been mapped at the surface (fig. 8). The Yxsjöberg mine is located on the northern flank of this positive anomaly. The mafic dikes observed at the surface typically appear to increase in thickness and are more densely spaced moving from east to west across the area of the map. This is consistent with the residual gravity anomaly, which reduces in amplitude towards the east. The positive gravity anomaly here can be interpreted to be due to the presence of mafic rocks at depth associated with the dikes observed at the surface (Olsson and Olsson, 1985). Ripa and Antal Lundin (2020) performed 3D geophysical modelling of the magnetic and gravity data around Yxsjöberg. In their study the prominent positive gravity anomaly was also interpreted as due to the presence of mafic rocks at depth. Andersson et al. (1986) describe gravity measurements performed at depth within the Yxsjöberg mine, which they use to conclude that the mafic dikes continue to at least 800 metres depth. The negative gravity anomalies on the map are interpreted to be associated with regions dominated by relatively low density, granitic rocks (Olsson and Olsson, 1985; Ripa and Antal Lundin, 2020). Some of these negative anomalies are thought to be associated with so called GP-granites (Late Svecokarelian Granite-pegmatite rock suites; Stephens et al., 2009). For example, the negative anomaly to the far east of Yxsjöberg is thought to be associated with the Mo-mineralised GP granite at Pingstaberg. The relationship between these GP granites and Mo-W mineralisation has been the focus of several investigations at SGU in recent years (Ripa and Antal Lundin, 2020; Bergman et al., 2020).

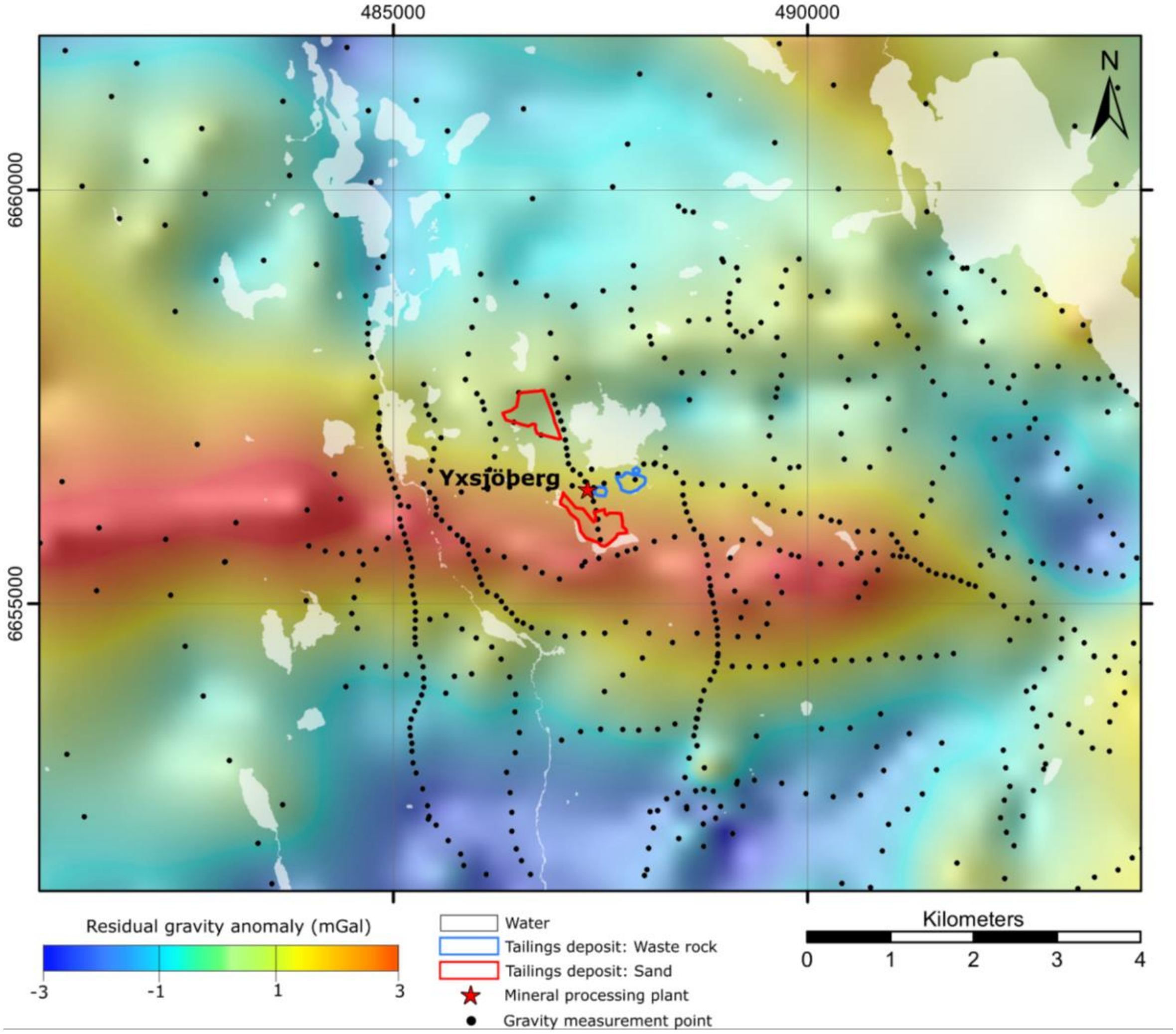

Figure 11. Map of the residual gravity anomaly for the area around Yxsjöberg. Gravity measurement points are shown as black dots.

Petrophysical data

Figure 8 shows a map of petrophysical data and magnetic susceptibility measurements taken at outcrop which are available in SGU's database for the area around Yxsjöberg. The available petrophysical data show that the highest magnetic susceptibilities are measured with samples of Fe mineralisation (often over 1 000 000 × 10^{-6} SI). This is consistent with observations from the residual magnetic anomaly map (fig. 9). Mean average density values for the felsic volcanic and mafic rocks are approximately 2650 kg/m^3 and 2990 kg/m^3, respectively. Whereas these two rock types have comparable average magnetic susceptibilities of around 3000 × 10^{-6} SI. This is consistent with the interpretation that the mafic rocks give rise to the positive gravity anomaly shown in figure 11 but do not give rise to an appreciable anomaly in the magnetic data (fig. 9). Table 5 shows the new petrophysical samples which were collected as part of this project, in this case from waste rock at the Yxsjöberg mine. Here the sample of skarn with W mineralisation had appreciably higher density and magnetic susceptibility than a sample from the surrounding felsic volcanic rock.

There are about 90 boreholes present in SGU's database for the area around Yxsjöberg (fig. 8). About 60 of these are located within about 2 km of the Yxsjöberg deposit and were drilled primarily between 1975 and 1986 by AB Statsgruvor.

Table 5. Table summarising the petrophysical results collected as part of this project from the area around Yxsjöberg.

Sample ID	Easting (m)	Northing (m)	Description	Density (kg/m3)	Magnetic susceptibility (10-6 SI)	J (mA/m)
PCY210207B	487504	6656382	Skarn with W mineralisation	3220	229972	2266
PCY210204D	487560	6656371	Felsic volcanic	2646	1349	30

Sampling of waste rock at Yxsjöberg

15 samples of waste rock at Yxsjöberg were collected from two locations, near Kvarnåsen mine and adjacent to the dressing plant as shown in the map in figure 12. Pieces of the waste rock near the dressing plant were typically smaller in size and are inferred from the location to have been crushed to a smaller size in preparation for further processing for mineral separation (fig. 13). Waste rock was dominated by a high percentage of volcanic host rock, with mineralised skarn comprising around 25% of the waste rock sampled. The small size of waste rock in some piles near the dressing plant necessitated a different sampling method than that of site at Kvarnåsen with larger pieces of waste rock (fig. 13), as much of the material was between 1 cm to gravel/sand in size. Two samples of the finer material were collected using a shovel from 30 cm depth to avoid weathered material and the disposition of the material was not recorded. The analyses of these two samples showed little deviation from the other material collected according to the methods presented in Sädbom and Bäckström (2018), and thus this "shovel collection" method appears to be a viable method of sampling fine crushed waste material.

Composite samples collected at Yxsjöberg show elevated levels of W (average 0.07%) as well as elevated levels of Zn, Cu, Bi, Be, In and Sn (fig. 14). Levels of CRMs including W and Be are typically higher by a small margin in the material that was sampled near the processing plant than that of the material in the vicinity of the mine. Full results of analyses are shown in table 6.

The richly mineralised ore sample collected at Yxsjöberg showed high levels of Fe, W, Bi, Be, Cu, Zn, and In. Scheelite occurs as 1 mm crystals evenly distributed through the sample, with small grains of sulphides also showing even distribution. Thin section observations showed that the dominant CRM containing mineralogy is scheelite (W), sphalerite (Zn), chalcopyrite (Cu), cassiterite (Sn), fluorite (F), and danalite (Be). When viewed under UV light the Yxsjöberg scheelite glows a strong blue colour, indicating little to no Mo in the mineral, which was confirmed by EDS analysis. Pyrrhotite is the dominant sulphide mineral observed in thin section.

Danalite, in solid solution with helvite (Mn-endmember) and genthehelvite (Zn-endmember) is the host of Be at Yxsjöberg (fig. 15). EDS analysis of danalite did not show the presence of Be due to the inability of the detector to identify Be, however the distinctive Si-S chemistry of danalite was used as an indicator of its presence. While In was found to be elevated in the sample, it was unobserved in EDS analysis, however it is likely contained within sphalerite.

The amount of accessible waste rock at Yxsjöberg lacks a clear estimate, however observations in the field showed limited amounts at the two sampling locations. Based on LiDAR data shown in the map in figure 12, waste rock appears to have been disposed of around the open pit mine, however thick overgrowth prevented any clear indication of the presence of waste rock. An unknown quantity of waste rock and tailings were used as backfill in Nävergruvan to prevent collapses, and to fill the open pits of the mines (AB Statsgruvor, 1990).

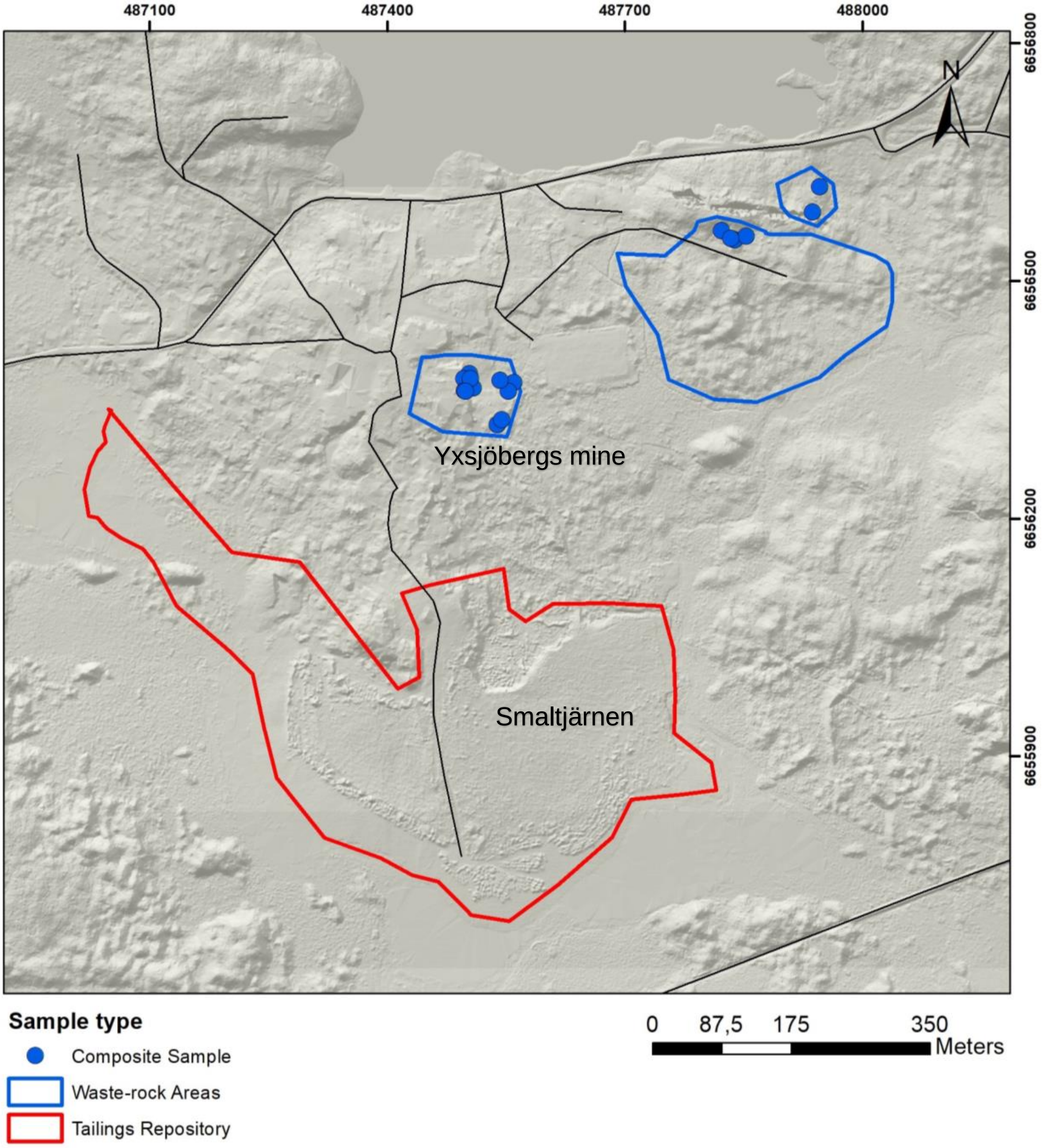

Figure 12. LiDAR image over the Yxsjöberg area showing the Smaltjärnen tailings repository and waste rock dumps.

Figure 13. A. Waste rock pile near the Yxsjöberg dressing plant. The fine material is visible where material has slumped in the centre of the picture. **B.** Waste rock pile near the Kvarnåsen mine showing larger size of material compared to material near the processing plant. Photo: Patrick Casey.

Table 6. Analyses of waste rock from Yxsjöberg mine.

Data	Object	W (ppm)	Cu (ppm)	Zn (ppm)	Be (ppm)	Sn (ppm)	Bi (ppm)
Mineralised Sample	W-Skarn	6590	4800	1100	815	577	1355
Composite Samples (n=15)	Yxsjöberg Mean	692	262	98	45	100	118
	Max	1770	1120	192	169	256	535
	Min	33	14	30	0.92	15	0.27

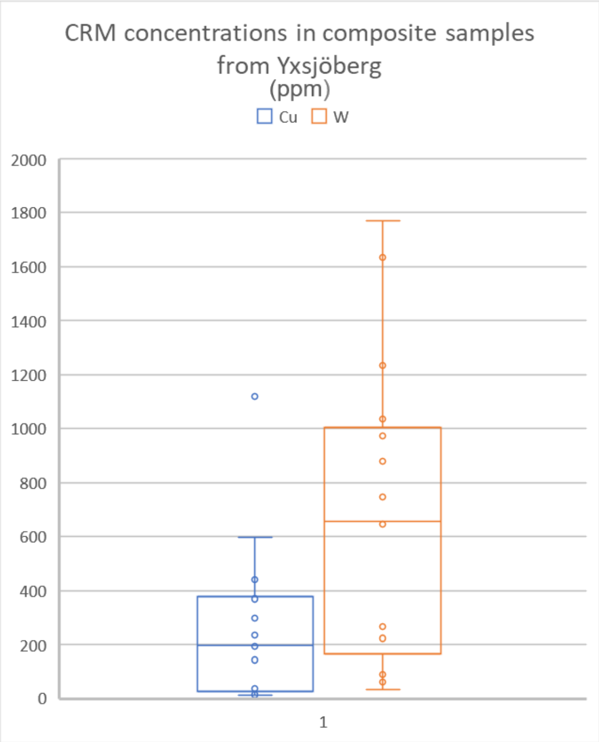

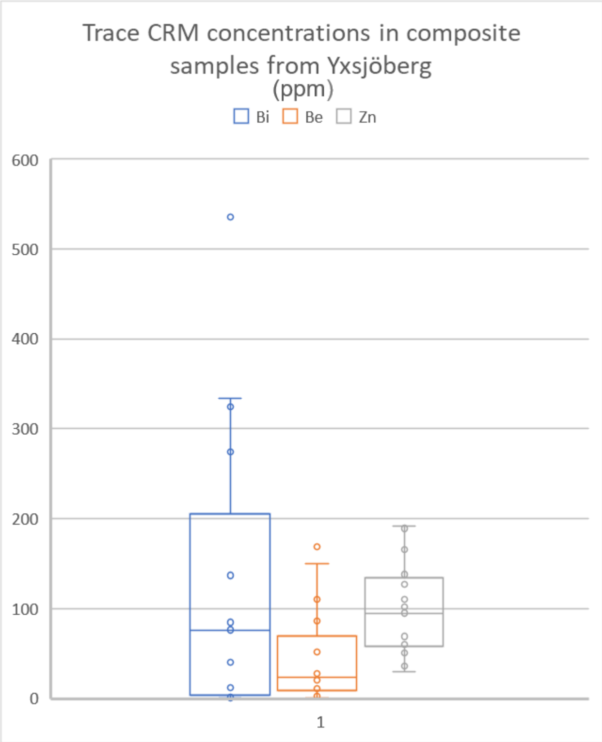

Figure 14. Box and whisker plot showing ranges of CRM concentrations in composite samples from Yxsjöberg.

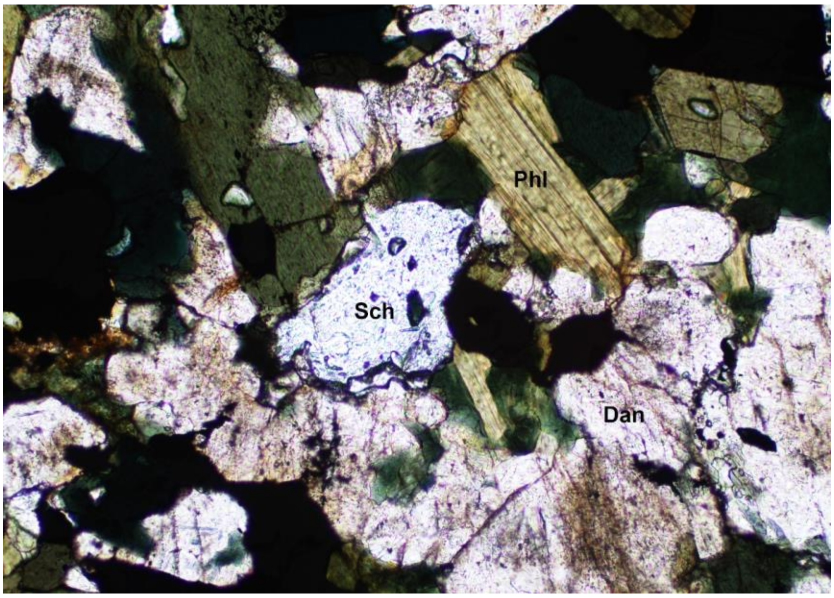

Figure 15. Image in plane polarized light of mineralised skarn sample from Yxsjöberg showing scheelite (Sch), danalite (Dan) phlogopite (Phl) and pyroxene. Opaque minerals are pyrrhotite. Micrograph: Patrick Casey.

Sampling of tailings at Yxsjöberg

Background

The tailings dam at Morkulltjärnen has an area of approximately 250 000 m^2 (fig. 16) Vegetation is dominated by sedges with some small groves of deciduous trees. The dam has a northerly downslope and grows increasingly swampier in the lower areas. Historic aerial photos show that the release points for the tailings were midway along the eastern side of Morkulltjärnen, and this point was later moved to the southern end of the dam, where the road curve inwards.

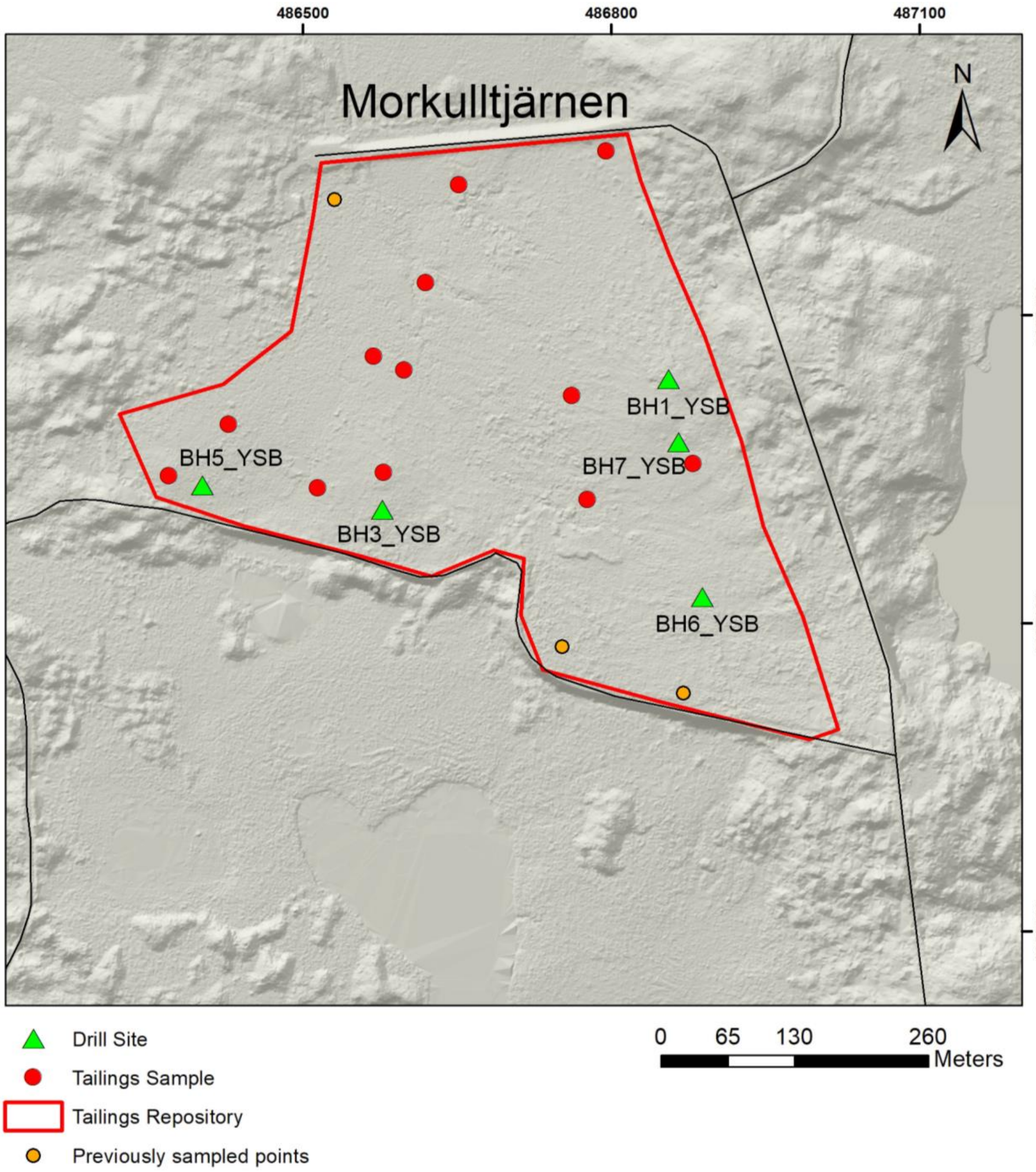

Figure 16. LiDAR image over the Morkulltjärnen tailings repository showing surface samples taken in this project and the location of boreholes.

Surface sampling of tailings at Morkulltjärnen

10 surface samples were collected at Morkulltjärnen. Samples were collected from between 0.75–1 metre in depth. For most samples this was below the oxidized layer, however several samples were taken of the oxidised layer as well. Differences in particle size were apparent during sampling depending on the sampling location. The higher elevation on the south and eastern sides of Morkulltjärnen contained coarser sand, typically medium grain, while the northern and western sides of the tailings repository contained very fine, silty material. The highest concentrations of W were found in the coarse material close to the former release point of the tailings (fig. 17), as well as in the finest fraction in the silty material to the northwest. Analysis of the tailings from surface samples showed high levels of W (average 1100 ppm), as well as increased levels of Sn, Cu, Bi, Zn, In and Be. The highest levels of W are found closest to the outflow pump from the enrichment plant where the material is the coarsest, and lower levels are found distal from this point. Very high levels (2200 ppm) of W are observed in the finest silty material in the northwest of Morkulltjärnen.

Figure 17. Morkulltjärnen circa 1975. The release point for the tailings is seen in the middle right where a large pile of tailings has formed. Photo: Lantmäteriet

Geophysical investigation of Morkulltjärnen

A geophysical investigation was conducted at Morkulltjärnen where four different methods including ERT, IP, RMT, and tTEM were utilized. The location of the geophysical measurements acquired at Morkulltjärnen are shown in figure 18. The tTEM has a very good coverage over the tailing area except for the north-western part that was very wet and not accessible for the ATV.

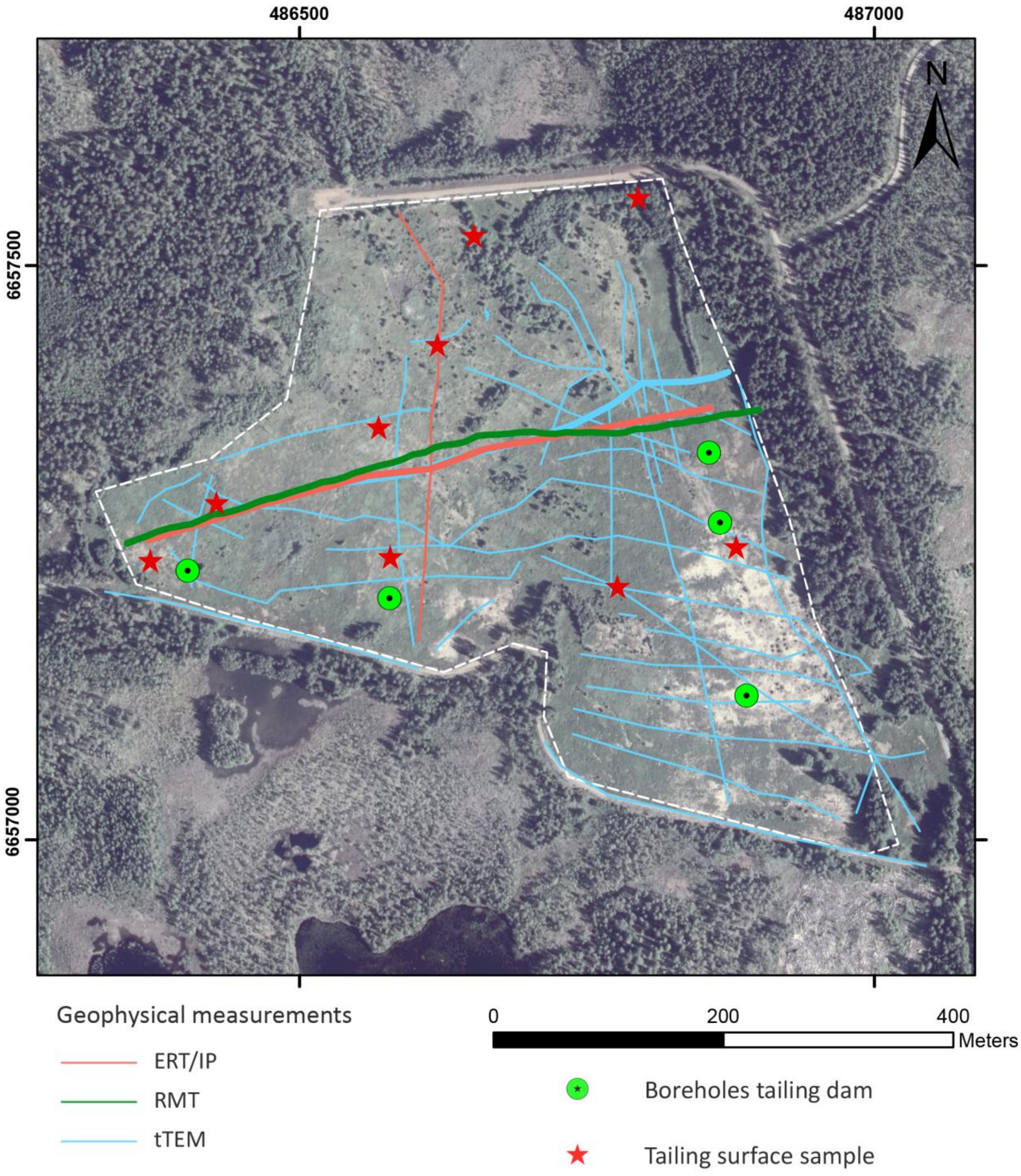

Figure 18. Orthophoto showing Morkulltjärnen tailings dam. The dashed white lines represent the boundary of the tailings. Ground geophysical measurements (lines in different colours), tailings surface samples (red stars), and boreholes (green dots). The thicker lines show the location of the profiles shown in figure 19.

The results from the IP measurements are not shown here but discussed in more detail in (Bastani et al. 2024, in prep.). The resistivity models obtained from the ERT, RMT and tTEM have all been used to determine the extent and depth of the tailings. They generally show quite similar results, however ERT and RMT have higher resolution and larger depth of investigation compared to tTEM.

The resistivity models from ERT, RMT and tTEM along an east-western profile (fig. 19A–C) show generally low resistivities at the top corresponding to the tailings and higher resistivities at the bottom corresponding to lake sediment and bedrock. The resistivity of the tailings varies between 10 and 30 ohmm and the thickness of the tailings is largest in the central part of the profile (10–12 m). The very thin (1–3 m) high resistive layer at the ground surface, present at some parts of the profile, is caused by dry sand.

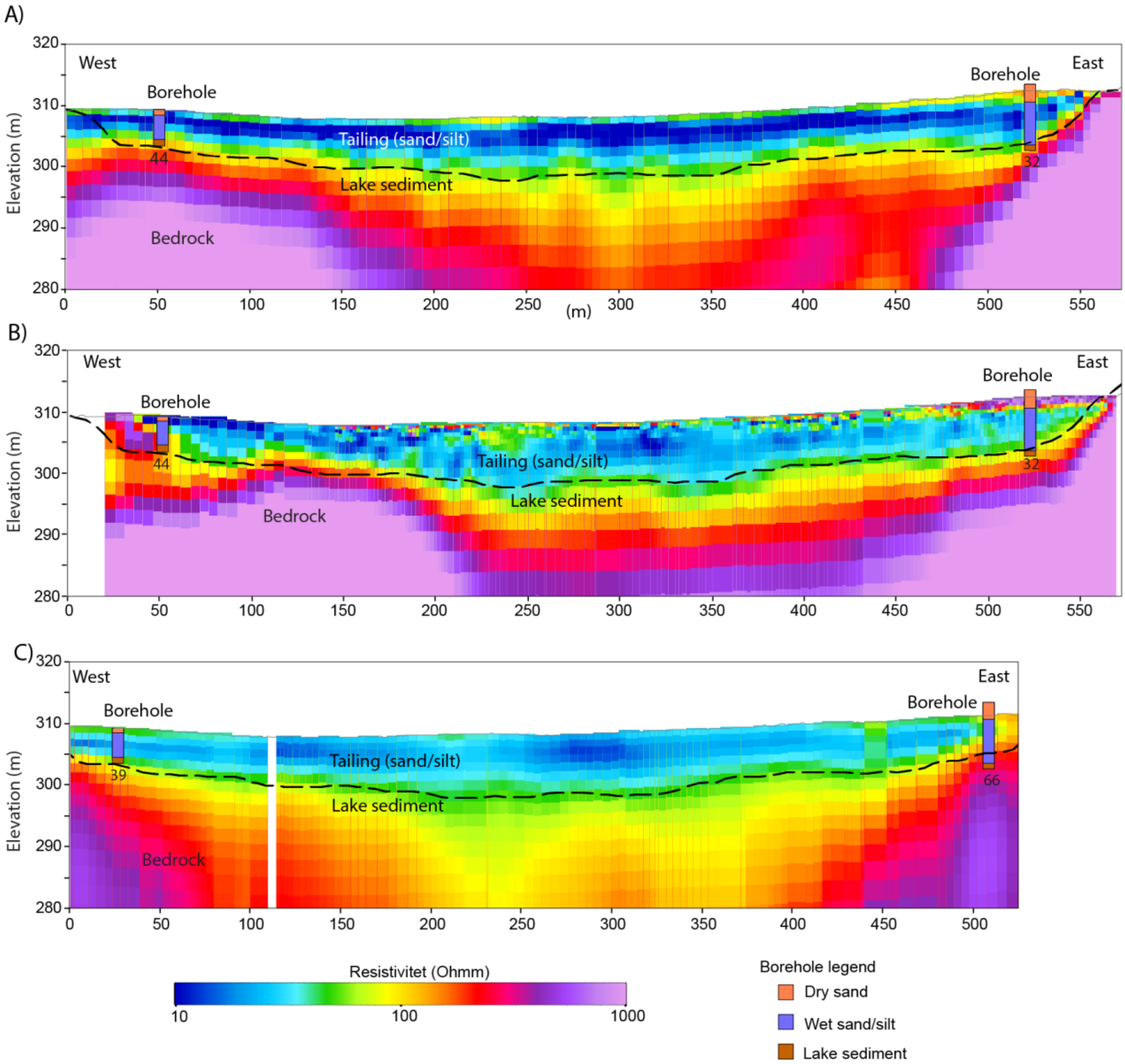

Figure 19. Resistivity models along an east-western profile obtained from three different geophysical methods **A**. RMT, **B.** ERT and **C.** tTEM. The two nearest borelholes are plotted along the profiles and the figures below show their distance from the profile. The black dashed line represents the bottom of the tailings interpreted from geophysical models and drillings. See fig. 18 for the location of the profiles.

The nearest boreholes are performed at a distance of 30 to 60 metres from the profiles and they correlate well with the resistivity models (fig. 18 and 19). The western borehole shows 5 m tailings (1 m dry sand followed by 4 m wet sand and silt) and eastern borehole show 10 m tailings (3 m dry sand followed by 7 m wet sand and silt).

The bottom of the tailings has been interpreted along all profiles and then interpolated to a surface that covers the tailing pond. Figure 20 shows the modelled tailing thickness based on the resistivity models and the five drillings. The thickness varies generally between 5 and 12 metres with the largest depth found in the central part.

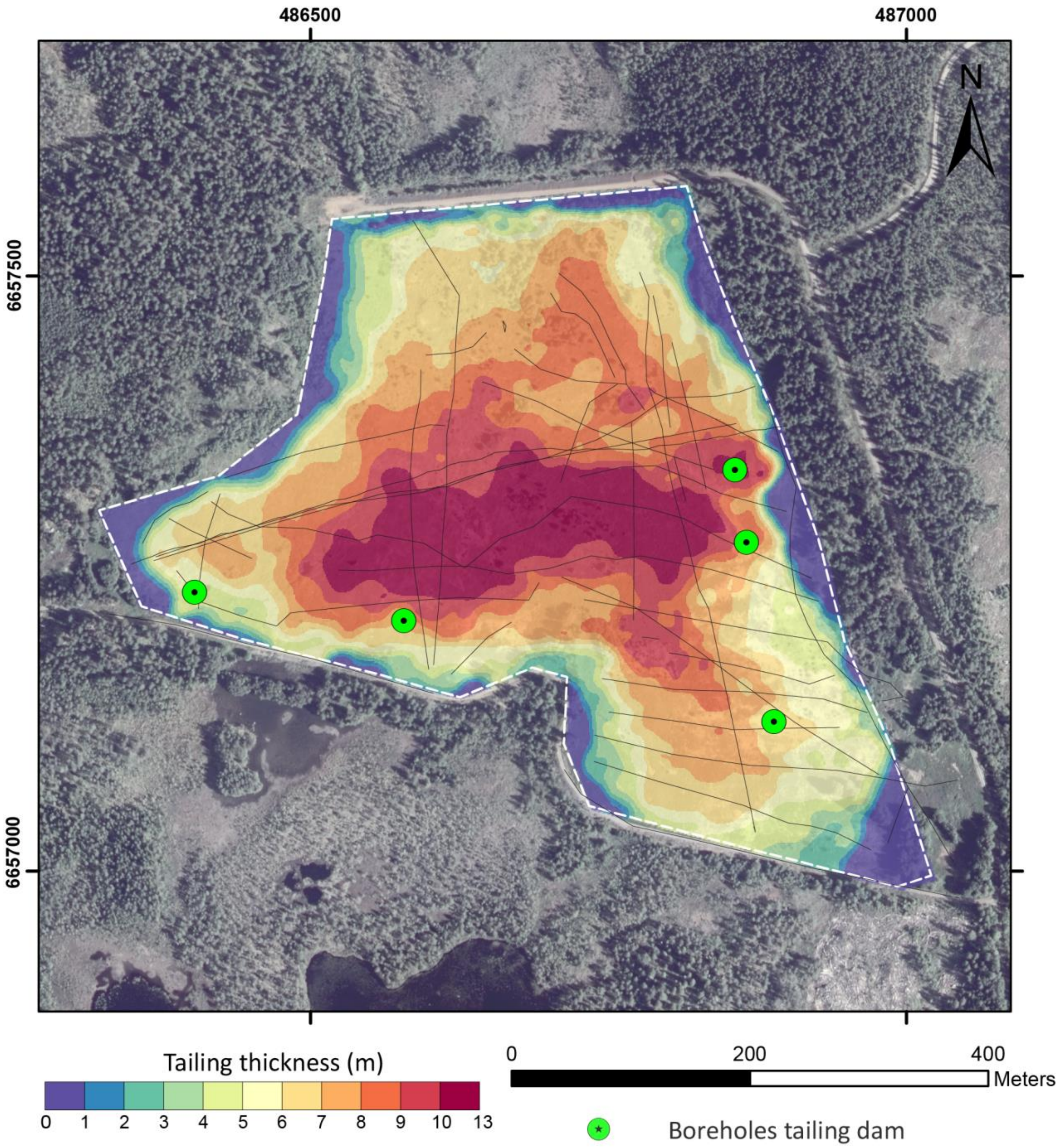

Figure 20. Modelled tailing thickness at Morkulltjärnen, Yxsjöberg based on geophysical measurements and drilling.

Drilling at Yxsjöberg

A total of 5 boreholes were sampled at Morkulltjärnen. The depths were typically between 5–10 metres. At each drill hole a distinct and abrupt change was seen in the tailings once the groundwater level was reached. Above groundwater the tailings were coarse and weathered, showing a strong rust brown colour. Below groundwater level the material was typically silty sand with occasional bands of silt and was light grey in colour.

The average W concentration in tailings at Morkulltjärnen is approximately 1100 ppm (table 7). Prior analyses of W in Smaltjärnen (Hallberg and Reginiussen, 2020) showed higher concentrations than in Morkulltjärnen, which these analyses confirm. This is most likely due to the increase in the recovery rate of W with the introduction of the flotation method. The average concentration of W in the upper tailings at Morkulltjärnen is approximately 75% of the total concentration of tungsten in the raw ore, providing evidence for the estimated recovery from the enrichment process from the refiner. A trend is seen in several of the drill holes of increasing concentration of W near the lowest levels of the tailings, possibly demonstrating the variation in W recover when using the older gravitation method before processing switched to the more effective flotation method. Concentrations of other critical raw material were similar to what was observed in the surface sampling campaign. Fluorine was analysed in the first unoxidized sample from each drill hole, as well as the lowest sample collected. These showed an average of 3.4% F in the tailings, which represents 1.7% average fluorite concentrations within the tailings, assuming no other F-bearing phases. Figure 22 shows a box and whisker plot with the concentrations of CRM within all boreholes sampled at Yxsjöberg. The largest variations occur in Zn and W concentrations.

A sample of separated tailings from Yxsjöberg was analysed using SEM-EDS (fig. 21) to identify the common mineralogy within the tailings. Scheelite and chalcopyrite were abundant in the tailings with small amounts of sphalerite and native bismuth observed. Scheelite typically showed good liberation from gangue minerals.

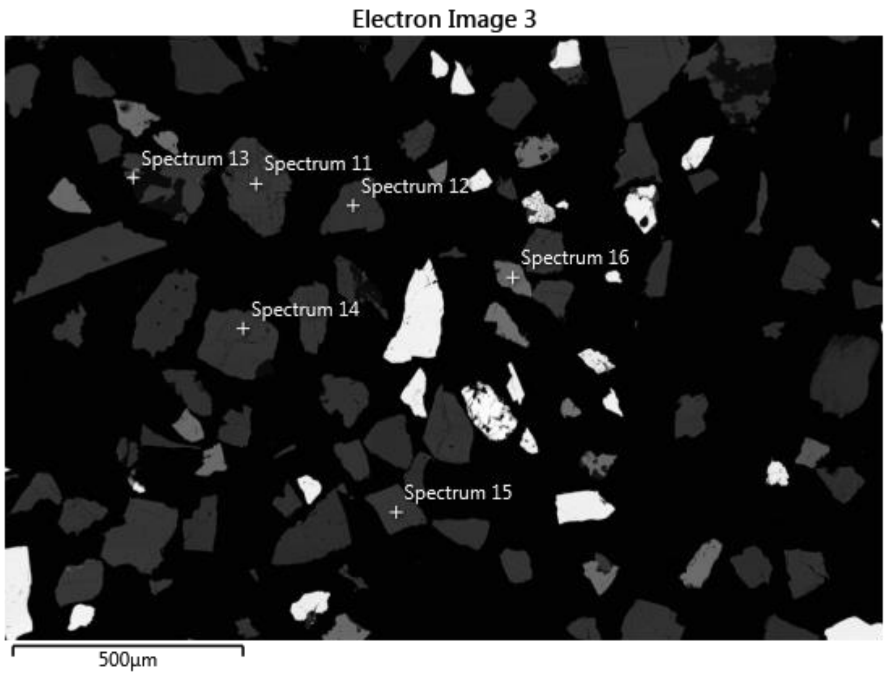

Figure 21. BSE image of tailings from Morkulltjärnen showing their high degree of liberation. Micrograph: Patrick Casey.

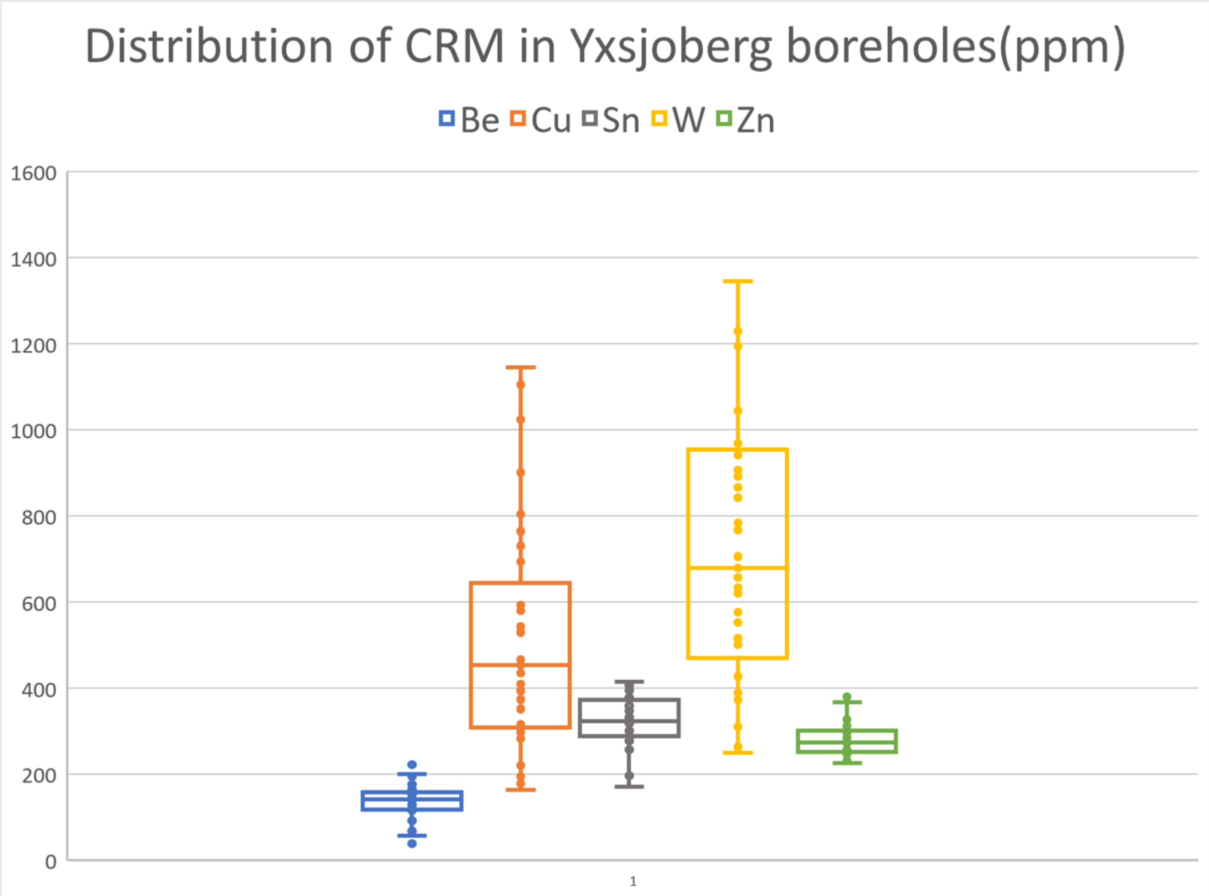

Figure 22. Box and whisker plot showing range of concentrations of CRM in the Yxsjöberg boreholes. Note that extreme outliers for W have been omitted for readability of the plot.

A grain size analysis of two surface samples as well as two samples of drilled tailings were conducted. Distribution of the size of the tailings was towards the finer fractions below 63 µm. Further geochemical analysis was not carried out on these fractions. Sieving of sample PCY210175 from the northwest corner of Morkulltjärnen showed nearly all the material in the northern part of the tailings pond is below 45 µm in size. Due to the fluorescence of scheelite, an estimation of the relative amounts of the mineral in each fraction could be carried out. In each sieved sample, the most concentrated scheelite grains were seen in the <45 µm fraction (fig. 23). This observation, in conjunction with the extremely high values of tungsten observed within surface samples taken in the northern part of Morkulltjärnen where the tailings were dominated by silt indicates that scheelite in the finest fraction was poorly recovered and likely remained in suspension and was carried downslope during release of the tailings into the pond.

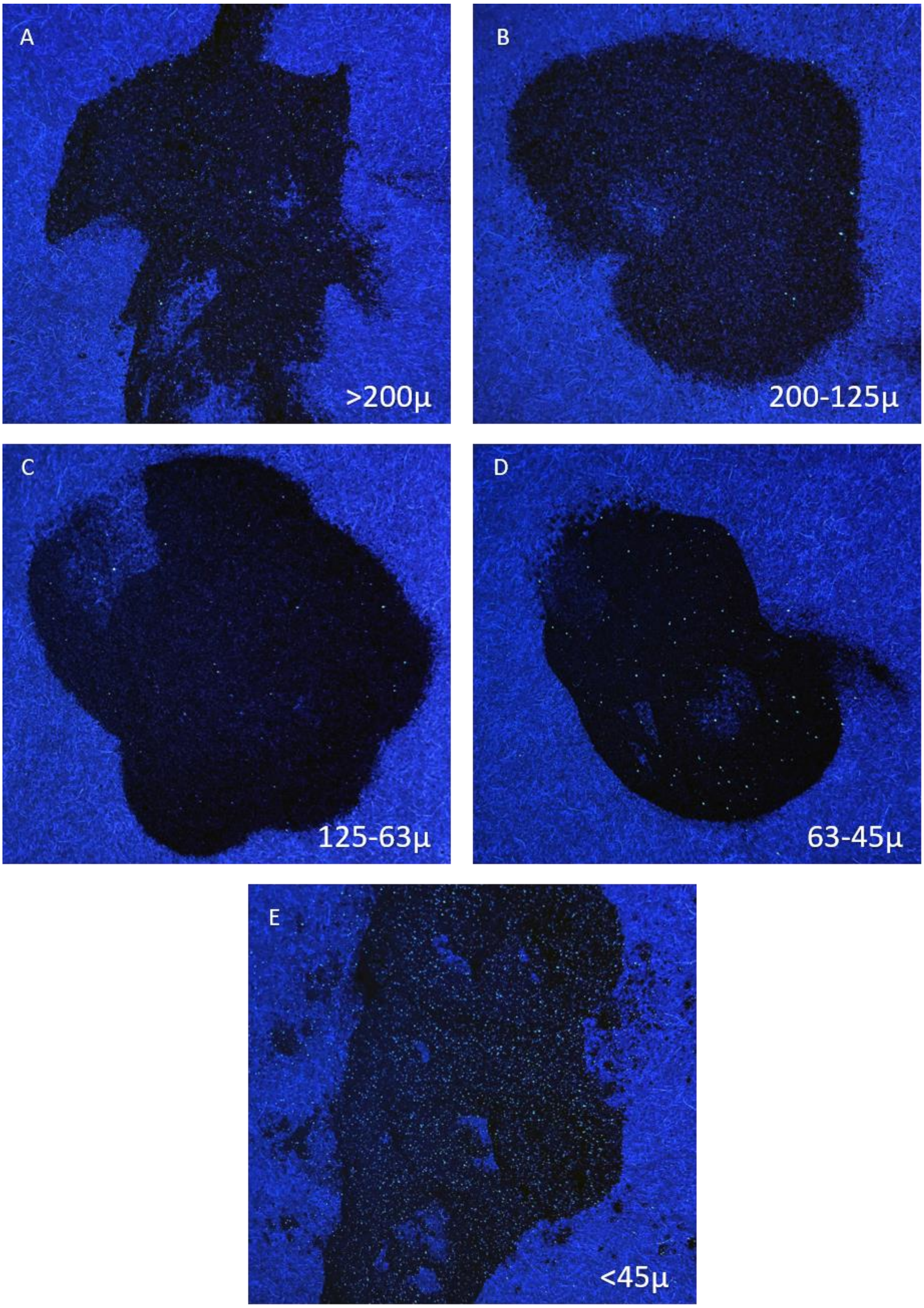

Figure 23. Separations of tailings from Morkulltjärnen under UV light. Scheelite crystals are the bright points within the sand. Photo: Patrick Casey.

Discussion

There is a large spread of W concentrations in the tailings from Morkulltjärnen depending on their location relative to the discharge point identified in historic aerial photos. This is likely due to sediment sorting processes during release of the material into the tailings pond. Scheelite is a heavy mineral with a specific gravity of 6, meaning that it will quickly settle, and not remain in suspension with other sediment thus limiting the range of transport within the tailings pond. Gravity and related downslope processes likely transported some denser material directly downslope of the outflow point. Drilling locations were limited by accessibility of the drill rig on the soft tailings and therefore concentrations of W may be higher further downslope where a W concentration of 2200 ppm was observed in a surface sample. It may prove prudent to conduct drilling during colder temperatures when the surface of the sand is frozen and able to bear the weight of heavy equipment to obtain a better distribution of sample locations and sediment types.

Scheelite fluoresces blue under short wave ultraviolet light; when exposed to UV light, the coarse fraction of the tailings showed a high level of scheelite grains, further demonstrating incomplete recovery (see fig. 23). Mulenshi et al. (2019) conducted mineral liberation analysis on different size fractions of tailings from Smaltjärnen and found that scheelite was typically poorly separated from gangue minerals. Their experiments have shown that finer crushing of the material can lead to increased liberation of scheelite and thus higher recovery percentages from the tailings. Backscatter SEM analysis of tailings from Morkulltjärnen showed a better grade of liberation compared to Smaltjärnen, which could lead to more economical remining.

Beryllium is present in the tailings at Yxsjöberg. Earlier sampling of the tailings at Morkulltjärnen (Hallberg & Reginiussen, 2020) found too wide a spread of Be in the samples to attempt to determine the amount of Be, however the surface sampling and drilling in this project provides average Be concentrations of around 100 ppm. Danalite is the dominant Be bearing mineral at Yxsjöberg. This mineral is not a predominant ore of Be, and as such estimates of recoverability are lacking for Yxsjöberg. Prior analysis of tailings conducted by LTU (Hällström et al., 2018) showed that the easily weathered danalite could only be identified in small amounts using XRD, and thus the Be may occur as free BeO due to the high affinity of Be for oxygen and likely further complicates potential recovery from the tailings.

A strongly oxidised layer was observed during both surface sampling and drilling. This layer was typically between 1–2 metres deep and ended once the ground water level was reached. The easily weathered pyrrhotite was the dominant sulphide mineral observed in thin section at Yxsjöberg. Weathering of pyrrhotite leads to the freeing of H^+ ions, resulting in a lower pH, increasing oxidation in the sediments above groundwater. Prior analysis of tailings (Hällström et al., 2018) at Smaltjärnen showed that there is enrichment in mobile elements at the base of oxidized zone where mobilised elements fell out of solution upon interaction with the more neutral groundwater where pH is buffered by carbonate minerals. Hällström et al. (2018) observed that this oxidation, which in turn freed the highly reactive F from fluorite produced a strong oxidation front that mobilized even typically immobile elements including Al. This strongly oxidised zone presents a risk for groundwater in the area due to the freeing of elements with toxic properties. Indeed, Hällström et al. (2018) found Be contamination in groundwater in the Yxsjöberg area to be the highest measured in the world, and suggested remining of the tailings as a potential method of reducing the environmental impact.

Table 7. Analytical results of tailings from Morkulltjärnen.

Data	Object	W (ppm)	Cu (ppm)	Zn (ppm)	Be (ppm)	Sn (ppm)	Bi (ppm)
Surface Sampling (n=9)	Morkulltjärnen Mean	1154	426	276	101	212	323
	Max	4090	939	312	125.5	250	455
	Min	312	153	200	79.8	186	212
Drilled Samples (n=44)	Morkulltjärnen Mean	844	476	274	134	215	503
	Max	3320	1145	380	223	320	1010
	Min	250	113	204	39.3	75	143

Potential resources at Yxsjöberg

Based on the assumption that no waste rock has been removed from Yxsjöberg the potential resources are 442 tonnes of W, 168 tonnes of Cu, 75 tonnes Bi, 64 tonnes Sn and 29 tonnes Be.

Based on the depth model in fig. 20 the estimated total volume of the tailings in Morkulltjärnen is approximatively 1.4×10^6 m^3. Using the average density of 1.6 ton/m^3 results in a total mass of 2.2 Mt of tailing which is in agreement with the historical production data of 2.43 Mt as an unknown quantity of tailings was used as back fill in the mine.

Based on the geochemical analyses and production data combined with the geophysical model of Morkulltjärnen, the tailings potentially contain approximately 1900 tonnes of W, 1000 tonnes Bi, 1000 tonnes Cu, 710 tonnes Sn, 600 tonnes Zn, 284 tonnes Be and 8 tonnes In. From the limited analyses of F, a potential 55000 tons are contained within the tailings.

Wigströmsgruvan

Background

Wigströmsgruvan (Sweref 6648189/499465) lies within the Yxsjöberg W-mineralisation field just west of Högfors in Örebro county (fig. 24). W mineralisation occurs in skarn-altered carbonate bodies in a within the supracrustal intermediate to felsic metavolcanic rock typical to Bergslagen. The skarn mineralisation occurred in relation to the emplacement of an intrusive body towards the end of the Svecokarelian orogeny in relation to the GP suite, likely coeval with the formation of the Yxsjöberg mineralisation. Tungsten mineralisation at Wigströmsgruvan occurs as scheelite ($CaWO_4$) and fluorite mineralisation is closely associated with the W mineralisation (AB Statsgruvor, 1983).

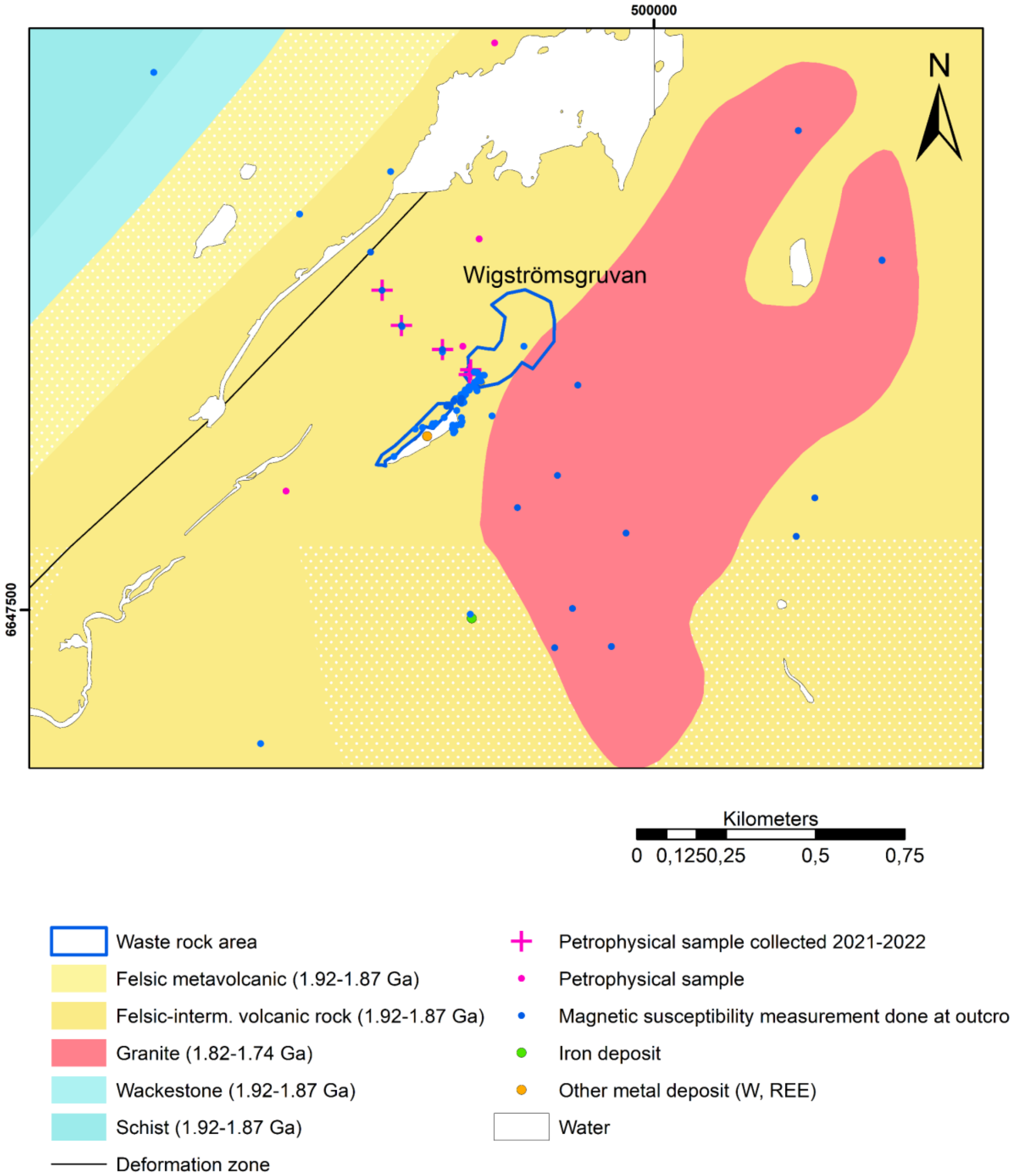

Figure 24. Bedrock map of area surrounding Wigströmsgruvan.

Production at Wigströmsgruvan began in 1978 as a complement to W production at Yxsjöberg, and material was transported there for refinement. The total ore extracted is shown in table 8, totalling approximately 0.13 Mt before mining operations ceased in 1981. Approximately 0.21 Mt of waste rock were produced during the short production period (AB Statsgruvor, 1983).

Waste rock observed at Wigströmsgruvan can be divided into two dominant types: skarn dominant waste rock near the northern end of the mine, where ore was loaded into trucks for transport to Yxsjöberg. A large portion of waste rock was used to construct a graded road from the base of the southern end of the mine to the northern end. The metavolcanic rock was the dominant waste rock used for building the graded road and was less accessible for sampling.

Table 8. Production statistics from Wigströmsgruvan.

	Total (Mt)	W (%)	CaF_2 (%)
Mined Ore	0.13	0.46	5.88
Waste-rock	0.21		

Available geophysical data for the Högfors district

Due to the close proximity of the 4 mines near Högfors studied in this report, i.e. Wigströmsgruvan, Ställberg, Mossgruvan and Basttjärn, the available geophysical data for all of these mines are presented together in this section. However, please note that the new investigations of the secondary resources for the Högförs Fe mines (i.e. Ställberg, Mossgruvan and Basttjärn) are presented later in the report in the chapter called "The Högfors district Fe mines".

Airborne data (magnetic, VLF, gamma spectrometry)

The oldest airborne surveys for the area shown in figure 25 were performed in 1969, 1972 and 1973 by SGU. For most of the area shown in figure 25 only magnetic and natural gamma spectrometry measurements were made, however in the 1973 survey VLF (1 transmitter) measurements were also collected, which cover a small part in the southwest of the map area. In 2016 and 2017, SGU performed modern airborne magnetic, natural gamma and VLF (2 transmitters) measurements over the area shown in figure 25. The acquisition parameters for the different airborne surveys collected over the area in figure 25 are shown in table 9.

A map of the residual magnetic intensity calculated using data from SGU's 2016 and 2017 measurements is shown in figure 25. Here it can be observed that the majority of the positive magnetic anomalies are associated with Fe-mineralisation, which lies predominantly within areas dominated by felsic metavolcanic rocks and is often associated with local carbonate or calc-silicate layers. In this area strong positive magnetic anomalies are not associated with older mafic rocks. However, younger dolerite dikes which crosscut the map area (with a northwest-southeast strike), predominantly on the eastern side of the map, are associated with clear albeit relatively weak positive magnetic anomalies. This is consistent with petrophysical measurements performed by Bergman et al. (2020), which show that the magnetic susceptibilities of the more recent diabase dikes are about an order of magnitude higher than those of the older mafic rocks. The older mafic rocks have in turn similar average magnetic susceptibilities to the granitic rocks in this area.

The mineralisation at both the Basttjärnsfältet and Ställbergs- Haggruvefälten is similar and can be described as manganese rich Fe-mineralisation (Magnusson, 1940). At both locations mineralisation occurs within a series of skarn layers interlayered with felsic metavolcanic rocks. Within both deposits the dominant ore mineral is magnetite (Magnusson, 1940), which likely gives rise to the strong magnetic anomaly observed at these deposits (fig. 25). A notable magnetic anomaly is not observed at Wigströmsgruvan. Here the main ore mineral is scheelite but molybdenite and fluorite also occur locally (Bergman et al., 2020). Hence, the lack of magnetic anomaly at Wigströmsgruvan is somewhat expected due to the lack of minerals with a high magnetic susceptibility. This is also consistent with petrophysical samples collected from Wigströmsgruvan as part of this study. These samples show that the mineralisation and surrounding felsic metavolcanic rock both have similar magnetic susceptibilities.

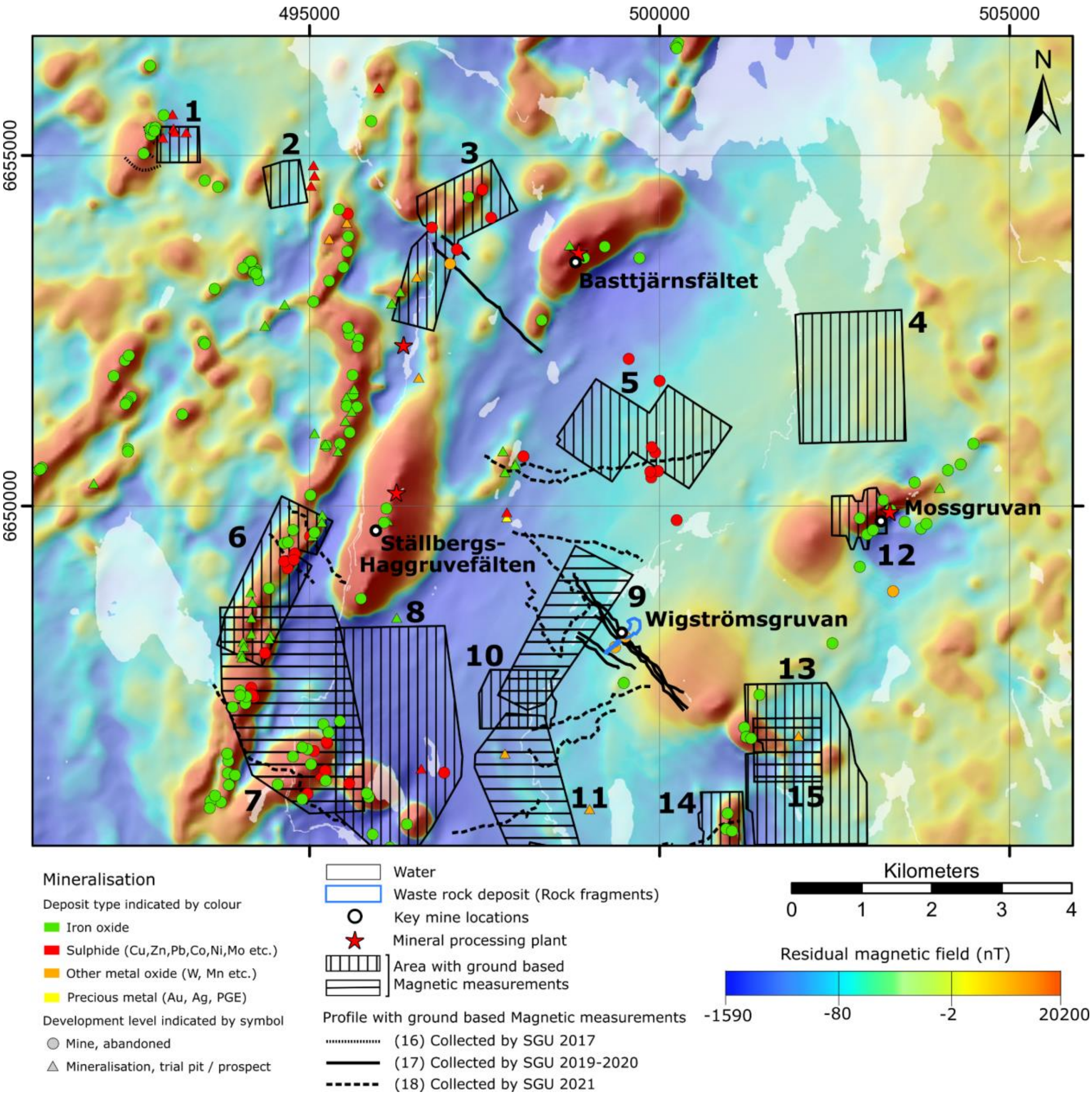

Figure 25. Map of residual magnetic field for the area around Basttjärnsfältet, Mossgruvan, Wigströmsgruvan and Ställbergs-Haggruvefälten. The location of ground-based magnetic measurements, listed in table 10 is shown. Note that profile measurements collected by SGU are grouped into 3 groups and shown with different line symbols. The number shown in the legend for each group of lines corresponds to the numbers in table 10.

Table 9. Complete list of airborne geophysical surveys performed in the area around Basttjärnsfältet, Mossgruvan, Wigströmsgruvan and Ställbergs-Haggruvefälten. Unless otherwise stated all data are collected using a small, manned aeroplane.

Year	Organisation	Geophysical methods used	Area (SGU map sheet)	Flight direction (degrees)	Flight line separation (m)	Flight altitude (m)
1969*	SGU	Magnetics, gamma spectrometry	11F	East–West (90°)	200	30
1972*	SGU	Magnetics, gamma spectrometry	Part of 12E and 12F	East–West (90°)	200	30
1973*	SGU	Magnetics, gamma spectrometry, VLF (1 transmitter)	11E	East–West (90°)	200	30
2016	SGU	Magnetics, gamma spectrometry, VLF (2 transmitter)	Part of 13F,13G, 12E, 12F, 12G, 12H, 11E, 11F, 11G and 11H	Northwest – Southeast (130°)	200	60
2017	SGU	Magnetics, gamma spectrometry, VLF (2 transmitter)	Part of 12E, 12F, 11E, 11F, 10E and 10F	Northwest – Southeast (130°)	200	60

* Not used for producing maps in this report.

Figure 26 shows a map of the apparent resistivity calculated from airborne VLF data collected in 2016 and 2017 for the area around Basttjärnsfältet, Mossgruvan, Ställbergs- Haggruvefälten and Wigströmsgruvan. Several low resistivity features can be observed some of which can be discarded as they are due to manmade structures such as powerlines and railways. However, a series of low resistivity features with an approximately northeast – southwest strike can be interpreted as deformation zones. One of these zones lies to the north of Wigströmsgruvan and several more to the east and southeast of it.

Ground-based EM, magnetic and IP measurements

Relatively large amounts of ground geophysical measurement data are available in SGU's database for the area around Basttjärnsfältet, Mossgruvan, Wigströmsgruvan and Ställbergs-Haggruvefälten (fig. 25; table 10). A total of 15 surveys have been performed over areas ranging in size from between approximately 0.3 km^2 and 5 km^2. These surveys can be split into two groups. The first group are those with a name beginning with "mgtmid" (see table 10) which were collected between 1977 and 1988. These represent older prospecting activities which have recently been digitized by SGU, often from analogue maps. The other group of surveys was collected as part of commercial prospecting activities between 2007 and 2014, predominantly by Kopparberg Mining Exploration AB. In recent years, a series of ground magnetic profiles have been collected in this area by SGU as part of various bedrock mapping projects. Profiles from one project are grouped and displayed with the same symbology on the map (fig. 25). The first group of profiles were collected in 2017 close to Pingstaberg (Ripa and Antal Lundin, 2020). Another group of profiles were collected between 2019 and 2020 as part of an investigation of W-Mo mineralisation associated with GP granites in Bergslagen (Bergman et al., 2020). Finally, additional profiles were collected as part of the Bergslagen etapp 3 bedrock project (Ripa and Brolin, 2022).

Table 10. Ground-based magnetic measurements for the area around Basttjärnsfältet, Mossgruvan, Wigströmsgruvan and Ställbergs-Haggruvefälten. Numbers correspond to the numbered polygons/lines shown in figure 25. Note that the numbers 16, 17 and 18 refer to groups of lines described in the figure and legend in figure 25.

Polygon/Line number and name	Method	Year acquired	Responsible	Comments
1.mgtmid1550	Magnetic	1979		Profile spacing of 20 m.
2.mgtmid216	Magnetic			Profile spacing of 50 m.
3.mgtmid363 – mgtmid371	Magnetic	1977		Profile spacing of 40 m.
4.mgtmid851	Magnetic	1977		Profile spacing of 80 m to 40 m.
5. Högfors nr 100	Magnetic	2007	Kopparberg Mining Exploration AB	Profile spacing of 50 m.
6. Kumla nr 100	Magnetic	2007	Kopparberg Mining Exploration AB	Profile spacing of 100 m.
7. mgtmid1001	Magnetic	1985		Profile spacing of 80 m
8. mgtmid996	Magnetic	1988		Profile spacing of between 40 m and 160 m
9. mgtmid1216	Magnetic	1986		Profile spacing of between 100 m and 200 m
10. Silverhöjden nr 200 (Båtberget)	Magnetic	2008	Kopparberg Mining Exploration AB	Profile spacing of 50 m.
11. mgtmid882	Magnetic	1986		Profile spacing of between 20 m and 200 m
12. Rundberget nr 3	Magnetic	2011–2014	Nordic Fe Ore AB	Profile spacing of between 50 m and 100 m
13. Utanheden nr 2	Magnetic	2009–2012	Kopparberg Mining Exploration AB	Profile spacing of 100 m.
14. Olovsgruvan nr 2	Magnetic	2009–2012	Kopparberg Mining Exploration AB	Profile spacing of 80 m
15. mgtmid1795	Magnetic	1982		Profile spacing of 80 m
16. MP17ILA0001 – MP17ILA0005	Magnetic	2017	SGU	
17. Several profiles collected by RBN	Magnetic	2019–2020	SGU	Profiles collected as part of Bergslagen etapp 2 project.
18. Several profiles collected by CJO	Magnetic	2021	SGU	Profiles collected as part of Bergslagen etapp 3 project.

The ground-based electromagnetic and IP measurements which are available in the SGU database for the area around Basttjärnsfältet, Mossgruvan, Wigströmsgruvan and Ställbergs-Haggruvefälten are shown in figure 26 and summarised in table 11. Within this area a total of 13 surveys which vary in size have been performed. The surveys include a series of older measurements, collected before 1990. These surveys (with names beginning with "mgtmid") are slingram measurements which have recently been digitized from analogue maps within SGUs archive. The more recent surveys have been collected as part of prospecting activities by Boliden Mineral AB and Kopparberg Mining Exploration AB and include IP, slingram and TEM measurements. Finally, a series of ground-based VLF profiles have been collected by SGU as part of several bedrock geology projects (Bergman et al., 2020; Ripa and Brolin, 2022).

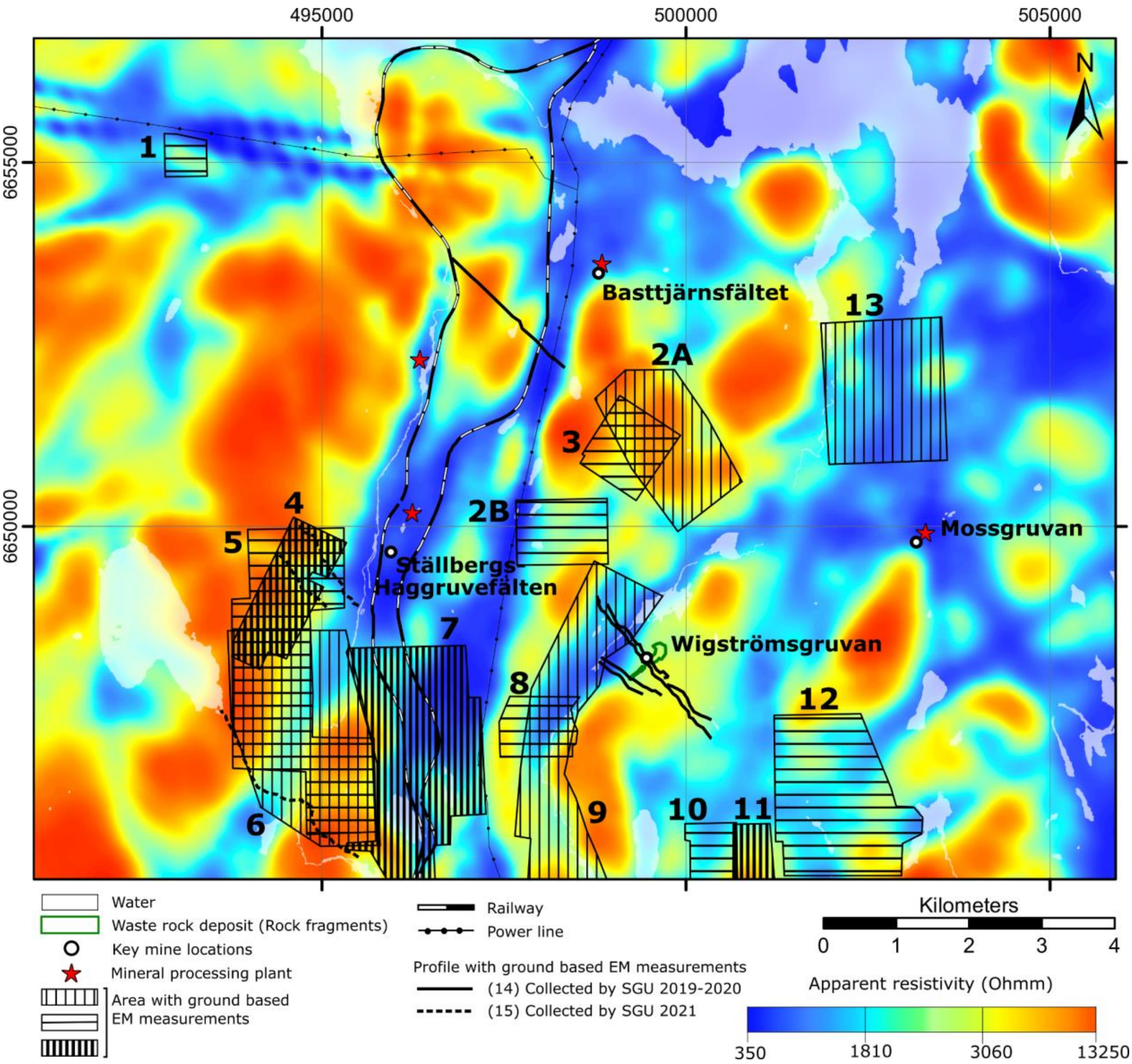

Figure 26. Map of apparent resistivity derived from airborne VLF data collected between 2016 and 2017 for the area around Basttjärnsfältet, Mossgruvan, Wigströmsgruvan and Ställbergs-Haggruvefälten. The location of ground-based electromagnetic and IP measurements, listed in table 11 is shown. Note that profile measurements collected by SGU are grouped into 2 groups and shown with different line symbols. The number shown in the legend for each group of lines corresponds to the numbers in table 11.

Table 11. Ground-based electromagnetic and IP measurements for the area around Basttjärnsfältet, Mossgruvan, Wigströmsgruvan and Ställbergs-Haggruvefälten. Numbers correspond to the numbered polygons/lines shown in figure 26. Note that the numbers 14 and 15 refer to groups of lines described in the figure and legend in figure 26.

Polygon/Line number and name	Method	Year acquired	Responsible	Comments
1. mgtmid4136 and mgtmid4137	Slingram, SR 18kHz	1979		Profile spacing of 40 to 20 m.
2A and 2B. Ställdalen nr 1004	TEM	2001	Boliden Mineral AB	Profile spacing of 200 m.
3. Högfors nr 100	IP	2007	Kopparberg Mining Exploration AB	Profile spacing of between 50 m and 100 m.

Table 11. Continuation.

Polygon/Line number and name	Method	Year acquired	Responsible	Comments
4. Kumla nr 100	IP	2006–2010	Kopparberg Mining Exploration AB	Profile spacing of 100 m.
5. Ställdalen nr 1006	TEM	2001	Boliden Mineral AB	Profile spacing of between 100 and 200 m.
6. mgtmid3243	Slingram, SR 18kHz	1985		Profile spacing of 80 m.
7. mgtmid4855, mgtmid5203	Slingram			Profile spacing of between 80 and 160 m.
8. Silverhöjden nr 200 (Båtberget)	IP	2008	Kopparberg Mining Exploration AB	Profile spacing of 50 m.
9. mgtmid4801, mgtmid4943, mgtmid5149	Slingram			Profile spacing of between 100 and 200 m.
10. Laxbro nr 2 and 3	Slingram	2007–2013	Kopparberg Mining Exploration AB	Profile spacing of 80 m.
11. Olovsgruvan nr 2	Slingram	2009–2012	Kopparberg Mining Exploration AB	Profile spacing of 80 m
12. Utanheden nr 2	Slingram	2009–2012	Kopparberg Mining Exploration AB	Profile spacing of 100 m.
13. mgtmid4874, mgtmid5220	Slingram			Profile spacing of between 40 and 80 m.
14. Several profiles collected by RBN	VLF	2019–2020	SGU	Profiles collected as part of Bergslagen etapp 2 project.
15. Several profiles collected by CJO	VLF	2021	SGU	Profiles collected as part of Bergslagen etapp 3 project.

Ground-based gravity

Figure 27 shows a map of the residual gravity anomaly for the area around Basttjärnsfältet, Mossgruvan, Wigströmsgruvan and Ställbergs-Haggruvefälten. The figure also shows the location of the gravity measurements used to generate the residual anomaly map. As part of this project 87 new gravity measurements were collected in this area, which are highlighted in the figure. The spacing between measurement sites is somewhat variable across the map, where it is highest in the northeast and southwest corners of the map (about 1–2 km between measurements). Within the central and north-western parts of the map the spacing between points is relatively small, about 150–300 metres between points along roads.

A series of clear, positive gravity anomalies with an approximately northeast – southwest strike, can be observed in the central and southwestern parts of the map area (fig. 27). The westernmost of these positive anomalies correlates strongly with the linear zone of Fe and sulphide mineralisation associated with carbonate and calc-silicate rocks within the felsic metavolcanic sequence. This positive gravity anomaly also correlates with a strong magnetic anomaly which can be seen in figure 25. It is possible that this positive gravity anomaly is associated with the carbonate / calc-silicate rocks and associated mineralisation, as these rocks tend to have higher densities than the surrounding extrusive and intrusive felsic rocks (based on inspection of petrophysical data in SGUs database). Another potential explanation for this positive gravity anomaly is that it is related to mafic rocks at depth. A series of mafic dikes can be observed approximately 1 km west of the westernmost positive gravity anomaly (figs. 27 and 28), which could be indicative of a larger mafic body at depth. The positive gravity anomaly at Yxsjöberg, which lies to the northwest of this area, has previously been attributed to mafic rocks at depth

(Ripa and Antal Lundin, 2020). The easternmost of these positive gravity anomalies with a northeast – southwest strike coincides with a region mapped as metasedimentary rocks (fig. 28). On inspection of the available petrophysical data, this predominantly mica rich metashale has a higher average density than the surrounding felsic rocks (Bergman et al., 2020). Hence, it is likely that this anomaly is associated, at least partially, with this region of metasedimentary rocks.

A series of negative residual gravity anomalies can be observed in figure 27 which are likely associated with granites which have been mapped in these areas and typically have relatively low densities. Notably, these negative anomalies are observed to the east of Wigströmsgruvan and Basttjärnsfältet and in the northwest corner of the map area, at Pingstaberg. At the Basttjärnsfältet, there is a small but clear positive anomaly, which is most likely related to the mineralisation and skarn rocks in the deposit.

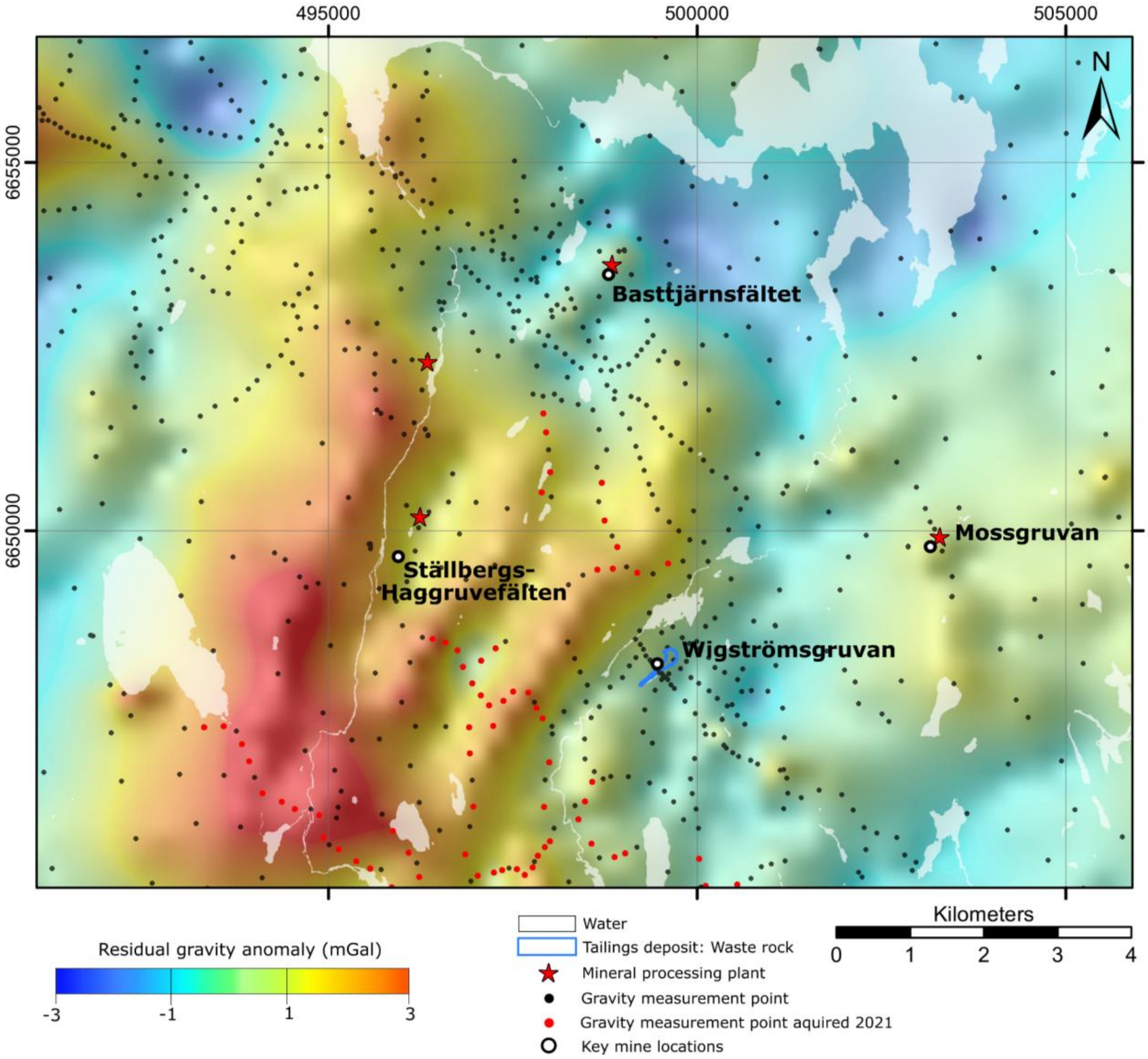

Figure 27. Map of the residual gravity anomaly for the area around Basttjärnsfältet, Mossgruvan, Wigströmsgruvan and Ställbergs-Haggruvefälten. Pre-existing and new gravity measurements are annotated as black and red dots, respectively.

Petrophysical data

Figure 28 shows the petrophysical data available for the area around Basttjärnsfältet, Mossgruvan, Wigströmsgruvan and Ställbergs-Haggruvefälten. The location of magnetic susceptibility measurements from outcrops are also shown. New measurements collected as part of this project and other ongoing projects at SGU (Ripa and Brolin, 2022) are highlighted. As a result of these new samples relatively large amounts of petrophysical data are available for the different rocks in this area. Some average petrophysical data for the different rocks in this area are summarised by Bergman et al. (2020). As part of this project two additional samples of mineralisation and surrounding felsic rocks were taken in the Wigströmsgruvan area. Data for these samples are shown in table 12.

A total of 78 boreholes are registered in SGU's database for the area shown in figure 28. These were drilled between 1961 and 2008. 32 of these wells are in the vicinity of Wigströmsgruvan and were drilled by AB Statsgruvor and LKAB prospecting between 1976 and 1978.

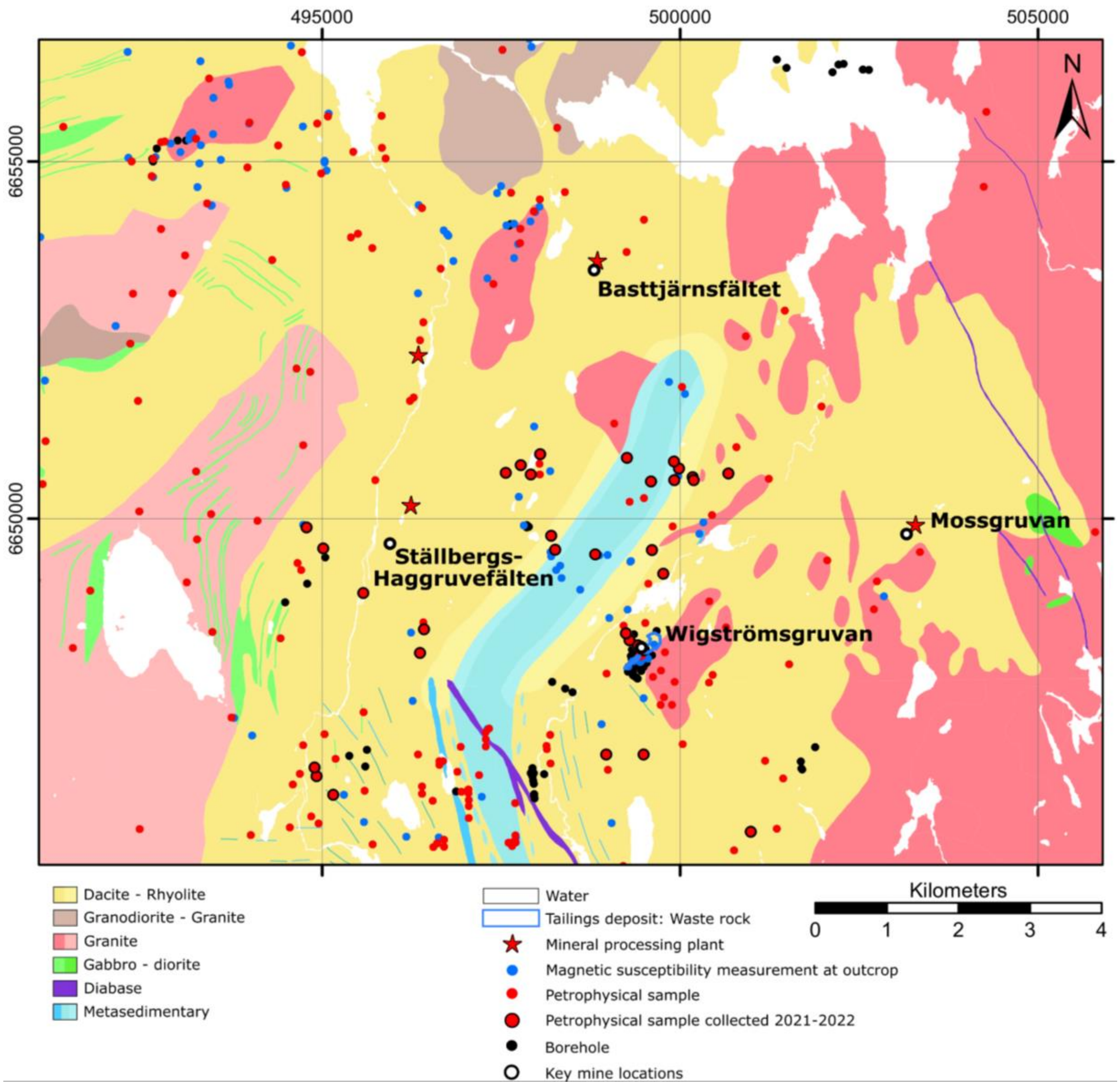

Figure 28. Map of the petrophysical data for the area around Basttjärnsfältet, Mossgruvan, Wigströmsgruvan and Ställbergs-Haggruvefälten.

Table 12. Table summarising the petrophysical results collected as part of this project from the area around Basttjärnsfältet, Mossgruvan, Wigströmsgruvan and Ställbergs-Haggruvefälten.

Sample ID	Easting (m)	Northing (m)	Description	Density (kg/m3)	Magnetic susceptibility (10-6 SI)	J (mA/m)
PCY210090C	499487	6648173	Felsic volcanic	2663	150	52
PCY210091B	499483	6648160	Skarn with W mineralisation	3486	1011	27

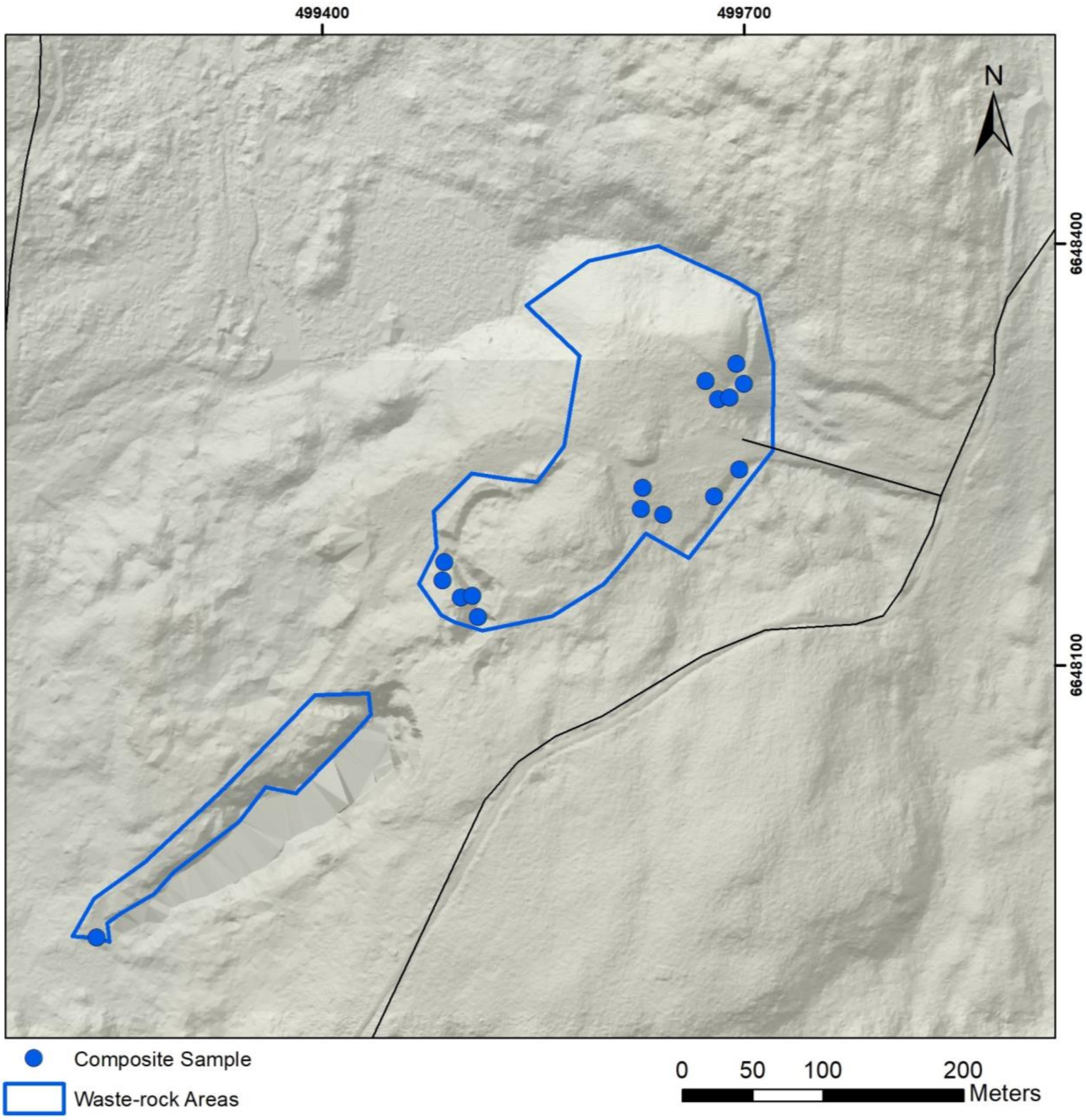

Figure 29. LiDAR image showing the extent of waste rock and sampling points at Wigströmsgruvan.

Sampling of waste rock at Wigströmsgruvan

A total of 16 composite samples of waste rock were collected at Wigströmsgruvan. Five samples were collected near the smaller, northern mine pit, 10 near what was interpreted as the loading area for the ore, and a single sample was collected from the graded road constructed from waste rock (fig. 29). Waste rock piles at Wigströmsgruva were typically moderately to heavily vegetated (fig. 30). Samples collected from the edge of the mine were predominantly metavolcanic rock with some fluorite rich skarn. Waste rock from the loading zone was predominantly skarn mineralisation and contained the highest levels of W, while the sample collected from the graded road material showed only trace amounts of W, confirming observations that much of the rock in that area is the country rock. The composite samples showed an average W content of 443 ppm, and molybdenum contents of 18 ppm. Slightly elevated levels of Bi, Zn, Nb, Ga and Be were also observed in the waste rock samples.

A richly mineralised specimen of skarn, and a Mo-mineralised specimen of metavolcanic rock were collected for further geochemical investigation and optical and electron microscopy. The mineralised sample was dominated by prehnite, garnet and fluorite with minor scheelite (fig. 31). Minor amounts of native bismuth were observed during SEM analysis. The metavolcanic Mo-mineralised specimen was quartz dominated with a brecciated texture. Molybdenite was observed as fracture fill, and not within the breccia, indicating a late-stage mineralisation common to Mo deposits found in Bergslagen.

Figure 30. Waste rock at Wigströmsgruvan. Photo: Patrick Casey

Scheelite forms a solid solution series with powellite ($CaMoO_4$) where Mo can contribute with up to 50% of the cations. Based on EDS analysis, scheelite at Wigströmsgruvan can contain approximately 3% Mo. Scheelite fluoresces bright blue under shortwave UV light, while small impurities of Mo cause a white/yellow to green fluorescence. Figure 32 shows scheelite from Wigströmsgruvan demonstrating numerous shades of fluorescence indicating varying amounts of Mo in the scheelite, from blue (0% Mo) to green (~3% Mo). Molybdenum mineralisation in Bergslagen commonly occurs within granite bodies from the GP suite, indicating the intrusive body at Wigströmsgruvan was the likely source of Mo.

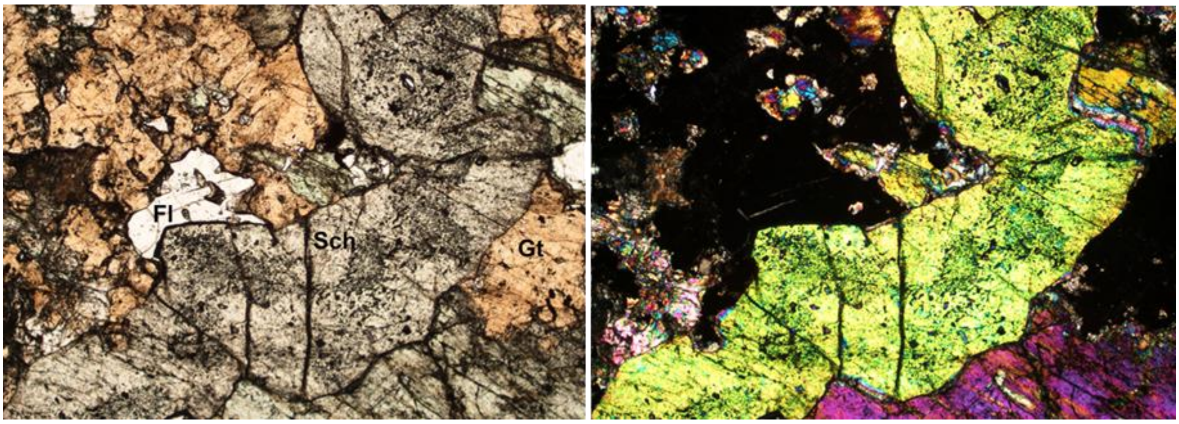

Figure 31. Scheelite crystal under XPL and PPL with garnet, fluorite and prehnite. Micrograph: Patrick Casey.

Figure 32. Richly mineralised skarn sample from Wigströmsgruvan under shortwave UV light showing the fluorescence of scheelite. Green = Mo rich, blue = Mo poor. Photo: Patrick Casey.

Table 13. Analysis of waste rock from Wigströmsgruvan.

Data	Object		W (ppm)	Zn (ppm)	Ga (ppm)	Nb (ppm)	Bi (ppm)	Mo (ppm)
Mineralised sample	W-skarn		850	662	10	4.1	71.7	27
Mineralised sample	Metavolcanic-Mo sulphide		6	14	29	32.7	68.5	4110
Composite samples (n=16)	Wigströmsgruvan	Mean	507	196	25.5	17.7	29.4	18.8
		Max	1610	421	23.3	11	1.67	3.8
		Min	68	89	31.4	26.4	70.9	27.9
EDS analysis	Scheelite Crystal		97.35% $CaWO_4$					2.65% $CaMoO_4$

Potential resources at Wigströmsgruvan

Based on the estimates of extracted waste rock data taken from MALMdb, and with the assumption that no waste rock has been removed from the site, using the data shown in table 13 it is estimated that Wigströmsgruvan may hold up to 128 tonnes of W, 125 tonnes of Zn and 4.5 tonnes of Nb within the waste rock.

FE OXIDE DEPOSITS

Grängesberg

Background

The Grängesberg Kiruna type Fe-oxide-apatite (IOA) deposit (Sweref 6660665/499847) represents the largest ore mineralisation in Bergslagen. The mines in Grängesberg were in operation during the intervals 1783–1789, 1791–1796, 1799–1881, 1883–1885, 1887–1989. Large scale mining of the IOA ores in Bergslagen did not begin until the later part of the 19th century when the Thompson process enabled efficient removal of phosphorus from Fe ore, as phosphorus contamination in steel leads to a brittle product. Mining was conducted at two fields (fält in Swedish), Exportfältet to the south of the mining area, and Risbergsfältet to the north, with Exportfältet producing the largest quantities of ore.

The mode of Fe mineralisation at Grängesberg, and indeed other IOA deposits like Kiruna-Malmberget are still debated, however an orthomagmatic process is typically invoked, and subsequent enrichment of Fe by metamorphic driven hydrothermal processes is discounted (Weis et al., 2022). Magnetite is the dominant Fe-oxide mineral at Grängesberg, although minor hematite occurs. Hematite mineralisation is dominant nearer to the structural footwall of the ore body. Fluorapatite is an important constituent of the deposit, with average P contents in drill cores of 4–5% (Hallberg and Reginiussen, 2020). Enrichment in LREE is typically observed in IOA deposits due tendency of LREE to remain in the melt and the propensity of the lanthanide elements to be enriched in phosphate minerals.

Much of the ore was lump ore and not concentrated further before smelting. Less rich ore was processed into tailings at two major concentrators. Tailings were originally deposited to the south of Exportfältet from smaller concentrators in operation through 1953, producing around 1 Mt of tailings. Two larger concentrators were built starting in the early 1950s and operating through the 1960s. The two major concentrators were Bergslagsschaktet processing ore at Risbergsfältet, and Södra verket processing ore from Exportfältet which was located to the southwest of Exportfältet. In the late 1960s, deposition of tailings shifted to two new tailings ponds, Svandammen which received tailings from Bergslagsschaktet, and Hötjärnen which received tailings from Södra verket (Fig. 33). The deposition of waste rock occurred predominantly at Exportfältet and just north of the open mine pit at Risbergsfältet.

The main mining areas at Grängesberg were the Exportfältet and Risbergsfältet where 132.8 and 20.36 Mt of ore, respectively, were mined to 650 metres below the surface. Recent estimates show that the ore extends to 1700 metres below surface level (Grängesberg Fe, 2014) and a confirmed remaining ore estimate of 33 Mt confirmed ore with Fe contents of 42.5% and phosphorus contents of 0.98%, and an inferred estimate of 115 Mt grading 40% Fe and 0.7% P (table 14). Previous work on mine waste at Grängesberg by SGU focused predominantly on the tailings repositories, and no previous analysis of waste rock has been conducted, however drill cores were analysed in conjunction with a previous study (Hallberg and Reginiussen, 2020) to confirm levels of phosphate in the ore at Grängesberg. The dominant CRMs at Grängesberg observed in this previous study were P, LREE, and elevated concentrations of Ti and V.

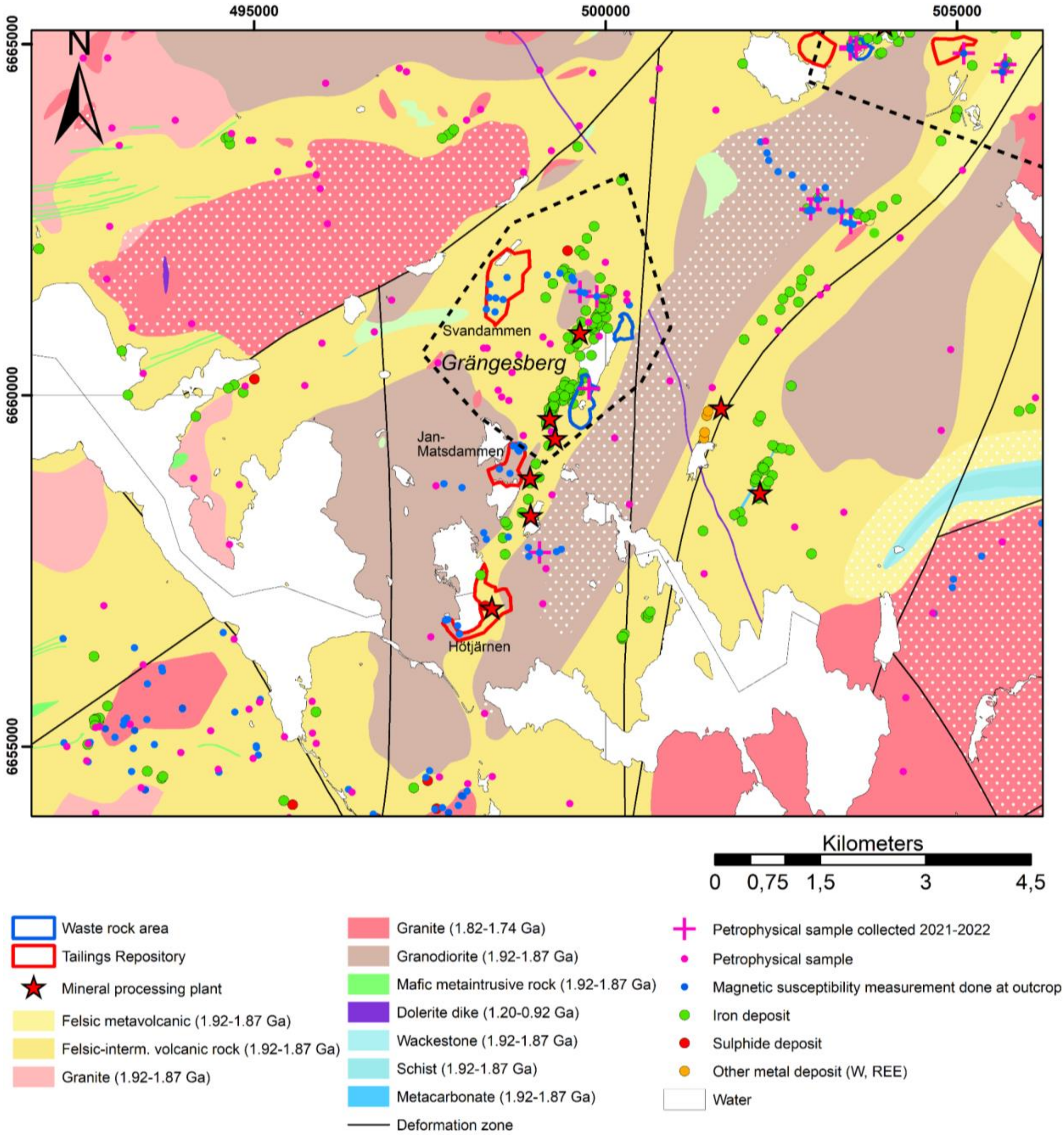

Figure 33. Bedrock map of Grängesberg area showing sampling sites as well as locations of available petrophysical data. White dot denotes porphyritic texture. Dashed black line denotes extent of geophysical mapping areas studied in this project.

Table 14. Ore production and waste produced at Grängesberg. Data from SGU's MALMdb.

Data	Object	Tonnage(Mt)	Fe_2O_3 (%)	P_2O_5 (%)
Mined ore	Grängesberg Exportfält	132.8	49.7	5.2
	Risbergsfältet	20.4	91	0.4
Waste rock generated	Exportfältet	73.7	12.1	0.65
	Risbergsfältet	0.62	8.35	2.5
Tailings produced	Bergslagsschaktet	8.4	17.2	1.2
	Södra verket	5.7	33.3	0.53

Available geophysical data

Airborne data (magnetic, VLF, gamma spectrometry)

Airborne geophysical data are available from several different surveys for the area around Grängesberg. The earliest of these surveys was collected in 1972 by SGU where magnetic and gamma ray measurements were performed. In 2008, TM resources AB collected Airborne TEM (SkyTEM) measurements in an area to the east of Grängesberg. Between 2016 and 2019, SGU performed a series of more modern airborne measurements which cover the area around Grängesberg. As part of these surveys new magnetic, natural gamma ray and VLF (2 transmitters) measurements were collected with a nominal flight height of 60 metres and line spacing of 200 metres. The different data collected in the area around Grängesberg are summarised in table 15.

Figure 34 shows a map of the residual magnetic field based on airborne measurements collected by SGU between 2016 and 2019 for the area around Grängesberg. The strongest magnetic anomalies, including the anomaly around Grängesberg are clearly associated with Fe mineralisation. The type of Fe mineralisation varies throughout the region but includes apatite-Fe oxide mineralisation and Fe mineralisation associated with carbonates / calc-silicates (Magnusson and Lundqvist, 1933). The Grängesberg Exportfält includes mainly apatite-Fe mineralisation with Fe contents of up to between 59 and 64%. Within the Grängesberg area the dominant mineral in the Fe mineralisation is magnetite but hematite can also occur in places (Magnusson and Lundqvist, 1933). Hence, the strong magnetic anomalies in this area are primarily associated with the presence of magnetite.

Figure 35 shows a map of the apparent resistivity over the Grängesberg area, derived from SGU's airborne VLF measurements between 2016 and 2019. In this area the zones of low resistivity mainly correspond to wetlands and lakes, as well as manmade objects such as powerlines and railways.

Table 15. Complete list of the airborne geophysical surveys collected in the area around Grängesberg (i.e. within the area shown in figure 34). Unless otherwise stated all data are collected using a small, manned aeroplane.

Year	Organisation	Geophysical methods used	Area (SGU map sheet)	Flight direction (degrees)	Flight line separation (m)	Flight altitude (m)
1972*	SGU	Magnetics, gamma spectrometry	Part of 12E and 12F	East–West (90°)	200	30
2008*	TM Resources AB	*Helicopter based measurements (SkyTEM)* Magnetics, TEM	part of 12FSV, Jonsmossen	Northwest – Southeast (135°)	100	30
2016	SGU	Magnetics, gamma spectrometry, VLF (2 transmitters)	Part of 13F,13G, 12E, 12F, 12G, 12H, 11E, 11F, 11G and 11H	Northwest – Southeast (130°)	200	60
2017	SGU	Magnetics, gamma spectrometry, VLF (2 transmitters)	Part of 12E, 12F, 11E, 11F, 10E and 10F	Northwest – Southeast (130°)	200	60
2019	SGU	Magnetics, gamma spectrometry, VLF (2 transmitters)	Part of 12E	East–West (90°)	200	60
2020*	SGU	*Drone based measurements* Magnetics, VLF multi-frequency	Small part of 12FSV, Blötberget	Northwest – Southeast (130°)	100	60

* Not used for producing maps in this report

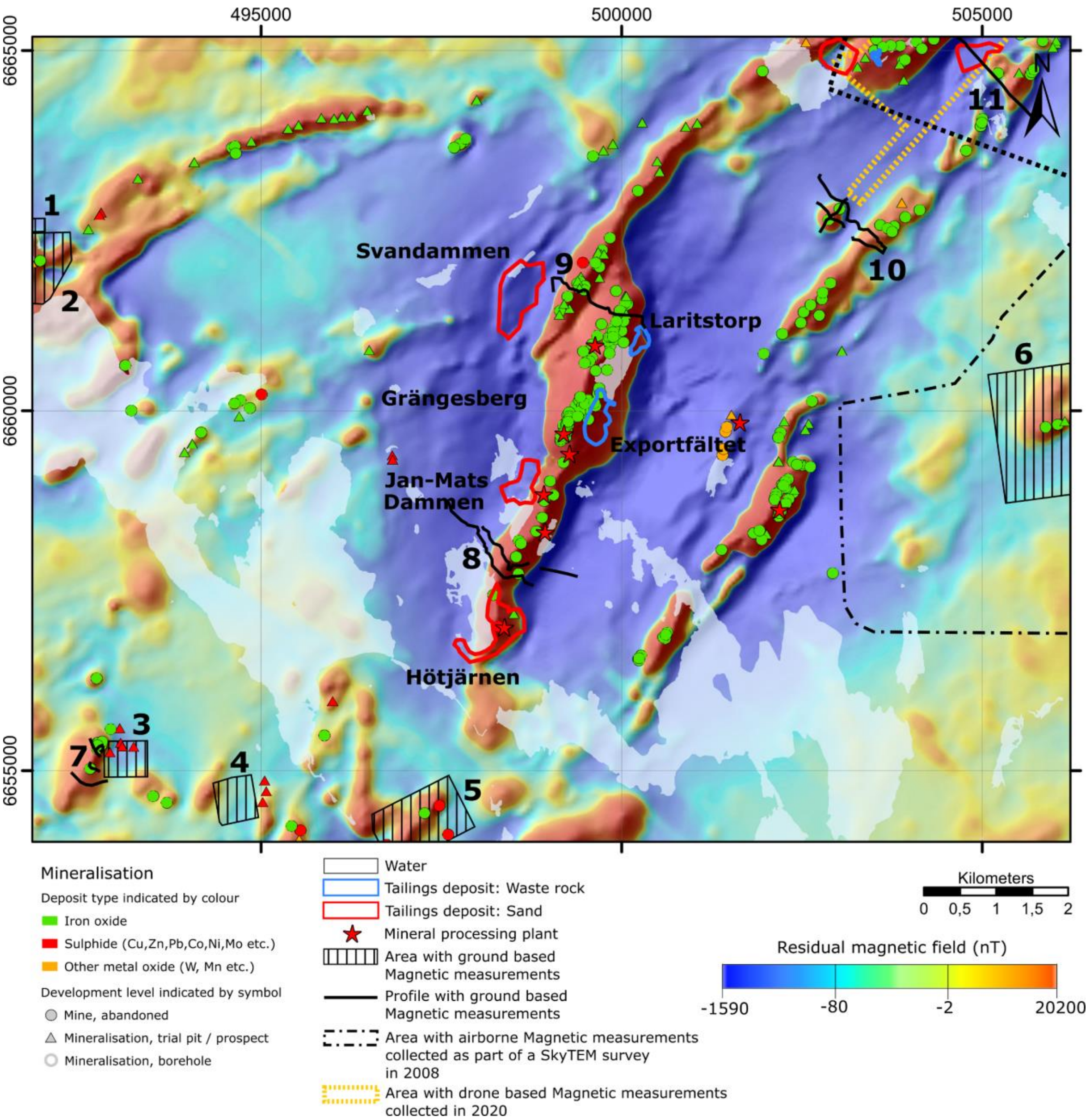

Figure 34. Map of residual magnetic field for the area around Grängesberg. The Blötberget mapping area (discussed later in the report) is shown as a polygon with a thick black dashed line in the north-eastern corner of the map. The location of ground-based magnetic measurements, listed in table 16 is shown. The location of magnetic measurements collected with a drone by SGU in 2020 is also shown.

Ground-based electromagnetic and magnetic measurements

Table 16 provides a summary of the ground-based magnetic measurement data in SGU's databases, which have been collected in the area around Grängesberg. The locations of these measurements are shown in figure 34. Between 1977 and 1982, ground magnetic measurements were performed over several small areas as part of mineral prospecting activities. Between 2017 and 2021, SGU collected a series of ground magnetic profiles within and around Grängesberg. These ground magnetic profiles were collected as part of ongoing and completed bedrock mapping projects (Lewerentz & Brolin, 2022).

Data from two ground-based electromagnetic surveys exist in SGUs databases, which were performed in the area around Grängesberg as part of mineral prospecting activities. These consist of both EM34 and slingram measurements and are detailed in table 17 and figure 35.

Table 16. Ground-based magnetic measurements for the area around Grängesberg. Numbers correspond to the numbered polygons/lines shown in figure 34.

Polygon/Line number and name	Method	Year acquired	Responsible	Comments
1. mgtmid1848	Magnetic	1982		Profile spacing of 20 m.
2. mgtmid1850	Magnetic			Profile spacing of 20 m to 10 m.
3. mgtmid1550	Magnetic	1979		Profile spacing of 20 m.
4. mgtmid216	Magnetic			Profile spacing of 50 m.
5. mgtmid363 – mgtmid371	Magnetic	1977		Profile spacing of 40 m.
6. mgtmid969	Magnetic			Profile spacing of 20 m.
7. MP17ILA0001 – MP17ILA0005	Magnetic	2017	SGU	Five profiles collected in this area
8. MP21CJO1006 – MP21CJO1008	Magnetic	2021	SGU	Three profiles collected in this area
9. MP21CJO1004	Magnetic	2021	SGU	One profile collected in this area
10. MP21CJO1001 – MP21CJO1003	Magnetic	2021	SGU	Three profiles collected in this area
11. MP21DSR0028	Magnetic	2021	SGU	One profile collected in this area

Table 17. Ground-based electromagnetic measurements for the area around Grängesberg. Numbers correspond to the numbered polygons/lines shown in figure 35.

Polygon/Line number and name	Method	Year acquired	Responsible	Comments
1. Saxberget nr 1004	EM34	2012	Boliden Mineral AB	Profile spacing of 100 m.
2. mgtmid4136 and mgtmid4137	Slingram, SR 18kHz	1979		Profile spacing of 40 m to 20 m.

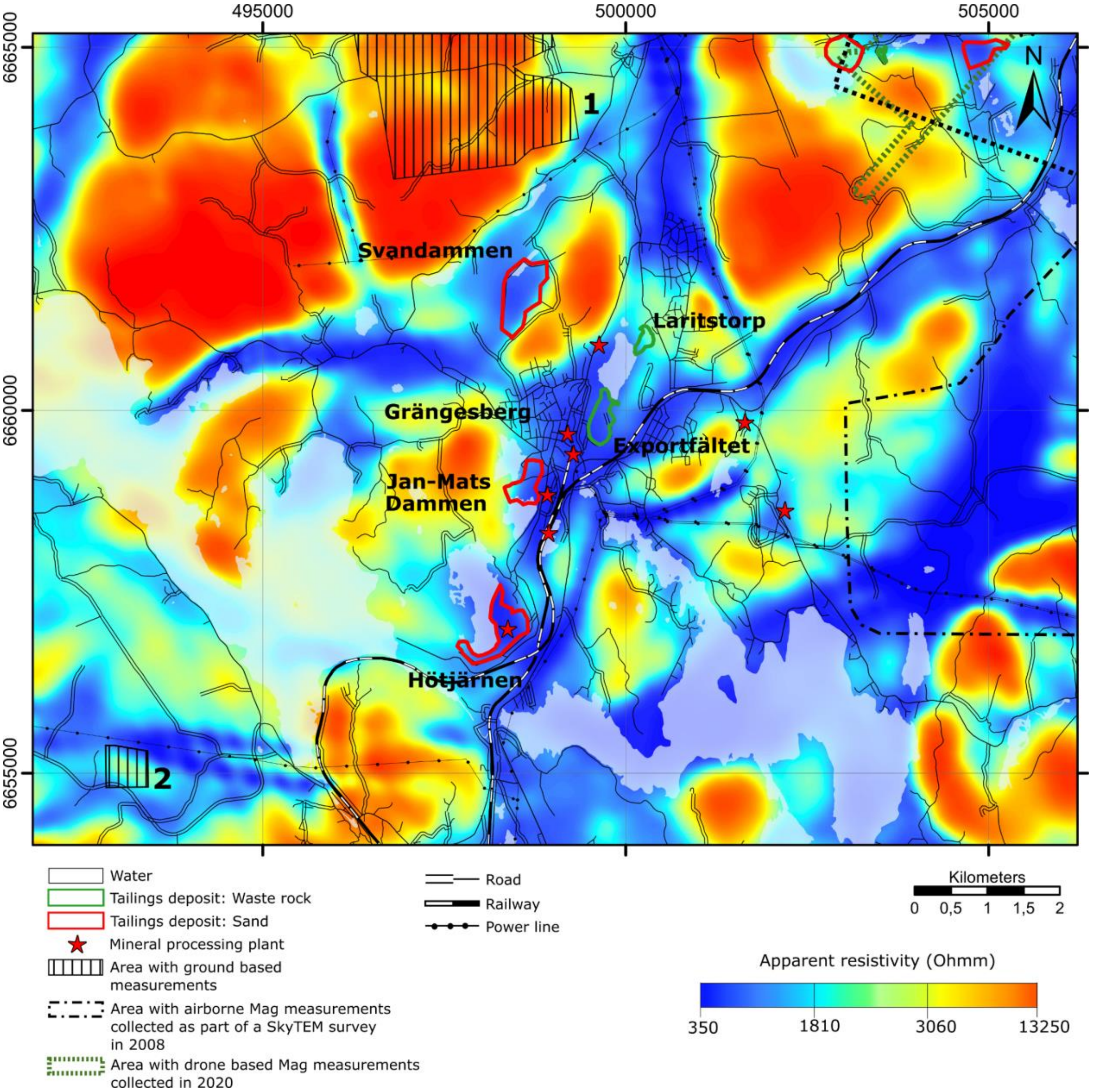

Figure 35. Map of apparent resistivity derived from airborne VLF data collected between 2016 and 2019 for the area around Grängesberg. The Blötberget mapping area (discussed later in this report) is shown as a polygon with a thick black dashed line in the north-eastern corner of the map. The location of ground-based electromagnetic measurements, listed in table 17 is shown.

Ground-based gravity

Figure 36 shows a map of the residual gravity anomaly for the area around Grängesberg using data from SGU's database. Prior to this project, the gravity measurements around Grängesberg had an average point spacing of about 2 km. To the southwest of the area shown in figure 36 the spacing between measurement points is somewhat lower, at about 500 m, at least along roads. As part of this project 258 additional gravity points were measured in the Grängesberg area, reducing the average point spacing to about 200–500 m (see fig. 36).

The main feature of the residual gravity anomaly map is a relatively large positive anomaly located at the position of the Grängesberg deposit. The peak of this anomaly corresponds well to the magnetic field anomaly and mineralisation documented at Grängesberg (fig. 34). Smaller gravity anomalies can also be observed to correlate with other regions of Fe mineralisation to the southeast and southwest of Grängesberg. A small gravity anomaly can also be observed to the immediate northwest of Grängesberg which appears to be associated with mafic rocks.

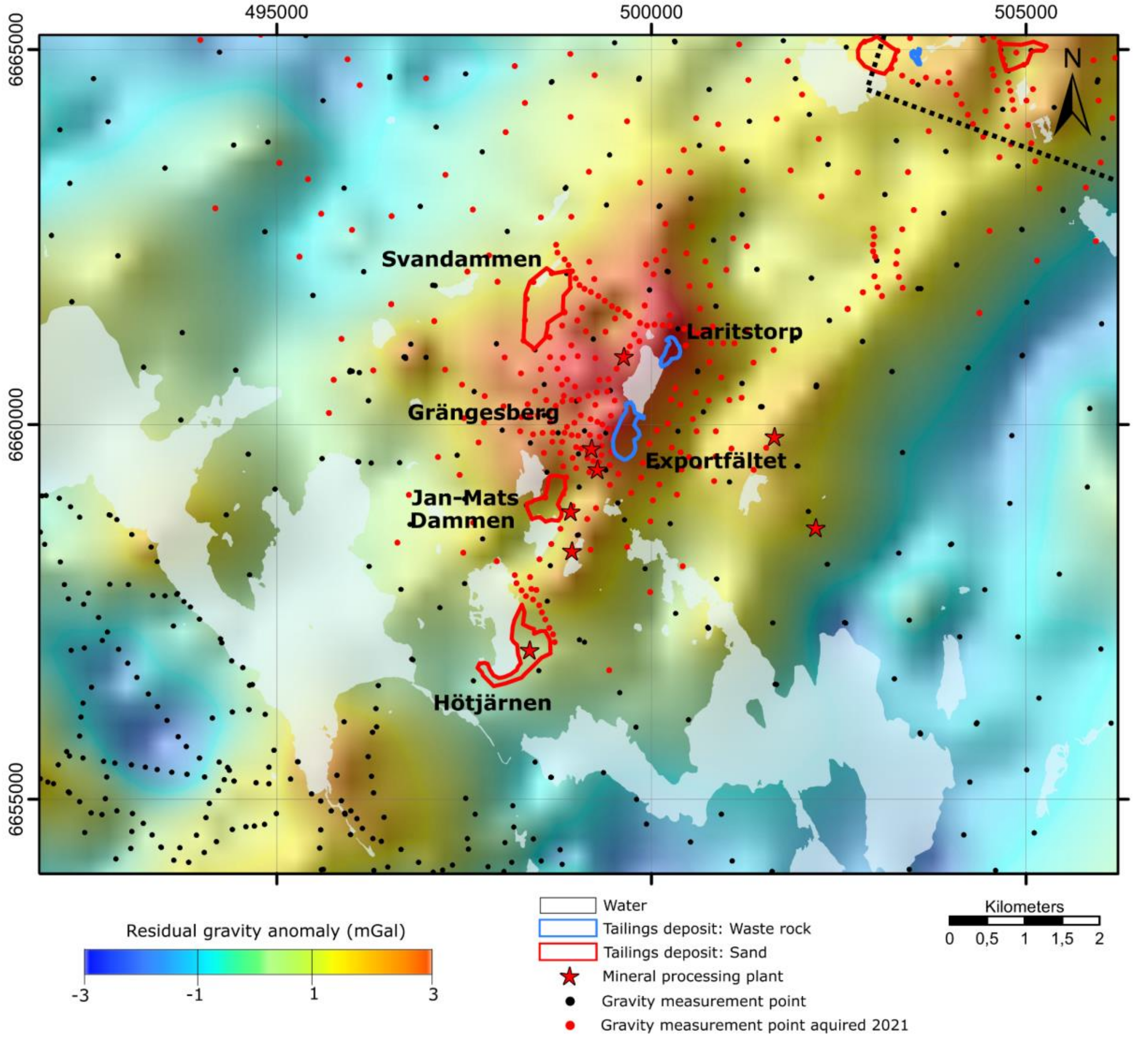

Figure 36. Map of the residual gravity anomaly for the area around Grängesberg. The Blötberget mapping area (discussed later in this report) is shown as a polygon with a thick black dashed line in the north-eastern corner of the map. Gravity measurement points are shown as black and red dots.

Petrophysical and borehole data

Figure 33 shows a map of the available petrophysical data in the Grängesberg area. Here it can be observed that the availability of petrophysical data is relatively good. However, to further improve the petrophysical database, several new petrophysical samples were collected as part of this project and a series of ongoing bedrock mapping projects (see fig. 33). The data for the additional petrophysical sample collected in the area around Grängesberg as part of this project is shown in table 18. A sample of Fe mineralisation taken from waste rock at Grängesberg shows relatively high density and magnetic susceptibility values, supporting the assumption that the gravity and magnetic anomalies here are linked to the Fe mineralisation. Measurements of magnetic susceptibility at outcrops have not been performed as standard during mapping projects over much of the Grängesberg area, however, some outcrop susceptibility measurement data are available from southwest of Grängesberg.

Figure 33 shows the boreholes within SGU's database for the area around Grängesberg. Many boreholes are documented in the database for the area immediately around the Grängesberg mines (over 700), which were drilled between 1962 and 1988 by a range of organisations, including Stora and SSAB.

Table 18. Table summarising the petrophysical results collected as part of this project from the area around Grängesberg.

Sample ID	Easting (m)	Northing (m)	Description	Density (kg/m3)	Magnetic susceptibility (10-6 SI)	J (mA/m)
PCY210123E	499763	6660093	Fe-oxide mineralisation	4670	58393920	7596

Sampling of waste rock at Grängesberg

Exportfältet

A total of 18 composite samples of waste rock were collected at Grängesberg Exportfält which are shown in figure 37. At present, the waste rock deposit at Exportfältet is used for industrial purposes such as ballast and much of the waste rock has already been removed. Samples were collected along the edges of the remaining open pit that is currently used for aggregates (fig. 38). Numerous piles of material were present in the active industrial area; however, no sampling of this material was done as the material has been sorted by size and magnetic material separated and disposed of.

Metavolcanic rock dominated the composite samples (60%) and approximately 20% of the samples are made up of granite. The remainder was skarn and Fe mineralisation. Concentrations of REE in the waste rock at Exportfältet average 500 ppm Elevated concentrations of V, Sn, and Ti were also observed.

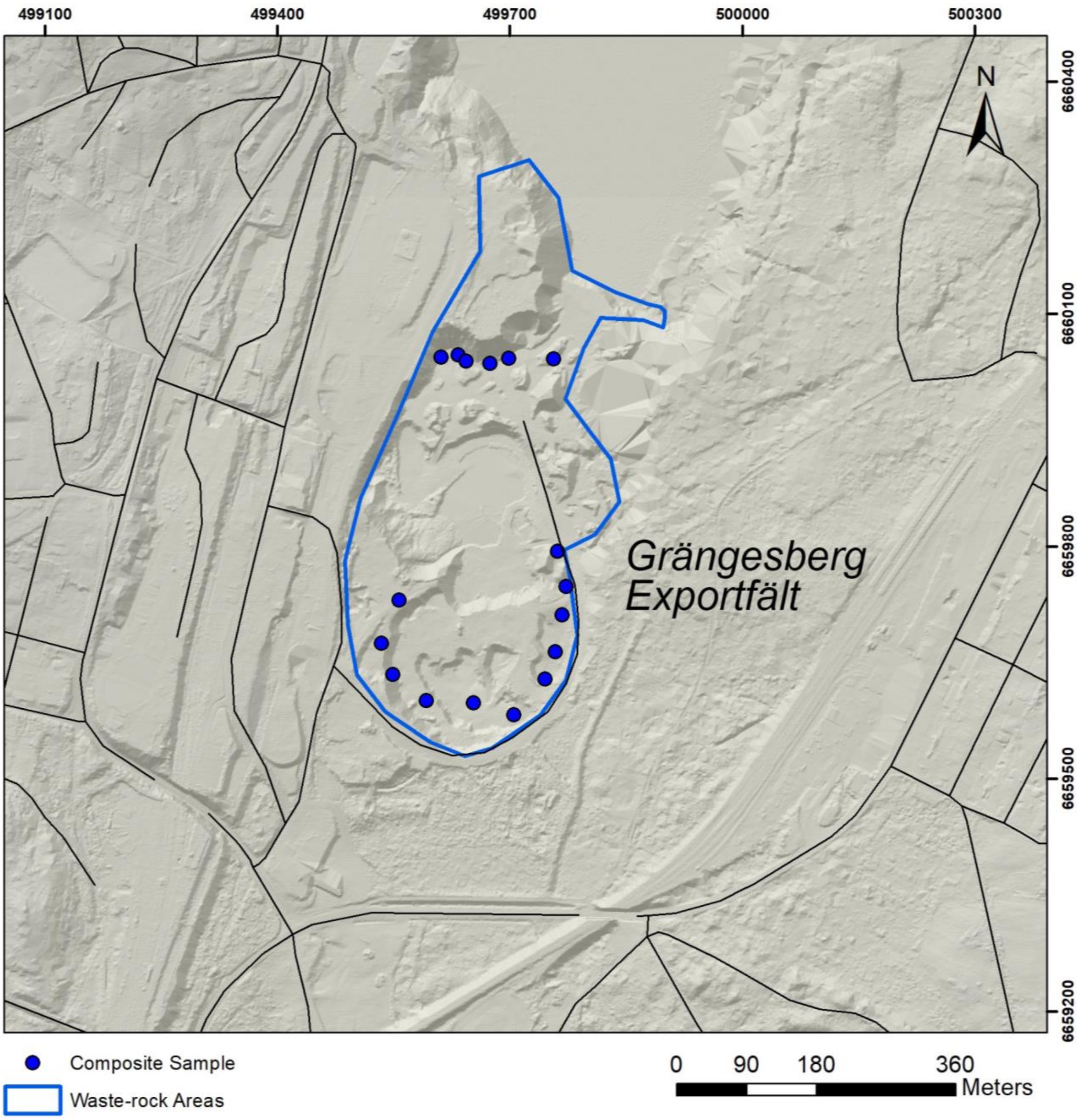

Figure 37. Lidar image of waste rock heaps and sampling points at Grängesberg Exportfält.

Figure 38. Image of sampling site at Exportfältet. Piles seen in foreground are sorted aggregates. Photo: Patrick Casey.

Risbergsfältet

The waste rock heap at Risbergsfältet is the largest waste rock source sampled within this project. It is approximately 25 metres in height, over 300 metres long and 100 metres wide, sloping towards the filled mine pit which can be observed in the LiDAR image in figure 39. Overgrowth on the tailings was limited to some small evergreen and deciduous trees. The waste rock heap at Risbergsfältet has been exploited to a minor extent for industrial mineral uses, however remains largely undisturbed. A total of 20 samples was collected from Risbergsfältet, 17 from the top of the waste heap and 3 from the base. Similar distribution between rock chips in the composite samples was seen at Risbergsfältet as at Exportfältet.

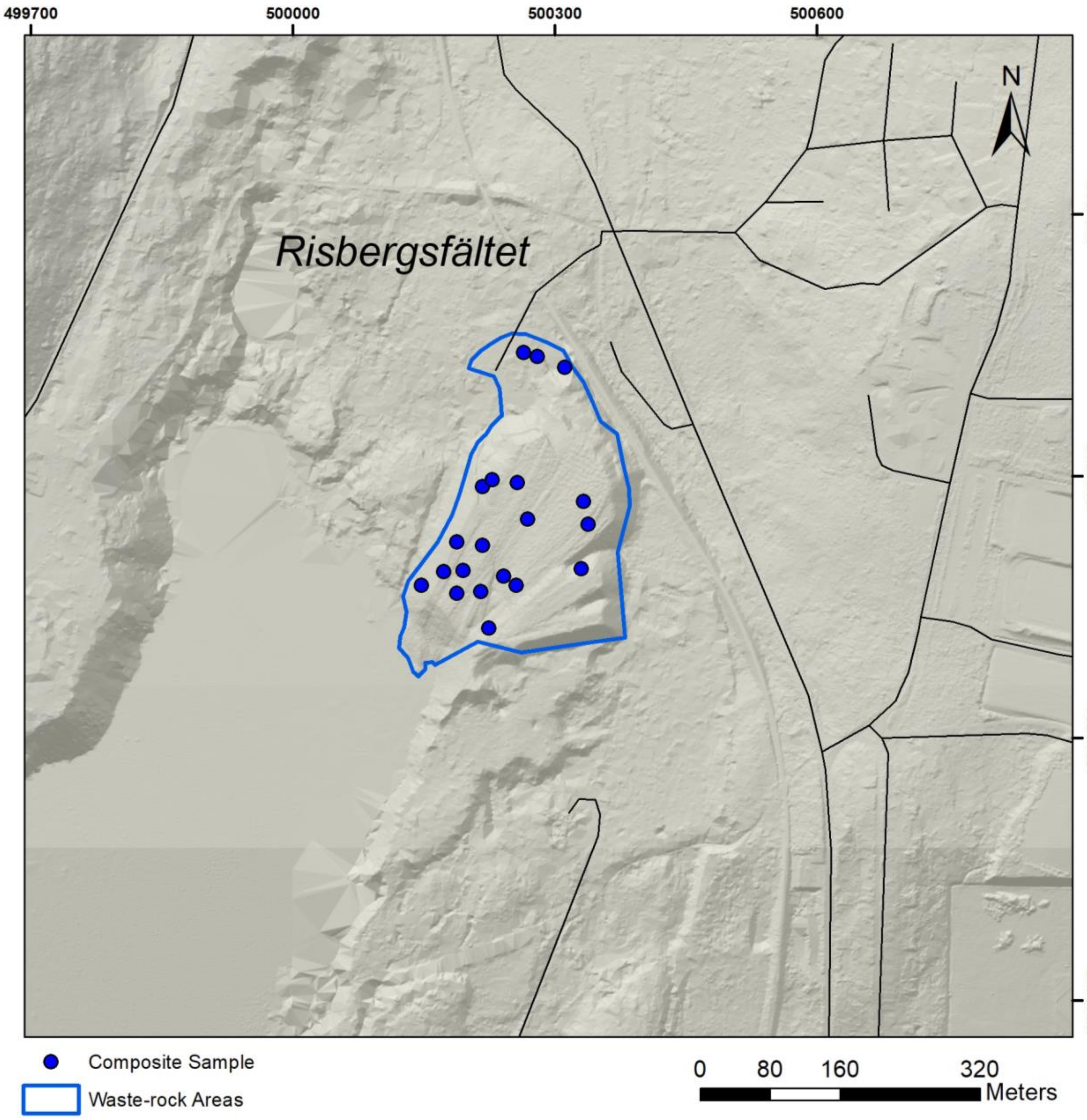

Figure 39. LiDAR image of waste rock heap at Risbergsfältet.

Results and discussion

Fe, phosphorus and REE contents were higher in the material from the Risbergsfältet samples, with average Fe contents of 17.2 % compared to 12.1% at Exportfältet. Phosphate showed a concentration of nearly double that of Exportfältet, at 1.2 %, and higher REE concentrations were also noted, 604 relative to 423 ppm in waste rock from Exportfältet (table 19).

A strong correlation of phosphorus content and REE content is seen in the waste rock analyses from Grängesberg (fig. 40). This correlation is due to the presence of REE within the apatite in the ore as well as in other phosphate minerals. Apatite at Grängesberg typically contains trace amounts of REE that were not measurable using EDS analysis, excepting for apatite occurring in proximity to monazite where up to 1–2% LREE was observed. EDS analysis of ore samples from Grängesberg showed the most common REE minerals are monazite, xenotime, and allanite. Monazite typically occurs as small inclusions along the C-axis of apatite (fig. 41C), as well as large crystals within the ore. Monazite, xenotime and allanite typically contain measurable quantities of radioactive elements such as U and Th, while apatite typically does not incorporate large quantities of these elements into its structure. EDS analysis confirmed the observation of low levels of Th in the monazite that were observed by Jonsson et al. (2015). Thorium was typically below EDS detection limit, while a small number of crystals contained ~2% Th.

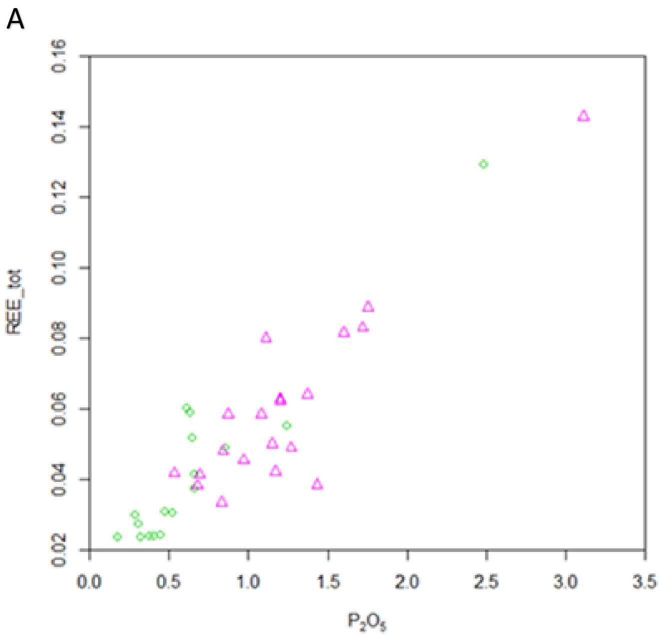

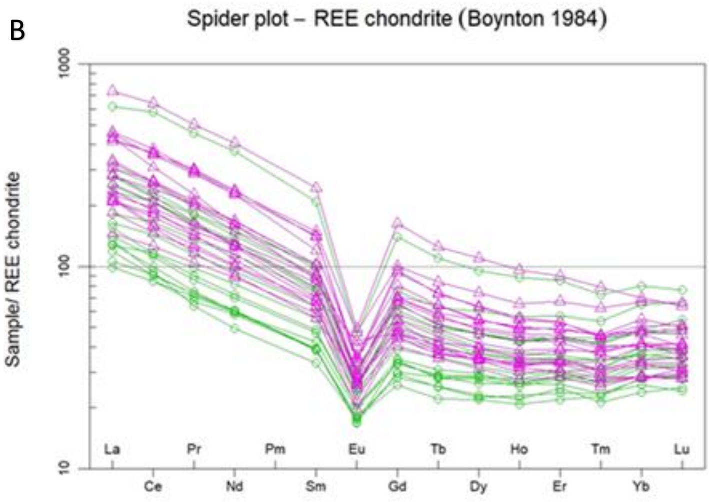

Figure 40. **A**: Binary plot showing strong correlation between phosphorus and REE in waste rock from Grängesberg.
B: Chondrite normalised REE pattern of waste rock. Normalised to Boynton (1984). Green = Exportfältet, pink = Risbergsfältet.

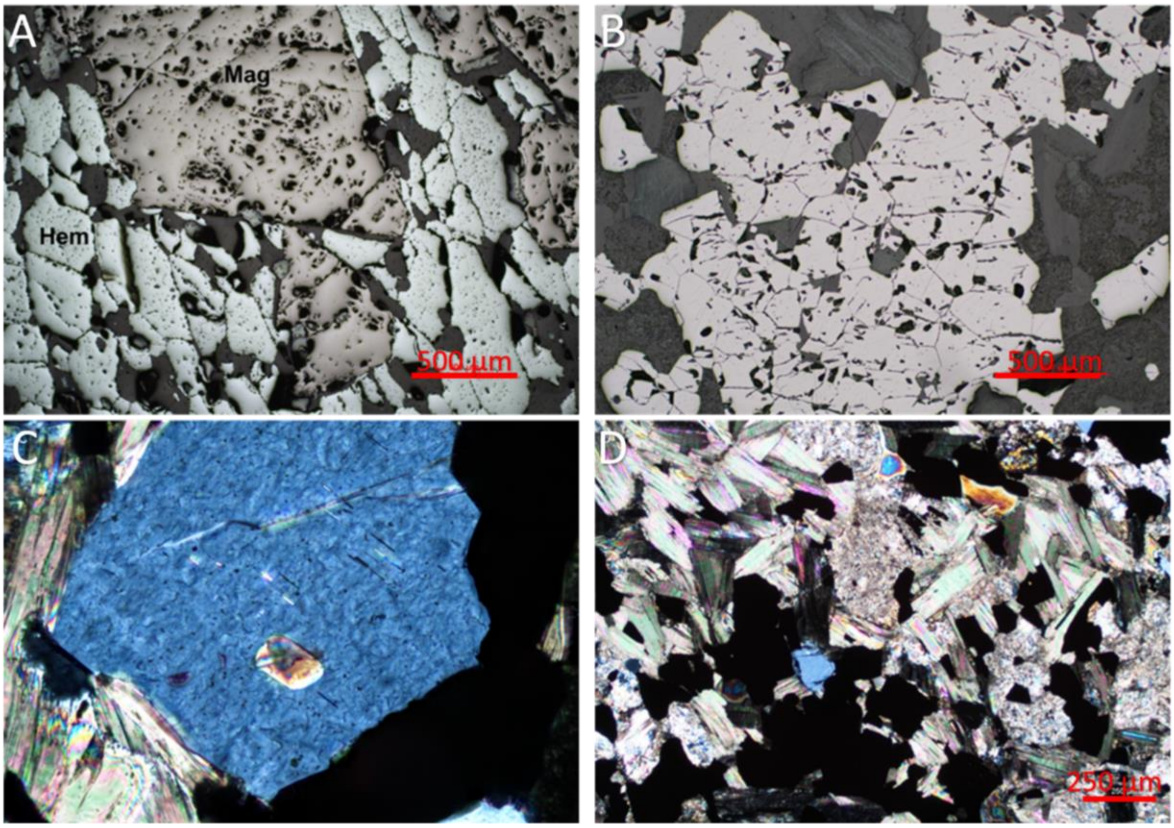

Figure 41. Thin section images from mineralised samples collected at Grängesberg. **A**. Magnetite blasts in hematite from a lump ore sample. **B.** Magnetite mineralisation in a skarn-rich sample. **C.** Apatite crystal in XPL showing a large monazite intergrowth as well as lathe like inclusions of monazite. **D.** Skarn-rich ore sample in XPL showing magnetite (opaque), chloritoid (anomalous interference colours) Apatite (1st order birefringence surrounded by magnetite) and monazite (high 3rd order birefringence). Micrographs: Patrick Casey

The low concentrations of Th observed in the monazite from Grängesberg indicate the monazites likely formed as secondary minerals from REE and phosphate liberated from primary apatite during fluid alteration. Low contents of Th in the monazite are a positive aspect for beneficiation of the material as the amount of potentially hazardous radioactive waste products can be minimized.

Allanite was often observed as alteration of epidote near other REE phases. In the backscatter images seen in figures 42 and 43, darker grey epidote is seen surrounding monazite crystals. Along the inner grain boundaries of the epidote lighter grey patches of allanite are observed. These most likely formed due to diffusion of REE from the monazite during fluid alteration.

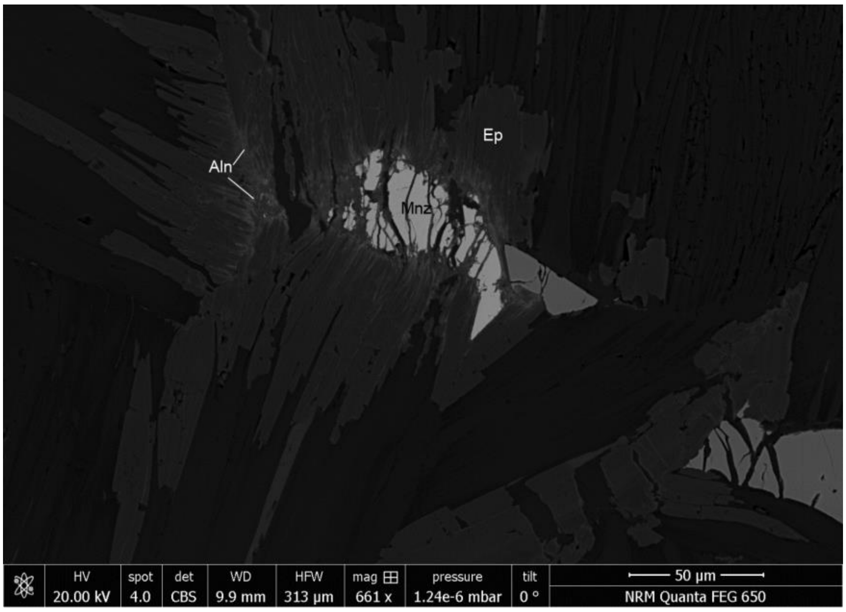

Figure 42. Backscatter electron image of monazite from Gränges-berg in epidote. The lighter grey portions of the epidote have been altered to allanite. Micrograph: Patrick Casey

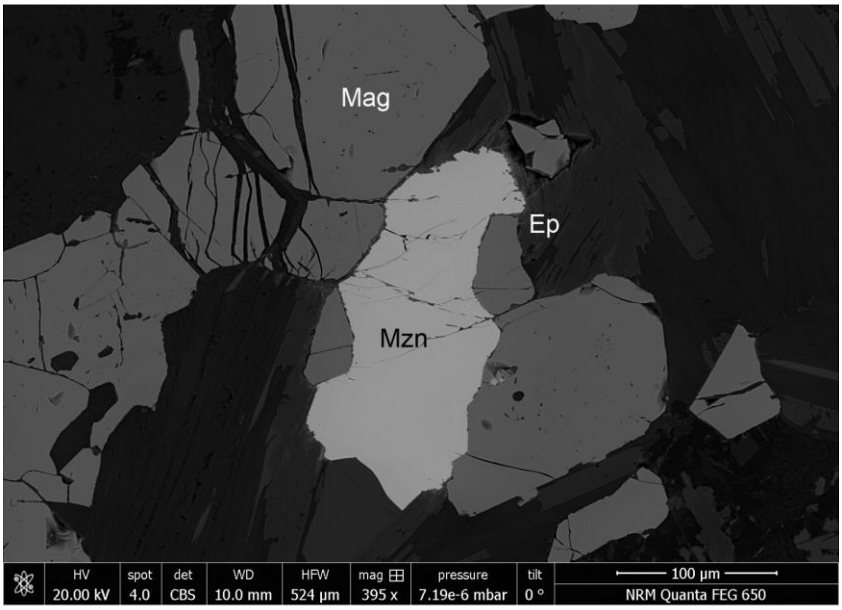

Figure 43. Backscatter electron image of monazite and magnetite from Grängesberg. Micrograph: Patrick Casey

Table 19. Analytical results of waste rock from Grängesberg.

Data	Object	Fe_2O_3 (%)	P_2O_5 (%)	REE (ppm)	V (ppm)	Sn (ppm)
Ore Sample	Fe-skarn	49.7	5.22	2797	490	28
	Haematite ore	91	0.4	2082	265	148
Composite samples (n=17)	Exportfältet	12.1	0.65	423	207	17
	Min	8.4	2.48	1290	132	6
	Max	19.3	0.17	234	303	56
Composite samples (n=20)	Risbergsfältet	17.2	1.2	604	268	37
	Max	33.3	0.53	333	99	5
	Min	7.5	3.1	142	471	107

Potential resources in waste rock at Grängesberg

Grängesberg potentially presents the single largest potential source for recovery of secondary REE in Bergslagen. Of the total tonnage of waste rock produced according to MALMdb (73 Mt) only a fraction is easily accounted for. Waste rock has been used for construction material, including ballast for the railway in the Grängesberg area, and for construction of the berms for the tailings ponds. Based on historical aerial photos much of the material was left in the open pit of the mine which is now covered by water, and volume estimates cannot be made.

Several large piles of waste rock remain in the area, and tonnage calculations of potential raw material only take into account this material. Calculations of volume of easily accessible material were made using LIDAR elevation data to calculate the surface area and height of these piles (figure 44). As the largest percentage of the material collected for chips observed was felsic metavolcanic rock, an average density of 2.9 tonne/m^3 was used based on density measurements conducted on a meta-rhyolite sample, and a porosity of 30% was assumed. The estimated amount of easily accessed waste rock at Grängesberg thus totals ~6.4 Mt.

Using this tonnage estimate, potential resources in easily accessible waste rock at Grängesberg is 660 kt Fe, 25 kt P, 11 kt Ti, 3200 tonnes REE, and 1500 tonnes Vi.

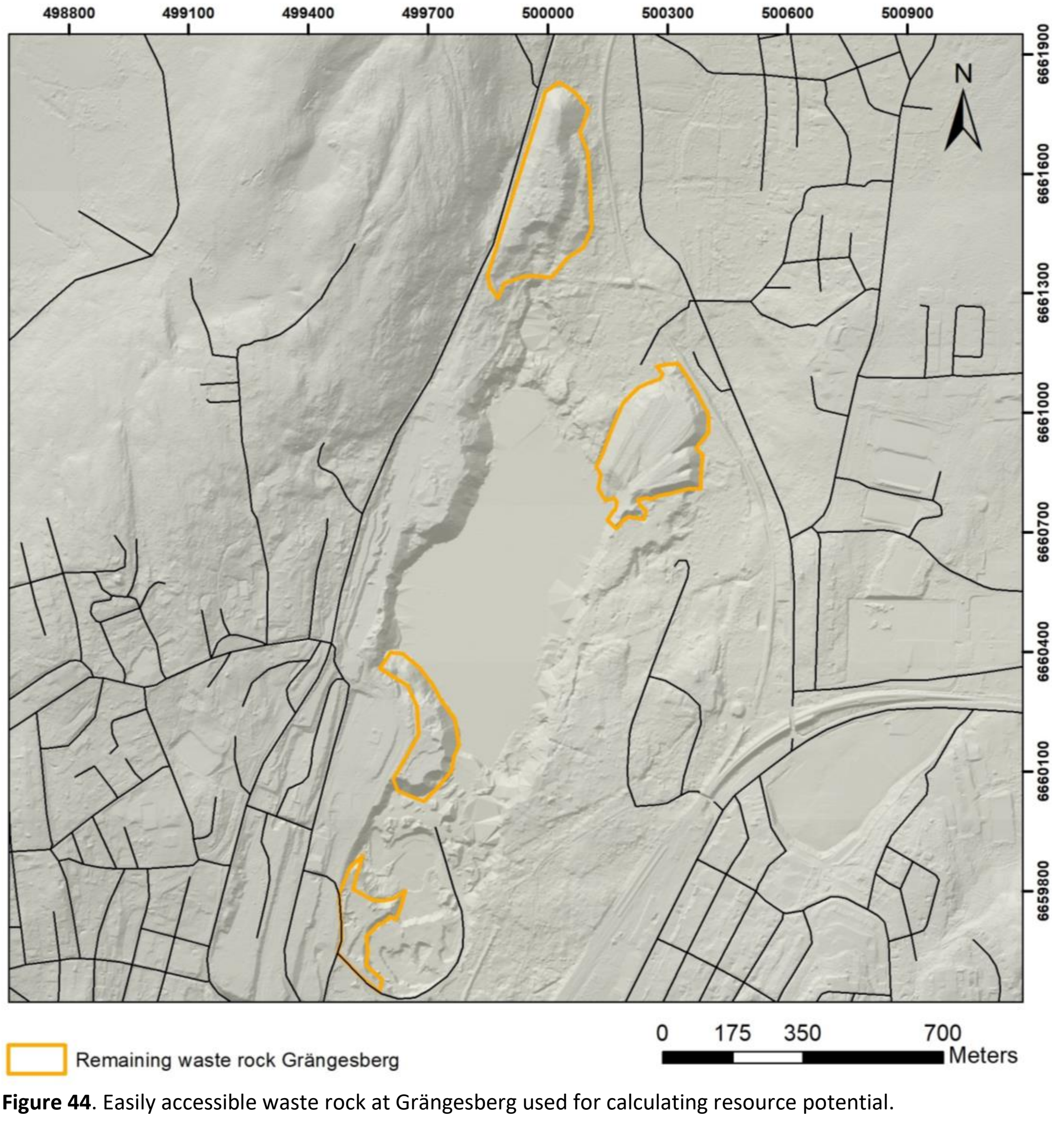

Figure 44. Easily accessible waste rock at Grängesberg used for calculating resource potential.

Sampling of tailings at Grängesberg

Ore refinement at Grängesberg originally began in small scale dressing plants just west of Exportfältet, and the tailings were deposited in a tailings dam at the southernmost end of Exportfältet until the early 1950 (the dam walls are visible in the bottom centre of the LiDAR image in fig 37) which was not sampled in this study. In the latter half of the 20^{th} century ore from Grängesberg was processed at two larger dressing plants, and deposited into three tailings ponds: Svandammen, which is currently used as a golf course, Jan-Matsdammen to the south east of the mine, and Hötjärnen further south of Jan-Matsdammen. Jan-Matsdammen was the first of the post-1950 tailings repositories to be used, with deposition starting between 1953 and 1955 based on historical aerial photos provided by Lantmäteriet. By 1975, Hötjärnen and Svandammen were also in use for the deposition of tailings.

Svandammen

Svandammen is the northernmost of the Grängesberg tailings repositories, with a surface area of approximately 372 000 m^2. It is currently occupied by a municipal golf course covering approximately 75% of the surface area (figures 45 and 46). Deposition of tailings began in the 1970s, ceasing in 1979. Overgrowth is rather sparse with deciduous and evergreen trees owing to maintained land use of the course. The material shows sorting, with the coarsest material to the east of the repository where the discharge occurred, fining to the west where it becomes waterlogged and silt dominated.

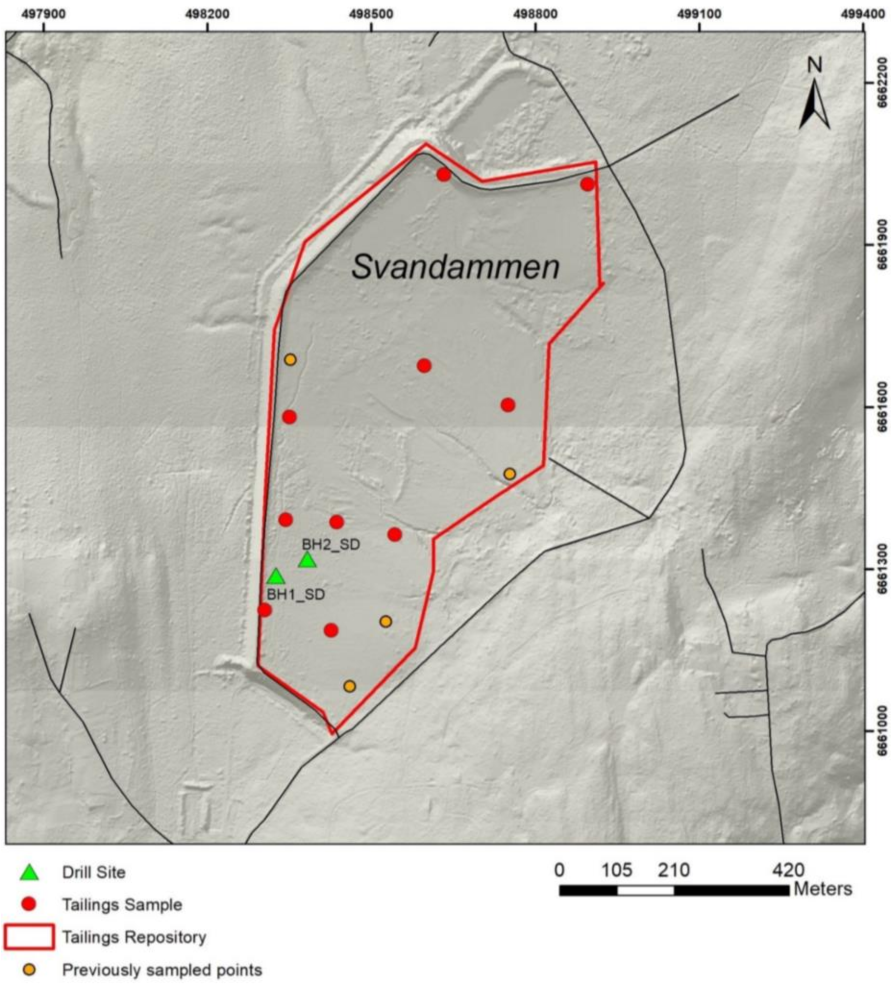

Figure 45. Sampling points for tailings from Svandammen.

Figure 46. Aerial photos of Svandammen in 1975 (below) and today (above). Photo: Lantmäteriet.

Geophysical measurements

The geophysical measurements at Svandammen were limited to the area of the tailings repositories not used as a golf course (fig. 47). Three methods were used, ERT, IP and tTEM. The tTEM measurements covered approximately 2.5 kilometres. Two ERT and IP profiles were measured, approximately 290 metres long each. The location of the measurements is shown in figure 47. Results from the ERT measurements show that the area in general has a high resistive layer (>1000 Ohm-m) in the approximately 5 metres closest to the surface. Drilling confirmed dry tailings of sand-silt at the top of the deposit and water saturated sediments in the lower parts. Figure 48 shows the resistivity model from inversion of ERT measurement together with the sites of three drillings and the interpretation of the deposits in each borehole. For borehole "GBS_3_sond" and "GBS_4_sond" no sampling or logging of the hole was performed. The drillings were only conducted to register the bottom of the tailings; however, it was noted that the material at the bottom was wet. From figure 48 it can be noted that there is a good correlation between the dry tailing deposits and the high resistivity layer at the top. However the bottom of the tailings is not recognizable from the ERT measurement. Along the eastern part of the profile, outcrops of the bedrock occur, and one can assume a thin layer of till overlying the bedrock. Following the topography and the indication of a bottom high resistive layer in the ERT model, the top of the bedrock has been interpreted in the eastern part of the profile. The tTEM measurements are not considered usable in this area because of lack of significant response, due to the relatively thick, high resistive layer at the top (seen in the ERT model).

A volume calculation for the Svandammen tailings deposits has been performed. The boreholes, topography and historical orthophoto was used to interpret the bottom of the tailings, and then a surface was interpolated. In the topography data (fig 45) it is evident that a dam wall has been constructed in the south, west and north enclosing the area. The interpretation in figure 48 is assumed to be valid for the whole area, with tailing's thickness in the central parts of approximately eight to ten meters. The constructed 3D-model yielded a volume of 2.18 million m^3.

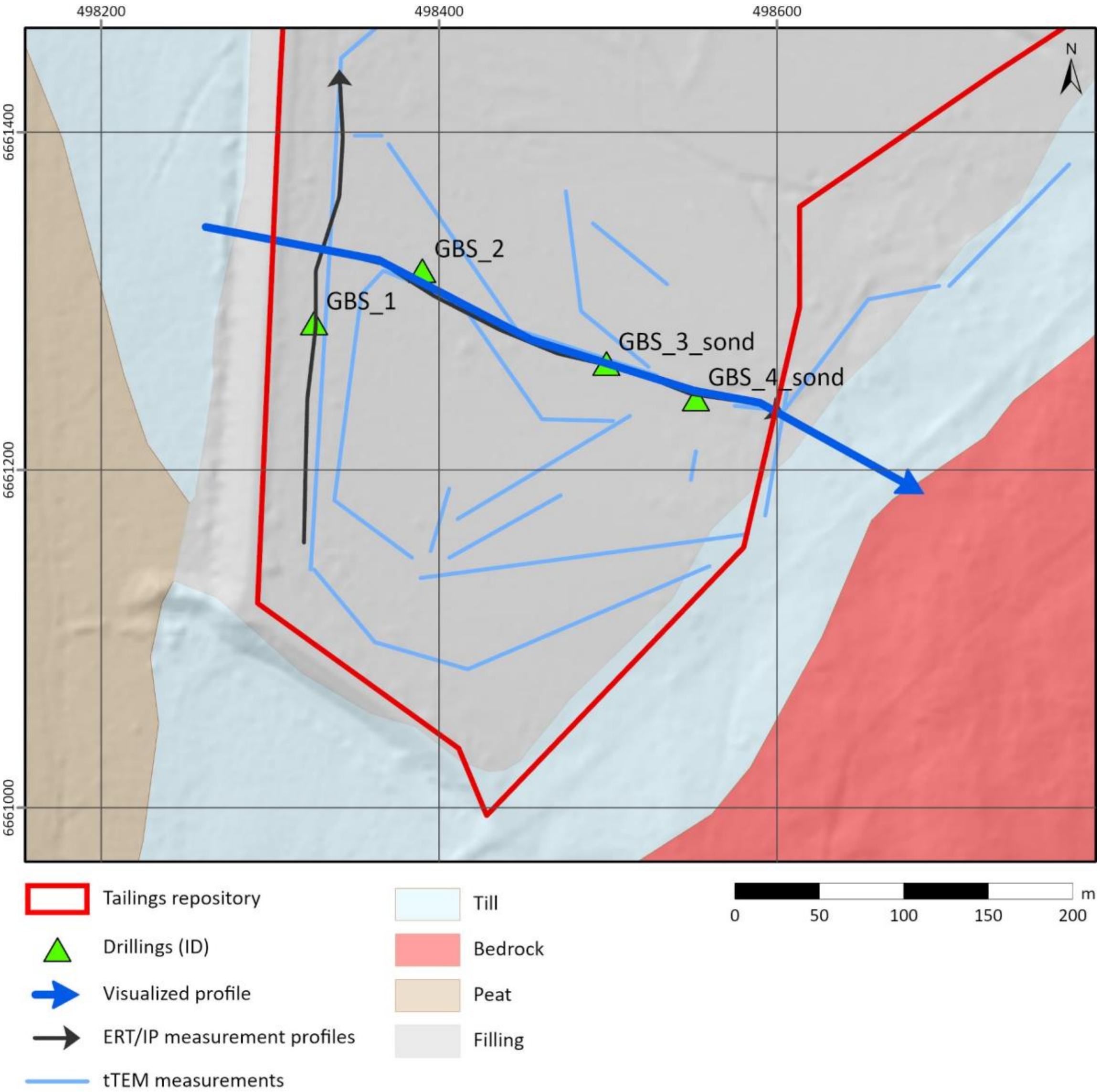

Figure 47. Geophysical measurement profiles and drill locations at Svandammen tailings in Grängesberg.

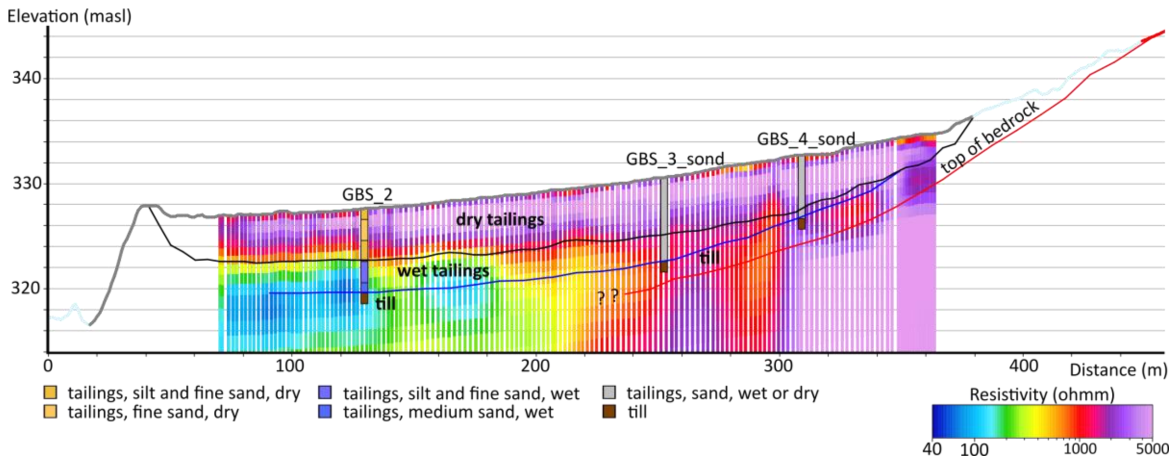

Figure 48. Resistivity cross-section for the blue profile shown in figure 47 (from west to east). Results from drillings and interpreted layers are visualised in the figure. The elevation is colour coded from the quaternary deposits shown in figure 47.

Sampling results

A total of 10 surface samples were collected from Svandammen. The samples showed elevated levels of Fe, P and REE, and minor enrichment in Sn and V. REE and phosphate values were notably lower in the surface samples at Svandammen when compared to the samples from Jan-Matsdammen and Hötjärnen, averaging 1000 ppm and 1.3%, respectively. Two boreholes were drilled at Svandammen. Svandammen is notably shallower in depth than the other Grängesberg tailings repositories, with a maximum depth of 10 metres, shallowing eastwards to around 5 metres.

Svandammen borehole 1 (BH1_SD; 6661288/498326) was drilled near the southwestern corner of the tailings dam. Tight pine and birch forest dominates here. The depth to till was 9 metres. The tailings were fairly water saturated at the surface and waterlogged starting at 4–5 metres. The material was generally fine to medium sand with abundant silt. Occasional bands of hematite of approximately 1 cm were observed, and the material was rich in mica. Results of geochemical analysis plotted along depth are shown in figure 49.

Svandammen borehole 2 (BH2_SD; 6661319/498390) was drilled along the E–W geophysical profile. Here the overgrowth was similar to the first location, though the trees were less sparse. The surface was notably drier, and the water table was reached at 5–6 metres. The tailings were silt to fine sand with occasional bands of medium sand. The lowest 3 metres were composed of medium to coarse sand and were dark grey to black in colour. Results of geochemical analysis plotted along depth are shown in figure 50.

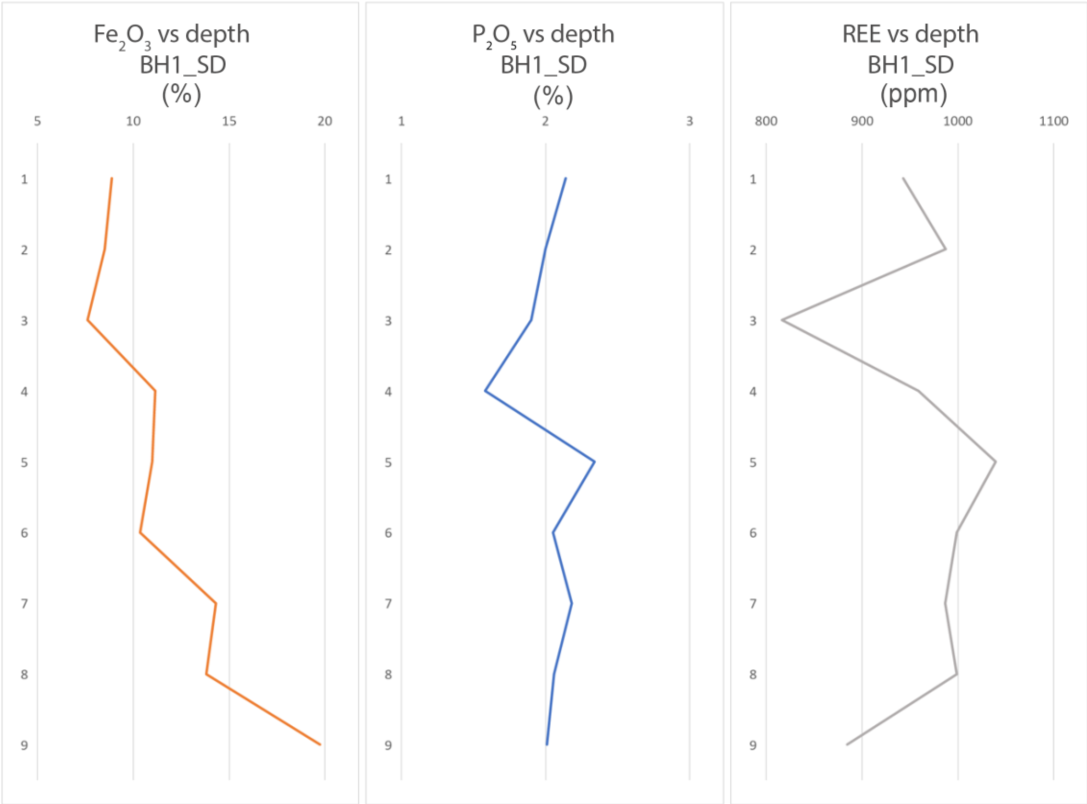

Figure 49. Iron-oxide, phosphate and total REE concentrations along the depth profile in BH1_SD.

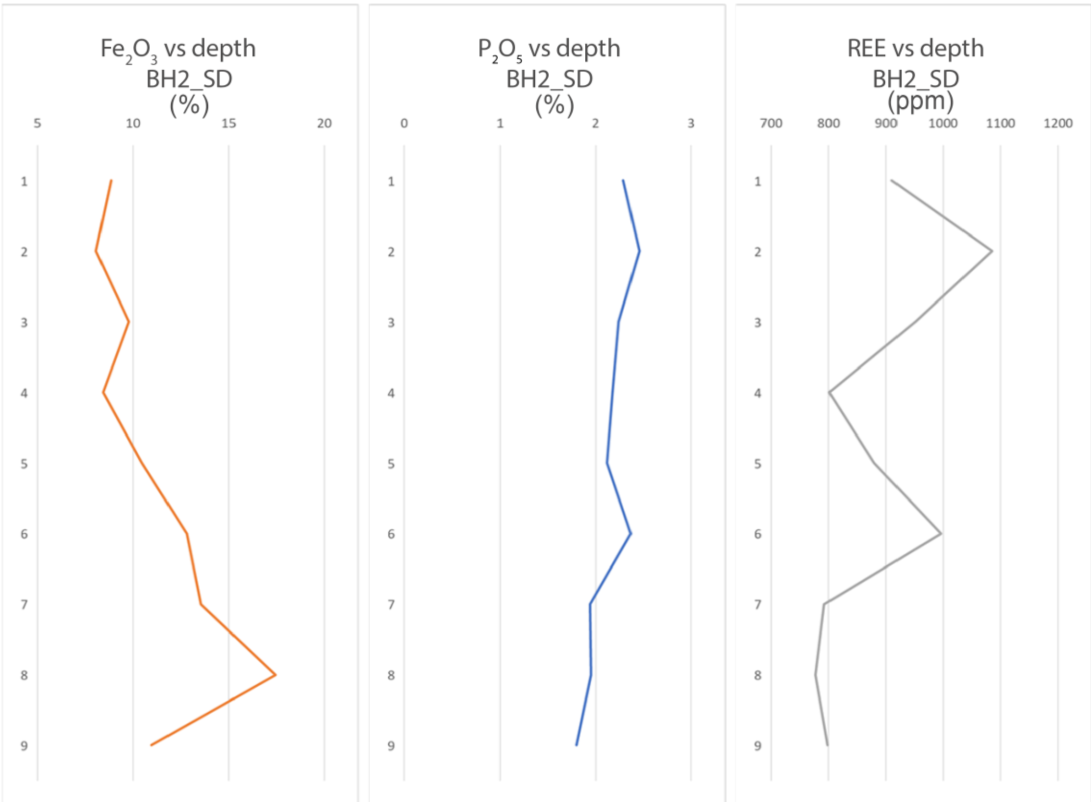

Figure 50. Iron-oxide, phosphate and REE concentrations along the depth profile in BH2_SD.

Discussion

Iron and P concentrations at Svandammen are notably lower than at the other sampled tailings ponds in Grängesberg. The highest Fe contents were observed in the towards the bottom of the boreholes (fig. 49;50). The ore processed at the Bergslagsschaktet was of lower grade (45.1% Fe and 0.6% P) than ore processed at Södra verket, and this combined with more effective recovery methods may have led to better recovery of Fe.

Rare earth element distribution in the tailings at Svandammen differ from those at Jan-Matsdammen, Hötjärnen, and the related Blötberget tailings repositories. These showed chondrite normalised REE patterns within the expected norm of a deposit formed from a magmatic body, with notable enrichment in light REEs, with a gradual depletion in the heavier REEs and strong negative Eu anomalies. The tailings from Svandammen show no to very slight negative Eu anomalies. The cause of the difference in the REE distribution from Svandammen is unclear, however a possibility is the ore body may have crystallized early before Eu fractionation occurred during plagioclase crystallization.

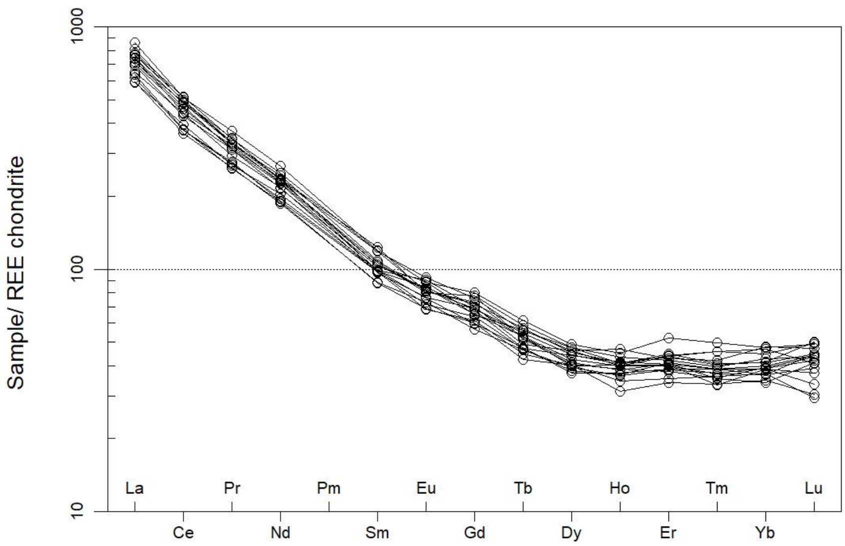

Figure 51. Chondrite normalised REE diagram for tailings from Svandammen. Chondrite values are from Boynton (1984).

Table 20. Analytical results of tailings from Svandammen.

Data	Object		Fe_2O_3 (%)	P_2O_5 (%)	REE (%)	V (ppm)	Ti (ppm)
Tailings (surface)	Svandammen (n=10)	Average	8.9	2.2	0.09	108	1332
		Max	12.4	2.6	0.11	151	1910
		Min	7.1	1.7	0.07	76	830
Drilled Tailings	Svandammen (n=20)		11.4	2.1	0.09	141	1291
			19.5	2.5	0.11	218	2240
			7.61	1.6	0.08	102	830

Jan-Matsdammen

Jan-Matsdammen (fig. 52) is the oldest of the three sampled tailings repositories at Grängesberg with deposition beginning between 1953-1955 (fig. 53). The area is densely overgrown with evergreen trees and becomes swampier closer to the lake. The remnants of the discharge pipes are found in the east, and the material in the vicinity of the discharge point is very coarse, with grain sizes up to 1 cm with the material fining downslope. Drilling at Jan-Matsdammen showed that the material was relatively dry and coarse through the entire upper part of the repository, while surface sampling showed water saturation below the water table closer to the edge of the lake.

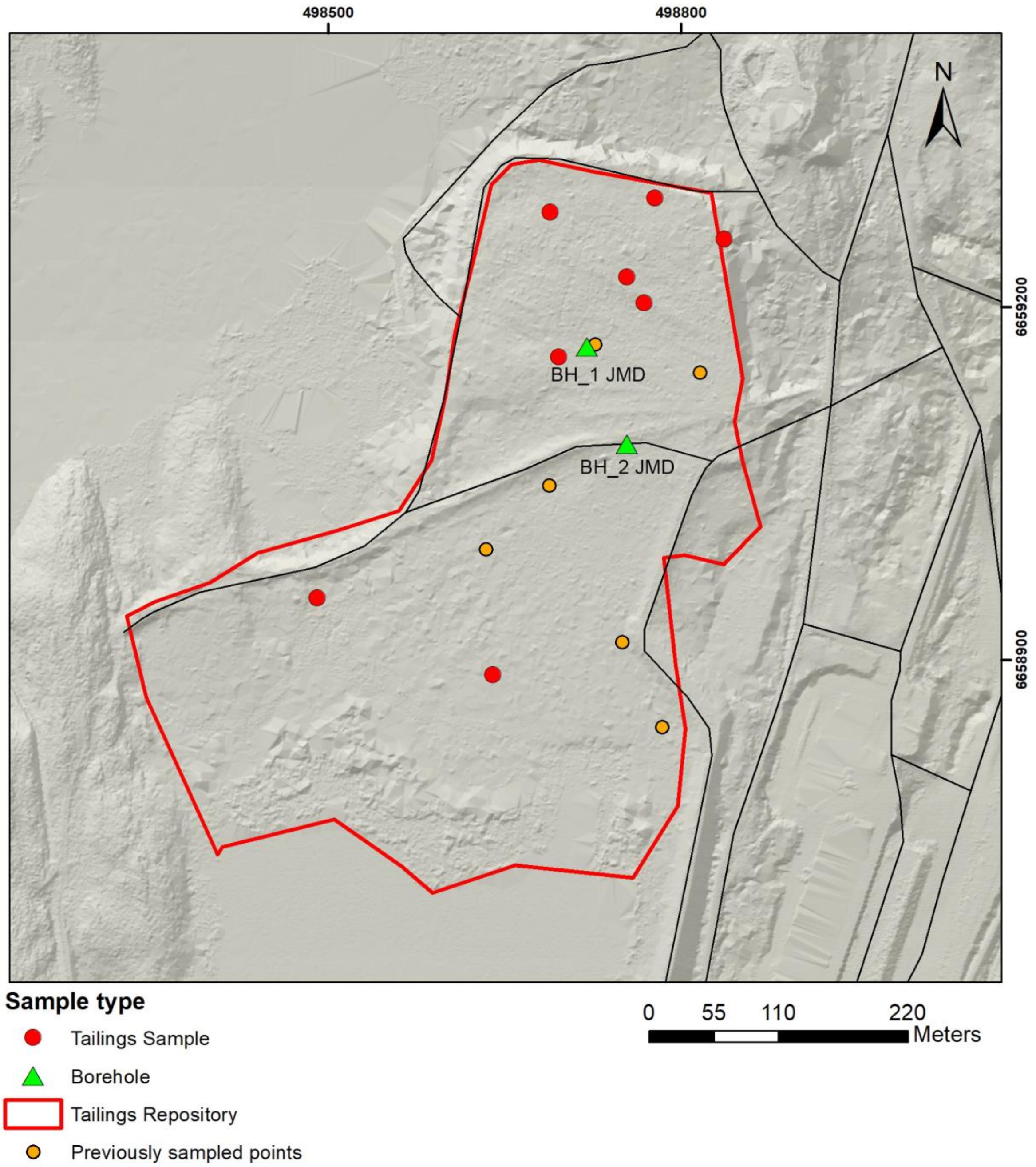

Figure 52. LiDAR image of the Jan-Matsdammen tailings repository showing sampling locations and boreholes.

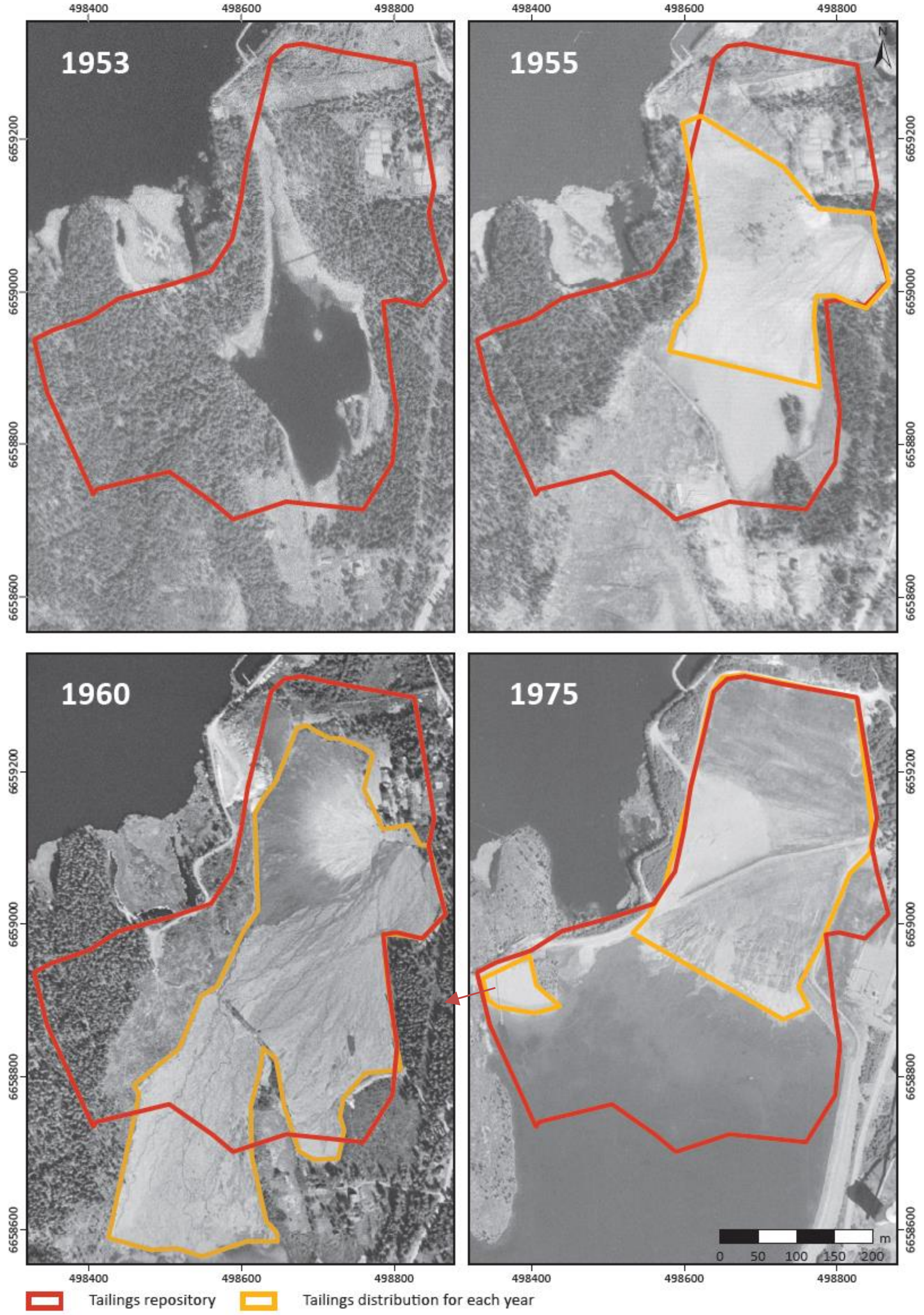

Figure 53. Historical orthophoto showing the evolution of the Jan-Matsdammen tailings repository. Photos: Läntmäteriet

Surface sampling results

Eight surface samples were collected at Jan-Matsdammen. Elevated concentrations of Fe, REE and phosphate were observed with an average of 16.2% Fe_2O_3, 0.19% REE and 5.4% P_2O_5 and elevated levels of V and Ti were also observed. The coarsest material near the release point marked in the aerial image from 1960 in CB_005 showed the lowest Fe, REE and P contents, while finer material showed significantly higher contents. A strong correlation was noted between REE and P_2O_5.

Geophysical measurements

At Jan-Matsdammen four geophysical methods were used to investigate the tailings deposits: ERT, IP, tTEM and RMT. Six profiles of ERT and IP measurements were conducted and along two of these profiles RMT measurements were also performed. The tTEM measurements covered approximately 1.5 km, also overlapping some of the ERT/IP profiles (fig. 54). The ERT and IP data are in general of high quality in this area, the measurements show correlation between each other but also outlines interesting differences. The RMT measurements were highly affected by the cultural noise in the area and the tTEM measurements had a limited access due to dense forest, the data that were collected did not show a significant response due to a high resistive layer at the top of the deposit.

The Jan-Matsdammen tailings deposit is under investigation (2022) for remining of the tailings by GRANGEX (Grängesberg Exploration Holding AB) and a scoping study has been published on their website (GRANGEX 2023). Results from drillings presented in the scooping study report have been valuable reference material when evaluating and interpreting the results from the geophysical measurements within this project. The location of the drillings used from GRANGEX and the two drillings performed within this project is shown in figure 54.

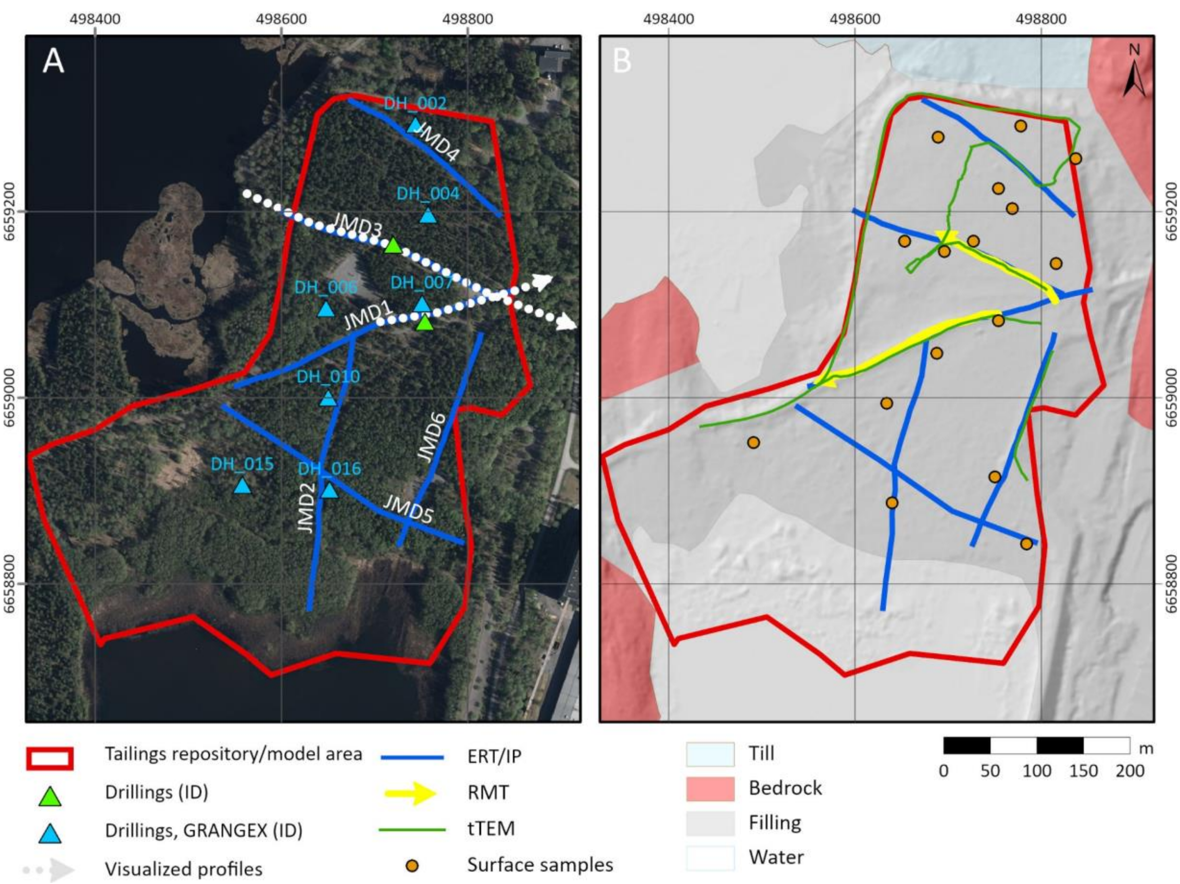

Figure 54. Geophysical measurement profiles, drilling and sampling locations at Jan-Matsdammen tailings repository in Grängesberg.

All ERT profiles show a high resistive layer at the top, about 10 meters thick, thinning out towards the lake Orrleken in the northwest and Jan-Matsdammen in the south of the area. At approximately 300 m.a.s.l. a low resistivity layer appears in all profiles which is interpreted as a groundwater level, it is also confirmed in one drilling (fig. 55). The resistivity within this layer is highest in the northernmost profile and the lowest in the southernmost profile. This is interpreted to correlate to the variation of water saturation in the sediments, with higher water-saturation closer to the lakes. The bottom of the tailings is not identifiable from the ERT measurements.

The tailing volume has been estimated. The input data has been the information from drillings and historical orthophotos. The deposition of the tailings started sometime between 1953 and 1955 and the distribution of the tailings has changed over time. The limits of the depositions are interpreted for each historical photo in figure 53 and the modelled area marked as the red area. As can be seen in the 1960s photo the depositions are more widespread than the model area boundary, and it can also be assumed that a lot of material is deposited in what today is covered by water in the Jan-Matsdammen. The calculated volume of sand is 1.43 million m^3 and should be seen as a low estimate. This compares well to the calculated value of 1.48 million m^3 stated in the scoping study (Lindholm, 2021) and an estimated tonnage of 2.55 Mt. From the ERT resistivity model about 60 percent of this is interpreted to consist of dry tailings deposits, i.e. located above the water table. A map of the thickness of the tailings deposits is presented in figure 57.

IP-data have been processed and inverted to obtain a phase model (called parameter phi). Data from all profiles but JMD2 (fig. 54) have been inverted and used to construct a 3D model. A high IP-effect is evident in the eastern part of the area at about four metres below the surface. Figure 57 B show a slice from the 3D-grid at the level of 302 m.a.s.l. masked to only show values above 27 milli radians (mrad). The figure shows a correlation between material with high IP-effect and vicinity to the discharge point and the area where a lot of material was deposited in the 1950s to the 1960s (compare with figure 53). There are three boreholes (DH_004, DH_007 and Borr_2_JMD) within this "high-IP" area which all show a significant increase in the Fe content at depth and at the level of high IP-effect in the material; figure 56 show the modelled IP parameter phi and one of these boreholes. This is an indication that older material had a higher Fe content and that this is giving rise to a high IP-effect observable in the data. These interpretations should be treated as indicative and a more thorough investigation, and probably more sampling and analyses, are needed to confirm or reject these hypotheses.

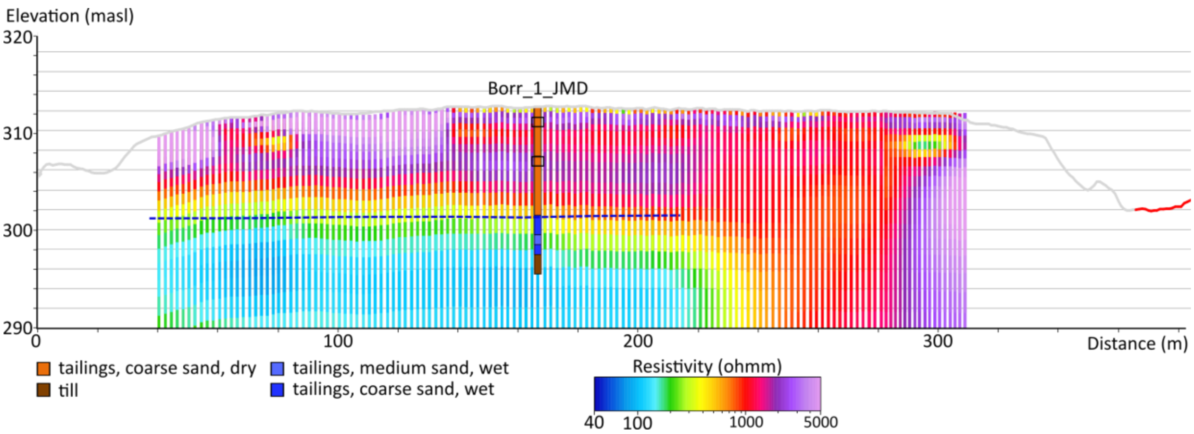

Figure 55. Cross section showing the resistivity and one borehole along profile JMD3 (white dotted arrow in figure 54A). The blue dashed line shows the interpreted water table. The line for the elevation is colour coded from the quaternary deposits shown in figure 54B.

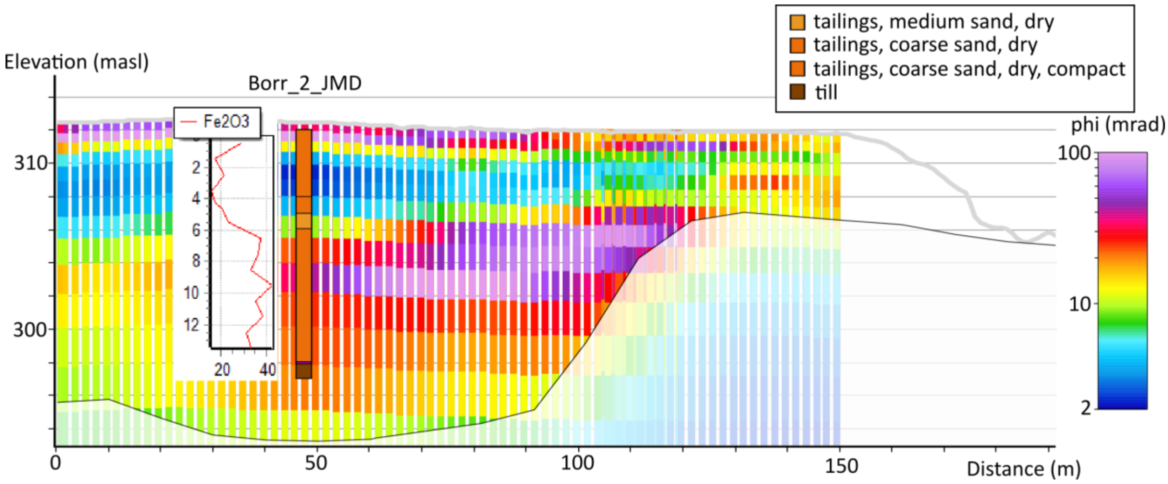

Figure 56. Cross section showing the IP-effect in terms of phi, along part of profile JMD1 (white dotted arrow in figure CB_004). In the figure is also shown a borehole with the results from chemical analysis of Fe_2O_3 (depth on the y-axis and percentage Fe_2O_3 on the x-axis). The white transparent area shows the area below the depth of investigation (DOI) for the IP-models.

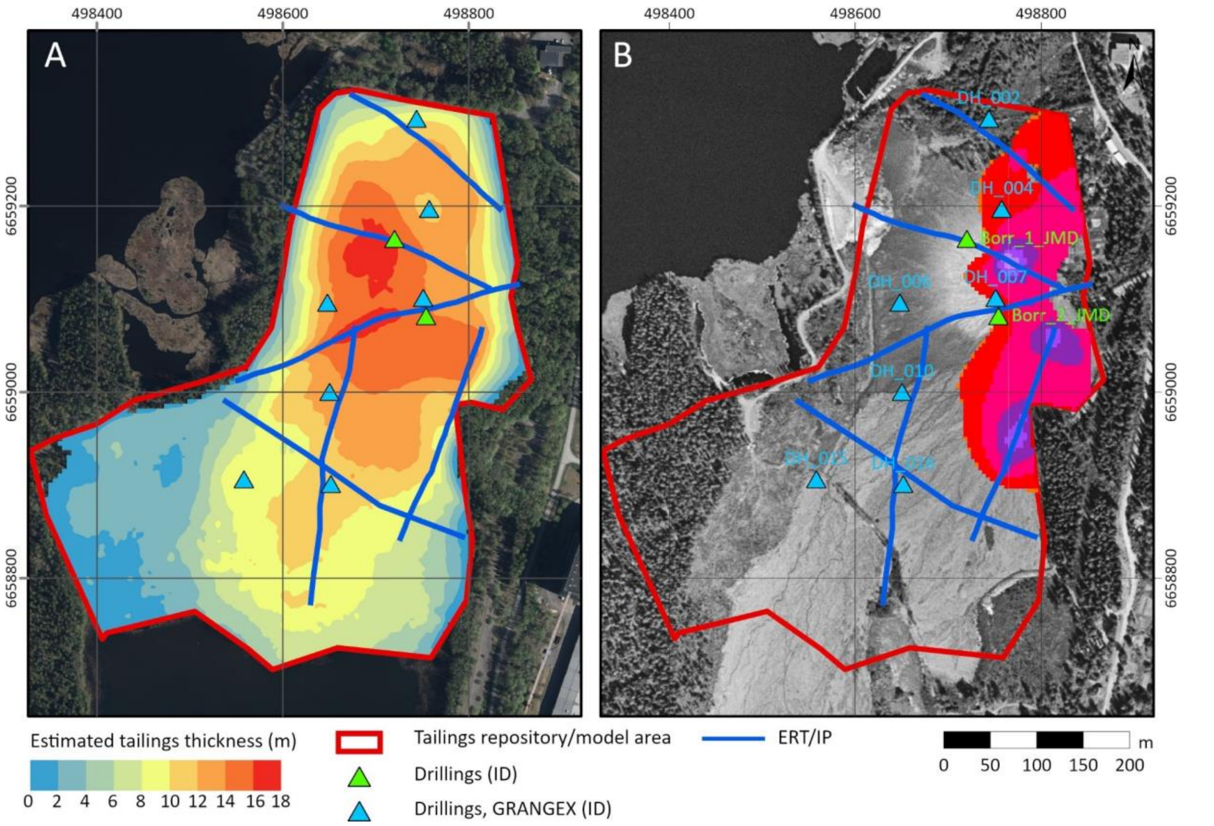

Figure 57. A. Modelled tailing thickness. **B**. Material with high IP-effect in the vicinity to the discharge point. The coloured area represents interpolated phi values to a 3D grid which is sliced at 302 m.a.s.l and masked to show values above 27 mrad (colour scale same as shown in figure 56).

Drilling results

Two boreholes were drilled at Jan-Matsdammen for sampling of tailings at depth. These sites were chosen based on concentrations of CRM in the analysed surface samples and variations in the properties of the tailings identified in the geophysical models.

Borehole 1 Jan-Matsdammen (BH1_JMD; 6659166/498720) was drilled in the vicinity of an outflow point as seen in the historic aerial photos taken of Grängesberg (fig. 53). Vegetation at the drilling location was dense pine forest. Tailings at the surface were coarse sand with occasional larger grains up to 1 cm in size. The tailings were dark in colour due to the presence of Fe-oxide minerals and rich in large flakes of mica. The depth of the borehole was 15 metres, and the bottom was a thin layer of peat overlaying till.

Analyses showed high levels of P_2O_5 and elevated levels of Fe_2O_3 and high levels of REE. Fe contents ranged between 12 and 22% with the highest values nearest the surface, decreasing with depth, and increasing again towards the bottom. Phosphate levels were between 4 and 6% and showed only a minor increase towards the bottom of the borehole. REE varied between 1700–2100 ppm, and generally correlated to P concentrations (fig. 58).

Grain size was consistent throughout the borehole, varying from coarse to medium sand with very little silt component. Sieving of samples showed that 60% of the tailings were over 200 µm in size.

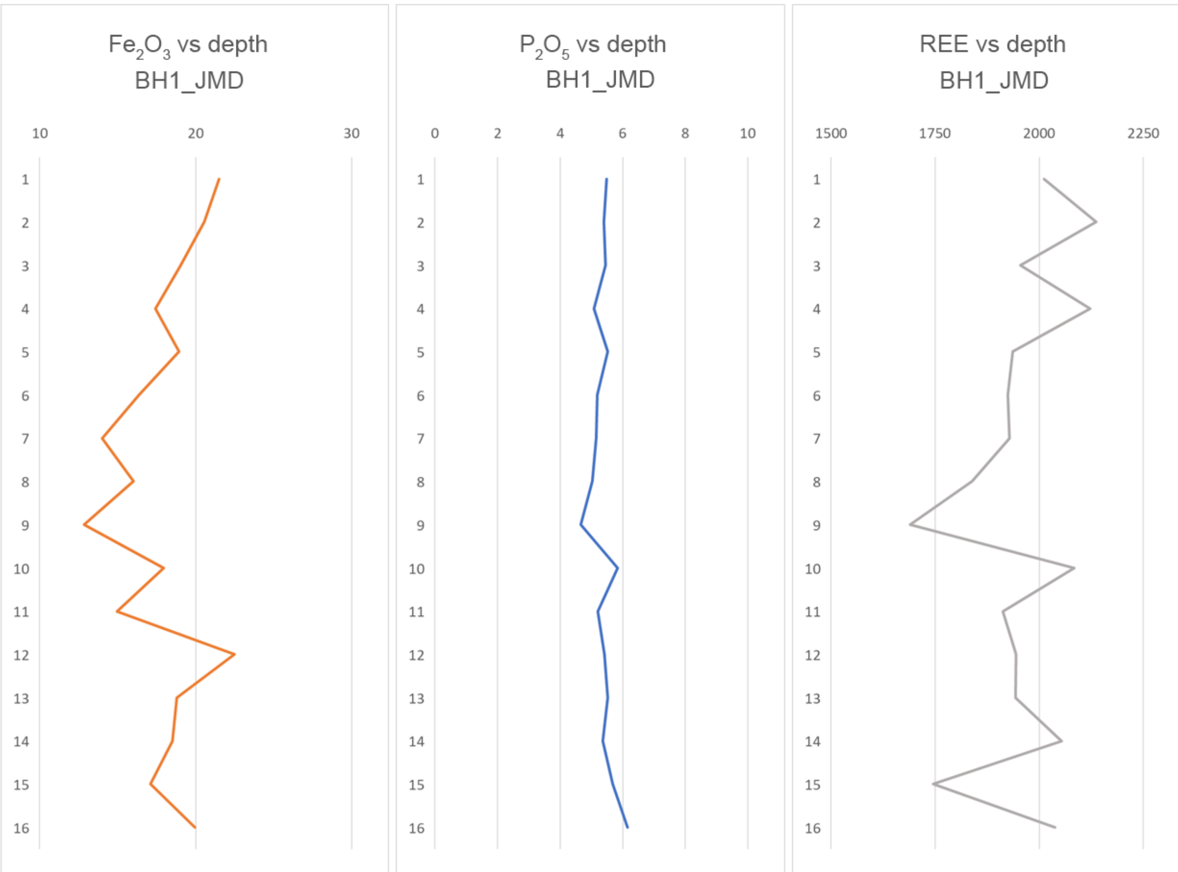

Figure 58. Iron-oxide, phosphate and total REE concentrations along the depth profile in BH1_JMD

Borehole 2 Jan-Matsdammen (BH2_JMD; 6659083/498754) was drilled between two outflow points observed in the historic aerial photo and was chosen based on an anomalous layer of lower resistivity between 4–5 metres observed by geophysical investigations. The depth of the borehole here was 16 metres. The tailings were similar to that of BH1_JMD, coarse sand, and with a limited silt fraction. They became wetter towards the bottom as the groundwater layer was reached at around 13 metres. An anomalous layer at 4 metres was very dry and hard packed. Historic aerial photos indicate that the borehole drilled through an old road across the tailings, and this layer was likely the compacted tailings produced by traffic over the road. The anomalously low resistivity may be due to alignment of grains due to compaction within this layer.

Geochemical analysis showed notably higher levels of Fe in the tailings when compared to borehole BH1_JMD. Fe decreases through the first 4 metres before rising rapidly to over 30%. Phosphate and REE concentrations are more correlated than in BH1_JMD (fig 59).

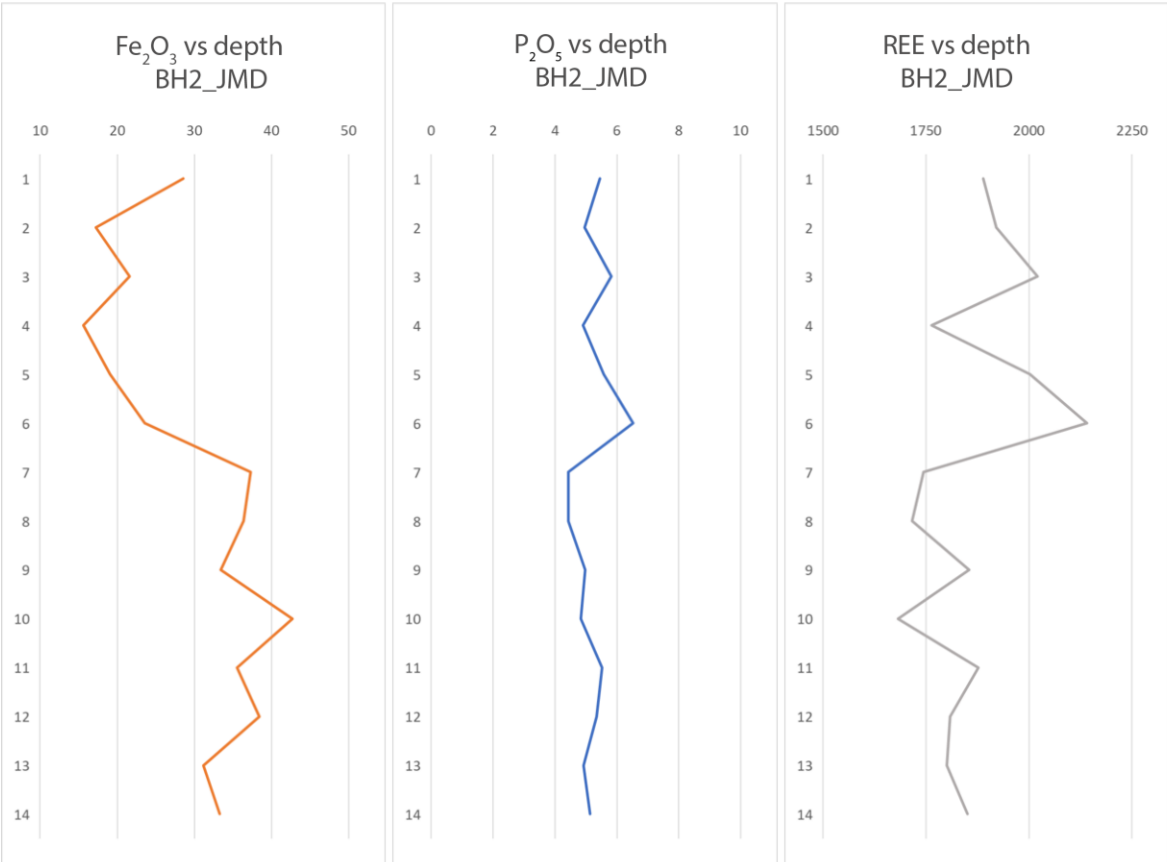

Figure 59. Iron-oxide, phosphate and total REE concentrations along the depth profile in BH2_JMD.

Discussion

Analyses showed rather consistent values for P and REE between boreholes. Iron shows significantly higher values in BH2_JMD, with concentrations exceeding 30 percent in the bottom 7 metres. This may be a result of the location of the borehole relative to the release point for the material where the heavier Fe-oxide minerals were not transported with lighter material in suspension or more efficient recovery percentages over time. Phosphorus and REE content of the drilled samples were in broad agreement with the average results of the surface sampling, with average concentrations of 5.4% P_2O_5, 0.17% REE and 22% Fe_2O_3. Concentrations of Ti averaged 980 ppm and V concentrations averaged 395 ppm. The high values for phosphate and REE indicate that only Fe was extracted at the concentrators during the period Jan-Matsdammen used for deposition of tailings. Chondrite normalised REE values show enrichment in LREE, with a moderate negative Eu anomaly.

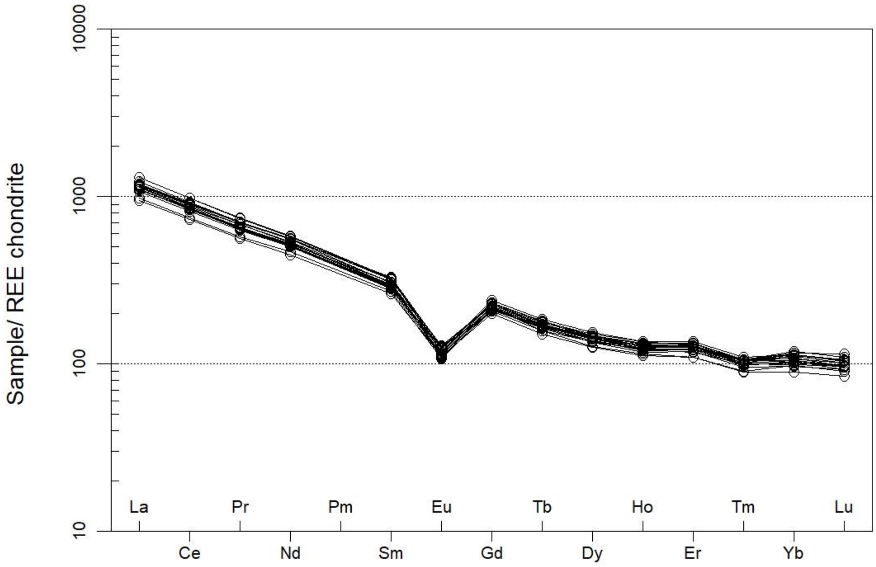

Figure 60. Chondrite normalised REE diagram of tailings from Jan-Matsdammen. Chondrite values are from Boynton (1984).

Table 21. Analytical results of tailings from Jan-Matsdammen.

Data	Object		Fe_2O_3 (%)	P_2O_5 (%)	REE (%)	V (ppm)	Ti (ppm)
Tailings (surface)	Jan-	Average	15.9	5.0	0.19	253	1118
	Matsdammen	Max	29.3	6.8	0.23	428	1530
	(n=8)	Min	8.0	1.2	0.07	117	880
Drilled Tailings	Jan-		22.8	5.3	0.19	395	980
	Matsdammen		42.7	6.5	0.22	662	1530
	(n=34)		12.9	4.4	0.17	233	770

Hötjärnen

Hötjärnen is the largest of the three tailings repositories in Grängesberg (fig. 61), in both surface area (430,000 m^2) and volume. Geophysical measurements showed an average depth of approximately 20 metres. The deepest sections of Hötjärnen reach up to 30 metres depth. The surface of the repository is flat, and in most areas sparsely vegetated with small evergreen trees and sedges dominating. The sand at the surface is coarse and black and rich in Fe-oxides.

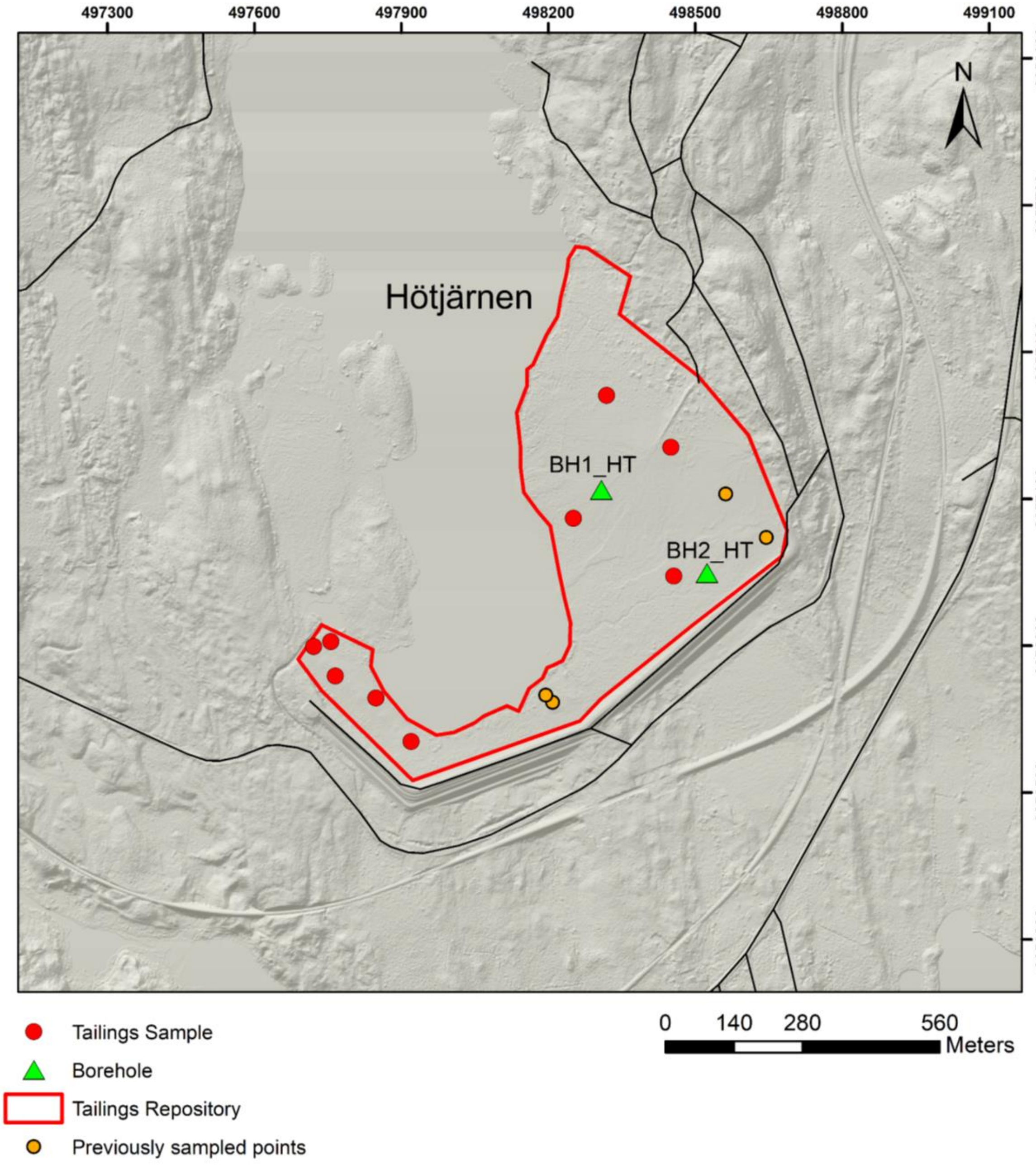

Figure 61. LiDAR map showing the boundaries of the Hötjärnen tailings repository with samples taken in 2021 in red, and prior sampling points in orange.

Geophysical measurements

The Hötjärnen tailings deposits is well suited for different geophysical measurements. It is easily accessible with car, mostly open or sparsely vegetated and flat. ERT and IP measurements were performed in two campaigns resulting in a total of seven profiles covering 2.6 kilometres (fig. 62). tTEM measurement were concentrated in the south-eastern corner of the respiratory and covered in total of 4.0 kilometres. In addition, two RMT profiles were measured along two of the measured ERT/IP profiles (fig. 62). Most data are of high quality, with good responses and in general a very good agreement with each other, however the IP-data are in general quite noisy. The processing and inversion of IP data set in this area is yet not fully satisfactory and will not be discussed here.

The results from ERT, RMT and some of the tTEM measurements have been used to identify the bottom of the tailings sand to calculate the tailings deposits volume. The pattern of the resistivity is exemplified by figure 63. Nearest to the surface is a 2-meter-thick high resistivity layer, which is thinning out and disappearing towards west, in vicinity to the dam. This is interpreted as dry tailings deposits, above the water table, with more water saturation closer to the dam. In the east of the profile, the underlying bedrock appears as a high resistive contrast which dips towards southwest, the same pattern is evident both in the RMT- and tTEM models. Further west, the bedrock cannot be identified, but the bottom of the tailings sand is interpreted as following the bottom of the low resistivity layer (grey line in figure 63). The tailings deposits show large variations in resistivity, with alternating high and low resistivity layers and zones. From the drilling one can observe a change in grainsize approximately at the shift in resistivity at 15 metres depth. A shift is also evident in the density, and for several elements (fig. 64) which is further discussed in the sections below. Relating all these parameters need further studies to outline, however it is possible to identify high or low resistive areas within the tailings. If the REE is related to smaller particle sizes which in turn determine the resistivity, then the resistivity models may provide a possibility of mapping REE content in the material.

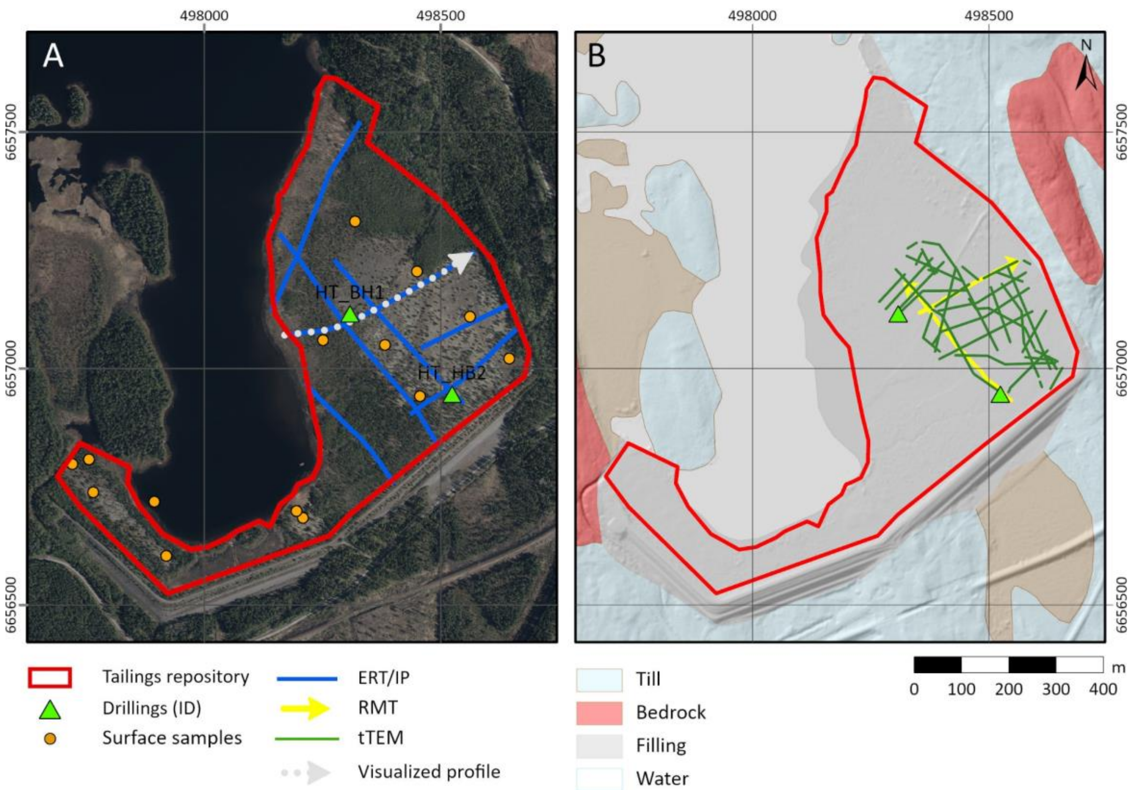

Figure 62. Geophysical measurement profiles, drilling and sampling locations at Hötjärnen tailings repository in Grängesberg.

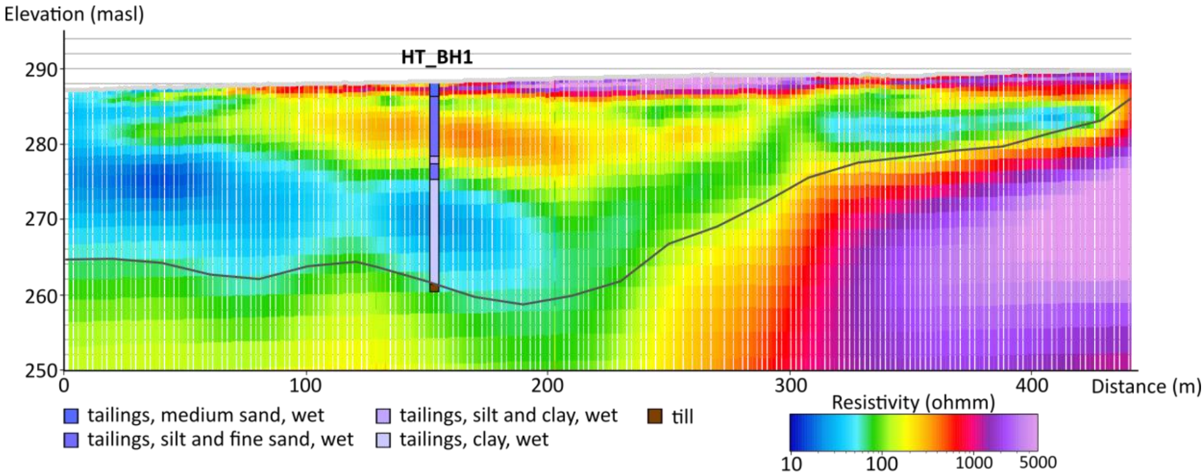

Figure 63. Cross section showing the resistivity from inversion of ERT data and one borehole along the white dotted line in figure 62. The dark grey line shows the interpreted bottom of the tailings deposit.

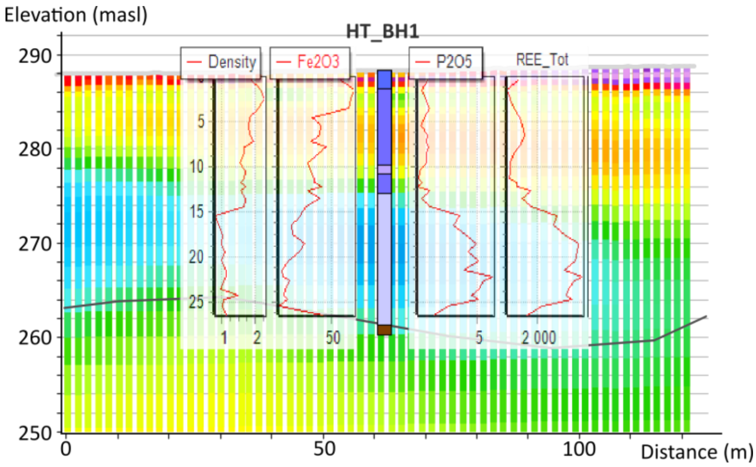

Figure 64. Zoomed in part of cross section shown in figure 63 with results from density measurements and geochemical analysis of Fe_2O_3, P_2O_5 and REE total (depth on the y-axis and percentage for Fe_2O_3, P_2O_5 and ppm for REE_tot on x-axis).

The bottom of tailings has been interpreted from the geophysical data, drillings, LiDAR and historical orthophotos, and a 3D model has been constructed. From this model the volume of the tailings is estimated to be $4.13 \cdot 10^6$ m^3, with a tonnage estimated at ~8 Mt. The model only covers area with geophysical measurements and here a model of tailings thickness has been constructed (fig. 65A). Figure 65B shows a historical orthophoto with reference year 1960 where no tailings yet have been deposited. In the area is a smaller lake and it can be assumed that this is probably the location of the thickest tailings deposits, which is also indicated in figure 65A.

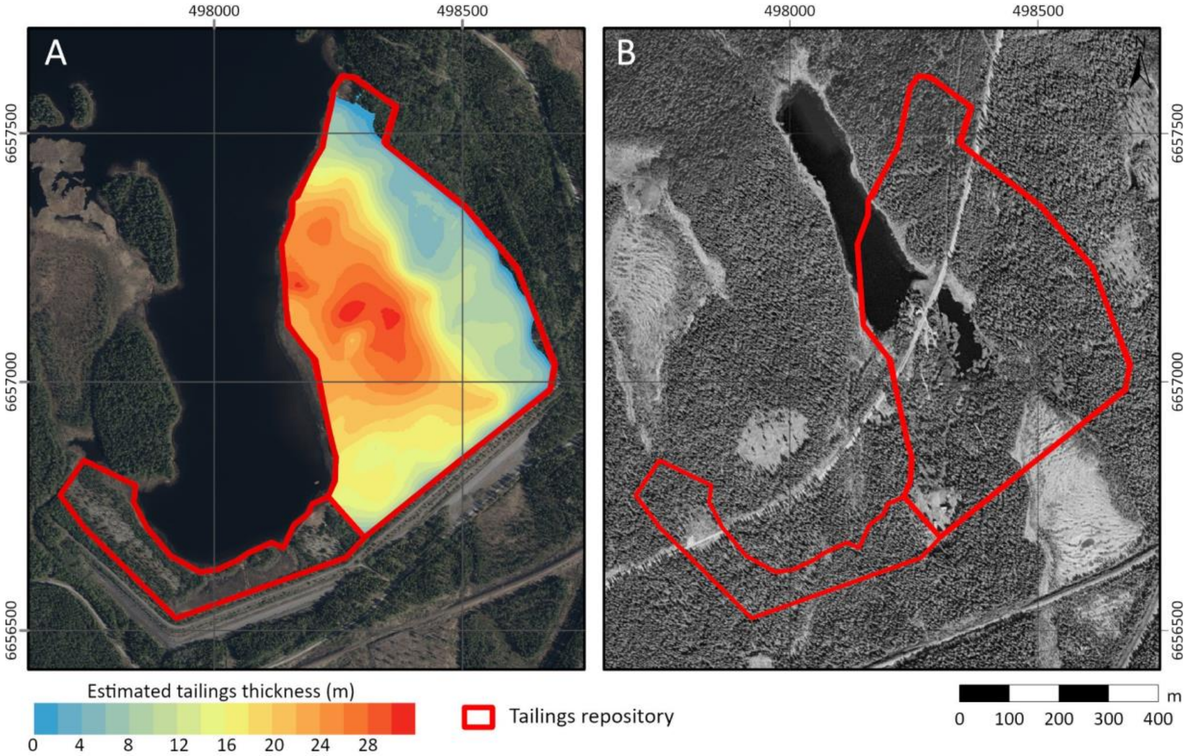

Figure 65. A. Modelled tailing thickness. **B.** Historical orthophoto, reference year 1960.

Surface sampling results

A total of 10 surface samples were taken at Hötjärnen. Most samples were taken from the south-eastern side of the tailings dam to get a better spread of concentrations where previous sampling had not been conducted. The tailings at the surface were typically medium sand with a high mica and Fe-oxide fraction. High levels of Fe were observed, averaging 37%, as well as lower levels of phosphate. REE levels were consistent with those at Jan-Matsdammen, despite lower phosphate levels.

Drilling results

Two boreholes were drilled at Hötjärnen BH1_HT and BH2_HT. BH1_HT had a depth of 27 metres and BH2_HT was drilled in sediment with a total depth of 21 metres, however, only the upper 10 metres were sampled.

Borehole 1 Hötjärnen (BH1_HT; 6657118/498308) was the deepest borehole drilled in Grängesberg at 27 metres. Based on historic aerial photos the borehole was drilled at a location that was previously near the centre of the lake that existed before being filled with tailings. The surface of the drilling site was covered by small sedges and small pine trees. The sand at the surface was dark black in colour and appeared to be made up predominantly of Fe-oxides. The water table was reached after 2 metres. At 14–15 metres BH1_HT showed a distinct shift in the properties of the tailings. The sediment transitioned from grey, mica rich, medium to fine sand to a very fine silt to clay like material (fig.66), typically a rusty red in colour with fine laminations. This silty clay like material is likely the finest fraction from the tailings that were released, which remained in suspension and settled out further from the discharge point. The cause of the oxidation that gives these sediments their red colour is unclear, however the small particle size may increase the oxidative rate. The increase in size of the tailings moving upwards through the borehole is likely due to changes in the sedimentary regime as the lake filled with the coarsest material being deposited on the top.

The transition from sand to silt is also noted within the geochemical analyses. The charts showing differences in P_2O_5, Fe_2O_3 and REE concentrations along depth show the upper 5 metres of the borehole had extremely high quantities of Fe, between 50 and 68%, dropping off around 5 metres, and again at 14 metres (fig. 67). Phosphorus shows concentrations of between 1 and 2% P_2O_5 between the surface and 14 metres, where it rapidly increases in the silty sediment to between 4 and 6 % and REE follow a similar trend to P.

Figure 66. Tailings in BH1_HT at **A.** the surface) and **B.** after the transition to the silty tailings. Photo: Patrick Casey

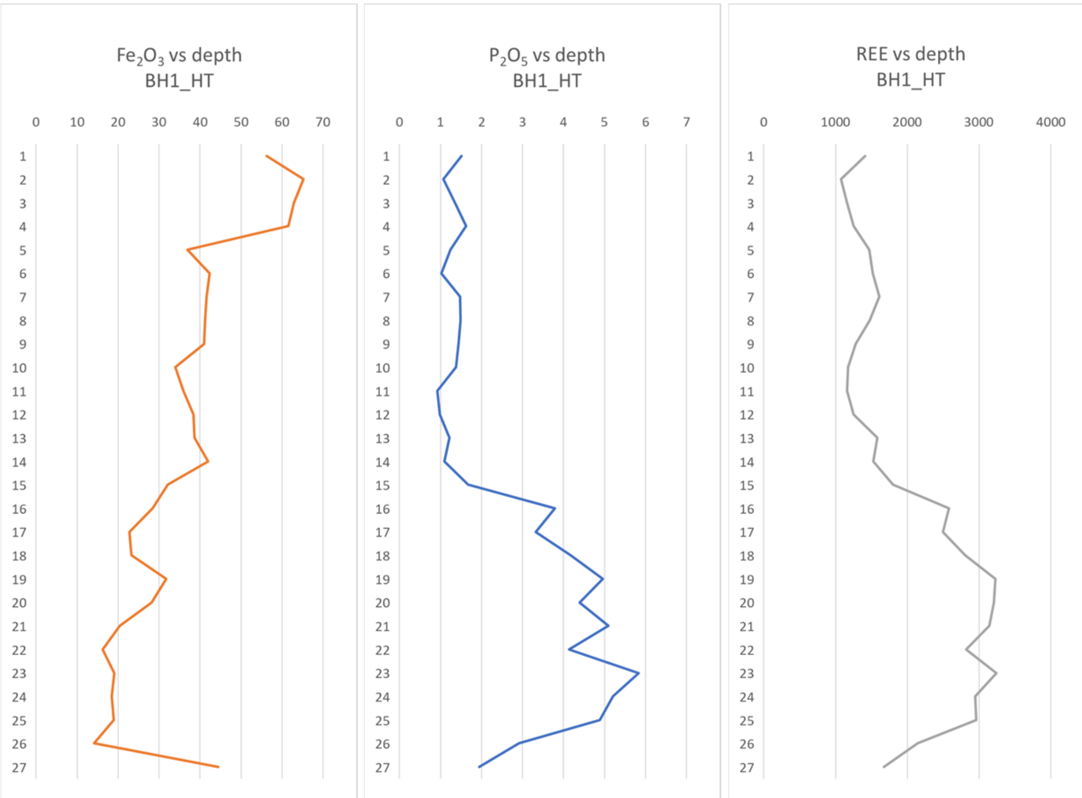

Figure 67. Fe-oxide, phosphate and total REE concentrations along the depth profile in BH1_HT.

Borehole 2 Hötjärnen (BH2_HT; 6656948/498524) was drilled closer to the retaining wall of the tailings dam. Here the sand was greyer in colour and notably more mica rich. The depth to the bottom of the sediment was measured to be 21 metres, however due to time constraints a complete profile was not sampled. The material in this hole was dominantly sandy with occasional silty bands of around 3–5 cm width. from around 12 metres the material became much more dominated by silt, with red silt bands occurring, similar to BH1_HT.

As observed in BH1_HT, this siltier material deeper in the profile showed a decrease in Fe, and a sharp increase in P_2O_5. REE contents at this site were typically over 2000 ppm, significantly higher than the upper 14 metres in BH1_HT, despite similar P_2O_5 concentrations (fig. 68).

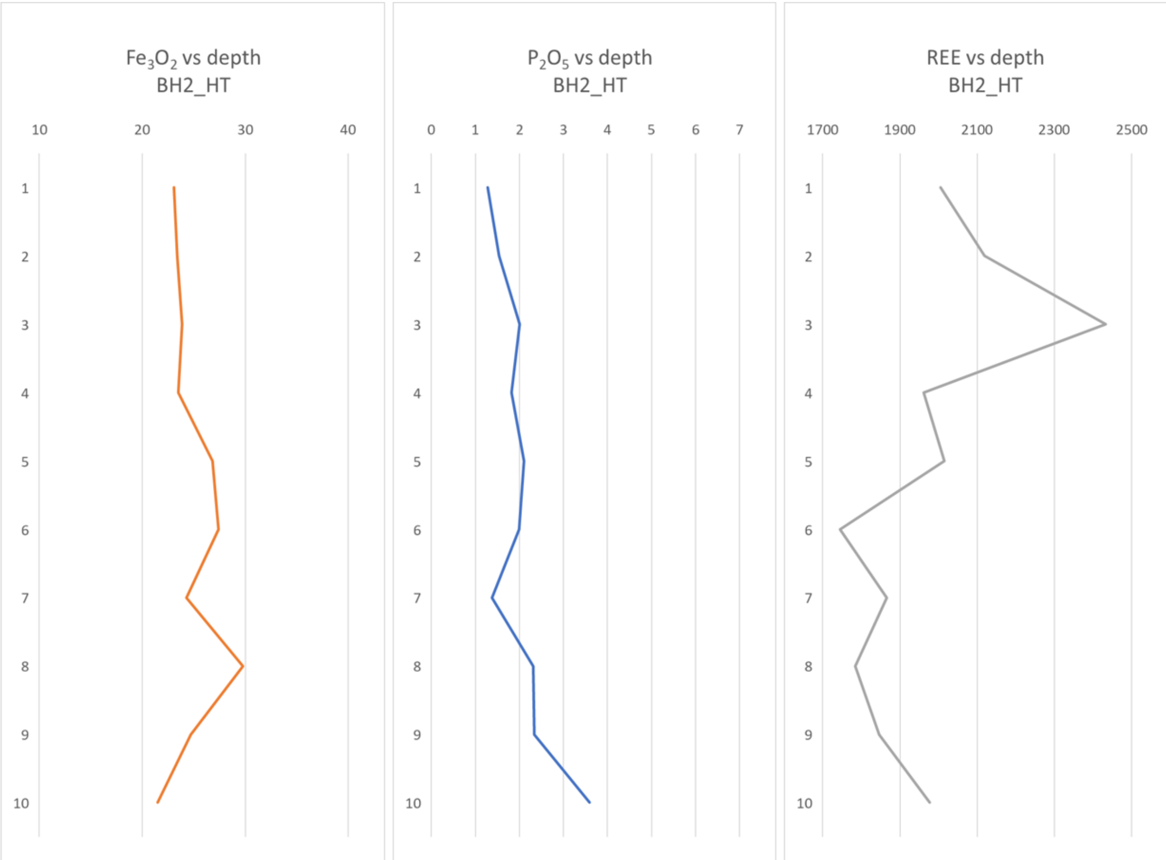

Figure 68. Variations in iron-oxide, phosphate and total REE along the depth profile in BH2_HT

Discussion

Iron-oxide contents in Hötjärnen are considerably higher in the upper levels of the sediment compared to the other repositories in Grängesberg. Surface sampling showed an average content of 38% Fe_2O_3, and results from borehole analysis show high levels of Fe_2O_3 in the upper 6 metres of up to 65%. This indicates poor recovery of Fe towards the end of production. A trend is seen with lower P_2O_5 levels where Fe levels are higher. This may point to preferential recovery of phosphorus at the end of the life of the processing plant, disposing of the Fe with the rest of the gangue fraction. REE levels in BH1_HT shows fairly strong correlation with phosphate, while BH2_HT shows a poor correlation. This may indicate that large amounts of REE may not be contained within apatite, and instead the sand contains high abundances of monazite, xenotime and allanite, which were not recovered through the methods used to separate the apatite.

Table 22. Analytical results from Grängesberg, Hötjärnen

Data	Object		Fe_2O_3 (%)	P_2O_5 (%)	REE (%)	V (ppm)	Ti (ppm)
Tailings (surface)	Hötjärnen (n=10)	Average	37.3	1.3	0.18	649	1008
		Max	57.2	2.0	0.25	914	1490
		Min	24.9	0.7	0.12	428	660
Drilled Tailings	Hötjärnen (n=46)		31.6	2.39	0.20	530	1295
			65.2	6.19	0.34	1055	2450
			14.2	0.8	0.11	292	630

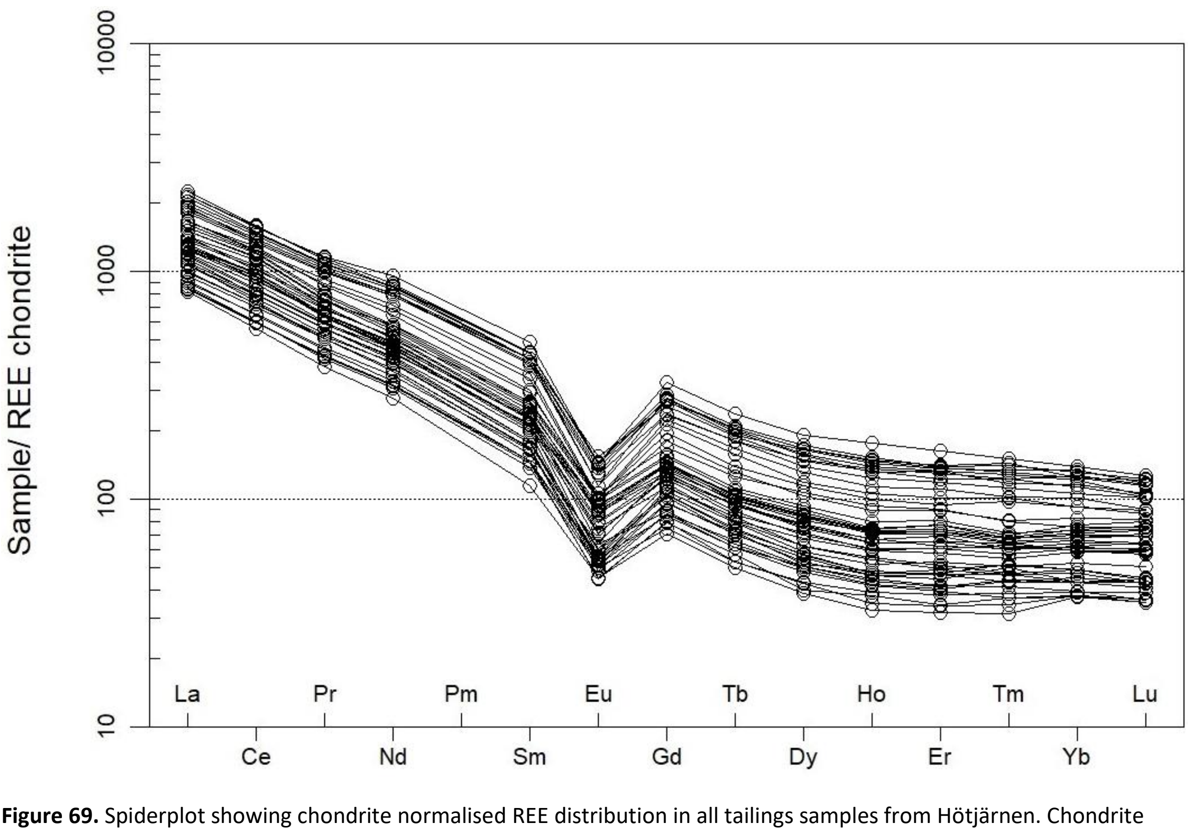

Figure 69. Spiderplot showing chondrite normalised REE distribution in all tailings samples from Hötjärnen. Chondrite values from Boynton (1984).

A distinct increase in the levels of P and REE is at approximately 15 metres depth, where the material becomes an extremely fine-grained muddy silt while Fe levels decrease. An increase in phosphate is seen also seen in BH2_HT below 10 m, nearly doubling in concentration.

This may be a result of sedimentary processes discussed above, where very fine grained, less dense material was carried further into the tailings pond during deposition or indicate a shift towards extraction of apatite starting at the 15-metre level. This finer material contains on average 0.26% REE. The fine material also contains higher concentrations of other heavy metals compared to the upper layers, showing enrichment in Zn, Co, Ni, Pb, As, and W. Concentrations of Sn are significantly lower in the drilled tailings than those in the surface samples likely reflecting the lower levels of Fe-oxides below the first few metres of the surface. The normalised REE distribution shown in figure 69 remains consistent for all samples regardless of REE content, with an enrichment in LREE, a negative Eu anomaly, and relative depletion in HREE in most samples, though a wide spread in concentrations is seen.

A heavy mineral separate of tailings was examined using SEM and EDS analysis. These analyses showed abundant magnetite and monazite. Monazite in Hötjärnen showed higher levels of Th than monazite in the mineralised samples from Grängesberg, averaging 2% Th. Additionally, small crystals of thorite were observed in association with monazite shown in figure 70.

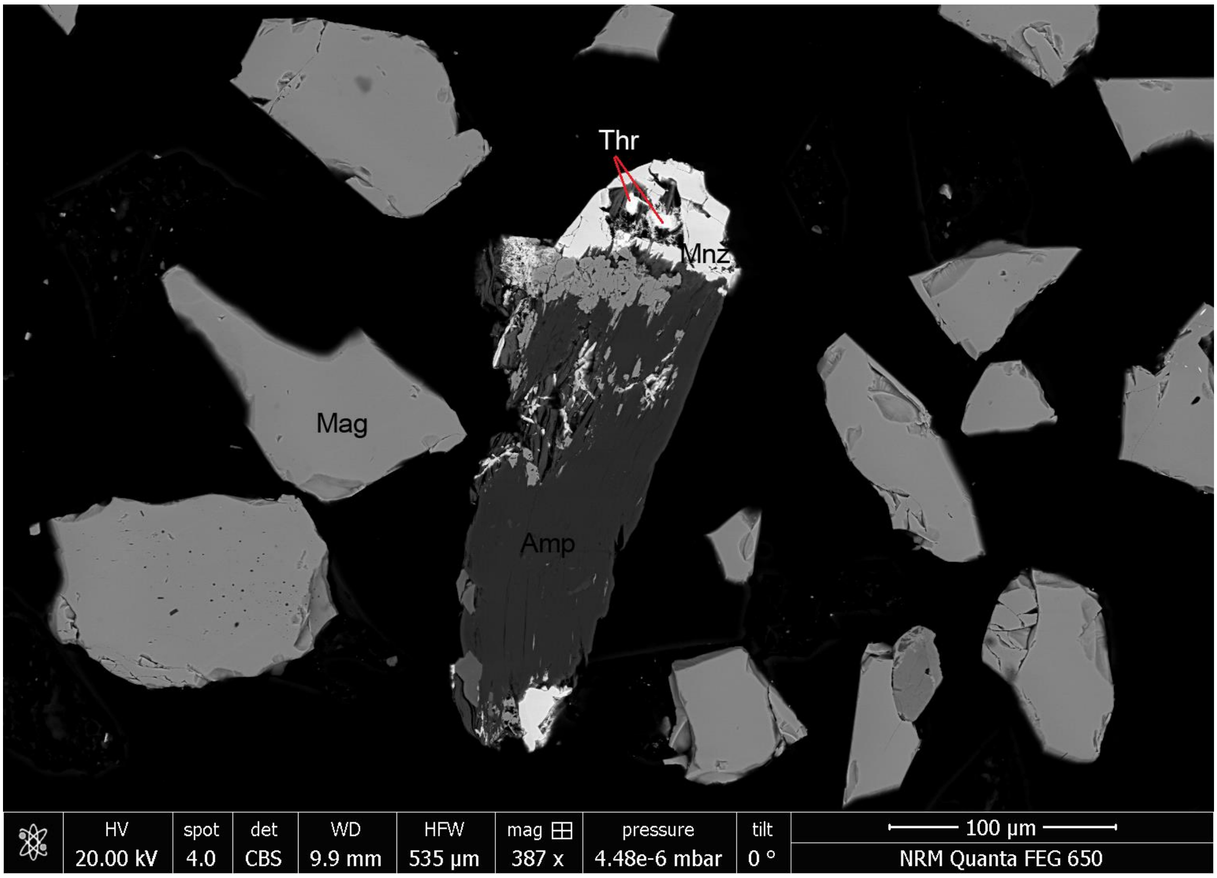

Figure 70. Backscatter electron image of tailings concentrate from Hötjärnen showing magnetite grains and high Th monazite growing within amphibole. The two bright white spots indicated with red lines are thorite crystals. Micrograph: Patrick Casey.

XRD analysis of tailings

A sample of tailings from each tailings dam was analysed using XRD to determine the mineralogy of gangue minerals. The results for each tailings repository showed a similar make up of minerals: quartz, biotite, actinolite, chlorite, hornblende, albite and microcline.

Grängesberg tailings discussion

Results from the three tailings ponds showed distinct differences in their contents of CRM (Fig 71). Hötjärnen showed the highest levels of REE, with an average content of 1900 ppm REE, and significantly lower values for phosphate, averaging 2.2 % by weight. Jan-Matsdammen showed the highest values for phosphorus with an average of 5.2% P_2O_5 and 1800 ppm REE. Svandammen showed the lowest values of P and REE of the three tailings repositories, with approximately 1% P and 0.1% REE on average.

The differences in the contents of the three tailings repositories is likely due to differing methods of extraction and refinement of the ore, as well as differences in the composition of the ore processed. At Jan-Matsdammen, the oldest of the tailings ponds, Fe was likely the only resource extracted, leaving a concentrate rich in P and other REE rich components. Processing of an apatite concentrate was carried out at Grängesberg in the 1980s, and likely also earlier. According to Hammergren (1988, unpublished report) 80 kt of apatite concentrates a year were produced at Grängesberg, and thus the lower phosphorus levels in the upper tailings at Hötjärnen, and at Svandammen, may be due to the extraction of apatite during the refinement process. In figure 72 a decoupling in the correlation of REE to phosphate can be seen in the Hötjärnen drill samples, which is likely related to the extract of phosphorus. Interestingly, despite the lower contents of phosphorus at Hötjärnen, the REE content remains roughly the same as that of Jan-Matsdammen, indicating higher REE concentrations in apatite, or a higher percentage of REE in other REE rich phases such as monazite, xenotime and allanite. Hammergren (1988, unpublished report) indicated that approximately 35% of REE remained in the tailings after removal of the apatite, as monazite and other REE rich phases fell out during production of the concentrate. The geochemical results show in HT_BH1 30–40% of the total REE is seen in the upper tailings compared to the lower sections of the borehole, which may point to the lower concentrations of phosphate as being related to the production of the apatite concentrate.

Potential resources in tailings at Grängesberg

Based on geophysical measurements a total tonnage of 14.14 Mt of tailings was calculated for Grängesberg. A weighed average of concentrations of CRM was taken weighted towards the tonnage of sand in each tailings dam. In the three tailings dams studied in Grängesberg, assuming that all material is recoverable, and that no tailings have been removed there is a potential for 2.2 Mt Fe, 156 kt P, 21.5 kt REE, 17.5 kt Ti and 5.7 tonnes V.

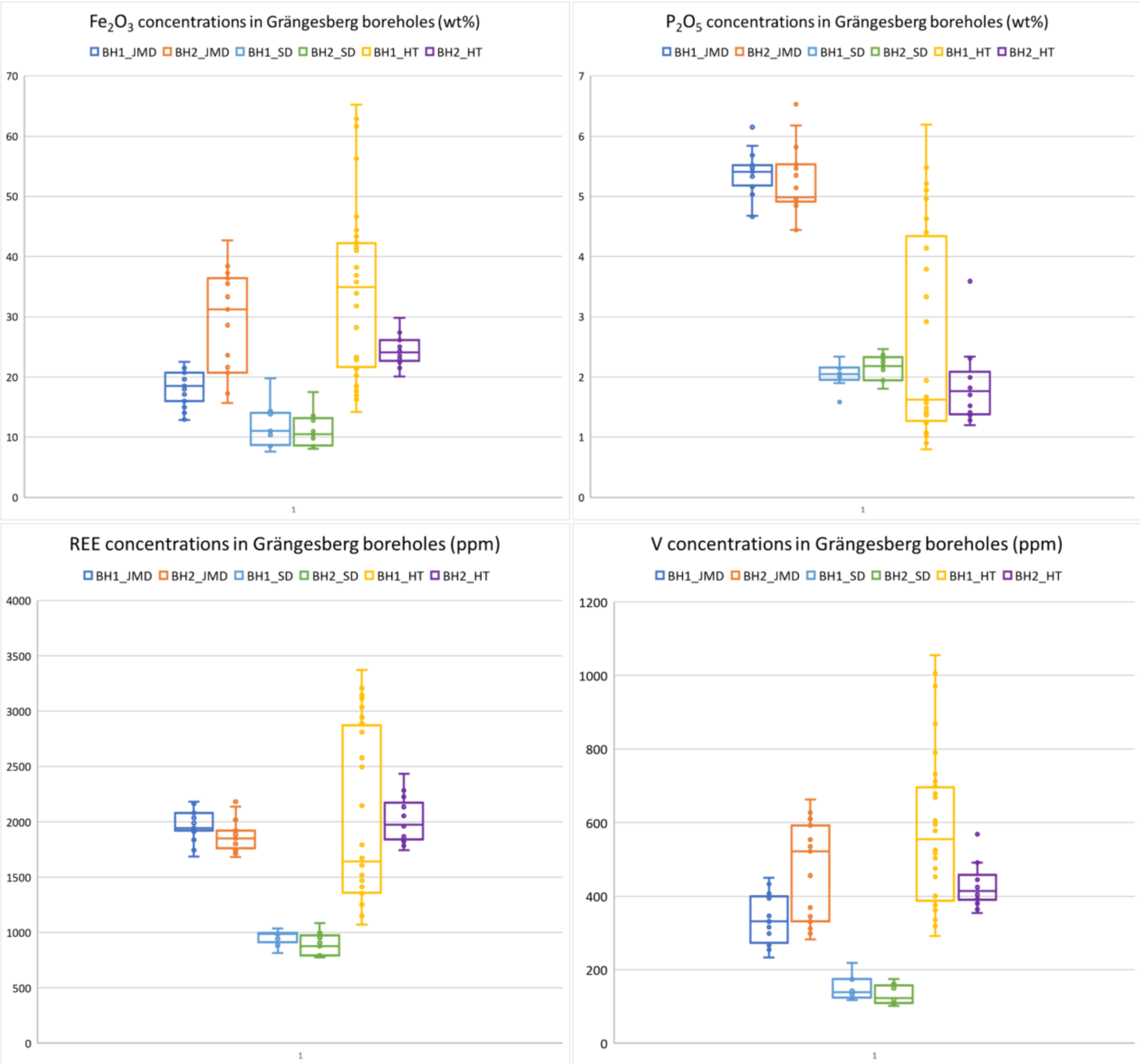

Figure 71. Box and whisker plots of concentrations of CRM in the Grängesberg boreholes.

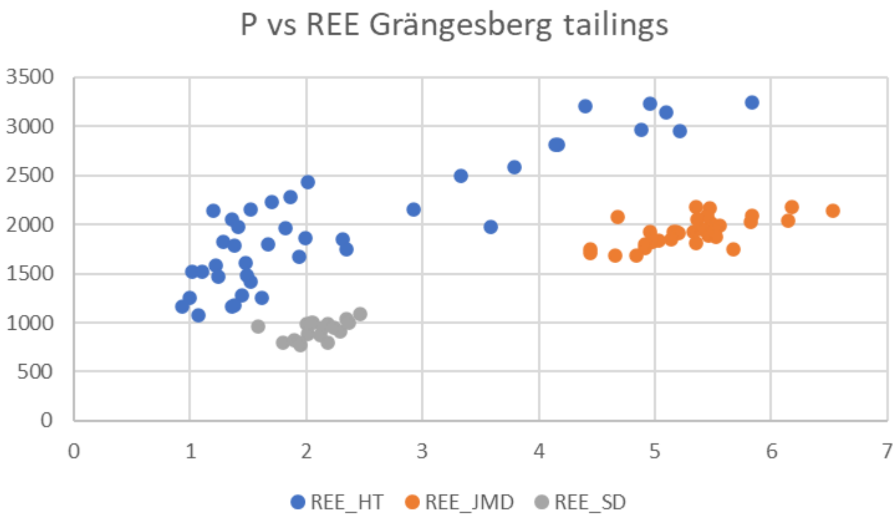

Figure 72. Relationship between phosphate (x-axis) and REE (y-axis) in tailings from Grängesberg. HT = Hötjärnen, JMD = Jan Matsdammen, SD = Svandammen.

Blötberget

Background

Blötberget (Sweref 6665277/504461) is an Fe-oxide-apatite deposit roughly 6 km northeast of Grängesberg (fig. 73) and was likely co-magmatic to the Grängesberg deposit. The Blötberget area has been mined for Fe ore at small scale since at least 1664. Large scale mining operations began in 1859 and the mine operated for the years 1859–1863, 1891, 1896–1897, 1900–1979.

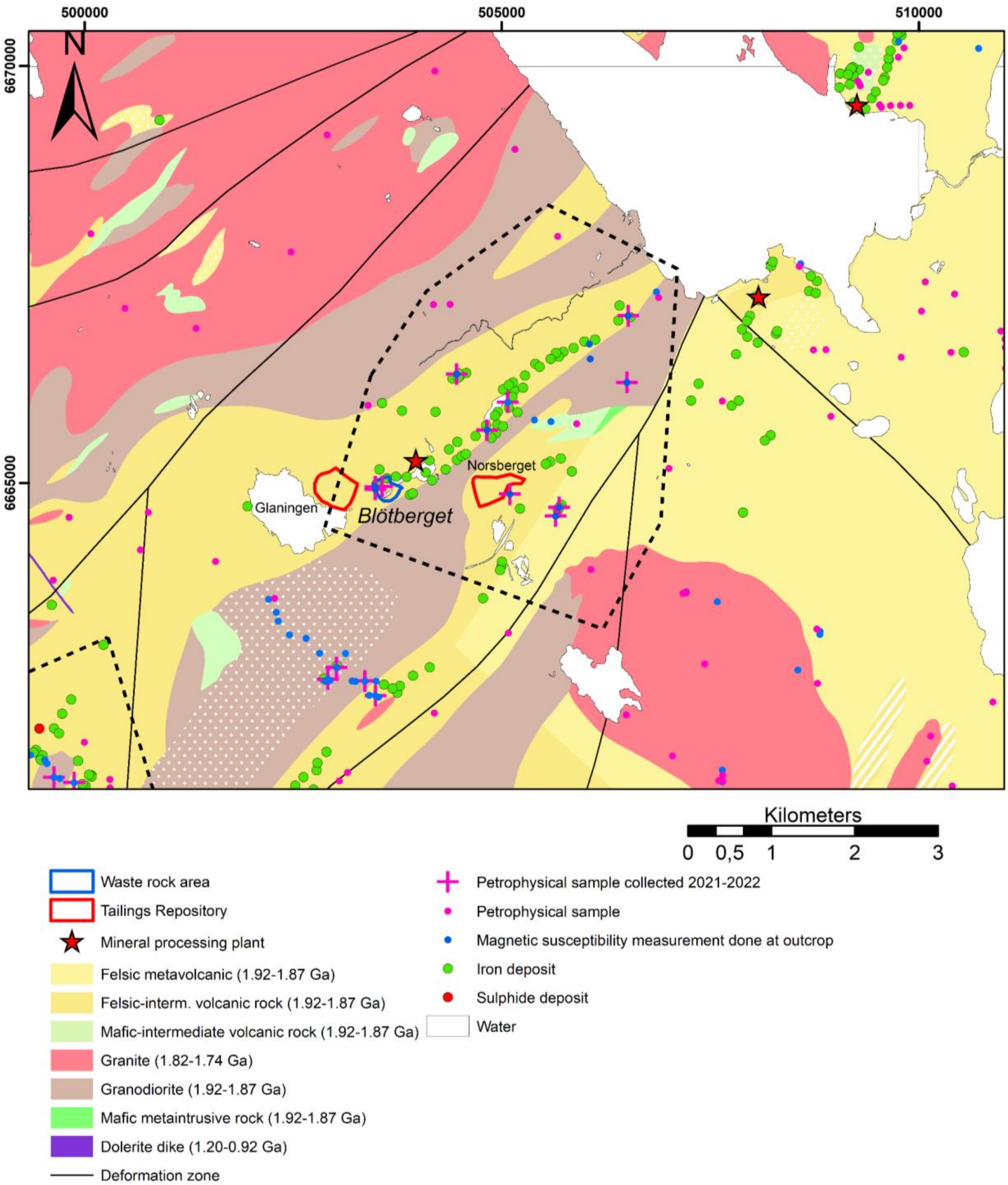

Figure 73. Bedrock map of the area surrounding Blötberget showing petrophysical and geophysical investigation points.

Approximately 15.8 Mt (table 23) of ore was produced from Blötberget until its closure in 1979 producing 4.21 Mt of waste rock (Svenskt Stål AB, 1981). Like Grängesberg, Blötberget contains rich Fe ore that is dominantly composed of magnetite with minor haematite and apatite. The host rock of the ore is the intermediate to felsic metavolcanic rock that dominates the metallogenic regions of Bergslagen. Pegmatite intrusions are common, cutting through the Fe ore bodies. Fe ore is also found in thin veins in granitic host rock, pointing to potential remobilization of the Fe during metamorphism.

Much of the ore was produced as lump ore, and less rich ore was processed in a dressing plant on-site using magnetic separation methods. 5.6 Mt of concentrate was produced, with 4.7 Mt of sand deposited in two tailings dams. The first tailings pond used was near lake Glaningen, and a second dry deposit dam was constructed to the east of Blötberget at Norsberget and was used from around 1960 until the closure of the mine. Estimated mineral reserves at Blötberget are 55 Mt of Fe, with an inferred estimate of an additional 11.8 Mt down to the 800-metre level (Nordic Fe Ore, 2014). A mining permit was granted to Nordic Fe Ore in 2010 who are in the process of attempting to restart production at Blötberget.

Table 23. Ore production and waste produced at Blötberget. Data from SGU's MALMdb.

Data	Object	Tonnage (Mt)	Fe_2O_3 (%)	P_2O_5 (%)
Mined ore	Blötberget	15.8	39.6	0.49
Reserves		66.8	41.7	
Waste rock generated		4.2		
Tailings produced		4.7		

Available geophysical data

Airborne data (magnetic, VLF, gamma spectrometry)

As part of this project an area around Blötberget was selected for additional bedrock mapping efforts. The motivation for this was to gain a better understanding of the bedrock and primary mineralisation from which the mining waste in this area has been generated. This area is shown in figure 74 delimited by a black dashed line and will be referred to subsequently as the Blötberget mapping area.

The earliest airborne measurements within SGU's database for the area around Blötberget were measured in 1972 by SGU (magnetic and natural gamma measurements). In 2008, TM Resources AB collected airborne transient electromagnetic (TEM) and magnetic data to the south-east of Blötberget (figure 74). In 2016, SGU collected more modern airborne magnetic, natural gamma and VLF (2 transmitter) data over the Blötberget area. These data were collected with a north-west – south-east line direction (approximately perpendicular to the predominant tectonic foliation in the area). These data were used to generate the residual magnetic field map shown in figure 74. In recent years, Blötberget has been the focus of several research projects to investigate how different geophysical methods can be applied to image mineral deposits, for example the EU project Smart Exploration (Malehmir et al., 2020). SGU has collaborated in various parts of these studies, which have been led by Uppsala University. The research activities have included physical property measurements of the Fe oxide mineralisation and host rocks as well as airborne and land based geophysical investigations (Maries et al., 2017; Almqvist et al., 2019; Markovic et al., 2020; Malehmir et al., 2020; Malehmir et al., 2021). In 2020, as part of the Smart Exploration project, SGU collected drone based magnetic and VLF multi frequency data over the Blötberget deposit (Malehmir et al., 2020) (figure 74). The different airborne geophysical surveys for the area around Blötberget are summarized in table 24.

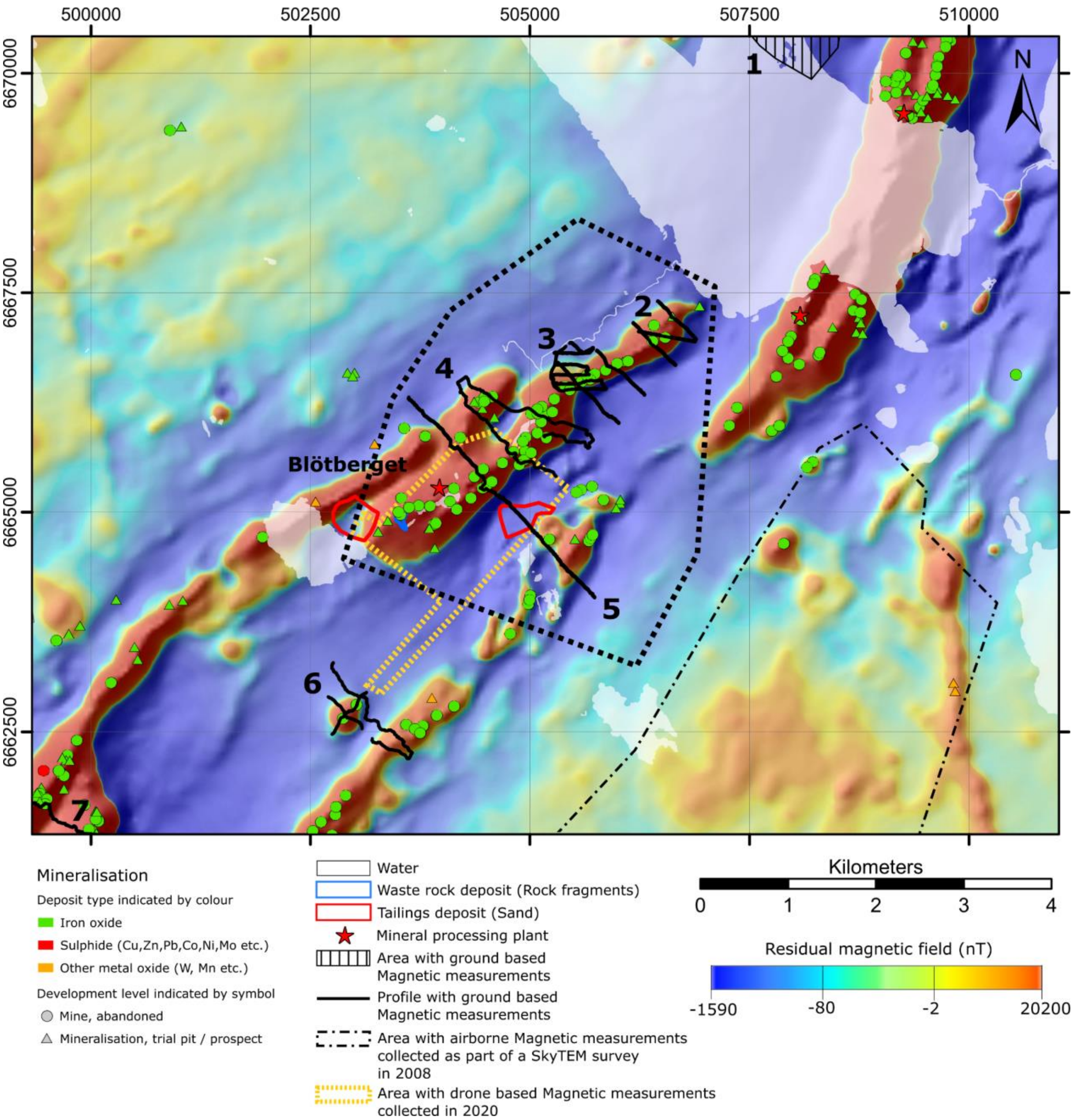

Figure 74. Map of residual magnetic field for the area around Blötberget. The Blötberget mapping area is shown as a polygon with a thick black dashed line. The location of ground-based magnetic measurements, listed in table 25 is shown. The location of magnetic measurements collected with a drone by SGU in 2020 is also shown.

Table 24. Complete list of the airborne geophysical surveys collected in the area around Blötberget. Unless otherwise stated all data are collected using a small, manned aeroplane.

Year	Organisation	Geophysical methods used	Area (SGU map sheet)	Flight direction (degrees)	Flight line separation (m)	Flight altitude (m)
1972*	SGU	Magnetics, gamma spectrometry	Part of 12E and 12F	East–West (90°)	200	30
2008*	TM Resources AB	*Helicopter based measurements (SkyTEM)* Magnetics, TEM	Part of 12FSV, Jonsmossen	Northwest – Southeast (135°)	100	30
2016	SGU	Magnetics, gamma spectrometry, VLF (2 transmitter)	Part of 13F,13G, 12E, 12F, 12G, 12H, 11E, 11F, 11G and 11H	Northwest – Southeast (130°)	200	60
2020*	SGU	*Drone based measurements* Magnetics, VLF multi-frequency	Small part of 12FSV, Blötberget	Northwest – Southeast (130°)	100	60

* Not used for producing maps in this report

Figure 74 shows a map of the residual magnetic field for the area around Blötberget. The map shows a series of strong magnetic anomalies with a northeast – southwest strike, which follow the general tectonic foliation of the felsic metavolcanic sequence in the region. This area of strong anomalies is clearly associated with Fe-oxide mineralisation. In general, the foliation and often also the mineralisation dips approximately 40–70º to the southeast. Several samples of Fe mineralisation collected from the Blötberget mapping area within this project had magnetic susceptibilities over 10 000 000 × 10^{-6} SI. The strong magnetic response in this area is attributed primarily to the presence of magnetite within the mineralisation (Maries et al., 2017; Almqvist et al., 2019). Hematite is also present within the mineralisation at Blötberget but has only a relatively small effect on bulk susceptibility. To the east of Blötberget, a relatively weak magnetic anomaly with approximately north-south strike can be observed which is presently mapped as a dolerite dike.

Figure 75 shows a map of the apparent resistivity calculated from airborne VLF measurements collected by SGU in 2016. On inspection many of the low resistivity features on the map can be correlated with regions with relatively high soil moisture or wetland (low lying topography) or man-made features, such as powerlines and railways. However, there is a low resistivity feature with an east-southeast strike, which intersects the eastern edge of the map area, about 1 km north of the south-eastern corner. As this feature does not correlate with topography, man-made structures or features on SGU's soil type map, it could potentially be a deformation zone in the bedrock.

Ground-based electromagnetic and magnetic measurements

Table 25 provides a summary of the ground-based geophysical data which are available for the area around Blötberget. The location of these data is also shown in figures 74 and 75 as numbered polygons and lines. The oldest ground-based data are magnetic measurements collected in 1976 over an area to the northeast of Blötberget (fig. 74). In 2021, several additional ground magnetic and VLF profiles were collected by SGU as part of this project and other ongoing bedrock mapping projects in the region (Lewerentz and Brolin, 2022). The objective of these new measurements was to improve the geophysical data available for this area to support mapping and geological modelling work in the future. These magnetic measurements include a series of profiles perpendicular to the strike of the mineralisation within the Blötberget mapping area (fig. 74). Furthermore, ground VLF measurements were collected over a small area to investigate a potential deformation zone. A GEM GSMV-19 instrument was used for these measurements.

As part of the research activity in recent years, mentioned earlier, several reflection seismic investigations have been performed at the Blötberget deposit. This includes both 2D and sparce 3D seismic reflection surveys (Markovic et al., 2020; Malehmir et al., 2020; Malehmir et al., 2021). At Blötberget, a strong seismic reflection is associated with the mineralisation, due to the large density contrast with the surrounding strata (Maries et al., 2017). This combined with the relatively gentle dip of the mineralisation (between 40 and 50º at the surface) means a good image of the mineralisation can be obtained using seismic reflection methods.

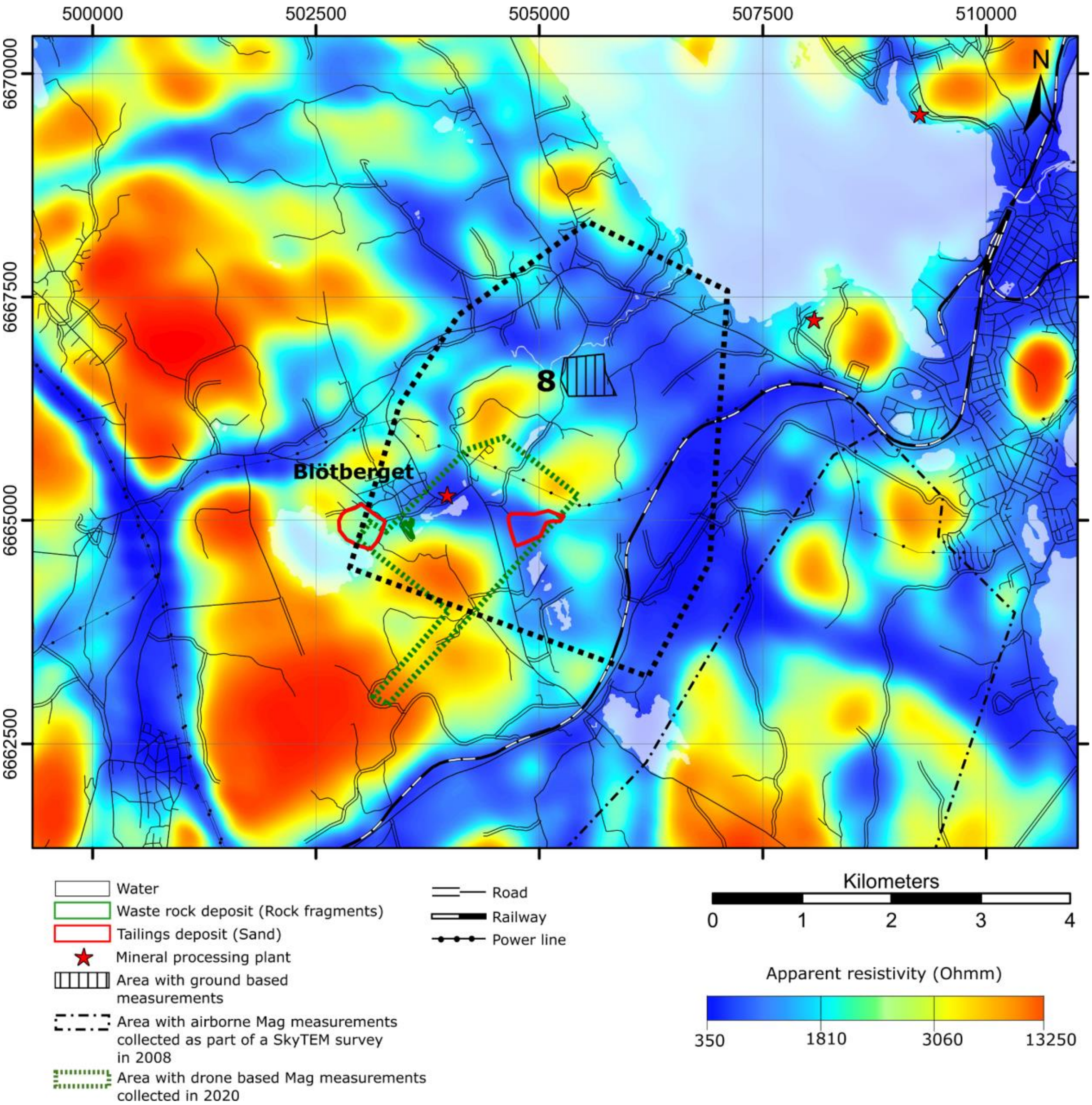

Figure 75. Map of apparent resistivity derived from airborne VLF data collected between 2016 and 2019 for the area around Blötberget. The Blötberget mapping area is shown as a polygon with a thick black dashed line. The location of ground-based electromagnetic measurements, listed in table 25 are shown.

Table 25. Ground-based magnetic and electromagnetic measurements for the area around Blötberget. Numbers correspond to the numbered polygons/lines shown in figure 74 and 75.

Polygon/Line number and name	Method	Year acquired	Responsible	Comments
1. mgtmid707	Magnetic	1976		Profile spacing of 40 m to 100 m.
2. MP21DSR0025 – MP21DSR0027	Magnetic	2021	SGU	Three profiles collected in this area
3. MP21DSR0023, MP21DSR0024 and MP21DSR0029	Magnetic	2021	SGU	Two northwest – southeast profiles and a series of short east – west profiles collected in this area
4. MP21CJO1005	Magnetic	2021	SGU	Two profiles collected in this area
5. MP21CJO1028	Magnetic	2021	SGU	One profile collected in this area
6. MP21CJO1001 – MP21CHO1003	Magnetic	2021	SGU	Three profiles collected in this area
7. MP21CJO1004	Magnetic	2021	SGU	One profile collected in this area
8. VP21DSR0028	VLF	2021	SGU	Several East – west profiles recorded in a small area

Ground-based gravity

About 220 new gravity measurements were made in the area around Blötberget as part of this project. Figure 76 shows two maps of the residual gravity anomaly calculated with different parameters as well as the pre-existing and newly acquired gravity measurement points. In figure 76A a grid spacing of 250 × 250 m was used to interpolate the Bouguer anomaly measurements. The residual anomaly was calculated by subtracting a version of the Bouguer anomaly grid which had been upward continued by 3 km, from the original grid. In figure 76B a grid spacing of 100×100 m was used and the residual anomaly was calculated by subtracting a version of the data which had been upward continued by 500 m. Hence, small, high frequency variations are more prominent in 76B than 76A. As a result of the new measurements the typical spacing between gravity points was reduced significantly to about 500 m across the Blötberget mapping area. However, as most new points were collected along the roads, there are a few regions where the spacing between points is still about 1 km.

There is a good correlation between the Fe mineralisation and the positive gravity anomalies in figure 76. This is due to the significantly higher density of the Fe mineralisation when compared to most of the other rock types in the area (Maries et al., 2017). At the Blötberget mine (located approximately at the southwestern mineral processing plant shown in figure 76A) and to the immediate southeast of it, there is a region with a small positive gravity anomaly. This is potentially due to the Fe mineralisation and its continuation beneath the surface to the southeast. There appears to be some small variations in the residual gravity anomaly along the northeast – southwest trending Fe-oxide mineralised zone (figure 76B). This could potentially be linked to the relative amount of Fe-oxide mineralisation present in different regions along this zone. However, within the Blötberget mapping area there is a region with mafic rocks (figure 73), which appears to coincide with a positive residual gravity anomaly. Hence, the presence of additional mafic rocks below the surface cannot be discounted as contributing to the positive anomalies observed in the Blötberget mapping area.

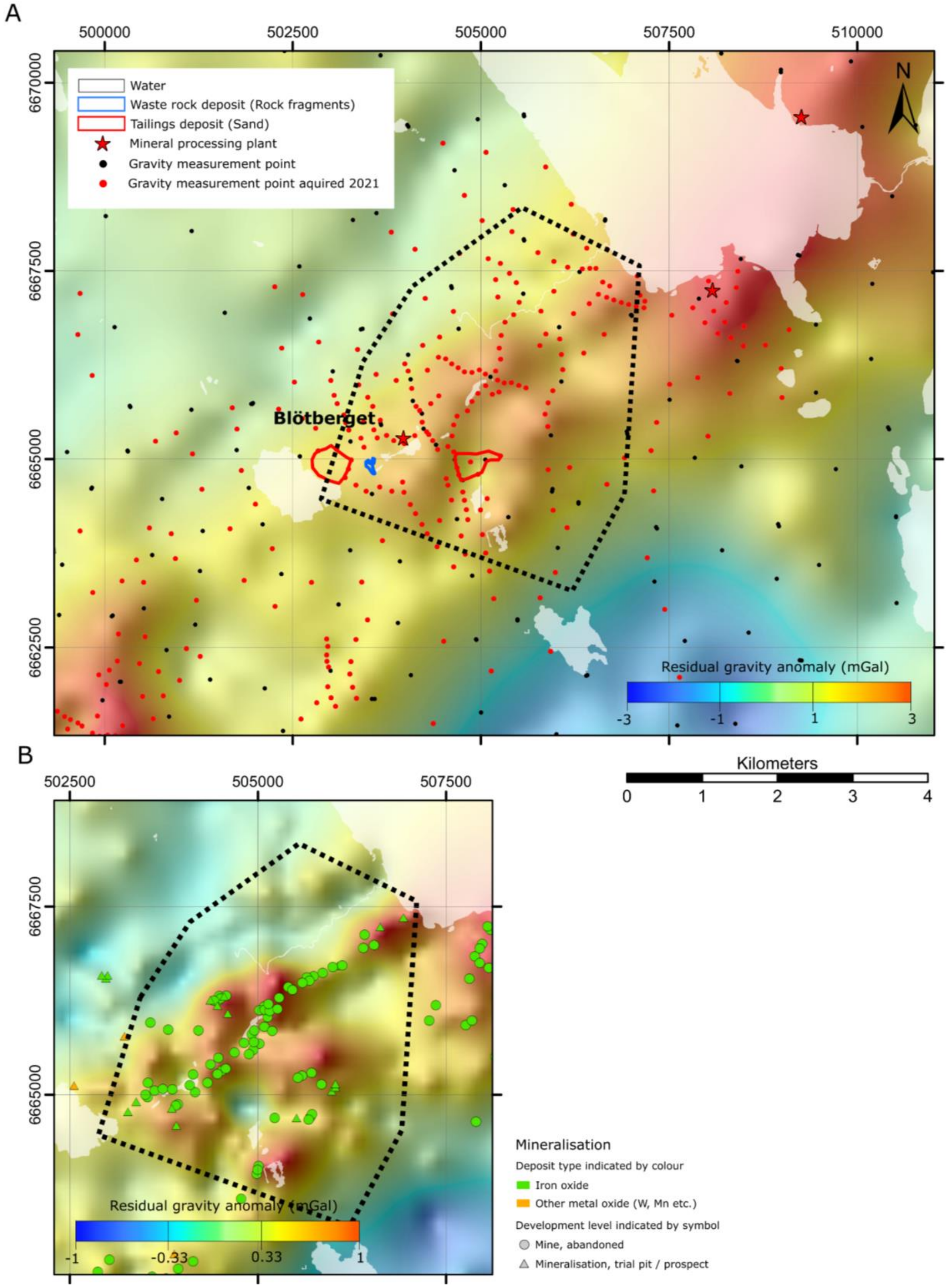

Figure 76. Map of the residual gravity anomaly over and around the Blötberget area. **A.** Residual gravity anomaly calculated with a 250×250 m grid spacing and 3 km upward continuation. Pre-existing and new gravity measurements are annotated. **B.** Residual gravity anomaly calculated with a 100×100 m grid spacing and 500 m upward continuation. Mineralisation is shown with red and orange symbols. The Blötberget mapping area is shown on both A and B with a thick black dashed line. Note that the distance scale for A and B is the same but they have different scales for the residual gravity anomaly values.

Petrophysical data

Figure 73 shows the available petrophysical data and measurements of magnetic susceptibility at outcrop within SGU's database for the area around Blötberget. Prior to this project the availability of petrophysical data within SGUs database was relatively low for this area, however, as part of this project an additional 14 petrophysical samples were collected. These new data points are highlighted in figure 73 and described in table 26.

From these new petrophysical measurements the samples taken from Fe mineralisation often have high magnetic susceptibilities (often >1 SI) and densities (often >4000 kg/m^3). This is consistent with the observed gravity and magnetic anomalies for this area (figure 74 and 76). These results are also consistent with other studies from this area such as Maries et al. (2017) who provide a description of the physical properties of the mineralisation and host rocks at Blötberget based on petrophysical laboratory measurements from core and downhole geophysical log measurements. Their study shows that the mineralised zones typically have far higher densities (>4000 kg/m^3) than the surrounding rocks. They observe that samples of mineralisation rich in magnetite are often associated with high magnetic susceptibilities while conversely samples dominated by hematite typically have relatively low magnetic susceptibility. Almqvist et al. (2019) performed a detailed investigation of the magnetic properties of drill core and hand samples taken from the Fe-oxide mineralisation at Blötberget. They observed that the bulk magnetic susceptibility is primarily dependant on the presence of magnetite (rather than hematite). However, they observed also that there is a strong correlation in magnetic anisotropy and the concentration of hematite.

The petrophysical data for the metavolcanic rocks (dacite and felsic volcanic) show far lower densities than the mineralisation (typically between 2716 and 3044 kg/m^3). The intrusive granitic rocks exhibit still lower densities of between 2614 and 2643 kg/m^3. The magnetic susceptibilities of these felsic rocks are also relatively low compared to the Fe mineralisation.

There are a total of 25 boreholes within SGUs borehole database located close to the Blötberget deposit and towards the southeast of Blötberget (figure 73). These wells were drilled between 1955 and 1975 by SSAB and Boliden, amongst others.

Table 26. Table summarising the petrophysical results collected as part of this project from and around the Blötberget mapping area.

Sample ID	Easting (m)	Northing (m)	Description	Density (kg/m3)	Magnetic susceptibility (10-6 SI)	J (mA/m)
DSR210035A	504822	6665635	Granite	2638	11935	26
DSR210035B	504822	6665635	Fe-oxide mineralisation	3851	5070449	452033
DSR210036A	505096	6664867	Fe-oxide mineralisation	3963	12787220	3473
DSR210037A	505646	6664603	Dacite	3044	818	-
DSR210038A	505688	6664708	Fe-oxide mineralisation	3591	1742904	43237
DSR210039A	503485	6664953	Granite	2623	140	12
DSR210039B	503485	6664953	Fe-oxide mineralisation	4739	23746370	1175
DSR210040A	503483	6664924	Dacite	2716	2811	85
DSR210041A	504459	6666306	Granite	2614	18464	397
DSR210041B	504459	6666306	Fe-oxide mineralisation	4449	8925774	17380
DSR210042A	506502	6666205	Granodiorite	2643	9056	46
DSR210045A	506515	6667007	Fe-oxide mineralisation	4337	11151330	100866
PCY210190C	503566	6664957	Fe-oxide mineralisation	4639	920122	3997
PCY210190E	503566	6664957	Felsic volcanic	2748	48354	644

Sampling of waste rock at Blötberget

A total of 16 waste rock samples were collected from Blötberget. Waste rock at Blötberget was only found within the area near the western end of the former open pit mine (fig. 77;78) The amount of waste rock observed was estimated to be far under the amount produced during production. Historic aerial photos show that the large open pit mine was filled in between the 1960 and 1975 using waste rock, accounting for the lack of large heaps of waste rock at Blötberget. Based on measurements of the volume of the open pit, up to 2 million m^3 of material may have been used as backfill.

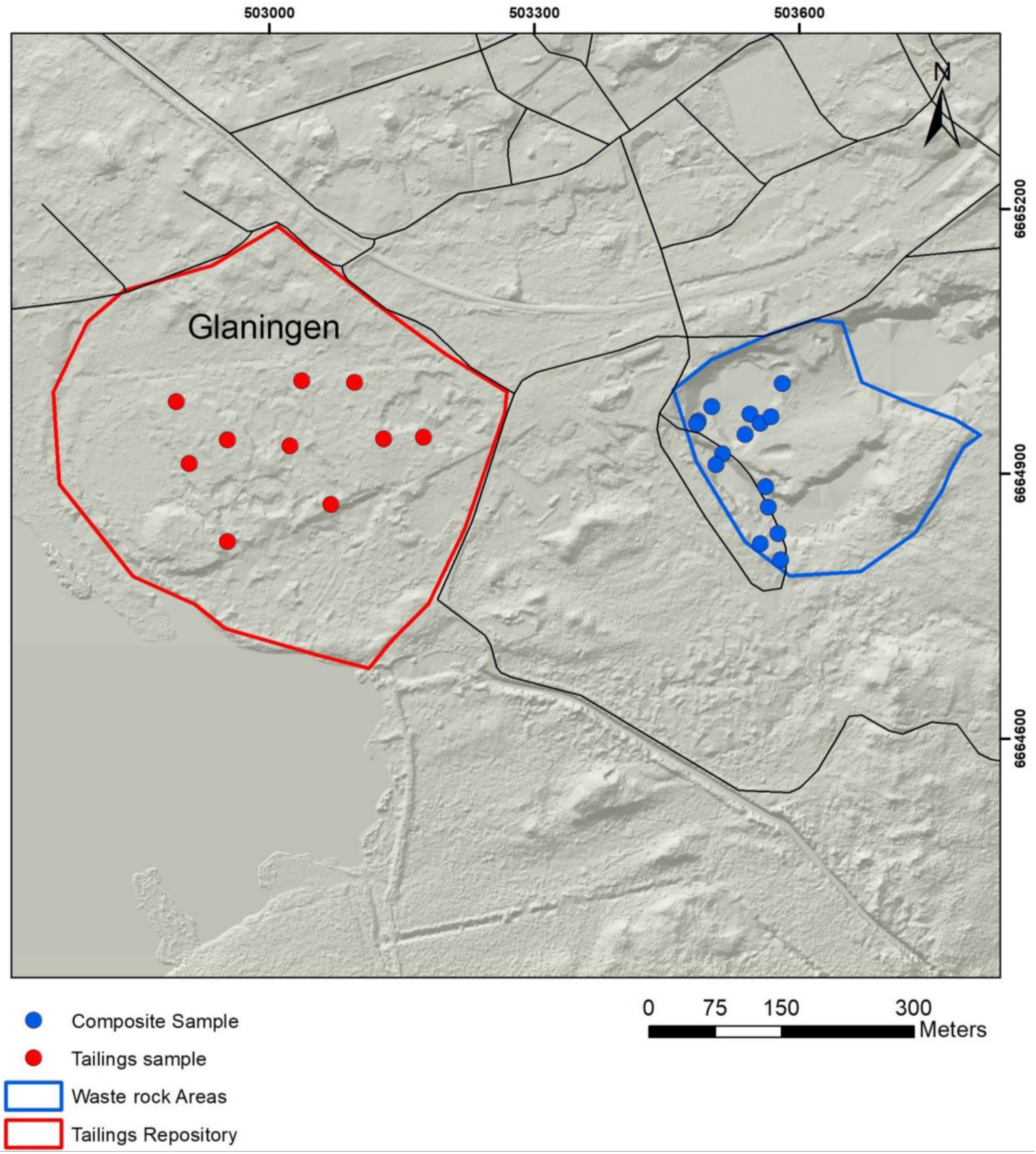

Figure 77. LiDAR image over the Blötberget mine and the Glaningen tailings dam.

Figure 78. Waste rock at Blötberget (6664966/503542). Photo: Patrick Casey

Waste rock was dominated by the metavolcanic country rock with a small portion of granite, skarn and ore. Ore chips collected from the waste rock heaps were either hematite or magnetite dominant, with magnetite samples composing approximately 75% of the mineralised chips sampled. Numerous granite samples observed contained veins of hematite.

Results are listed in table 27, and showed high concentrations of Fe_2O_3, as well as modest enrichment in P, REE, V and Ti and minor enrichment of Sn. Blötberget waste rock shows similar enrichment patterns in LREE as Grängesberg, however, many samples show a less pronounced negative Eu anomaly.

The mineralised sample collected for chemical analysis showed 84% Fe_2O_3 and 1.26% P_2O_5. Vanadium concentration was 527ppm, and REE 1700 ppm. Thin section analysis showed dominant magnetite with subordinate haematite, as well as abundant apatite. The REE mineralogy at Blötberget is relatively simple, with monazite as the dominant REE mineral, with minor xenotime and allanite. Bastnäsite was observed growing near calcite in the sample, most likely a later alteration product produced by the breakdown of monazite (fig. 79). Apatite showed little enrichment in REE in EDS analysis, though small (~5 µm) growths of monazite were common in apatite (fig. 79). EDS analysis showed Sn and V occur within the Fe oxides. Vanadium likely occurs as substitution for Fe, while Sn likely occurs as microcrystalline cassiterite growths within the Fe-oxides.

Large crystals of monazite were abundant in the mineralised sample from Blötberget (fig 79). Several 45 second analyses of 1 µm points and raster areas were conducted to determine Fe and trace element (table 28) and REE distribution as well as levels of Th (table 29). REE in monazite was dominated by the LREE with Ce comprising 27% and La 12%. Thorium was below detection limit in most analyses, though some monazite crystals showed ~1% Th, with an average concentration of 0.13%. These analyses indicate that, like Grängesberg, residual Th from REE extraction is likely to be of limited concern.

REE distribution (fig. 80) of the composite samples followed typical patterns for other mineralisations in Bergslagen, with pronounced Eu anomalies, and enrichment of LREE.

Table 27. Analytical results of waste rock from Blötberget.

Data	Object	Fe (%)	P (%)	REE (ppm)	V (ppm)
Composite Samples (n=15)	Average	15.7	0.26	589	173.9
	Max	31.9	1.07	1730	272
	Min	17.3	0.13	226	61
Mineralised sample		84.0	1.46	1813	1010

Table 28. Results of EDS analysis of magnetite from Blötberget.

Data	Mineral	Fe (%)	Sn (%)	V (%)
EDS analysis	Magnetite (n=7)	71.3	0	0.20

Table 29. Results of EDS analysis of monazite from Blötberget.

Data	Object	P (%)	Ce (%)	Th (%)
EDS analysis	Monazite (n=9)	12.5	27.2	0.13

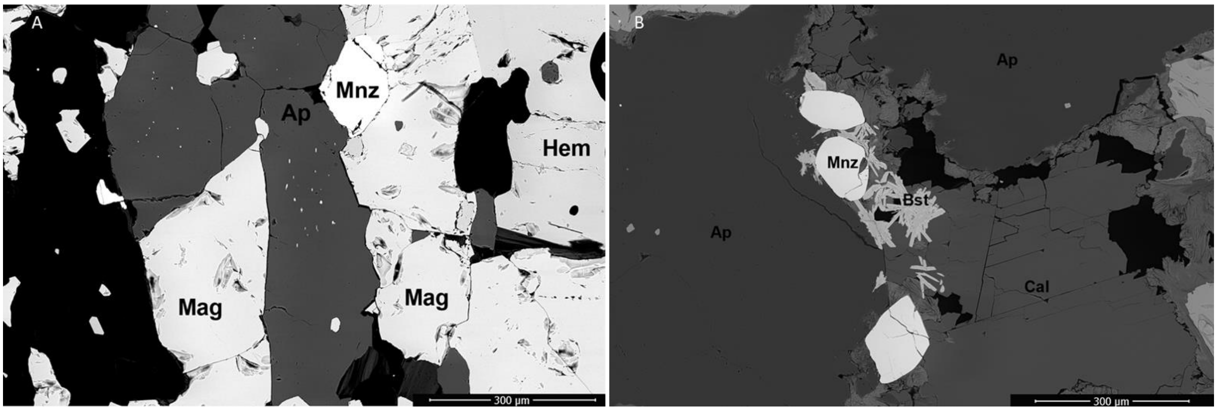

Figure 79. SEM images a of mineralised sample from Blötberget. **A.** image showing Fe-oxides (magnetite and hematite), apatite (dark grey) with monazite (white) blebs within apatite, as well as a single large monazite crystal. **B.** Large apatite crystals with monazite, bastnäsite and calcite. Micrograph: Patrick Casey

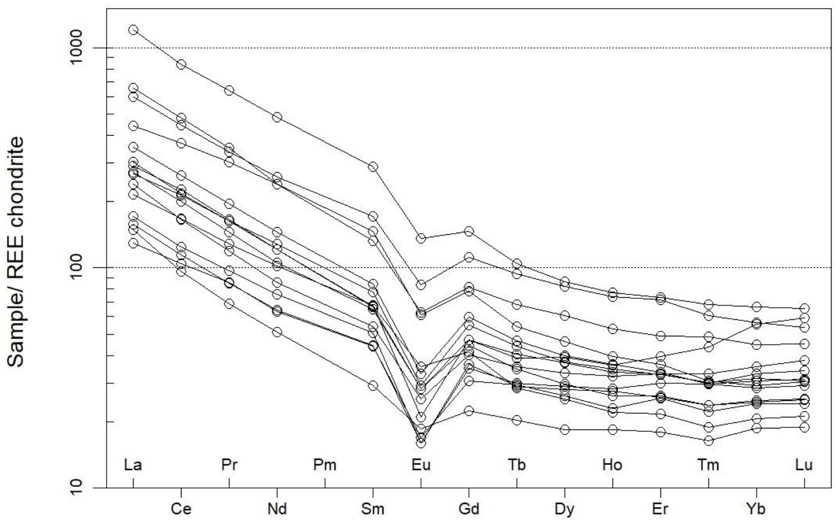

Figure 80. Chondrite normalised REE patterns from composite samples at Blötberget. Chondrite values taken from Boyton (1984).

Sampling of tailings at Blötberget

Surface sampling results at Glaningen

The Glaningen tailings repository at Blötberget was identified in aerial pictures and LiDAR data during preparations for composite sampling. This tailings repository had not been sampled in previous SGU fieldwork, and its identification aids in the estimation of potential recoverable resources at Blötberget. Based on historic aerial images provided by Lantmäteriet, Glaningen was the first of the tailings repositories to be used at Blötberget.

The tailings dam at Glaningen appears to be shallow in depth. An approximately 1.5 metre wall surrounds the tailings, and the tailings reach only partly up the wall in most areas. No geophysical measurements were conducted due to unfavourable conditions, and no depth sounding was conducted due to difficulty of access with equipment. However, depth was estimated to be around 1.5 metres, and estimations based on remaining tailings calculated from geophysical models of the Norsberget tailings dam and production data from MALMdb, an estimated 300 kt of sand covering to a depth of 1.3 metres remains in the tailings dam.

The area is overgrown with deciduous and evergreen trees (fig. 81), with occasional small bushes. A total of 10 surface samples were taken. The tailings have a wide grainsize distribution from silt to coarse sand within each sample and are typically rich in white micas. A grain size analysis was conducted and indicated roughly even distribution between coarse, medium and fine fractions. Analyses showed high levels of Fe, P, REE and modest enrichment in V, and slight enrichment in Sn.

Figure 81. Vegetation and tailings in the Glaningen tailings dam (6664939/503130). Photo: Patrick Casey.

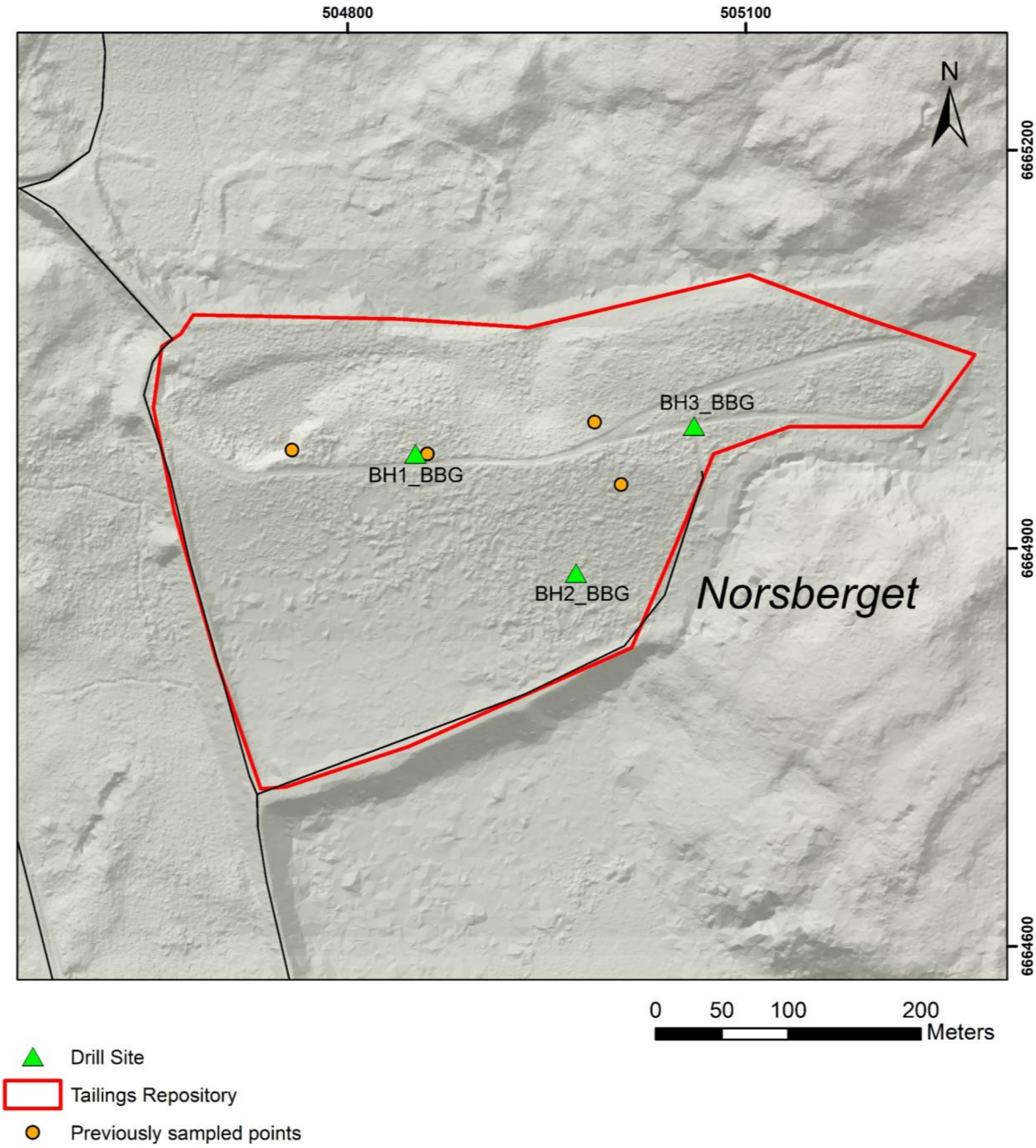

Figure 82. LiDAR image showing the tailings dam at Norsberget.

Drilling at Norsberget

A second tailings dam was built to the east of the Blötberget mine in the Norsberget area (fig. 82) and entered use by 1975 based on Lantmäteriet aerial images. Two sections were built to receive tailings, an upper dam and a lower dam, however, only the upper dam was used before the mine was closed in 1979. No surface sampling was conducted during this project; however, several samples were taken during a previous sampling campaign, which showed approximately 13% Fe_2O_3, 2% P_2O_5 and 1100 ppm REE. The north-western side of the tailings dam has been subjected to limited extraction of sand for industrial purposes, which is evident in the LiDAR image in figure 82. This excavation has left an exposed face of sand that provides an excellent overview of the layering contained within the tailings, and evidence of sedimentary processes that occurred during deposition (fig. 83). The surface of the tailings is dry and coarse, and the tailings turn finer and wetter with the sloping of the tailings towards the south wall of the tailings dam. Vegetation at Norsberget is thick grass and sedges with occasional deciduous trees. Toward the southern wall groves of evergreen trees are present.

A total of 3 boreholes were sampled at the Norsberget tailings dam. The boreholes showed a consistent particle size of fine sand with silt as well as silt layers, with the coarsest sand typically at the top and bottom of each borehole. Occasional bands of hematite sand were observed within the tailings. Depth probing was conducted at all three boreholes, showing a depth between 15–20 metres until till was reached. BH1 and BH3 were aborted after 9–15 metres, respectively, due to the sampling screw repeatedly getting stuck within the tailings. The cause for this is unknown and was speculated to be caused by friction from contact with the dry tailings, or the screw being caught on a piece of scrap metal dumped within the tailings. Tailings at Blötberget were typically dry and the water table was reached around the 14–15 metre level.

Figure 83. Photos showing the exposed sedimentary layers of the tailings at Norsberget. Image **B** shows detail of the tailings, including an approximately 3 cm band of hematite rich sand just above the knife. (6667983/504755). Photo: Patrick Casey.

Geophysical measurements

Geophysical measurements were conducted in May 2022 at the eastern Blötberget (Norsberget) tailings repository. Three ERT/IP profiles and four RMT profiles were measured (fig. 84). At the time of the measurements parts of the ground was still frozen and there was a 10 cm thick ice layer. Therefore, before the ERT/IP measurements, the electrodes had to be hammered through the ice layer for higher current injection. Moreover, by using saltwater at the location of electrodes a relatively better contact, though not good enough, was achieved. The effect is visible showing a thin high resistive layer close to the surface in the resistivity models, and there may be more effects on data which are yet not fully evaluated. The RMT measurements are not affected by frost in the ground and show a good result.

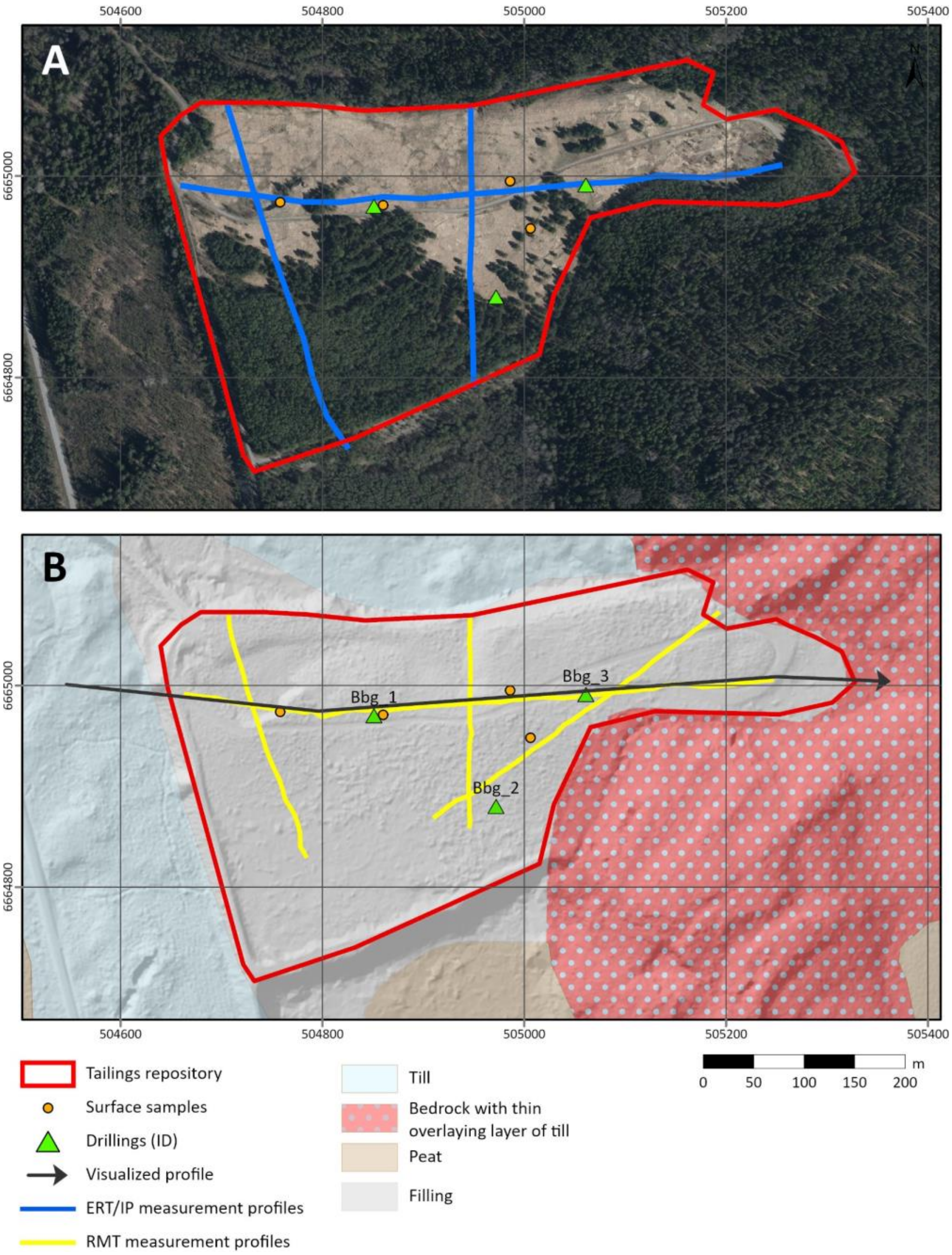

Figure 84. Geophysical measurement profiles, drilling and sampling locations at the eastern Blötberget (Norsberget) tailings repository.

Compared to ERT, the RMT method has a limited resolution close to the surface but deeper penetration. For the Blötberget area, the method worked well to identify the top of the bedrock (fig. 85). This layer can be approximated with the bottom of the tailings by assuming that the bedrock is overlain by a "thin" layer of till or peat. A 3D-model over the tailings deposit has been constructed based on the results from 2D inversion of RMT data and the three drillings conducted in the area together with study of historical maps and orthophotos. The volume of the sand was estimated to be 2.36 million m³. The estimated thickness of the tailings deposit is shown in figure 86.

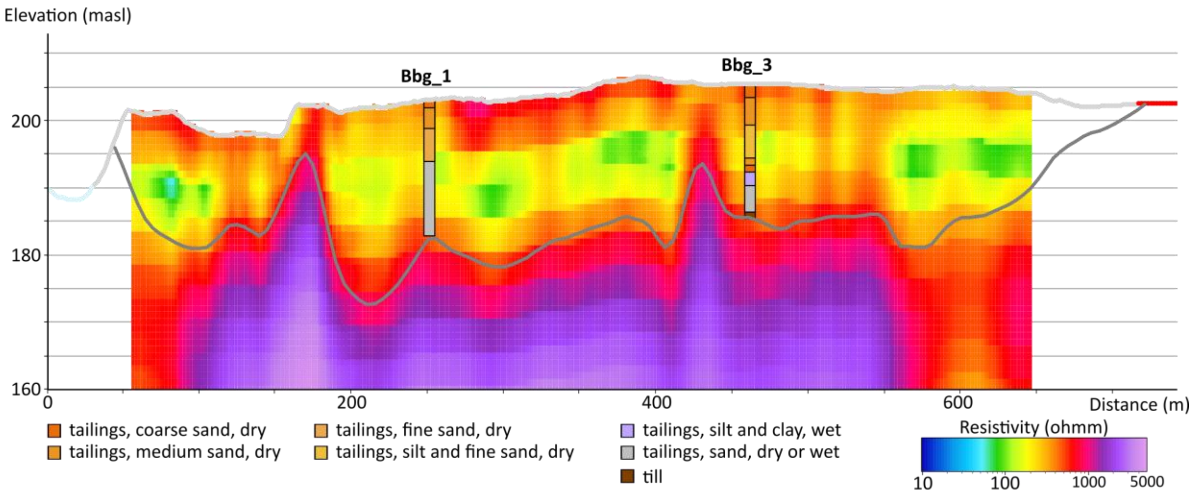

Figure 85. Cross section with resistivity from RMT measurements, location of profile showed in figure 84. The grey line is the interpretation of the bottom of the tailings.

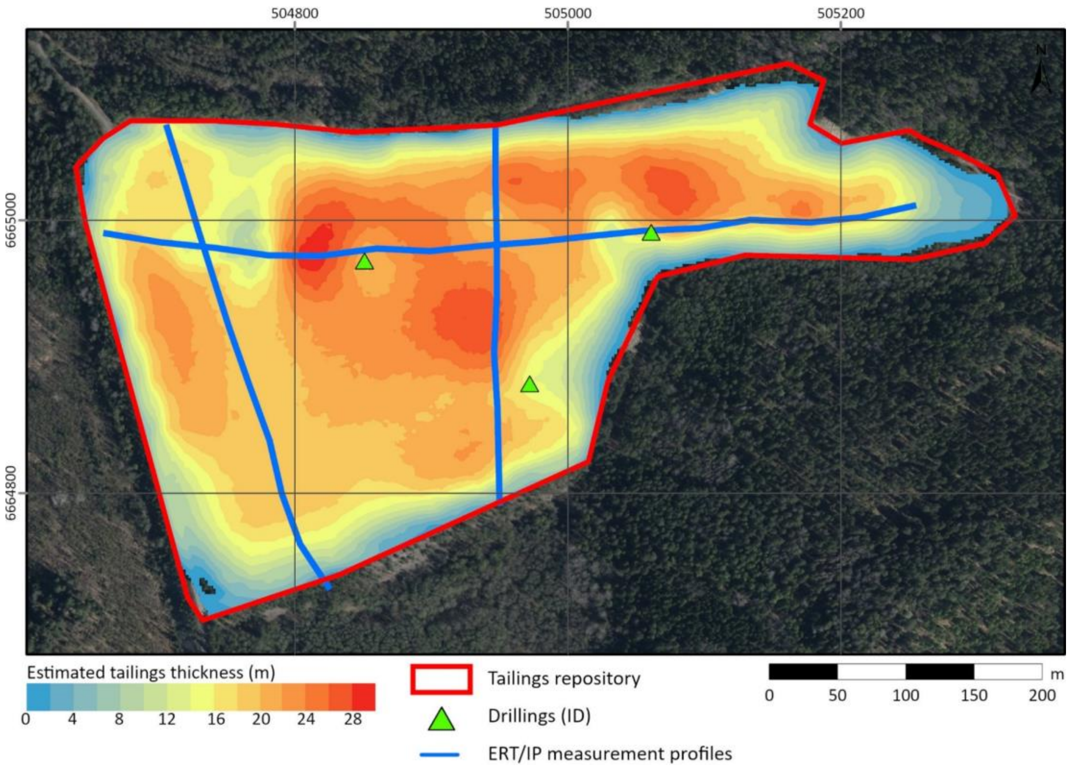

Figure 86. Modelled tailing thickness at Norsberget.

Blötberget drilling results

Borehole 1 Blötberget (BH1_BBG; 6664971/504851) was sampled at the highest topographic point of the tailings repository. The total depth to the top of the till layer was 20 metres. Sampling occurred only to the 9-metre level due to the sampler getting stuck, possibly due to the friction from the coarse, dry tailings. The tailings in the sampled 9 metres were generally coarse to medium sand.

Analysis of the tailings showed rather consistent levels of Fe_2O_3 averaging 13.5%, and consistent levels of P_2O_5 around 1.3 % (fig. 87). Total REE concentrations averaged 900 ppm.

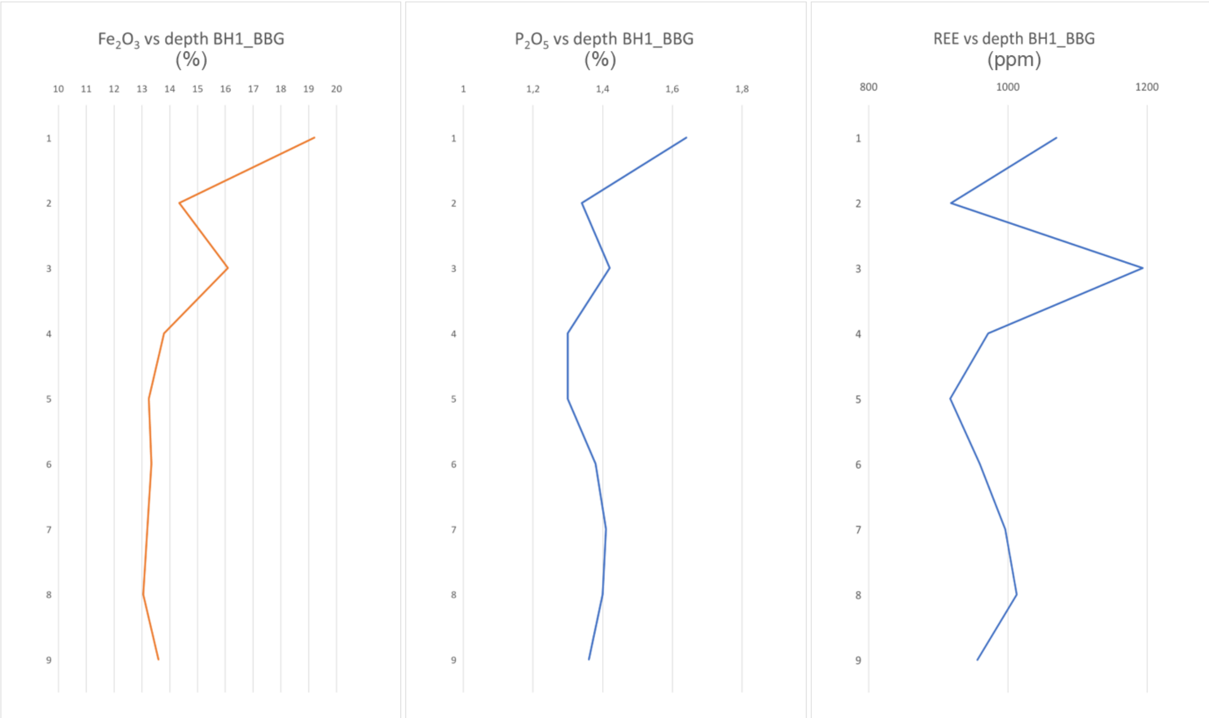

Figure 87. Fe-oxide, phosphate and REE concentrations along the depth profile in BH1_BBG.

Borehole 2 Blötberget (BH2_BBG; 6664881/504972) was sampled near the southern boundary of the tailings repository. The surface was notably moister, and the location was near a pine forest. The water table at this drill site was reached at around 9 metres. The upper levels of the borehole contain medium sand transitioning to silty fine sand to silt at around 6 metres depth.

Analysis of the tailings showed more variation than at the other drilling sites (fig. 88). Iron values were higher at the top of the borehole, averaging 15%, before falling to near 10% at the bottom of the drill hole where the material was finer. Phosphorus levels followed a similar profile of the highest levels between 3–12 metres, where the average was 1.75% P_2O_5 before dropping closer to 1%. It was also between these levels that REE contents were highest, correlating strongly to the phosphorus levels. The highest REE contents of over 2000 ppm were at metre 7, and averaged 1500 ppm throughout these intervals before falling to under 1000 ppm again near the bottom of the profile.

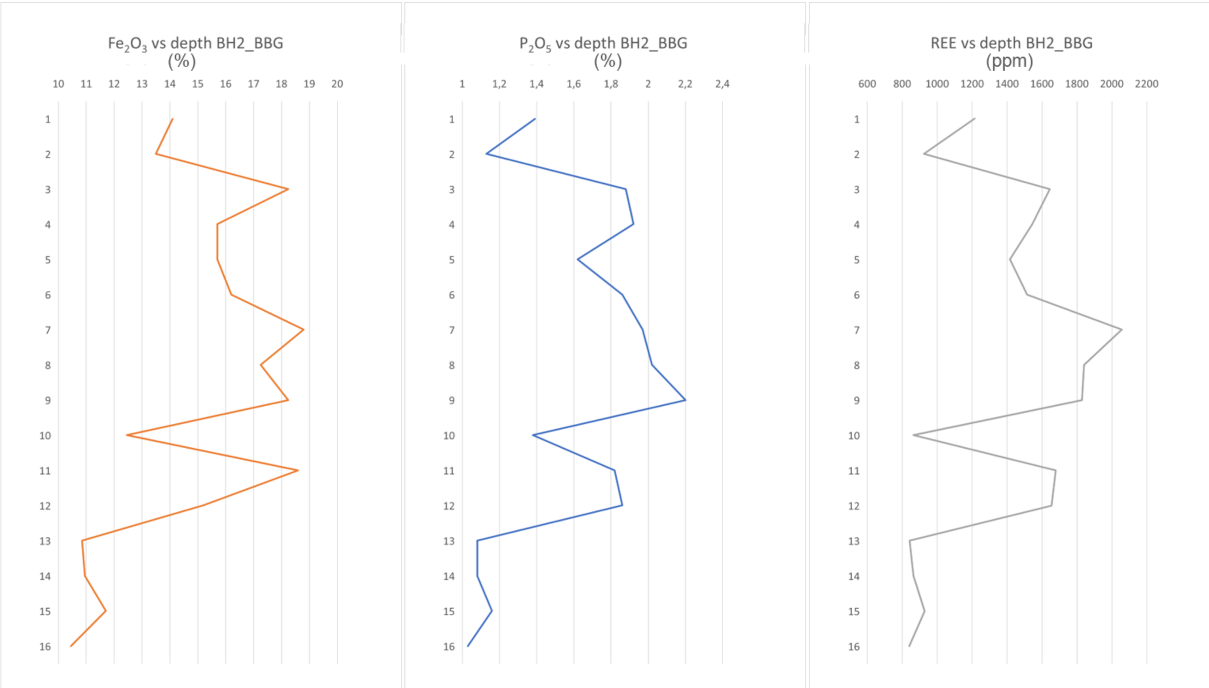

Figure 88. Fe-oxide, phosphate and REE concentration along the depth profile in BH2_BBG.

Borehole 3 Blötberget (BH3_BBG; 6664992/505061) was sampled near the eastern edge of the tailings repository. The depth to the bottom was 19 metres. The sand was typically medium to fine silty sand. The material here was again very dry until the 15-metre level. Due to the sampler becoming stuck at the 15-metre level, sampling was not carried out below this point.

Metre 3 of this borehole showed the highest Fe contents of all samples within Blötberget, at 43% Fe_2O_3, while other samples contained around 15% Fe_2O_3 on average, likely due to the presence of abundant bands of hematite sand observed at this level. Phosphate averaged 1.3% throughout the borehole with a wide variation between different sampled levels of 1%, while REE averaged near 1000 ppm, with some samples over 1200 ppm (fig. 89). Phosphate and REE were strongly correlated.

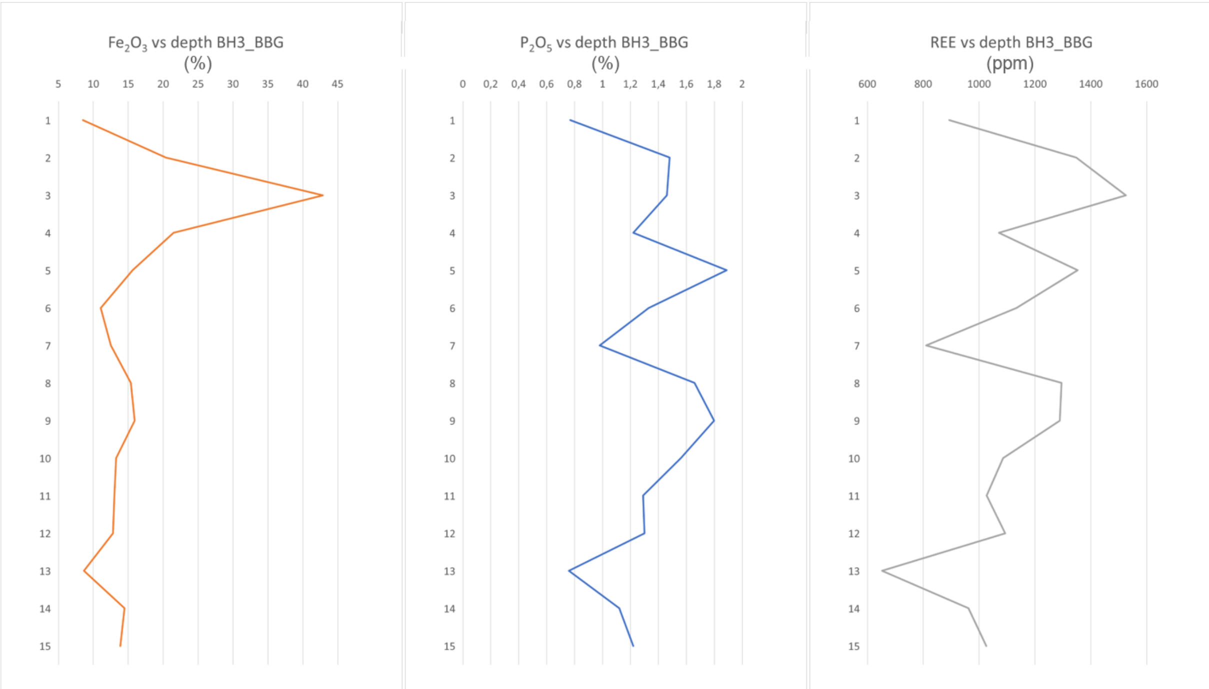

Figure 89. Fe-oxide, phosphate and REE concentrations along the depth profile in BH3_BBG.

Discussion

While drilling at Blötberget provided numerous obstacles, a clearer image of the levels of CRM (figs 90 and 91) remaining were able to be established. Phosphate levels were generally consistent between 1 and 2 %. These levels are similar to the levels found in the newer tailings in Grängesberg, however, no indication of apatite concentrate production was noted in production statistics from Blötberget, indicating a generally lower concentration of P in the ore rather than a fraction of the phosphate having been extracted. Iron concentrations are lower (fig. 90) particularly in comparison to Grängesberg, indicating good recovery percentages through the end of the lifetime of the mine. Hematite appeared to be the dominant Fe-oxide in the tailings based on the observation of frequent bands of hematite sand, which may point to magnetite separates having a higher recovery percentage. REE levels are notably higher in the drilled samples than surface samples (table 30).

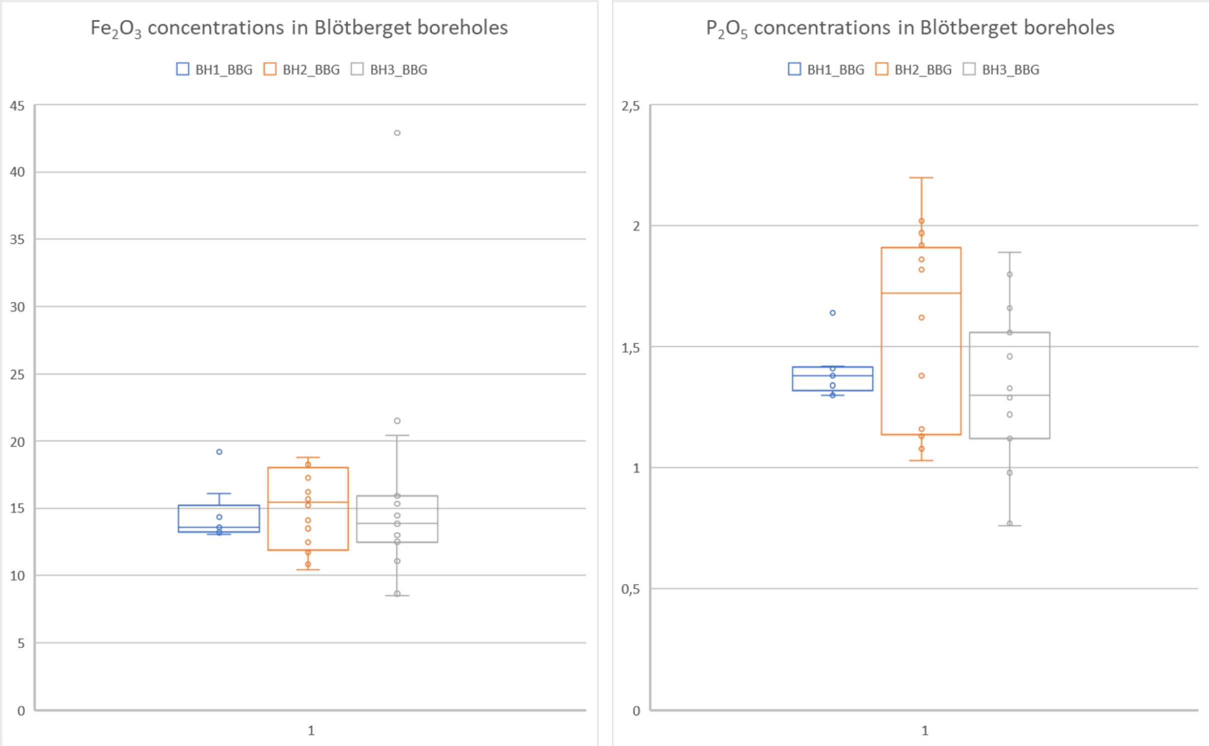

Figure 90. Distribution of Fe_2O_3 and P_2O_5 in boreholes from Blötberget.

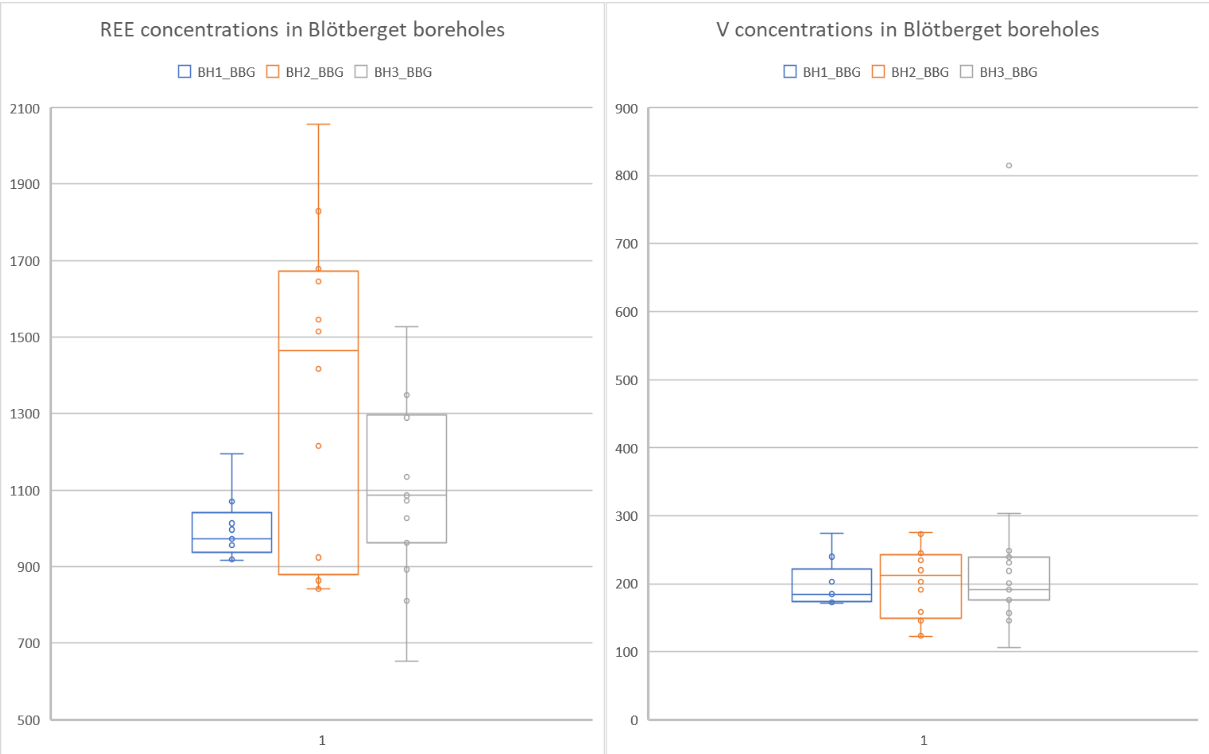

Figure 91. Distribution of concentrations of REE and V in boreholes from Blötberget.

Table 30. Analytical results of tailings from Blötberget

Data	Object	Fe (%)	P (%)	REE (%)	V (ppm)	Ti (ppm)
Tailings/Surface	Glaningen	19.0	1.0	0.12	294	1105
	(n=10)	39.5	1.3	0.17	738	1590
		5.23	0.78	0.09	165	490
Tailings/Drilled	Norsberget	10.4	0.64	0.12	210	732
	(n=41)	30	0.96	0.21	815	1610
		6.0	0.33	0.065	106	490

Potential resources at Blötberget

The amount of available waste rock that is easily accessible is unclear. Figure 77 in section *Sampling of waste rock at Blötberget* shows the extent of the easily accessible waste rock at Blötberget that was sampled, as well as apparent heaps of waste rock that were too overgrown for sampling. The amount of waste rock observed was clearly well below the 4 Mt recorded in MALMdb at the final report (AB Svenskt Stål, 1981). Aerial images provided by Lantmäteriet (Fig. 92) show that between 1960 and 1975 the open pit at Blötberget was filled in with waste rock. Using data from mine maps an estimated 1.6 million cubic metres of material would fit into the open pit. It is likely that most waste rock was dumped in the open pit after the shift to underground mining at Blötberget.

Based on the mine productions statistics from MALMdb and assuming that no waste rock has been removed from the site there is a potential for 650,000 tonnes of Fe, 11,000 tonnes of P, 2,400 tonnes of REE, 1,000 tonnes of V and 3,400 tonnes of Ti.

With the assumption that the average concentrations of both sampled tailings repositories represent a baseline average for CRM, the tailings repositories at Blötberget can potentially contain up to 500,000 tonnes of Fe, 30,000 tonnes of P, 5,500 tonnes of REE, 1,000 tonnes of V and 3,000 tonnes of Ti.

Figure 92. Aerial images showing the backfill of waste rock into the open pit at Blötberget. Photo: Lantmäteriet.

Mossgruvan and Sköttgruvan

Background

Mossgruvan and Sköttgruvan (Sweref 6649949/503301) are located approximately 15 km south of Grängesberg. The mines were in operation from 1868 through 1972, with the longest continual duration of mining between 1882–1925 and 1933–1972, exploiting a skarn Fe ore. The skarn Fe ore formed in carbonate layers and contained approximately 40% Fe, with between 2 and 5% Mn. Total production at Mossgruvan was approximately 3.2 Mt with 1.31 Mt of waste rock produced (Table 31).

A tailings dam lies approximately 1 km south of the mine. These tailings were sampled previously by SGU, and showed elevated levels of Fe and Mn, with no elevated levels of other CRM observed.

The waste rock at Mossgruvan is separated into two dominant areas marked in the map in figure 93. One area has been exploited for construction material and waste rock piles in the south-east have been transformed into a motocross raceway (fig. 94). A large portion of the waste rock at Mossgruvan was granitoid rock. Slag was common throughout the waste rock and was avoided during sampling.

During collection of composite samples, it was noted that mineralised samples were under-represented in the waste rock compared to other sites sampled in western Bergslagen. Iron-rich chips were typically calcite or dolomite rich marbles with disseminated grains of magnetite, often showing minor Mn weathering crusts. Occasional sulphide grains and fracture fills were observed, though uncommon. Minor molybdenite was observed in several of the skarn samples. It is possible that much of the waste rock here has been mixed with other waste rock during construction of the motocross track. Other waste rock piles were observed to the north-west of the sampling area, however thick overgrowth precluded their inclusion in sampling. The geophysical data which is available for the area around Mossgruvan is summarised earlier in the report (see the section for Wigströmsgruvan).

Table 31. Production statistics from Mossgruvan.

	Total (Mt)	Fe (%)	Mn (%)
Mined Ore	3.22	40.3	1.9
Processed in dressing plant	2.16		
Tailings[1] (n=4)	1.26	12.5	2.5
Waste rock	1.31		

[1]Tailings data collected during previous sampling.

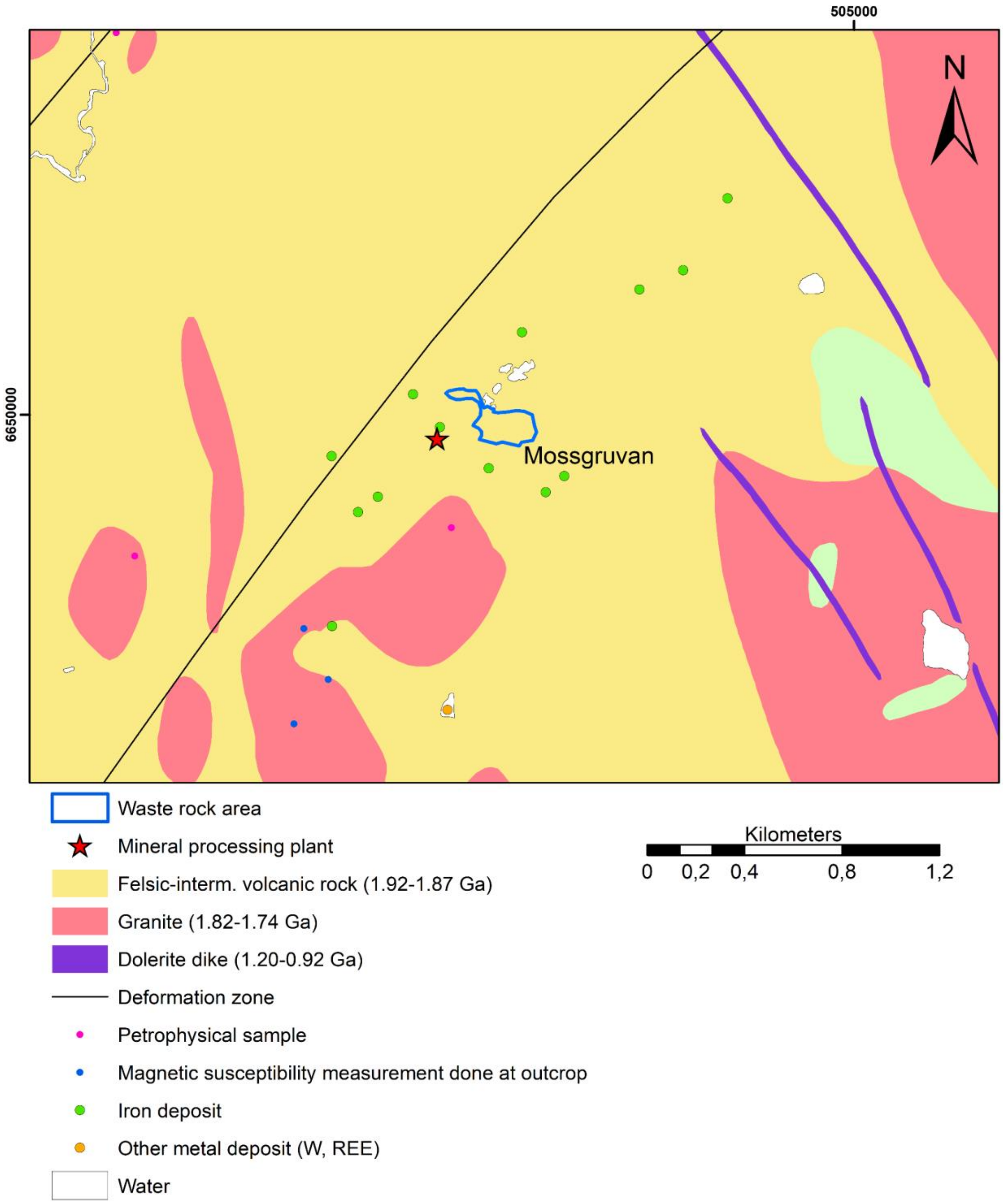

Figure 93. Bedrock map of the area surrounding Mossgruvan.

Figure 94. Waste rock at Mossgruvan showing the motocross track cutting built on the waste rock (6649925/503494). Photo: Stefan Persson.

Sampling of waste rock at Mossgruvan

A total of 15 composite samples were collected from Mossgruvan. The samples showed no appreciably elevated levels of CRM. Low levels of Fe were observed, with an average of 9.3% Fe_2O_3 and 0.5% MnO (table 32). One sample showed moderately elevated levels of Mo possible related to late Svecokarelian intrusions that formed the Mo-W deposit at the nearby Wigströmsgruvan. A single richly mineralised sample was analysed and showed 50% Fe-oxide and 5.9% MnO. Manganese was significantly lower in concentration at Mossgruvan, likely owing to the limited levels of remaining ore within the waste rock.

Microscopy of a thin section from this sample showed massive magnetite as the host of most Fe, with abundant olivine. Olivine was predominantly fayalite (Fe), with a proportion of forsterite (Mg) and tephroite (Mn) in solid solution (fig 95).

The appropriation of the waste rock into use as a motocross raceway is unlikely to have skewed the results of the composite samples as similar results were obtained from the undisturbed waste rock from the northwest pile.

Potential resources at Mossgruvan

With the assumption that no material has been removed from the site, waste rock at Mossgruvan may hold up to 85 000 tonnes of Fe, and 5 500 tonnes of Mn.

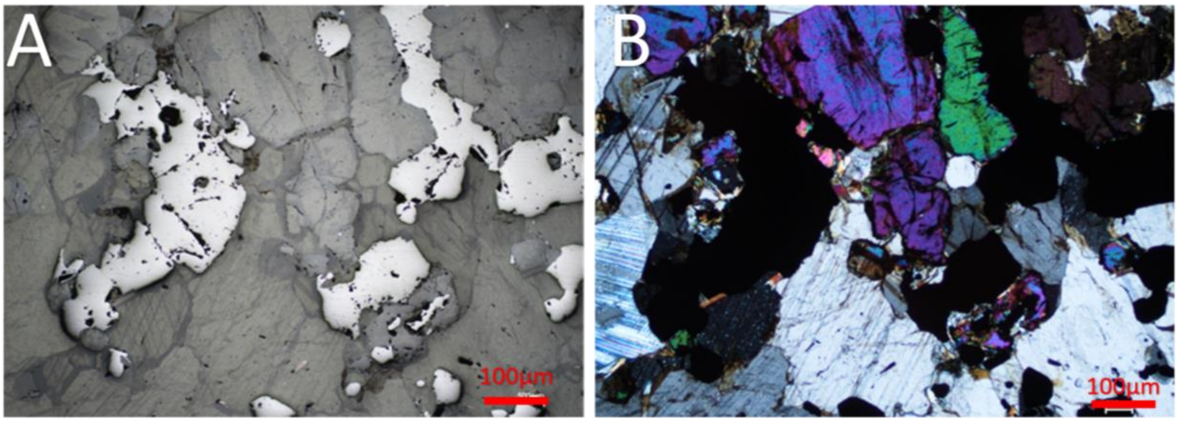

Figure 95. Thin section images from richly mineralised sample from Mossgruvan. **A**. Reflected light image showing magnetite and small oval blebs of pyrrhotite. **B**. Thin section in XPL showing calcite (pale grey to high birefringence) and olivine (high second order birefringence). Micrographs: Patrick Casey

Table 32. Analytical results from Mossgruvan

Data	Object	Fe (%)	MnO (%)
Mineralised sample	Mossgruvan	51.8	5.90
Composite samples (n=15)	Average	9.3	0.55
	Max	15.8	1.25
	Min	6.4	0.25

Basttjärn

Background

The Basttjärn iron mine (Sweref 6653477/498800) (fig. 96) was located 6 km south of Grängesberg in the Högfors district and operated from 1959 to 1978. Mineralisation occurs in skarn altered carbonate bodies that is to some extent weathered at depth, known as "mullmalm" (eng. *limonite ore*). This weathering is believed to have been caused due to fluid infiltration along large fault zones. During operation, the mine produced 1.38 Mt of ore with approximately 33% Fe and 4% Mn from three mine shafts (table 33).

Ore was processed at a dressing plant on site, and approximately 0.72 Mt of tailings were produced, and deposited in a tailings dam to the west of the mine. Surface sampling of the tailings was not conducted, however, a single analysis was conducted during a previous study showing 16% Fe and 5.0 % MnO, with somewhat elevated levels of Cu and Pb. Only the westernmost of the mines was sampled for waste rock due to extensive overgrowth of the other two mines.

The tailings were sampled previously by SGU, and analyses showed enrichment in Fe and manganese and elevated levels of Cu, Pb and Zn.

The geophysical data which is available for the area around Basttjärn is summarised earlier in the report (see the section for Wigströmsgruvan).

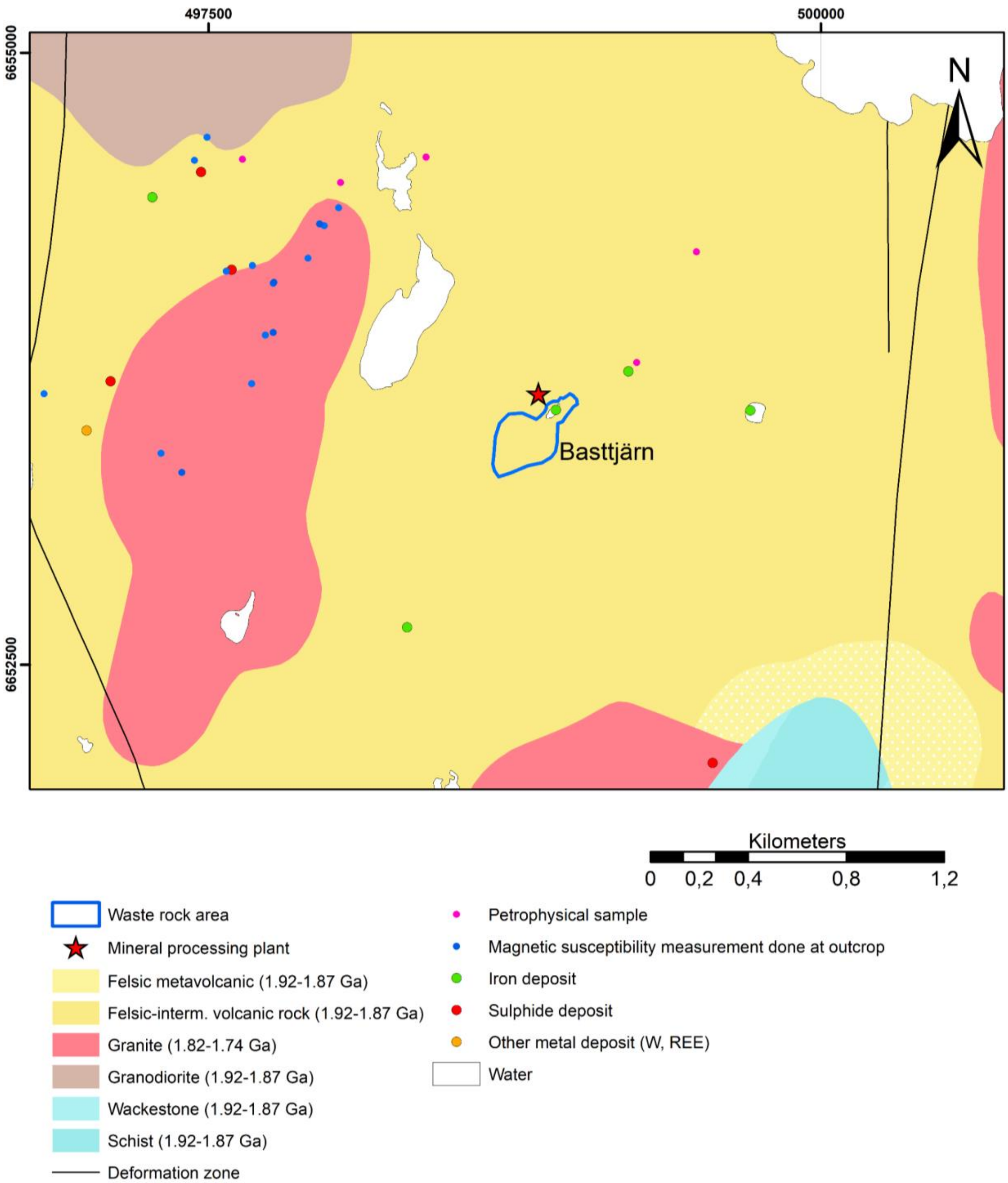

Figure 96. Bedrock map of the area around the Basttjärn mines.

Table 33. Production statistics from Basttjärn

	Total (Mt)	Fe (%)	Mn (%)	Cu (ppm)	Pb (ppm)	Zn (ppm)
Mined Ore	3.75	40.9	4.0			
Processed in dressing plant	1.38					
Tailings[1] (n=2)	0.77	11.9	4.1	520	211	249
Waste rock	2.57					

[1]Tailings data collected during previous sampling.

Sampling of waste rock at Basttjärn

A total of 15 composite samples were collected at Basttjärn (figure 97). The waste rock is dominated by marble, both calcitic and dolomitic. The Fe ore is skarn hosted and contains high levels of carbonate, and often shows the typical blue-purple crust associated with Mn weathering (figure 98). Field observations indicated the dolomitic marble was richer in Fe-oxides than calcitic marble. Silicate skarn is also relatively common, dominantly composed of amphibole and garnet with occasional disseminated grains of sulphide minerals and sulphide fracture fill. Sulphide mineralisation is dominated by pyrite and pyrrhotite with lesser chalcopyrite and galena.

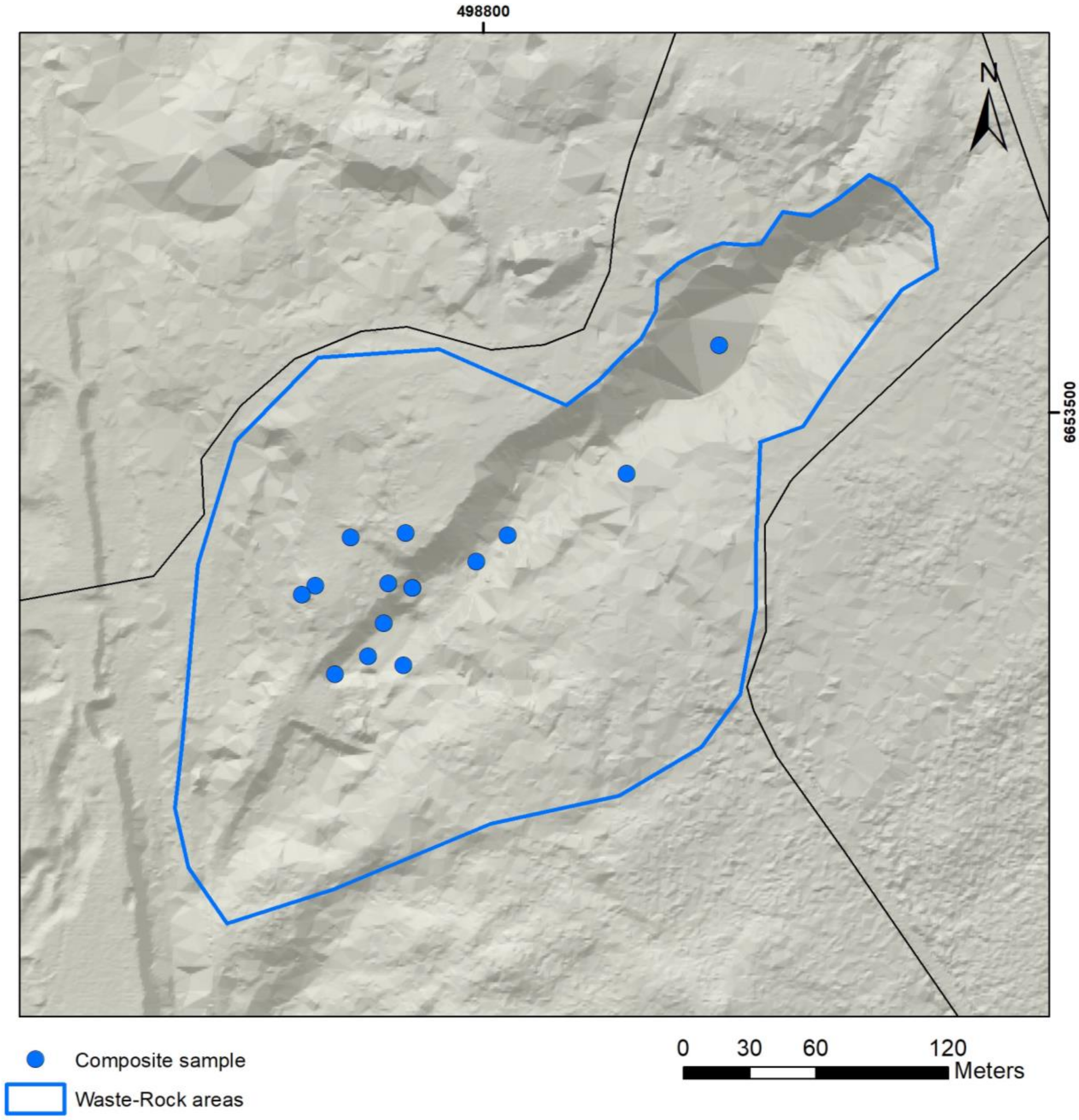

Figure 97. LiDAR image of the waste rock heaps and abandoned Fäbobacksgruvan mine pit at Basttjärn.

Composite samples showed high levels of Fe remaining within the waste rock, averaging 20% Fe_2O_3. MnO concentration averaged 3% (table 34). Analysis showed higher levels of Cu (163 ppm), Pb (114 ppm) and Zn (210 ppm) within these composite samples compared to the other Fe-Mn skarn mineralisation sampled in the Högfors district. Arsenic concentrations at Basttjärn are anomalously high, with some samples containing over 1000 ppm As. A richly mineralised ore sample analysed showed 46% Fe_2O_3 and 4.3% MnO. Elevated levels of sulphide associated elements such as Zn (256 ppm) and Cu (113) were noted as were high levels of As (839 ppm) (fig 99). SEM-EDS analysis was conducted on this sample and found disseminated grains of pyrrhotite, sphalerite, and galena as well as abundant arsenopyrite. EDS analysis of magnetite showed that it contained 2.9% Mn on average. Fayalite was the most abundant silicate.

Figure 98. Waste rock at Basttjärn containing a large amount of ore material (dark rock) demonstrating typical Mn weathering (6653532/498851). Photo: Patrick Casey.

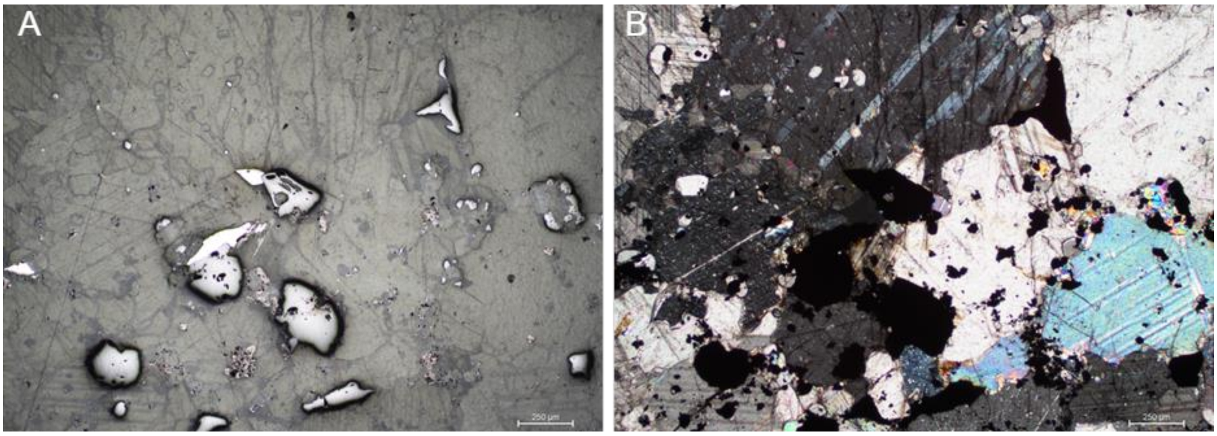

Figure 99. Thin section images from mineralised skarn sample from Basttjärn mine. **A**. Small magnetite crystals (grey) with arsenopyrite (white rhombic crystals). **B**. Thin section in XPL demonstrating the abundant carbonate (dolomite) in the ore. Micrographs: Patrick Casey

Table 34. Analytical results from Basttjärn.

Data	Object	Fe_2O_3 (%)	MnO (%)	Cu (ppm)	Zn (ppm)	Pb (ppm)	As (ppm)	Ti (ppm)
Mineralised sample	Basttjärn	51.8	5.9	108	172	10	839	50
Composite sample (n=15)	Average	19.6	3	163	210	115	229	477
	Max	30.8	3.9	479	294	442	1225	810
	Min	10.7	2.1	10	145	16	11	210

Potential resources at Basttjärn

With the assumption that no material has been removed from Basttjärn, potential resources at are 315000 tonnes Fe, 59000 tonnes Mn, 1200 tonnes Ti, 540 tonnes Zn, 420 tonnes Cu, 295 tonnes Pb.

Ställberg

Background

Ställbergsgruvan (Fig. 100) was in operation from 1867 through 1977 mining an Fe-Mn skarn ore body formed in carbonate interbeds in the regional rhyolitic metavolcanic rock. Total mined tonnage from Ställberg was 6.5 Mt of ore, and it produced 5.48 Mt of waste rock (table 35). Ore dressing was conducted on site in the early 20th century, producing only a small amount of tailings, which are now found northwest of the mine shaft and spread over some of the waste rock piles. The edge of the tailings berm can be seen in the LiDAR image of the Ställberg mine in figure 101. The waste rock has been used for construction and fill material, and the remaining tonnage is unclear. A summary of the available geophysical data for the area around Ställbergsgruvan is provided in the background description for Wigströmsgruvan, earlier in the report. The geophysical data which is available for the area around Ställbergsgruvan is summarised earlier in the report (see the section for Wigströmsgruvan).

Table 35. Production statistics from Ställberg.

	Total (Mt)	Fe (%)	Mn (%)
Mined Ore	6.53	49.8	4.71
Processed in dressing plant[1]	0.005		
Tailings	0.017	8.5	4.0
Waste rock	5.48		

[1]Tailings data were collected during a prior SGU sampling campaign.

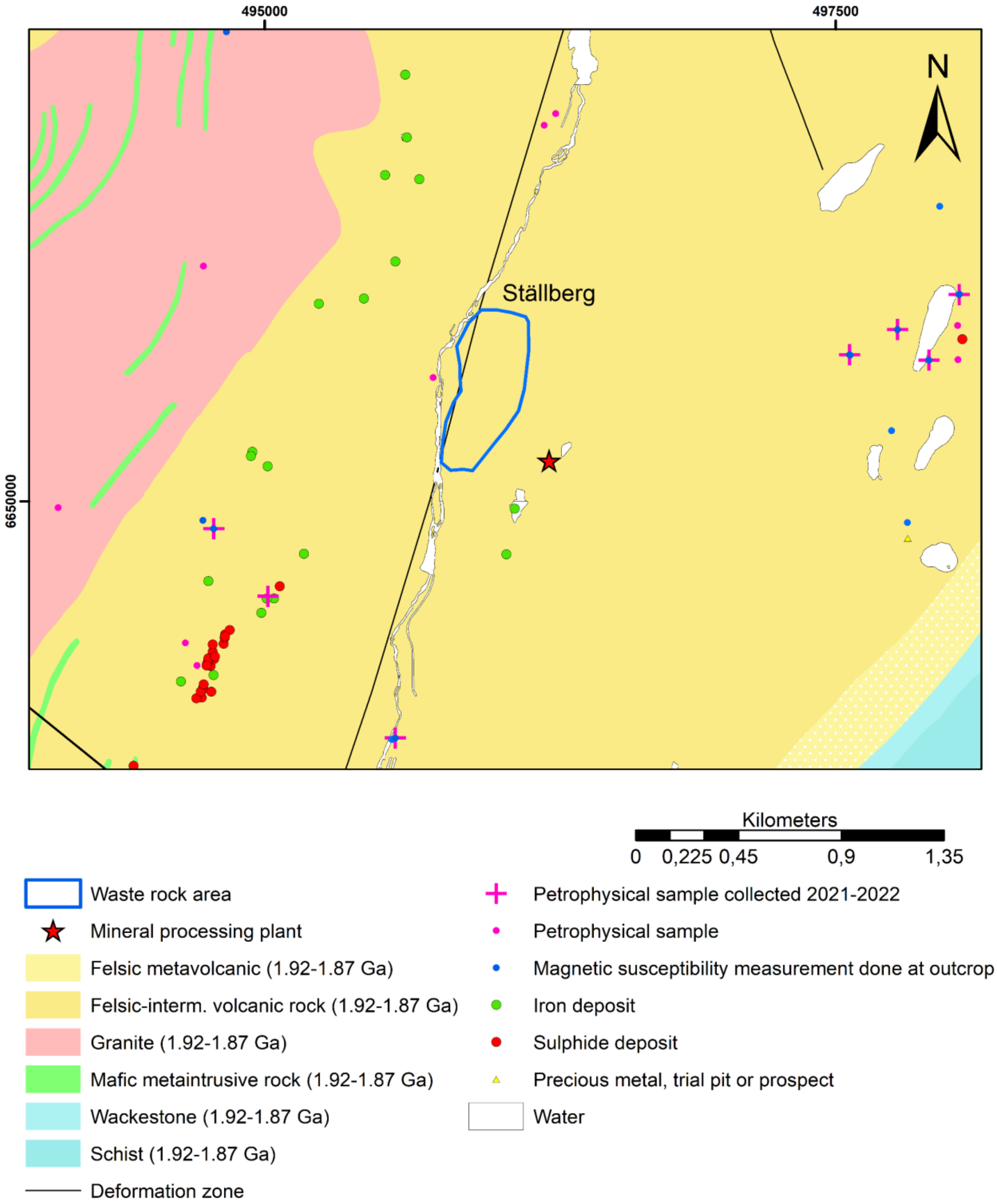

Figure 100. Bedrock map of the area surrounding Ställbergsgruva.

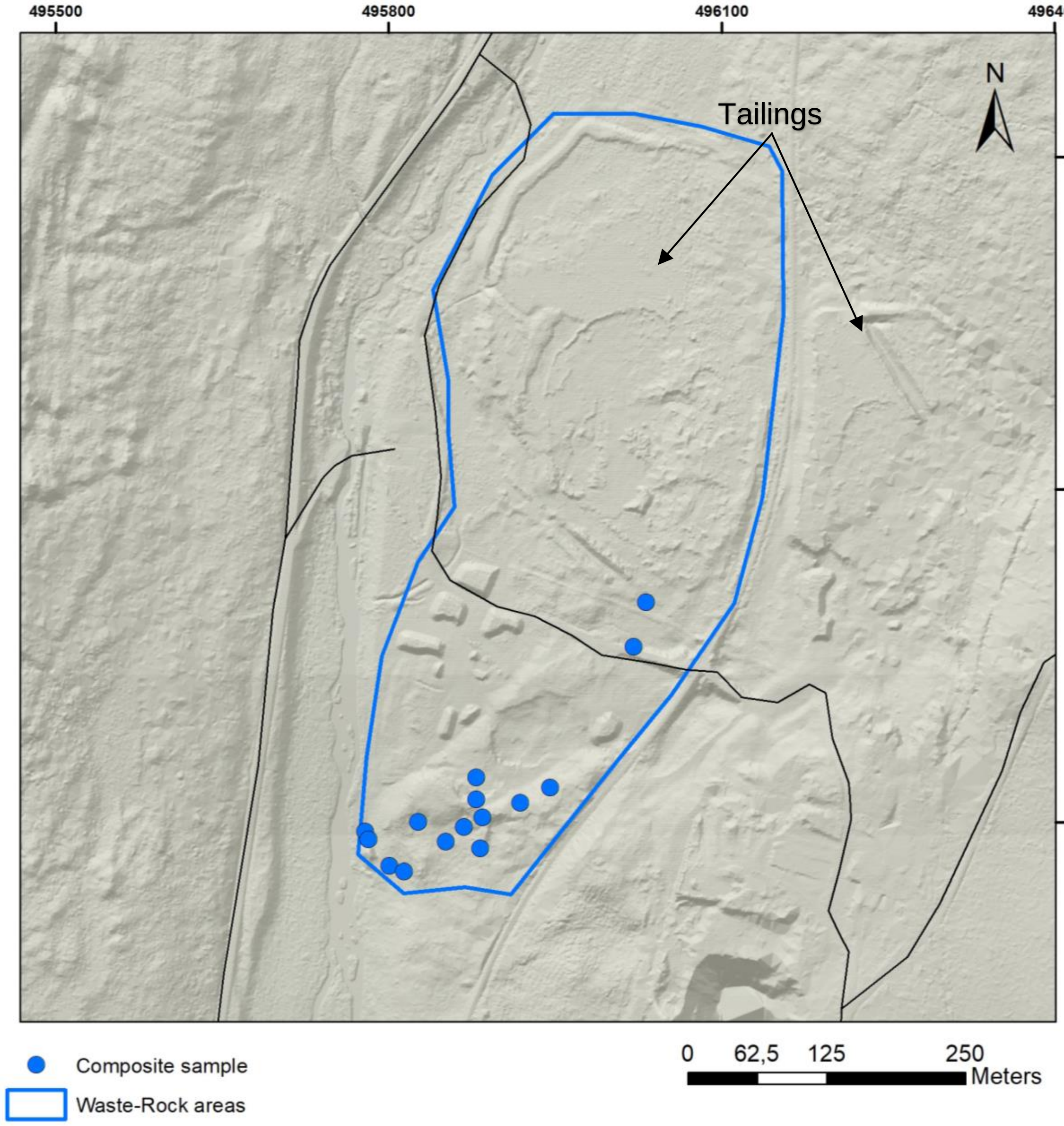

Figure 101. LiDAR image of the Ställberg waste rock dump. The wall of the former tailings dam can be seen in the northwest corner of the waste rock dump.

Sampling of waste rock at Ställberg

A total of 15 composite samples collected at Ställberg show moderate enrichment in Fe, with an average concentration of 17.4 % Fe_2O_3 and 3% MnO. The dominant waste rock was the local extrusive felsic metavolcanic rock as well as silicate and calc-skarn (Fig. 102). The calc-skarn was calcitic to dolomitic in composition, and typically contained disseminated magnetite crystals with occasional grains of sulphide or sulphide fracture filling. Somewhat elevated levels of Cu were observed in some samples up to 150 ppm. A single richly mineralised ore sample was analysed with high Fe_2O_3 contents at 81.3% and 6.9% MnO. No appreciable elevations in CRM was noted in either the composite samples or the richly mineralised sample.

Microscopy of the richly mineralised sample showed magnetite as the dominant Fe bearing mineral (Fig 103). EDS analysis showed up to 3% Mn within the magnetite. Small grains of arsenopyrite were also observed. Olivine was a common alteration mineral, dominantly fayalite, with lesser amounts of the manganese and magnesian chemistry present.

Figure 102. Sampled waste rock heap at Ställberg (6649891/496105). Photo: Stefan Persson

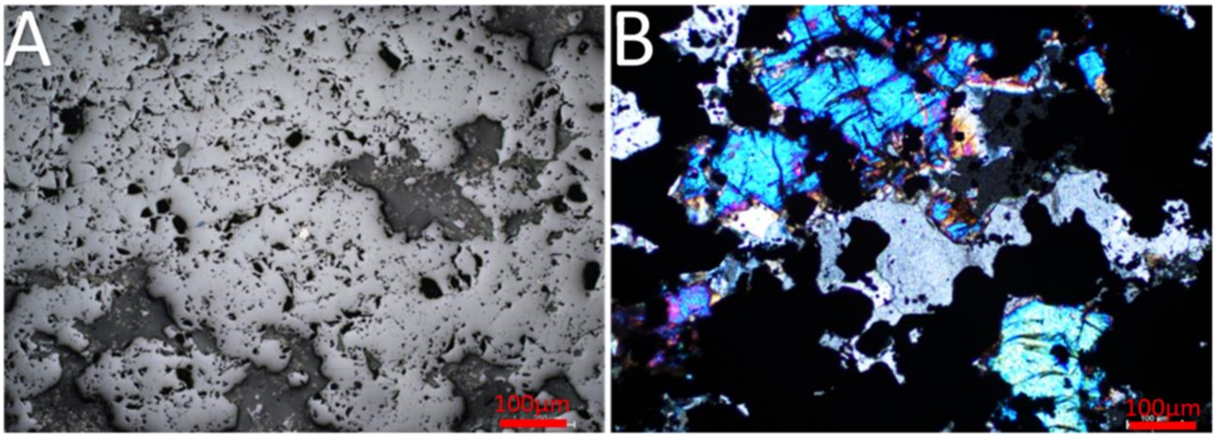

Figure 103. Thin section images from mineralised Ställberg sample. **A.** Magnetite with small sulphide grains (centre of image). **B**. Calcite (colourless) and fayalite (2nd – 3rd order birefringence) in XPL with magnetite (opaque). Micrograph: Patrick Casey

Potential resources at Ställberg

The results of the analyses of the Ställberg composite samples are shown in table 36. With the assumption that no waste rock has been removed from Ställberg, the potential resources in the waste rock are 668 kt Fe, 123 kt Mn and 3,700 tonnes Ti. The numbers presented here are a maximum value, as waste rock from Ställberg has been used as aggregate, and data are lacking for the amount of material removed from the site.

Table 36. Analytical results from Ställberg

Data		Fe (%)	MnO (%)	Ti (ppm)
Mineralised sample		81.3	6.9	970
Composite sample (n=15)	Average	17.0	2.9	679
	Max	26.5	4.1	1580
	Min	11.2	1.9	360
Tailings* (n=6)		8.5	4.0	480

*Tailings data were collected during a prior SGU survey.

BASE METAL DEPOSITS

Hällefors

Background

Hällefors Silvergruva is one of the oldest mines sampled during this study. Initial production began in 1635, with interruptions due to lack of capital and poor yields. Renewed production started in 1896, and during the 20th century production occurred in brief spurts, with the final production, run by Boliden Mineral AB, for one year in 1979. At the end of its life ore was transported to the Saxberget mine for refining, and the tailings were deposited in the Saxberget tailings pond. Hällefors is a stratabound Zn-Pb-Ag deposit with abundant Fe and Mn mineralisation. The primary ores are found as lens like bodies in within skarn altered carbonate bodies, with later remobilization of sulphides occurring during regional metamorphism creating fracture fill veins rich in sulphides and sulfosalts. Two modes of mineralisation are present at Hällefors. The westernmost ore bodies are dominantly stratabound sulphide mineralisation with abundant Fe-oxide and manganese mineralisation. The eastern part of the field is dominantly Fe-Mn deposits with limited sulphide mineralisation occurring in the remobilized veins of sulphide/sulfosalts (Wagner et al., 2005).

Silver production at Hällefors totalled 12 tonnes, with nearly a third being recovered during the one year that Boliden Mineral AB was producing from the mine in the 1970s, a testament to the efficiencies of modern production. Estimates of the produced waste rock at Hällefors are difficult owing to the lack of records during the first 300 years of production. The final year of production by Boliden Mineral Ab produced approximately 0.09 Mt of ore according to MALMdb (Table 37).

Sampling of the waste rock was conducted at the waste heap nearest to Jan-Olafs gruva and Parallelgruvan. Two other large waste rock piles were not sampled and are outlined in figure 104.

Table 37. Production statistics from Hällefors (SGU's MALMdb)

	Total (Mt)	Zn (%)	Pb (%)	Cu (%)	Ag (ppm)	Au (ppm)
Mined Ore[1]	0.74	4.34	4.00	0.07	99.60	0.2
Waste rock[1]	0.095					

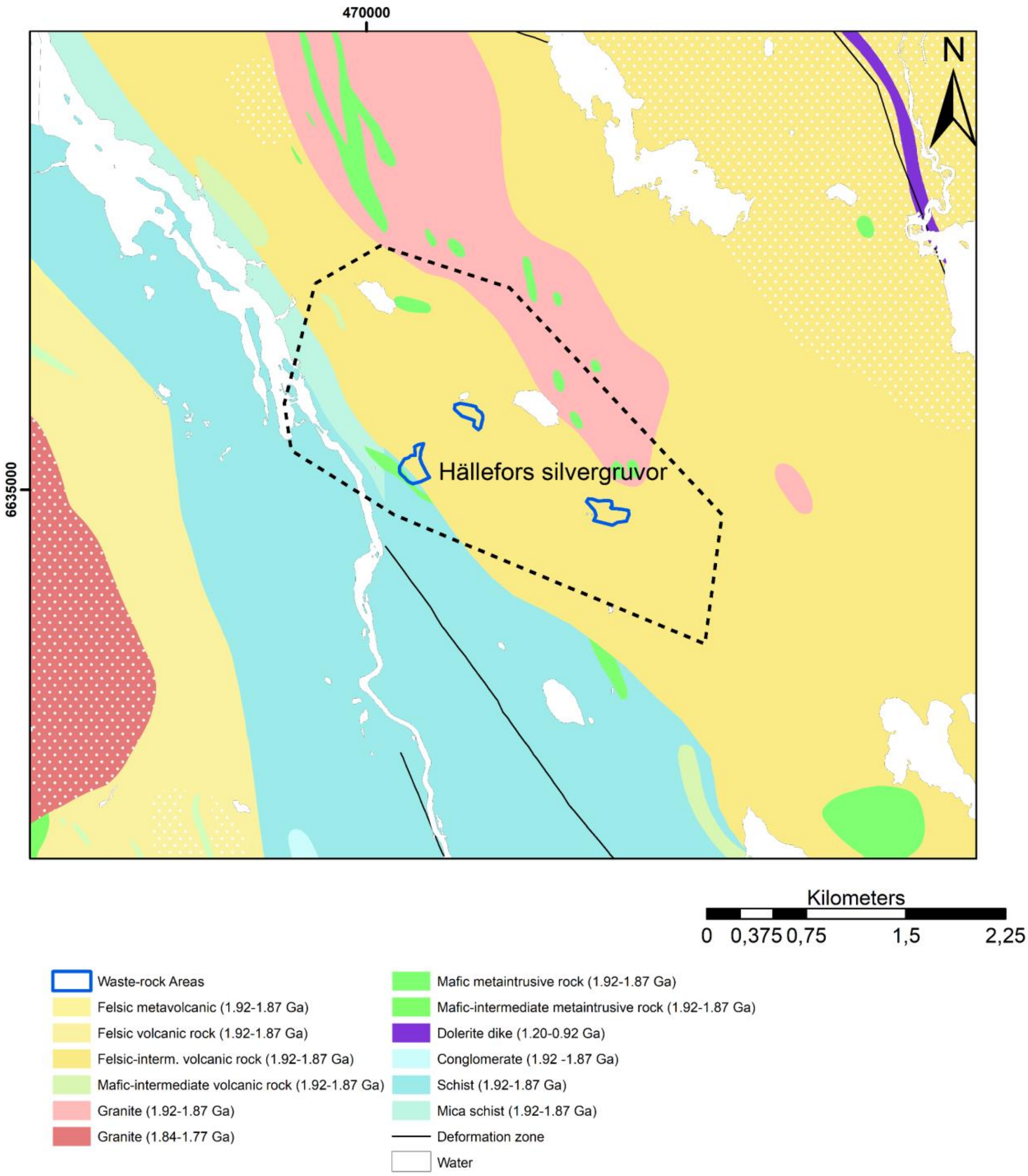

Figure 104. Bedrock map of the Hällefors area with the three waste rock areas denoted.

Available geophysical data

Airborne data (magnetic, VLF, gamma spectrometry)

As part of this project an area around the Hällefors Silver mines was selected for additional bedrock mapping efforts. The motivation for this was to gain a better understanding of the bedrock and primary mineralisation from which the mining waste in this area has been generated. This area is shown in figure 105 as a black dashed line and will be referred to subsequently as the Hällefors mapping area.

Airborne geophysical measurements were first performed in 1973 by SGU over and around the Hällefors mapping area. They included natural gamma, magnetic and VLF (1 transmitter) measurements. In 1985, LKAB collected additional airborne data over an area to the west of the Hällefors mapping area where natural gamma, magnetic, VLF (2 transmitters) and slingram measurements were performed. The most modern airborne data which are available for the area around the Hällefors silver mines were collected by SGU in 2017. For this survey natural gamma, magnetic and VLF (2 transmitters) measurements were recorded. Information about the different airborne geophysical data which are available are shown in table 38.

Figure 105 shows the residual magnetic field for the area over and around the Hällefors mapping area. Several magnetic anomalies are present. To the north of the Hällefors mapping area there is a region with felsic and mafic intrusive rocks which gives rise to a broad positive anomaly with an approximate southeast-northwest strike. To the south of the Hällefors mapping area there is another linear anomaly with similar strike (southeast-northwest) which is interpreted to be associated with the contact between the metasedimentary rocks to the south and the felsic volcanic rocks which lie within the centre of the Hällefors mapping area. Within the Hällefors mapping area there are several small positive magnetic anomalies which are associated with documented mineralisation. Firstly, to the north, there is a small positive anomaly, most likely associated with Fe mineralisation. Secondly, to the east of the Hällefors mapping area there is another magnetic anomaly associated with the mineralisation in the Eastern field (Östra fältet) of the Hällefors silver mines. Similar magnetic anomalies are not associated with the other mineralisation, which is documented in the Hällefors mapping area, namely the Western field (Västra fältet) and Stollberget. This is consistent with previous investigations of the minerology for the different deposits in the Hällefors area (Sundius et al., 1966), where significant amounts of both magnetite and pyrrhotite are documented in the Eastern field (Östra fältet). Whereas only relatively small amounts of pyrrhotite are documented in the Western field (Västra fältet; Sundius et al., 1966).

Figure 106 shows a map of the apparent resistivity calculated from the 2017 airborne VLF data. On inspection of this map, the regions of low resistivity appear to mainly correspond to areas with high soil moisture, such as lakes or wetlands, for example the region of low resistivity in the centre of the Hällefors mapping area. Some anomalies shown on the map are also associated with power lines.

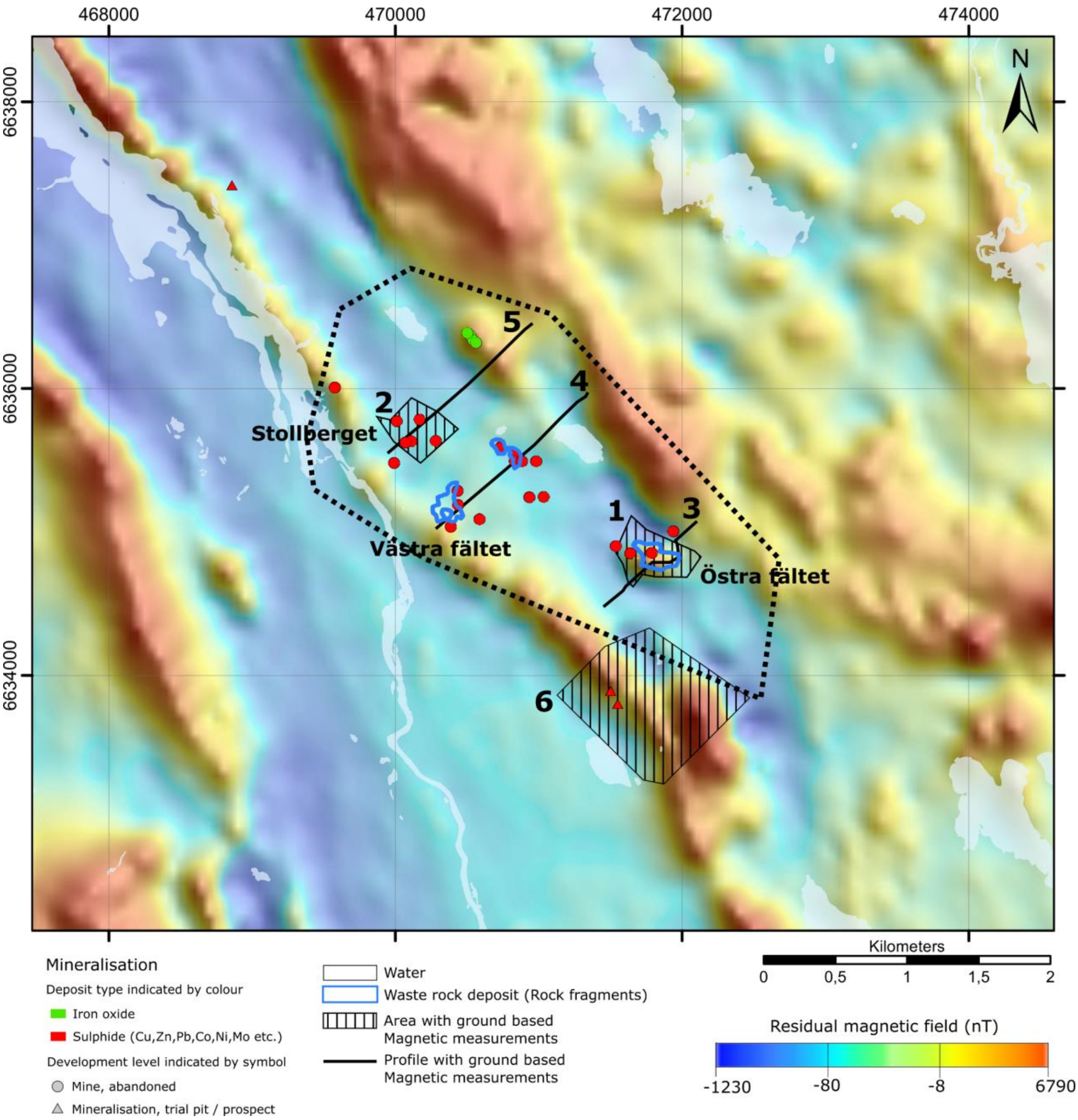

Figure 105. Map of residual magnetic field for the Hällefors focus area. The Hällefors mapping area is shown with a thick black dashed line. The location of ground-based magnetic measurements, listed in table 39 is shown.

Table 38. Complete list of the airborne geophysical surveys over and close to the Hällefors focus area.

Year	Organisation	Geophysical methods used	Area (SGU map sheet)	Flight direction (degrees)	Flight line separation (m)	Flight altitude (m)
1973*	SGU	Magnetics, gamma spectrometry, VLF (1 transmitter)	11E	East–West (90°)	200	30
1985*	LKAB	Magnetics, gamma spectrometry, slingram, VLF (2 transmitters)	Part of 11E	Northeast–Southwest (30°)	100	30
2017	SGU	Magnetics, gamma spectrometry, VLF (2 transmitters)	Part of 11E and 10E	East–West (90°)	200	60

* Not used for producing maps in this report

Ground-based electromagnetic and magnetic measurements

Prior to this project the only ground-based geophysical measurements available in this area were magnetic measurements collected in 1987 to the south of the Hällefors mapping area. These data have a line spacing of between 120 and 40 m and cover part of the magnetic anomaly which lies to the south of the felsic volcanic sequence (fig. 105).

As part of this project new ground-based geophysical measurements were performed with the objective of supporting mapping efforts and as input to geophysical and geological modelling of the bedrock and mineralisation.

These new measurements include three northeast-southwest profiles which were collected across different parts of the Hällefors mapping area, perpendicular to the dominant strike of the bedrock units. Both magnetic and VLF measurements (16.4 and 24.0 kHz) were collected (figs. 105 and 106) using a GEM GSMV-19 instrument. In addition, VLF and magnetic measurements were performed over two areas where mineralisation has previously been documented (Stollberget and the Östra fältet). For these areas an approximate line spacing of 60 m was used. Details of the ground-based geophysical measurements from the Hällefors mapping area can be seen in table 39 and figures 105 and 106.

Table 39. Ground-based magnetic and electromagnetic measurements within the Hällefors area. Numbers correspond to the numbered polygons/lines shown in figure 105 and 106.

Polygon/Line number and name	Method	Year acquired	Responsible	Comments
1. MP21DSR0012, VP21DSR0017, VP21DSR0018 and VP21DSR0019	Magnetic and VLF	2021	SGU	VLF data collected over an area with approximately 60 m line spacing. Three VLF frequencies measured (16.4, 22.2 and 24.0 kHz)
2. MP21DSR0013 VP21DSR0020, VP21DSR0021 and VP21DSR0022	Magnetic and VLF	2021	SGU	VLF data collected over an area with approximately 60 m line spacing. Three VLF frequencies measured (16.4, 22.2 and 24.0 kHz)
3. MP21DSR0011, VP21DSR0015 and VP21DSR0016	Magnetic and VLF	2021	SGU	One profile collected in this area, two VLF frequencies (16.4 and 24.0 kHz measured)
4. MP21DSR0010, VP21DSR0013 and VP21DSR0014	Magnetic and VLF	2021	SGU	One profile collected in this area, two VLF frequencies (16.4 and 24.0 kHz measured)
5. MP21DSR0009, VP21DSR0011 and VP21DSR0012	Magnetic and VLF	2021	SGU	One profile collected in this area, two VLF frequencies (16.4 and 24.0 kHz measured)
6. mgtmid1298	Magnetic	1987		Profile spacing of 120 to 40 m.

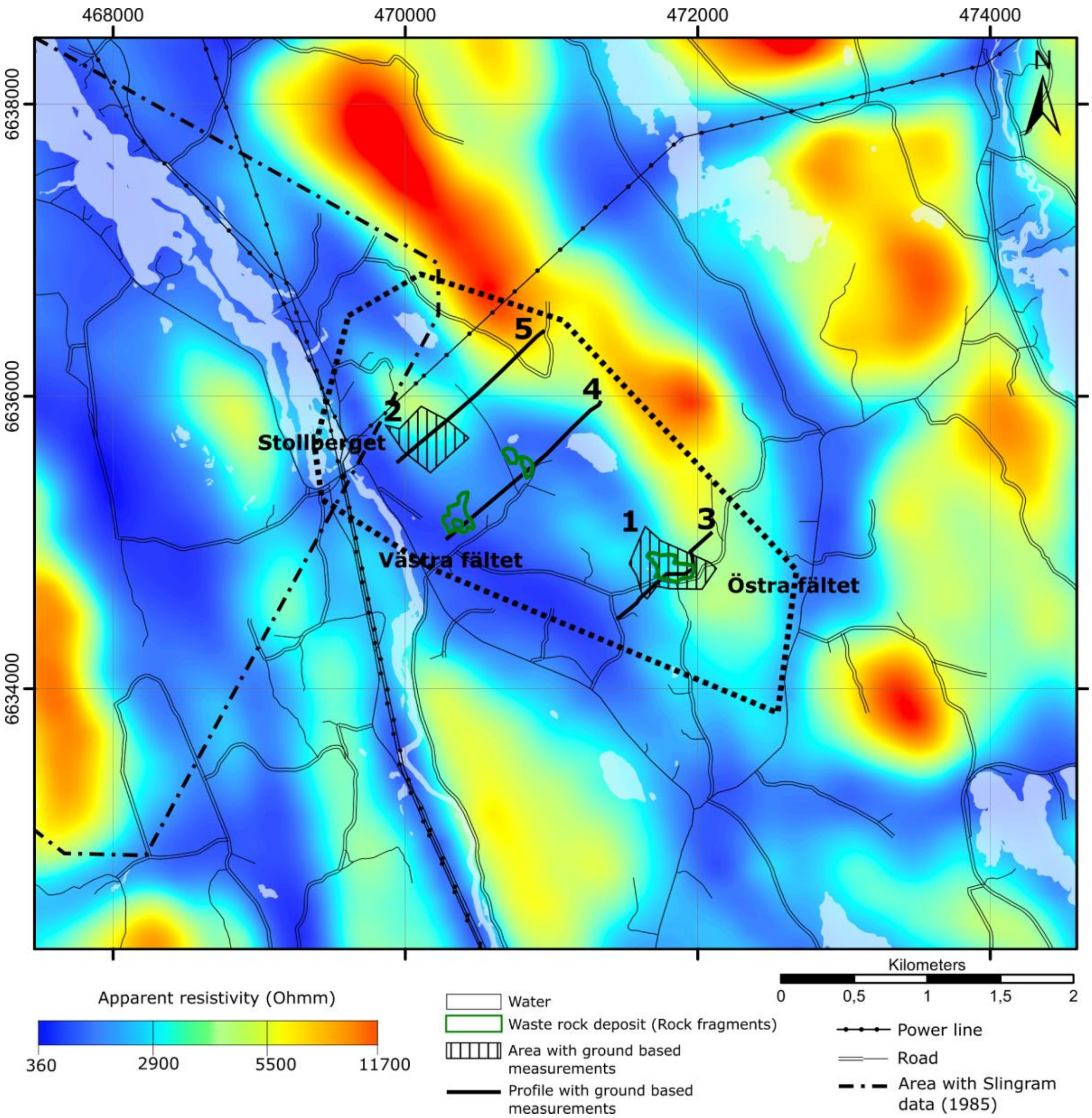

Figure 106. Map of apparent resistivity derived from airborne VLF data collected in 2017 for the Hällefors area. The Hällefors mapping area is shown with a thick black dashed line. The location of ground-based electromagnetic measurements, listed in table 39 are shown.

Ground-based gravity

Prior to this project some ground-based gravity measurements were available for the area around the Hällefors mapping area, however these had a relatively large average spacing of 1–2 km between points. As part of this project 209 additional gravity measurements were collected in 2022. As a result of the new measurements the spacing between points has been reduced to about 100–300 m across the Hällefors mapping area. Figure 105 shows two maps of the residual gravity anomaly calculated with different parameters as well as the pre-existing and newly acquired gravity measurement points. In figure 107A a grid spacing of 100×100 m was used to interpolate the Bouguer anomaly data. The residual anomaly was calculated by subtracting a version of the Bouguer anomaly grid which had been upward continued by 3 km, from the original grid. In figure 107B a grid spacing of 50×50 metres was used and the residual anomaly was calculated by subtracting a version of the data which had been upward continued by 300 m. Hence, small, high frequency variations are more prominent in figure 105B than figure 107A.

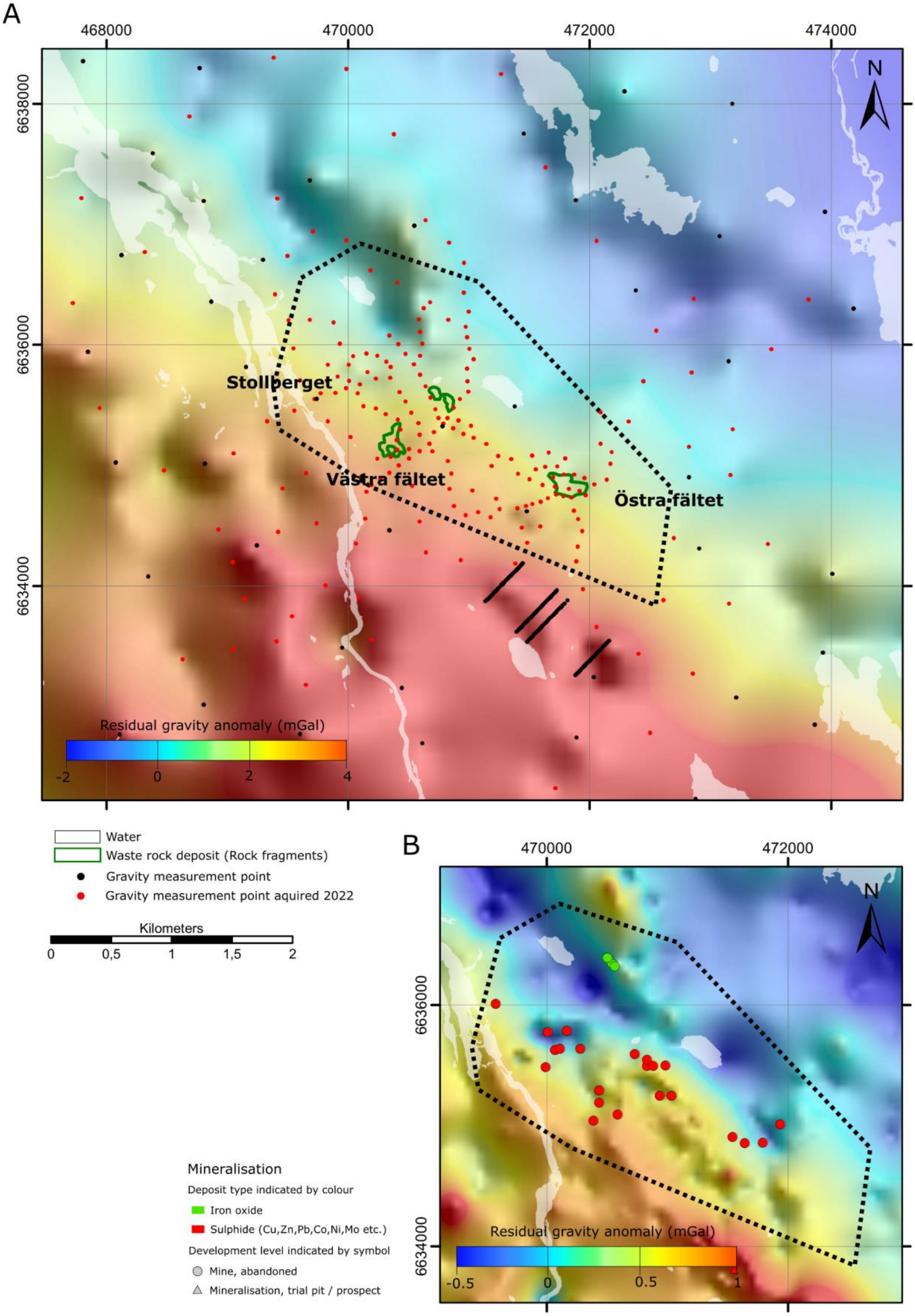

Figure 107. Map of the residual gravity anomaly over and around the Hällefors area. **A.** Residual gravity anomaly calculated with a 100×100 m grid spacing and 3 km upward continuation. Pre-existing and new gravity measurements are annotated. **B.** Residual gravity anomaly calculated with a 50×50 m grid spacing and 300 m upward continuation. Mineralisation is shown with red and green symbols. The Hällefors mapping area is shown on both A and B with a thick black dashed line. Note that the distance scale for A and B is the same but they have different scales for the residual gravity anomaly values.

The gravity response within the Hällefors mapping area is predominantly characterised by a gradient, from high values to the southwest to lower values in the northeast. This could be partially associated with the transition from predominantly felsic intrusive and extrusive rocks (with densities around 2650 kg/m^3) in the northeast to metasedimentary strata (with densities around 2800 kg/m^3) to the southwest. However, it could also be associated with variations in rock at depth (for example, due to the presence of mafic rocks below the surface). There appears to be several small-scale variations in the gravity anomaly within the mapping area (fig. 107B). The most prominent of which is a linear positive anomaly which coincides with Fe mineralisation and mafic rocks in the northwest part of the mapping area. Within the southern and central parts of the Hällefors mapping area (around the Västra fältet) there appears to be several low amplitude positive anomalies which follow the overall strike of the bedrock units in the area. Hence, these anomalies could potentially be associated with variations in the layering within the sequence, such as layers containing more mafic minerals or layers with more carbonate. However, it is also possible that these small anomalies could be associated with variations in the rocks at depth or the geometry of the contact between the metasedimentary strata and the felsic volcanic sequence. It should be noted that the Stollberget and Östra fältet coincide with small negative anomalies (about 0.5 mGal lower than the surrounding area, see figure 107B). This is not expected as the mineralisation typically has far higher density than the surrounding rocks (see table 40). One possible explanation is that these anomalies are due to the open space within the old mines, however, such an anomaly is not clearly observed at the Västra fältet where mining has also occurred. Hence, it could indicate that these anomalies are related to variations in rock at depth and not related directly to the mineralisation or mining activity.

Petrophysical and borehole data

Figure 108 shows the petrophysical data available for the Hällefors mapping area. As part of this project additional petrophysical data have been collected to provide a better characterisation of the physical properties of the rocks in this area. The new data are shown in table 40.

The majority of the new petrophysical data have been collected from felsic metavolcanic rocks, which dominate within the Hällefors mapping area. These rocks can locally include phenocrysts consistent with volcanic processes. However, in other areas they can be relatively fine grained and homogenous and almost devoid of phenocrysts. These more homogenous rocks are often referred to as hälleflinta in other reports and texts (Sundius et al., 1966). These felsic metavolcanic rocks typically have relatively low densities of between 2650 and 2750 kg/m^3 and low magnetic susceptibilities of less than 200 × 10^{-6} SI. The samples taken from carbonate and skarn also appear to exhibit similar physical properties as the felsic metavolcanic rocks. One sample was taken from granitic rocks to the north of the Hällefors mapping area which exhibits a low density of 2641 kg/m^3 and magnetic susceptibility of 209 × 10^{-6} SI. New and pre-existing samples taken from the metasedimentary strata to the southwest of the Hällefors mapping area typically show density values of around 2800 kg/m^3, which is typically slightly higher than those of the felsic metavolcanic rocks.

Two samples of sulphide mineralisation were collected, one from the eastern field (Östra fältet) and one from the western field (Västra fältet, see figure 105). Both samples exhibit high density values. However, the magnetic susceptibility varies markedly between the two sites, where the mineralisation from the eastern field has a high susceptibility of 2 982 742 × 10^{-6} SI and the mineralisation from the western field has a relatively low susceptibility of 1113 × 10^{-6} SI. This is consistent with the airborne magnetic measurements which show a large magnetic anomaly at the eastern field but almost no anomaly at the western. This is also consistent with the observations of Sundius et al. (1966) who document large amounts of magnetic minerals such as magnetite and pyrrhotite in the eastern field but not in the western field. This difference could well be linked to the different modes of mineralisation between the two deposits, where the eastern field is stratabound and associated with carbonate layers in the felsic metavolcanic sequence, whereas the mineralisation in the western field occurs more as fracture filling material and cuts across the strike of the surrounding rocks (Sundius et al., 1966).

A sample collected to the north of the Hällefors mapping area, within the area noted as mixed mafic and felsic intrusive rocks on the bedrock geology map (fig. 108), was classified as a fine grained, Fe mineralisation. This sample exhibits a relatively high density and magnetic susceptibility.

In the SGU database 16 boreholes are listed in the vicinity of the Hällefors Silver mines and they are shown in figure 108. These were drilled between 1988 and 1997 by NSG and Lundin mining Exploration AB.

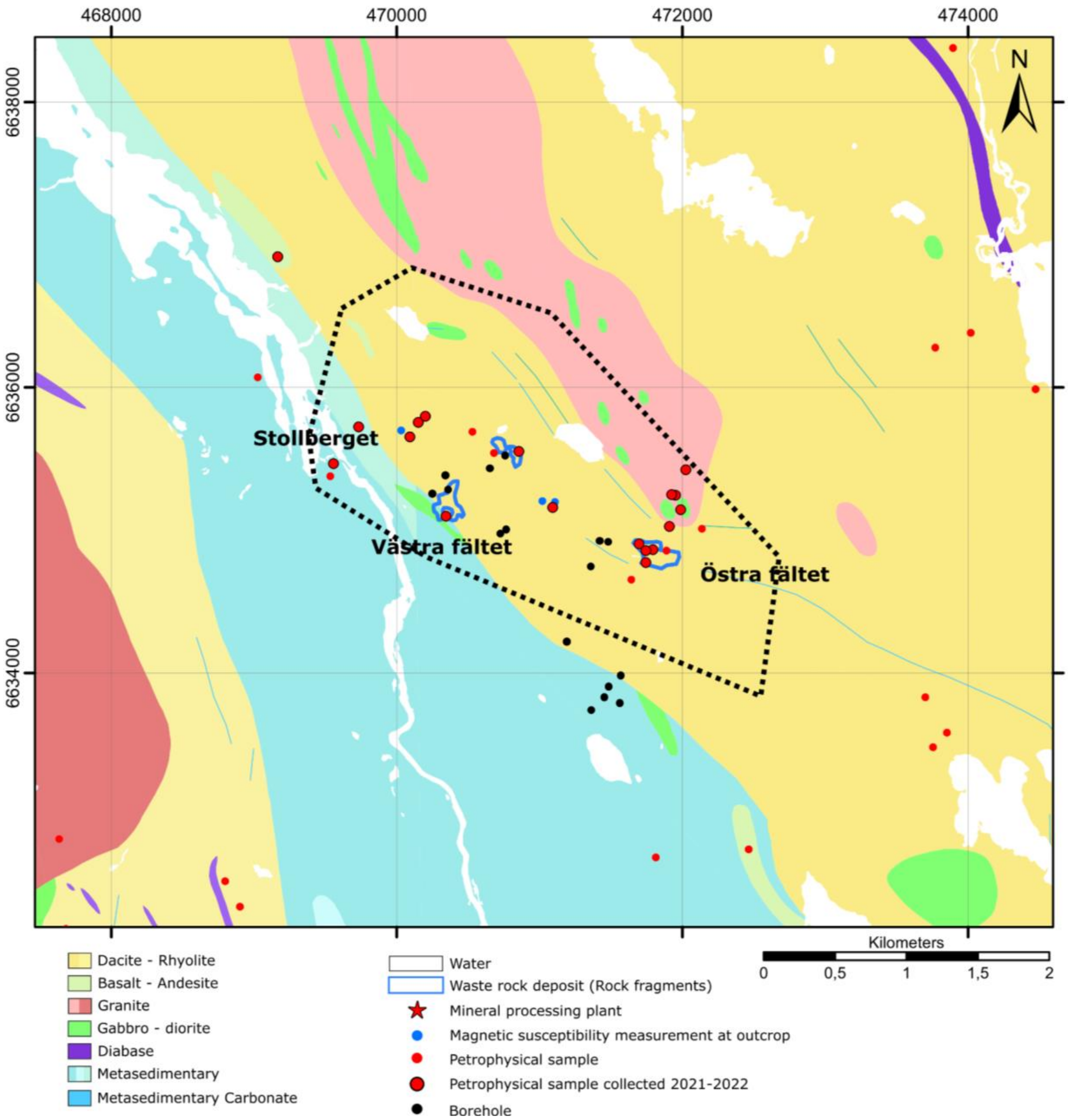

Figure 108. Map of the petrophysical and borehole data from and around the Hällefors study area. The Hällefors mapping area is shown with a thick black dashed line.

Table 40. Table summarising the petrophysical results collected as part of this project from the Hällefors mapping area.

Sample ID	Easting (m)	Northing (m)	Description	Density (kg/m3)	Magnetic susceptibility (10-6 SI)	J (mA/m)
DSR210017A	471793	6634864	Felsic metavolcanic	2703	151	30
DSR210017B	471793	6634864	Carbonate	2702	37	44
DSR210018A	471743	6634858	Sulphide mineralisation	4202	2982742	607677
DSR210019A	471907	6635028	Felsic metavolcanic	2721	190	21
DSR210019B	471907	6635028	Skarn	2751	232	38
DSR210020A	471924	6635251	Granite	2641	209	49
DSR210020B	471924	6635251	Fe oxide mineralisation	2941	94079	2519
DSR210021A	470343	6635100	Felsic metavolcanic	2718	126	69
DSR210021B	470343	6635100	Sulphide mineralisation	4498	1113	253
DSR210022A	470854	6635553	Felsic metavolcanic	2707	136	55
DSR210024A	471090	6635161	Felsic metavolcanic	2568	26	56
DSR210026A	470090	6635656	Felsic metavolcanic	2640	44	76
DSR210028A	470150	6635757	Felsic metavolcanic	2710	87	25
DSR210029A	470200	6635800	Felsic metavolcanic	2770	116	20
PCY210014A	469556	6635467	Shale	2757	424	55
PCY210015B	471744	6634775	Sulphide mineralisation	4179	9453	1509
PCY210027B	471695	6634905	Felsic metavolcanic	2710	126	34
PCY210034A	472024	6635424	Meta-intrusive	2670	203	52
PCY210035B	471950	6635247	Meta-intrusive mafic	2979	103778	207
PCY210036B	471988	6635144	Porphyritic volcanic	2727	408	35
PCY210040A	469164	6636916	Extrusive mafic	2859	635	63
PCY210043A	469732	6635726	Intermediate extrusive	2763	653	72

Sampling of waste rock at Hällefors

A total of 19 composite samples were collected from Hällefors. Figure 109 shows the locations of these samples, as well as where other waste rock heaps are located. These samples showed high levels of Fe and manganese, with up to 10% manganese. Much of the waste rock at Hällefors showed the typical purplish weathering crust common in Mn rich ores. High levels of Pb and Zn were observed, with lower levels of Cu. Sphalerite and galena were the dominant sulphide minerals observed, with pyrite and minor chalcopyrite present. Silver was present in some samples up to 100 ppm, strongly associated with Pb. Throughout its history galena was the most important mineral at Hällefors as a carrier of Ag and a strong correlation is seen between Ag and Pb content in the waste rock. EDS analysis showed silver mineralisation within argentiferous galena, as well as argentotetrahedrite. While geochemical analysis showed limited amounts of Sn, cassiterite was somewhat common in thin section. Antimony was enriched in most samples, averaging 50 ppm.

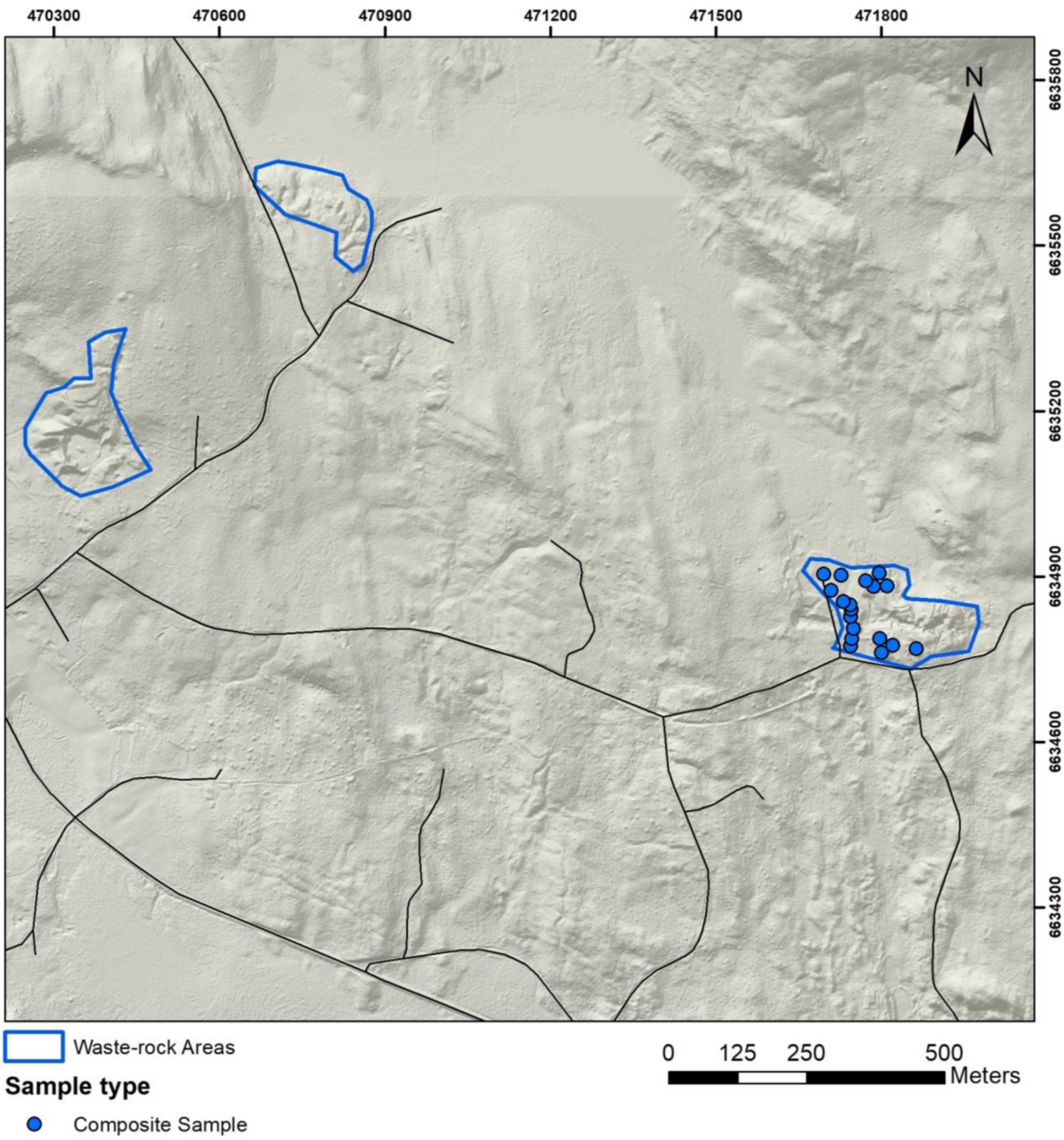

Figure 109. LiDAR image of area surrounding the Hällefors mines. Waste rock areas, including those not sampled in this study are shown.

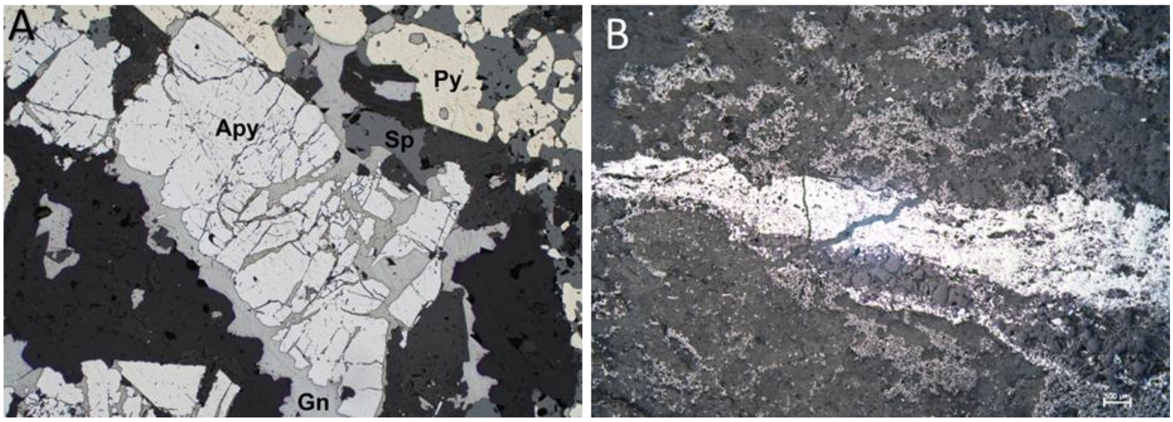

Figure 110. A: Thin section image of a sulphide rich sample from Hällefors demonstrating the fracturing of arsenopyrite and later remobilisation of galena filling in the fractures. **B:** Arsenopyrite vein intruding magnetite in the Fe rich sample. Micrograph: Patrick Casey.

Two richly mineralised samples were analysed, a sulphide rich sample (PCY210015B) and an Fe-Mn rich sample (PCY210018B). PCY210015B demonstrated extreme enrichment in sulphides, with 16.3% Pb and 14.4% Zn. Silver contents were 444 ppm and Sb was above the detection limit of 250 ppm. As and Cd were above the maximum detection limit of 1%. Based on summation of the other major components of the sample, 15% of the sample is unaccounted for, pointing to extreme enrichment in these two elements. Based on EDS analysis showing 0.5 % Cd in sphalerite, this points to 0.7% Cd and up to 14.3% As in this sample.

PCY210018B showed high levels of Fe_2O_3 and MnO, with 48.1 and 15.5%, respectively, of the sample composed of these two elements. Lead and Zn were approximately 0.5%. Antimony was again over detection limit. Arsenic was above detection limit as well. Arsenopyrite veins were observed cutting through the sample as shown in Fig. 110B. Based on summation of other components, As composes up to 8% of the mineralised sample (table 41).

Table 41. Analytical results of waste rock from Hällefors

		Fe (%)	Zn (%)	Pb (%)	Cu (ppm)	Ag (ppm)	Sb (ppm)
Mineralised sample (Fe-Mn)		48.1	0.55	0.58	89.25	69	>250
Mineralised sample (Sulphide)		20.3	14.5	16.4	168	444	>250
Composite Samples (n=18)	Average	10.4	1.4	0.97	113	31.6	49.4
	Max	21.5	6.2	3.9	348	101	137.5
	Min	3.3	0.205	0.012	12	0.7	2.4

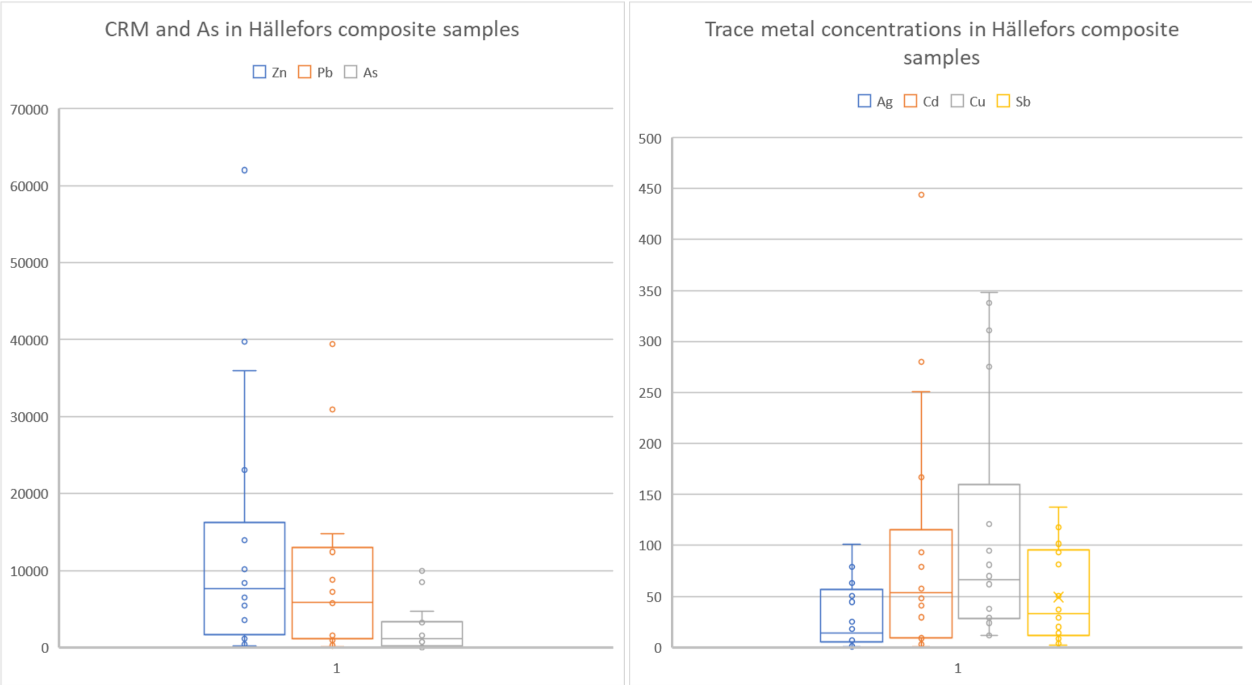

Figure 111. Distribution of CRM and elements of environmental concern in composite samples at Hällefors.

Potential resources at Hällefors

SGU's MALMdb indicates 94 kt of waste rock at Hällefors Silvergruva. Working on the assumption that no material has been removed from the site, the potential resources are up to 9700 tonnes of Fe, 1200 tonnes Zn, 900 tonnes Pb, 10 tonnes Cu, 3 tonnes of Ag and 4 tonnes of Sb. This estimate of waste rock is from the operation of the mine by Boliden Mineral AB during the 1970s. Additional waste rock from older mining operation was not sampled, and thus these amounts are a likely an underestimation.

Bedrock mapping of the Hällefors district

As part of this project the Hällefors district was selected for additional bedrock mapping efforts. Figure 112 shows the observations made during mapping.

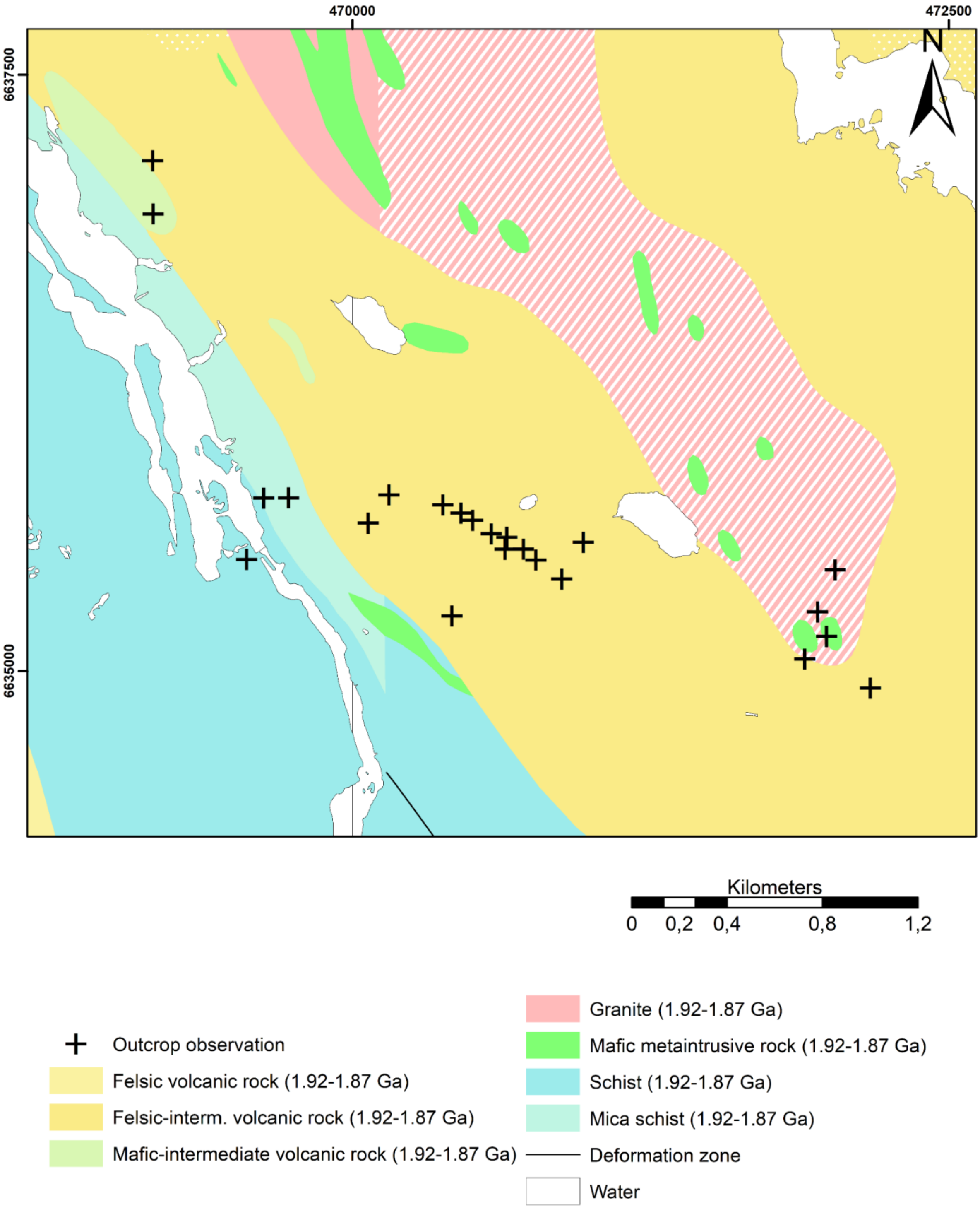

Figure 112. Map showing observations made (crosses) during mapping in the Hällefors area. Light grey marks outcrops shown in SGU's outcrop database.

Summary of observations

Supracrustal volcanic and volcanic sedimentary rocks

The Hällefors area is dominated by extrusive metavolcanic rhyolites. These rocks are dominantly fine grained to extremely fine grained (referred to as leptite and hälleflinta, respectively, in older Swedish literature). The textures are the result of varying degrees of recrystallisation during metamorphosis. In Hällefors the appearance of the metavolcanic supracrustal rocks varies from grey quartz to feldspar porphyritic, to pale to bleached white altered rocks with small quartz phenocrysts. Disseminated grains of sulphide minerals are common in the meta-rhyolite, and occasionally sulphides were observed as fracture fill.

Volcanic rocks with sedimentary structures were observed mostly to the east of Hällefors, where bedded meta-rhyolites were noted, with varying thicknesses in the bands. These outcrops have typically a creamy white colour on weathered surfaces, and a dark grey colour on the interior, and displayed rounded quartz phenocrysts up to 3 mm in diameter as well as occasional fragments of what were interpreted as pumice.

Also found in the Hällefors area are numerous examples of coherent meta-basic lava flows. These have been metamorphosed to amphibolite facies, and commonly display a "salt and pepper" texture of white feldspars and black amphiboles and contain no quartz.

Sedimentary rocks

Due west of Hällefors is a suite of schistose rocks. Mica schists were observed stratigraphically under the mica poor schists. These rocks are dark in colour, finely laminated, and are likely post volcanic, formed during the deepening of the depositional basin during a period of quiescence.

Carbonate beds were observed at a single outcrop in the vicinity of Parallelgruvan. These beds were typically thin dolomite bands, with bands of skarn alteration of varying thickness. A stromatolite was observed and can be seen in fig. 112C under the handle of the knife.

Intrusive rocks

The intrusive rocks in the Hällefors area are part of the GDG suite (granite-diorite-gabbro) and show a dominant composition between granite and diorite with occasional basic intrusions. They were emplaced early during the formation of the region during the extensional phase as evidenced by their intrusion into volcanic rocks and S1 fabric following the regional trend of 330° A single direct contact between an intrusive granite and extrusive rock was observed east of Parallelgruvan (fig 115c) at Hällefors where the contact between the rocks was strongly hydrothermally altered and serpentinized. Intrusive rocks show signs of alteration, with plagioclase typically sericitised to varying degrees. The metabasites typically show abundant amphibole.

Microscopy

Samples of the rhyolite commonly retains a porphyritic texture with sub-rounded to rounded dark coloured quartz phenocrysts ranging up to 3 mm in size with occasional plagioclase phenocrysts. In more altered samples of the volcanic rock, plagioclase has been replaced with sericite or show signs of low-grade sericite alteration around grain boundaries. Occasional disseminated opaque minerals were observed. These were dominantly magnetite and pyrite with occasional pyrrhotite.

A single thin section of strongly Mg altered meta-rhyolite of the "hälleflinta" type was studied (Fig. 113A). This sample showed fine grained quartz groundmass with typical grainsize of 0.005 mm to sub-micron in size with several larger quartz phenocrysts. Larger inclusions of sericite are interpreted as feldspar phenocrysts that underwent magnesian alteration.

Analysis of felsic subvolcanic rocks showed quartz and common chlorite and biotite. Plagioclase showed varying degrees of alteration to sericite (Fig. 113 B; F). Mafic subvolcanic rocks showed abundant amphibole, sericitised feldspars and opaque minerals. Opaque minerals were predominantly Fe-oxides with occasional pyrite grains.

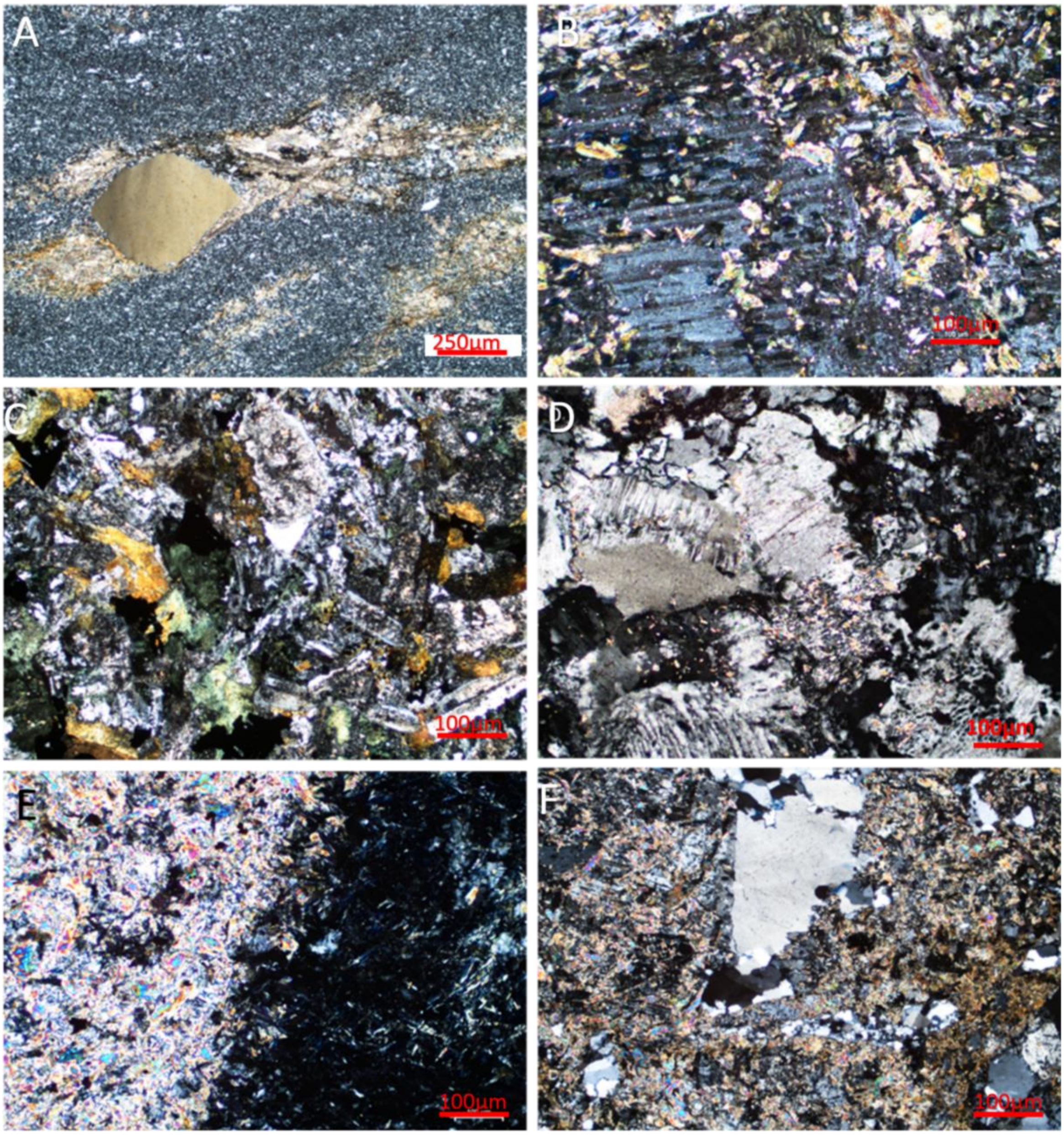

Figure 113. Thin section images from Hällefors. **A.** Quartz phenocryst and sericite altered plagioclase in an extremely fine quartz groundmass. **B.** Partial sericitisation of a feldspar crystal in a granite. **C.** Amphiboles and sericite in a mafic meta-intrusive. **D.** Myrmekite texture and partial sericitisation of plagioclase crystals in granite. **E.** Talc and serpentine minerals from meta-rhyolite from a contact. **F.** Near complete sericite alteration of feldspars within granite. Micrographs: Patrick Casey

Three samples from the serpentinized contact between the granite and the supracrustal rocks were analysed. The granite showed signs of stronger alteration, including myrmekite texture within plagioclase crystals (Fig. 113D). The serpentinised rock showed abundant serpentine minerals as well as talc (Fig. 113E).

Structure

Regional scale deformation during the Svecokarelian orogeny produced a regional 330° NNW foliation that was observed at all studied outcrops.

Northeast of the mine area preservation of primary bedding is observed with various well bedded units shown in fig. 114. In these beds upwards fining and sharp erosive contacts are seen, pointing towards a high energy environment likely situated in a subaqueous environment proximal to a volcanic source. These beds are likely formed by alternating pyroclastic deposition, both from gradual deposition of ash falling through the water column, and more energetic pyroclastic flows. Measurements of the bedding showed an upwards direction of 270° which is consistent with earlier work in Hällefors (Allen et al., 1996). Further evidence of the younging direction of the stratigraphy was provided by a stromatolite in a carbonate bed observed at Parallelgruvan (fig 114c), which showed a similar upwards direction to the bedding in the bedded supracrustal rocks.

Figure 114. A. Banded meta-rhyolite (6635631/470504) **B.** Detail of bedding in the schist overlaying the Hällefors supracrustal meta-rhyolites (6635462/469556). **C.** Carbonate and skarn layers near Parallelgruvan with stromatolite below knife handle. (6634885/471787). **D.** Sharp contact between bedding in meta-rhyolite in a fining upwards sequence (6635694/470379).

West of the Hällefors mines bedrock is dominated by schist. The schist is finely bedded, with beds ranging from 0.4 to 2 cm in thickness. Based on the bedding trend of 110° in the stratigraphically lower rocks, these beds represent a period of quiescence and basin deepening during an interlude of volcanic quiescence.

Figure 115. Intrusive and coherent volcanic rocks from the Hällefors area. **A+B**: Intrusive intermediate to basic rock showing foliation (6635247/471950) **B.** Detail of **A** showing dark mafic minerals and larger plagioclase crystals. **C.** Contact between granite (top) and supracrustal rhyolite with a serpentinised zone in the middle. Talc nodules are visible above the hammer (6635050/471896). **D**. Metabasite from north of Hällefors (6636916/469164).

Interpretation of the new ground-based geophysical data

Figure 116 shows some results from ground-based geophysical measurements for the area around Stollberget, located in the western part of the Hällefors mapping area. The figure shows the total magnetic field measurements as well as the apparent resistivity calculated from ground VLF measurements (using 24 kHz frequency). Lastly, a 2D resistivity model is shown, calculated from the ground-based VLF measurements.

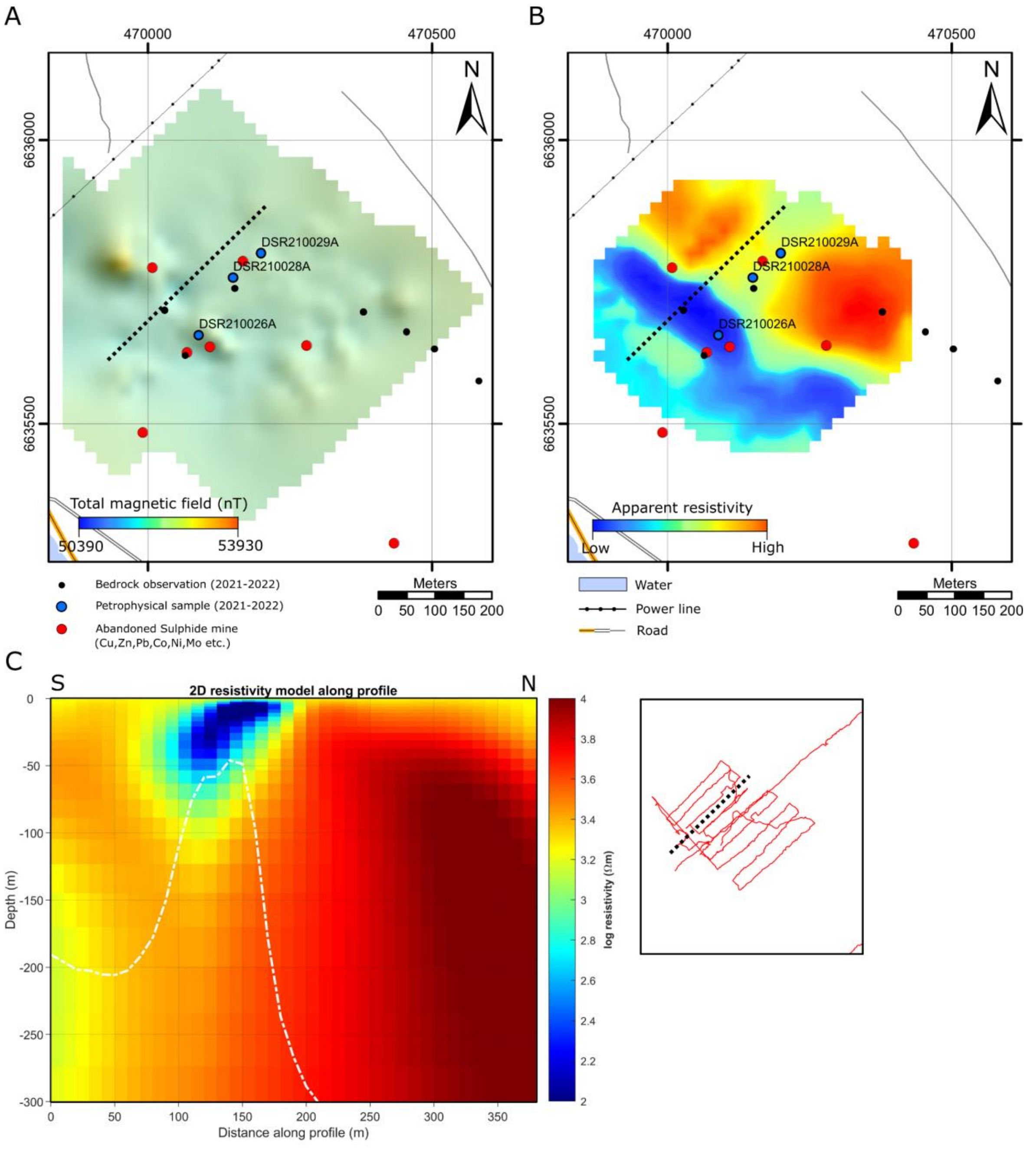

Figure 116. Results from ground geophysical measurements around Stollberget (shown as area 2 in figure 103). **A.** Total magnetic field intensity from ground measurements. **B.** Apparent resistivity map calculated from ground-based VLF measurements 24kHz. **C.** 2D resistivity model obtained by inverting the ground-based VLF data along a profile. The white dashed line shows the depth of investigation, below which the model is largely unconstrained. The location of the ground measurements is shown in the inset map in the bottom right-hand corner of the figure. The location of the 2D cross section is shown as a black dashed line on maps A, B and on the inset map.

The apparent resistivity map (fig. 116B) shows a linear conductive (low resistivity) feature with northwest – southeast strike within the survey area. This feature correlates with documented mineralisation in the southern part of the Stollberget area where mining activity has previously taken place. Hence, it is interpreted to be associated with sulphide mineralisation. Some of the documented mineralisation in the northern part of the survey area does not correspond to low resistivity features in the data, which implies that the mineralisation is most prevalent to the south. The anomaly lies approximately parallel to the general strike of the foliation in this area, hence it is interpreted as this mineralisation is stratabound and associated with carbonate/calc-silicate layers within this sequence. This is consistent with results from 2D resistivity modelling performed using the ground-based VLF data (figure 116C), which indicate that the low resistivity anomaly dips to the south, which is also consistent with the typical foliation in the area. The 2D modelling results indicate that the low resistivity feature is relatively shallow (constrained to the upper 50–100 m), however, it should be noted that as the inversion only includes one frequency (24 kHz) and the vertical resolution in the model is somewhat limited. The ground magnetic measurements show that there are no significant magnetic anomalies within the survey area. Hence, this implies that the mineralisation in this area does not contain significant amounts of magnetic minerals, such as magnetite or pyrrhotite. As a result, with regards to the geophysical properties, the mineralisation at Stollberget is more similar to that in Västra fältet than that in Östra fältet (Sundius et al., 1966). However, several subtle magnetic anomalies can be observed at the same location of the low resistivity feature which can potentially be associated with small amounts of magnetic minerals within the sulphide mineralisation. The conductive anomaly appears to continue to the southeast and to the northwest, away from the documented mineralisation.

Figure 117 shows maps derived from the ground-based geophysical measurements made around the Östra fältet, to the east of the Hällefors mapping area. The total magnetic intensity map shown in figure 117 shows a clear magnetic anomaly associated with the mineralisation within the Östra fältet, which unlike the Västra fältet contains magnetite and pyrrhotite (Sundius et al., 1966). The magnetic anomaly has an approximately east-west strike and appears to dip to the south, following the typical foliation in this area. There are several small anomalies along strike, to the east and west of the Östra fältet which are potentially associated with additional mineralisation. In the apparent resistivity map a corresponding zone of low resistivity can be observed at the Östra fältet with the same strike as the magnetic anomaly, which is interpreted to be linked to the mineralisation. This anomaly appears to be strongest on the eastern side of the magnetic anomaly and extends to the eastern side of the surveyed area. In the southwestern part of the surveyed area a subtle region of low resistivity with an east-west strike can be observed, which appears to correlate with a weak magnetic anomaly. This could potentially be linked to additional mineralisation.

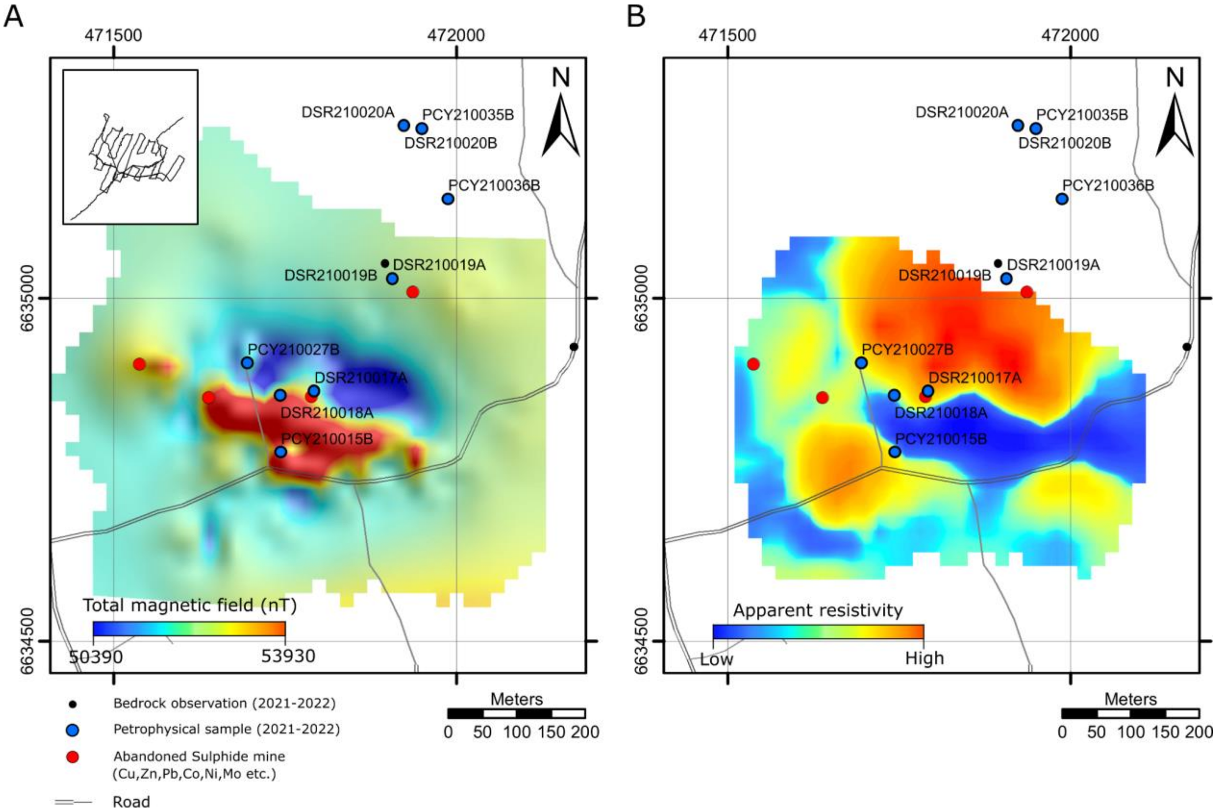

Figure 117. Results from ground geophysical measurements around Östra fältet (shown as area 1 in figure 103). **A.** Total magnetic field intensity from ground measurements. **B.** Apparent resistivity map calculated from ground-based VLF measurements 24 kHz. The location of the ground measurements is shown in the inset map in the top left-hand corner of the figure.

Kopparberg

Background

Two sulphide mines were located within the area surrounding the village of Kopparberg, the Ljusnarsberg mines and the Kaveltorp mines (fig 118). The history of mining in Kopparberg dates back to the 17th century when Cu deposits were found and mining began in small scale. The mineralisation at these mines consists of skarn ore lenses which were dominated by Cu-Pb-Zn +Ag mineralisations.

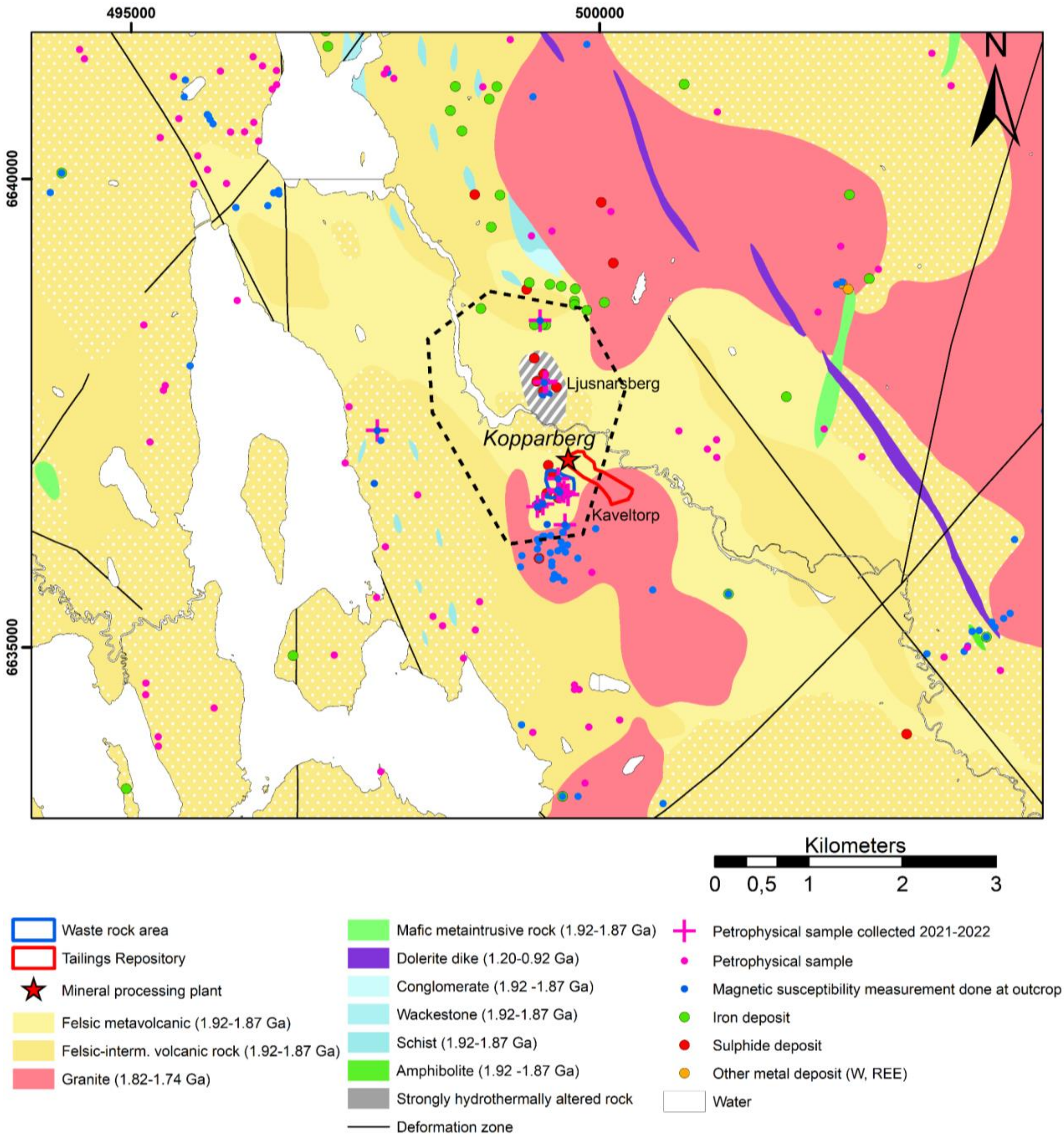

Figure 118. Bedrock map of the Kopparberg area showing petrophysical data collected in the course of the present study as well as previous studies.

Available geophysical data

Airborne data (magnetic, VLF, gamma spectrometry)

In this project an area has been specified for additional bedrock mapping, with the aim of improving the understanding of the geology linked to the original mineralisation, from which the waste material has been generated. A polygon showing the area identified for further geological mapping and geophysical investigations is shown as a black dashed line in figure 119. We refer to this in subsequent text as the Kopparberg mapping area. Within this area two mines are highlighted Kaveltorpsfältet (Kaveltorp mines) and Ljusnarsbergsfältet (Ljusnarsberg mines) located to the south and north of the village of Kopparberg, respectively (fig. 119).

The oldest airborne measurements over the area shown in figure 119 were collected by SGU as part of a campaign about 50 years ago. Most of the area shown in the map is covered by measurements made in 1969, however, a small section to the west of the map area was surveyed in 1973. During these older surveys magnetic, natural gamma and VLF (1 transmitter) measurements were made. In 2017, SGU collected modern airborne magnetic, natural gamma and VLF (2 transmitter) data which were used to produce the maps shown in figures 119 and 120. Details of the different airborne surveys which cover the area shown in figure 119 are summarised in table 42.

Figure 119 shows a map of the residual magnetic anomaly, calculated from airborne measurements. The strongest magnetic anomalies observed in figure 119 are mostly related to Fe mineralisation which is prevalent in the region. A relatively strong magnetic anomaly is observed at the Ljusnarsbergsfältet where both sulphide and Fe oxide mineralisation occur. A sample of skarn Fe mineralisation collected from the northern part of the Ljusnarsbergsfältet during this project exhibits a relatively high magnetic susceptibility of over 1 SI. The presence of magnetite, which is documented within the mineralisation at Ljusnarsbergsfältet (Magnusson, 1940), is likely associated with the strong magnetic anomaly.

A weaker but significant magnetic anomaly is associated with the Kaveltorpsfältet. The mineralisation at Kaveltorpfältet is predominantly sulphide mineralisation, but magnetite and pyrrhotite are also documented to occur (Magnusson, 1940). Magnetite crystals can be observed in samples taken from the Kaveltorp mines during this project. In some cases, the magnetic susceptibilities of samples taken from outcrop and waste rock from the Kaveltorp mines are also relatively high (over 1 SI). On the eastern side of the map shown in figure 119 several weak linear anomalies can be observed with an approximately northwest – southeast strike. These are mapped as dolerite dikes which crosscut the older felsic metavolcanic and granitic rocks.

Figure 119shows a map of the apparent resistivity calculated from airborne VLF data collected in 2017. Here it can be observed that many of the areas of low resistivity correspond to areas of wetland and lakes or manmade structures such as railways and power lines. However, to the east of the map there is a broad conductive feature with an approximately northeast-southwest strike. This feature can potentially be interpreted as a large-scale deformation zone.

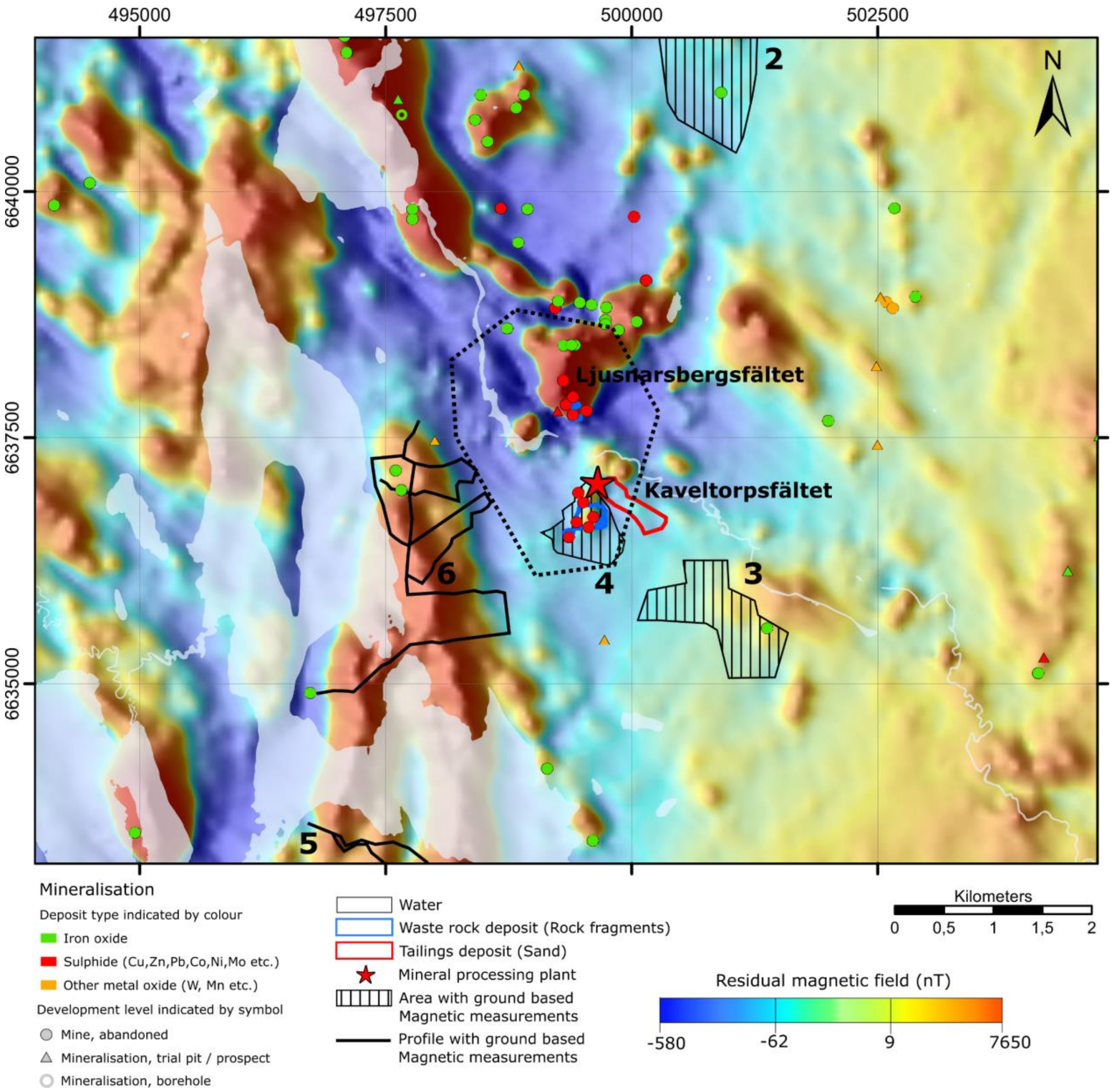

Figure 119. Map of residual magnetic field for the area around Kopparberg. The Kopparberg mapping area is shown as a polygon with a thick black dashed line. The location of ground-based magnetic measurements, listed in table 43 is shown.

Table 42. Complete list of the airborne geophysical surveys collected in the area around Kopparberg. Unless otherwise stated all data are collected using a small, manned aeroplane.

Year	Organisation	Geophysical methods used	Area (SGU map sheet)	Flight direction (degrees)	Flight line separation (m)	Flight altitude (m)
1969*	SGU	Magnetics, gamma spectrometry, VLF (1 transmitter)	11F	East–West (90°)	200	30
1973*	SGU	Magnetics, gamma spectrometry, VLF (1 transmitter)	11E	East–West (90°)	200	30
2017	SGU	Magnetics, gamma spectrometry, VLF (2 transmitters)	Part of 12E, 12F, 11E, 11F, 10E and 10F	Northwest – Southeast (130°)	200	60

* Not used for producing maps in this report

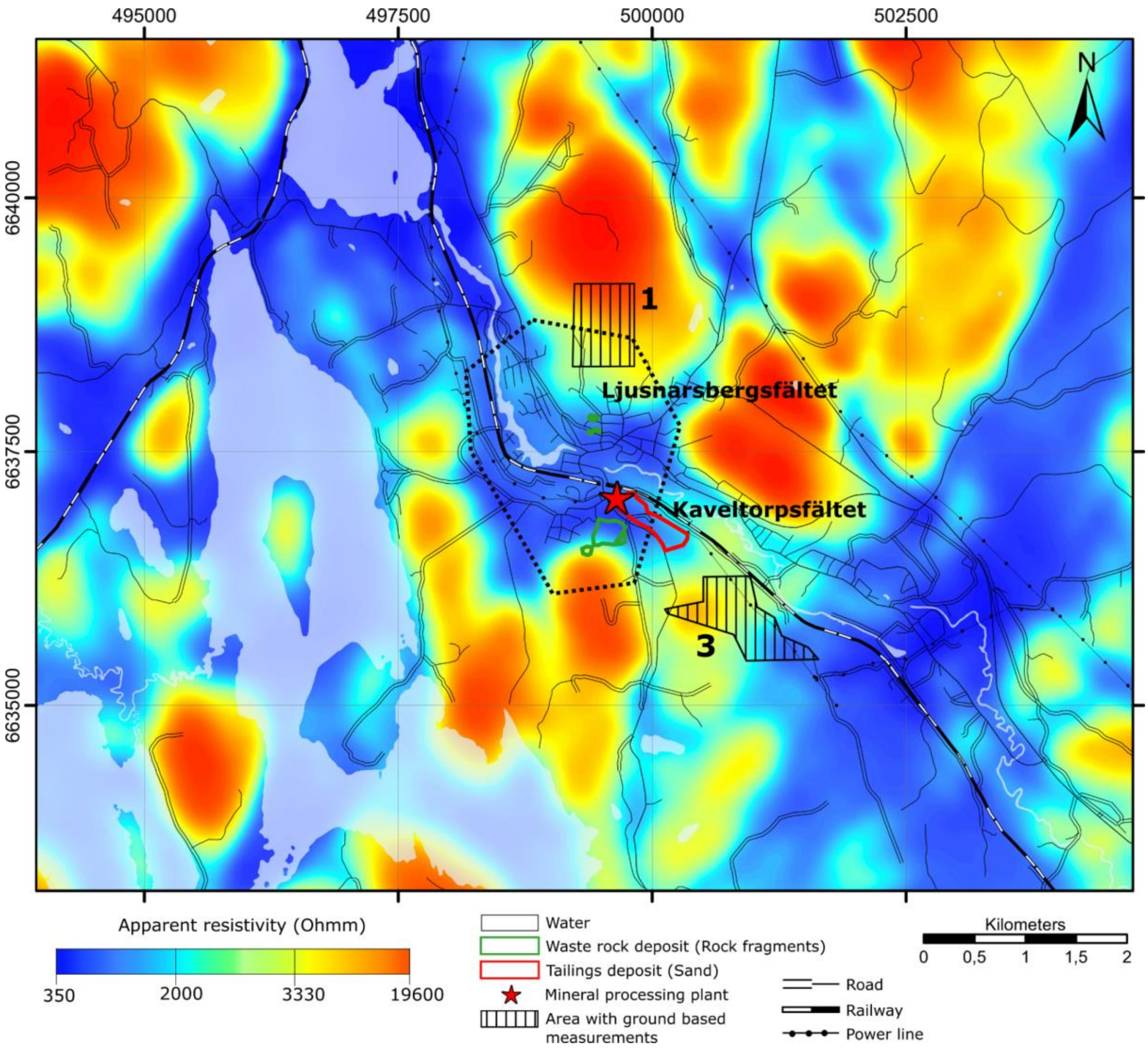

Figure 120. Map of apparent resistivity derived from airborne VLF data for the area around Kopparberg. The Kopparberg mapping area is shown as a polygon with a thick black dashed line. The location of ground-based electromagnetic measurements, listed in table 43 is shown.

Ground-based electromagnetic and magnetic measurements

Table 43 gives a summary of the ground-based geophysical measurements available within SGUs database for the area around Kopparberg. The oldest ground-based measurements in the database are electromagnetic and were recorded by Boliden Mineral AB using an EM3 instrument over the northern part of Ljusnarsbergsfältet. Additional magnetic and slingram measurements were performed between 2007 and 2013 in areas to the north and to the southeast of Kopparberg by Kopparberg mining Exploration AB (fig. 119 and 120). In 2021, as part of the Bergslagen etapp 3 mapping project, a series of ground magnetic profiles were collected by SGU to the west and southwest of Kaveltorpsfältet (Ripa and Brolin, 2022).

As part of this project additional ground magnetic measurements were performed by SGU over an area of approximately 0.45 km^2, including the Kaveltorpsfältet and an area to the south of this (labelled as 4 in table 43 and figure 119). The objective of these measurements was to map and characterise the magnetic response of the Kaveltorpsfältet and identify any additional anomalies to the south of the old mining area. For this survey a GEM GSMV-19 instrument was used which registered magnetic measurements together with GPS coordinates every second. The measurements were collected with approximately east-west profiles and nominal profile spacing of 70 m.

Table 43. Ground-based magnetic and electromagnetic measurements for the area around Kopparberg. Numbers correspond to the numbered polygons/lines shown in figure 117 and 118.

Polygon/Line number and name	Method	Year acquired	Responsible	Comments
1. Ställdalen nr 1004	EM3	2001	Boliden	Profile spacing of 100 m.
2. Laxbro nr 2 and 3	Magnetics	2007–2013	Kopparberg Mining Exploration AB	Profile spacing of 80 m.
3. Bångbro nr 1	Magnetics and Slingram	2008	Kopparberg Mining Exploration AB	Profile spacing of between 200 and 100 m.
4. MP21DSR0020 – MP21DSR0022	Magnetics	2021	SGU	Data acquired over an area with nominal profile spacing of 70 m.
5. MP21CJO2004 – MP21CJO2005	Magnetics	2021	SGU	Measurements in this area split over two profiles.
6. MP21CJO2006 – MP21CJO2008	Magnetics	2021	SGU	Measurements in this area split over three profiles.

Ground-based gravity

Figure 121 shows a map of the residual gravity anomaly for the area around Kopparberg as well as gravity measurement points. Prior to this project the spacing between measurement points in this area was about 1–2 km. As part of this project 260 new gravity points were collected to reduce the spacing between measurement points and improve the spatial resolution of the gravity information in this area. As a result, within the Kopparberg mapping area, the spacing between measurement points has been reduced to about 500 m overall and about 150 m along roads. Figure 121 shows two maps of the residual gravity anomaly calculated with different parameters as well as the pre-existing and newly acquired gravity measurement points. In figure 121A a grid spacing of 250 × 250 m was used to interpolate the Bouguer anomaly data. The residual anomaly was calculated by subtracting a version of the Bouguer anomaly grid which had been upward continued by 3 km, from the original grid. In figure 121B a grid spacing of 100 × 100 m was used and the residual anomaly was calculated by subtracting a version of the data which had been upward continued by 500 m. Hence, small, high frequency variations are more prominent in 121B than in 121A.

On inspection of figure 121A it is apparent that there is a region on the eastern side of the map area which typically has lower gravity anomaly values than in the west. This transition is consistent with the mapped surface geology where in the west a felsic metavolcanic sequence with carbonate layers and Fe mineralisation is mapped. This will most likely have a higher average density than the mixed felsic metavolcanic – granite sequence to the east, which is relatively sparse in mineralisation. In general, positive gravity anomalies in figure 121 correlate with regions with high magnetic anomaly values and mapped Fe mineralisation (fig. 119).

In figure 121B positive gravity anomalies are associated with the Ljusnarsbergsfältet and the Kaveltorpsfältet. This is most likely due to the presence of mineralisation and associated carbonate and skarn rock types which typically have densities higher than the surrounding felsic metavolcanic and granitic rocks. The residual gravity anomaly appears to be higher for the Ljusnarsbergsfältet than the Kaveltorpsfältet. In figure 121B there appears to be an indication that both Ljusnarsbergsfältet and Kaveltorpsfältet are linked by a region of slightly higher gravity anomaly values.

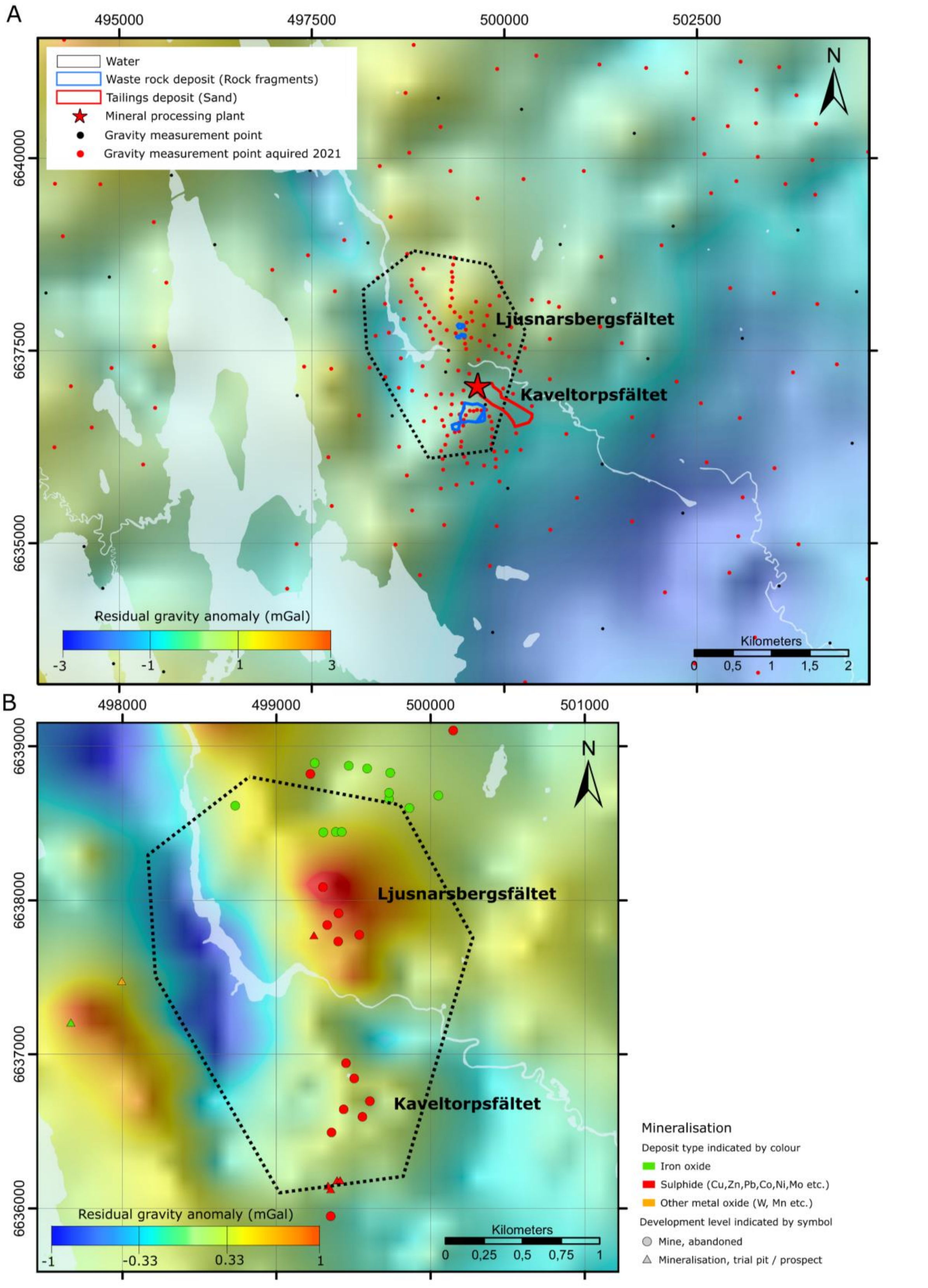

Figure 121. Map of the residual gravity anomaly over and around the Kopparberg area. **A.** Residual gravity anomaly calculated with a 250×250 m grid spacing and 3 km upward continuation. Pre-existing and new gravity measurements are annotated. **B.** Residual gravity anomaly calculated with a 100×100 m grid spacing and 500 m upward continuation. Mineralisation is shown with red, orange and green symbols. The Kopparberg mapping area is shown on both A and B with a thick black dashed line. Note that the distance scale and gravity anomaly colour scales are different for A and B.

Petrophysical and borehole data

Figure 118 shows the petrophysical data available for the area around Kopparberg. Due to the lack of pre-existing data from the Kopparberg mapping area additional petrophysical data were collected as part of this project to improve the understanding of the physical properties of the rock types in this area. The newly collected data are shown in table 44.

From these new results it is apparent that the felsic metavolcanic and granitic rocks which make up the bulk of the bedrock in the study area typically have relatively low densities of between 2615 and 2753 kg/m^3 and relatively low magnetic susceptibilities (<10 000 × 10^{-6} SI). Samples taken from skarn which are not visibly mineralised typically have relatively high densities of between 2830 and 3017 kg/m^3 and magnetic susceptibilities of (<50 000 × 10^{-6} SI) (fig. 122). With regards to mineralisation, samples of skarn Fe mineralisation typically have high densities of between 3298 and 3887 kg/m^3 and very high magnetic susceptibilities (in some cases over 9 000 000 × 10^{-6} SI). In these samples magnetite crystals were often observable, as documented previously by others (Magnusson, 1940), which likely gives rise to the high magnetic susceptibility (fig. 120). Samples classified as sulphide mineralisation (where appreciable amounts of sulphide minerals could be observed) typically had high densities of between 3588 and 4116 kg/m^3 but relatively low magnetic susceptibilities (when compared to the Fe mineralisation) of between 2920 and 144 767 × 10^{-6} SI.

There are 62 boreholes within the Kopparberg mapping area in SGUs database. These were drilled during the 1960s by Boliden and are located around the Kaveltorp mines (fig. 118).

Table 44. Table summarising the petrophysical results collected as part of this project from the Kopparberg mapping area.

Sample ID	Easting (m)	Northing (m)	Description	Density (kg/m3)	Magnetic susceptibility (10-6 SI)	J (mA/m)
DSR210046A	499554	6636679	Skarn	3006	51571	1026
DSR210047A	499575	6636653	Skarn Fe mineralisation	3887	9561647	20004
DSR210047B	499575	6636653	Sulphide mineralisation	4116	2920	53
DSR210048A	499556	6636797	Skarn	2830	26504	32
DSR210048B	499556	6636797	Skarn Fe mineralisation	3298	549052	48980
DSR210049A	499395	6636528	Granite	2630	56	25
DSR210050A	499335	6636499	Skarn	3017	500	42
DSR210050B	499335	6636499	Felsic metavolcanic	2753	340	66
DSR210052A	499630	6636306	Granite	2615	601	50
DSR210053A	499410	6637825	Skarn Fe mineralisation	3380	1318888	17217
DSR210053B	499410	6637825	Sulphide mineralisation	3734	144767	7323
DSR210054A	499364	6638486	Skarn	3589	8464	1954
DSR210054B	499364	6638486	Skarn Fe mineralisation	3777	1194301	109190
PCY210057B	499663	6636627	Felsic metavolcanic	2752	1638	14
PCY210059B	499619	6636657	Sulphide mineralisation	3588	6552	141
PCY210108B	499431	6637834	Felsic metavolcanic	2747	66644	684

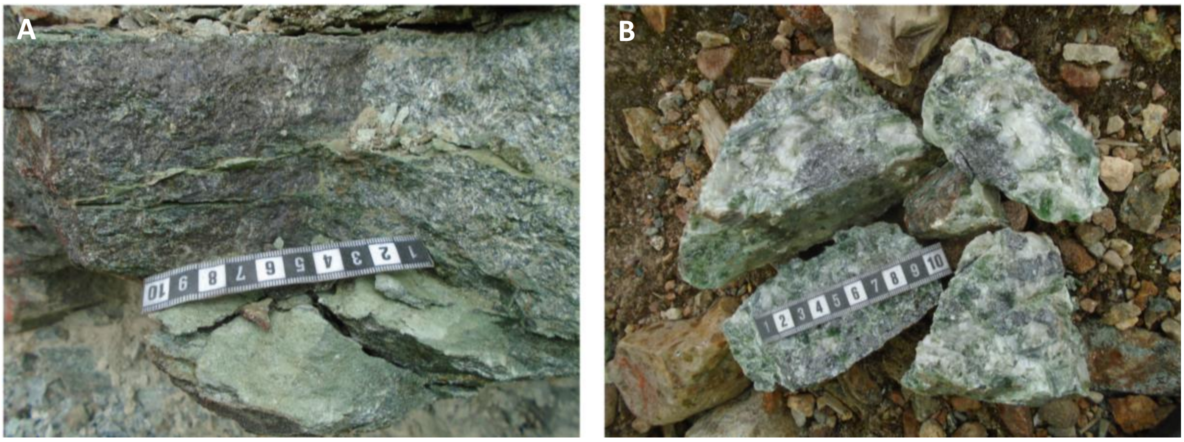

Figure 122. Example of skarn and skarn Fe mineralisation from the Kaveltorpsfältet. **A.** Example of medium-grained skarn rock in outcrop (DSR210046A, 6636679/499554). **B.** Example of skarn Fe mineralisation found within waste rock, with large amphibole crystals (>10 mm) and aggregates of magnetite crystals (DSR210047A, 6636653/499575).

Interpretation of the new ground-based geophysical data

Figure 123 shows a map of the total magnetic anomaly derived from ground-based measurements conducted in 2021 (Table 43) around the Kaveltorpsfältet. The Kaveltorpsfältet consists of several smaller mines, the locations of which are indicated approximately by the red dots in the figure.

The ground magnetic data shows several strong positive anomalies located within the central area of the Kaveltorpsfältet. The anomalies appear strongest in the northern part of the survey area, reducing in amplitude to the south. The layered skarn-felsic volcanic rock sequence within the Kaveltorpsfältet is strongly deformed and folded, however, overall across the area, the layered sequence typically dips to the east-southeast at about 28º (Magnusson, 1940). This is somewhat consistent with the ground magnetic data, where some of the strongest positive anomalies from the central part of the Kaveltorpsfältet appear to have an approximate north-northeast strike (i.e. the anomaly at DSR210048A). Several other anomalies, including the anomaly close to Haraldsgruvan appear to the southwest, along strike from the anomaly at DSR210048A. Several small anomalies are present which do not correspond to documented mineralisation, one to the southwest of Haraldsgruvan and another to the southeast of the central part of Kaveltorpsfältet. It is possible that these small anomalies are indications of additional mineralisation that has not yet been documented.

In figure 123 a close-up from the residual gravity anomaly map from figure 121B is shown. Here the positive gravity anomaly associated with the Kaveltorpsfältet appears to have an approximate northeast – southwest strike. The anomaly also extends further to the east than the magnetic anomalies from the ground-based measurements. This is consistent with an approximately northeast – southwest striking mineralisation dipping to the southeast (Magnusson, 1940).

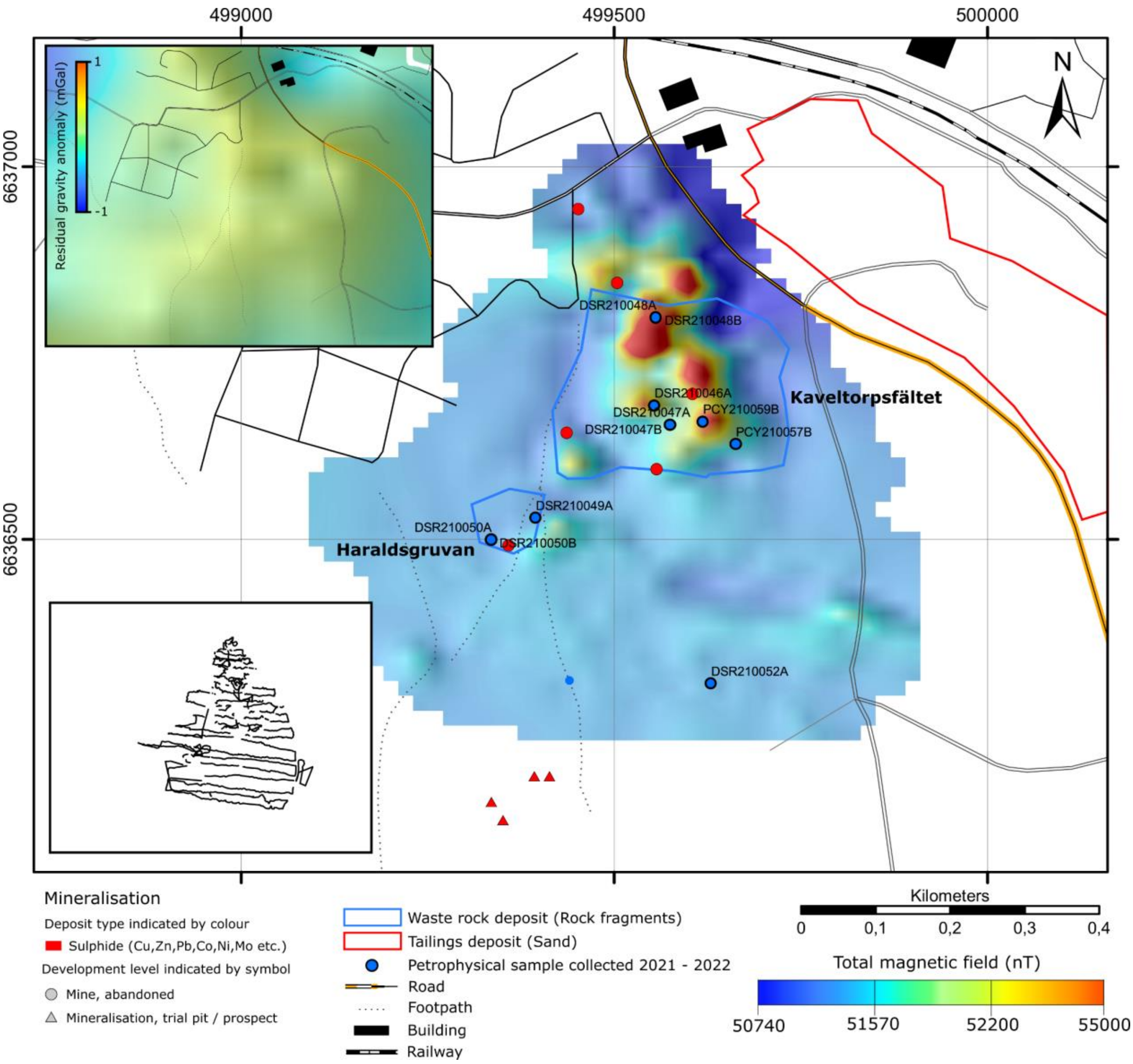

Figure 123. Map showing the total magnetic anomaly from ground measurements collected around the Kaveltorp mines. Mineralisation from SGUs database as well as new petrophysical samples collected between 2021 and 2022 are shown. The inset in the top left corner shows the residual gravity anomaly (100 m grid size, 500 m upward continuation). The inset map in the bottom left corner shows the measurement points used to generate the map. The extent of both inset maps is the same as that of the main map.

Kaveltorp Mines

Background

The Kaveltorp Zn-Pb-Cu (Ag) mines (fig. 124), located just south of the Ljusnarsberg field in Kopparberg were in operation from 1874 through the mid-1970s with mining operations terminated and restarted multiple times in 1874–1920, 1922–1949, 1952, 1967–1971. Mineralisation at Kaveltorp occurred in skarn bodies rich in Pb, Zn, and Cu, with minor Fe. Galena, sphalerite, chalcopyrite and magnetite were the dominant economic minerals mined from Kaveltorp. Total production at Kaveltorp was 0.92 Mt of ore and 0.23 Mt of waste rock was produced according to the SGU MALMdb (table 45).

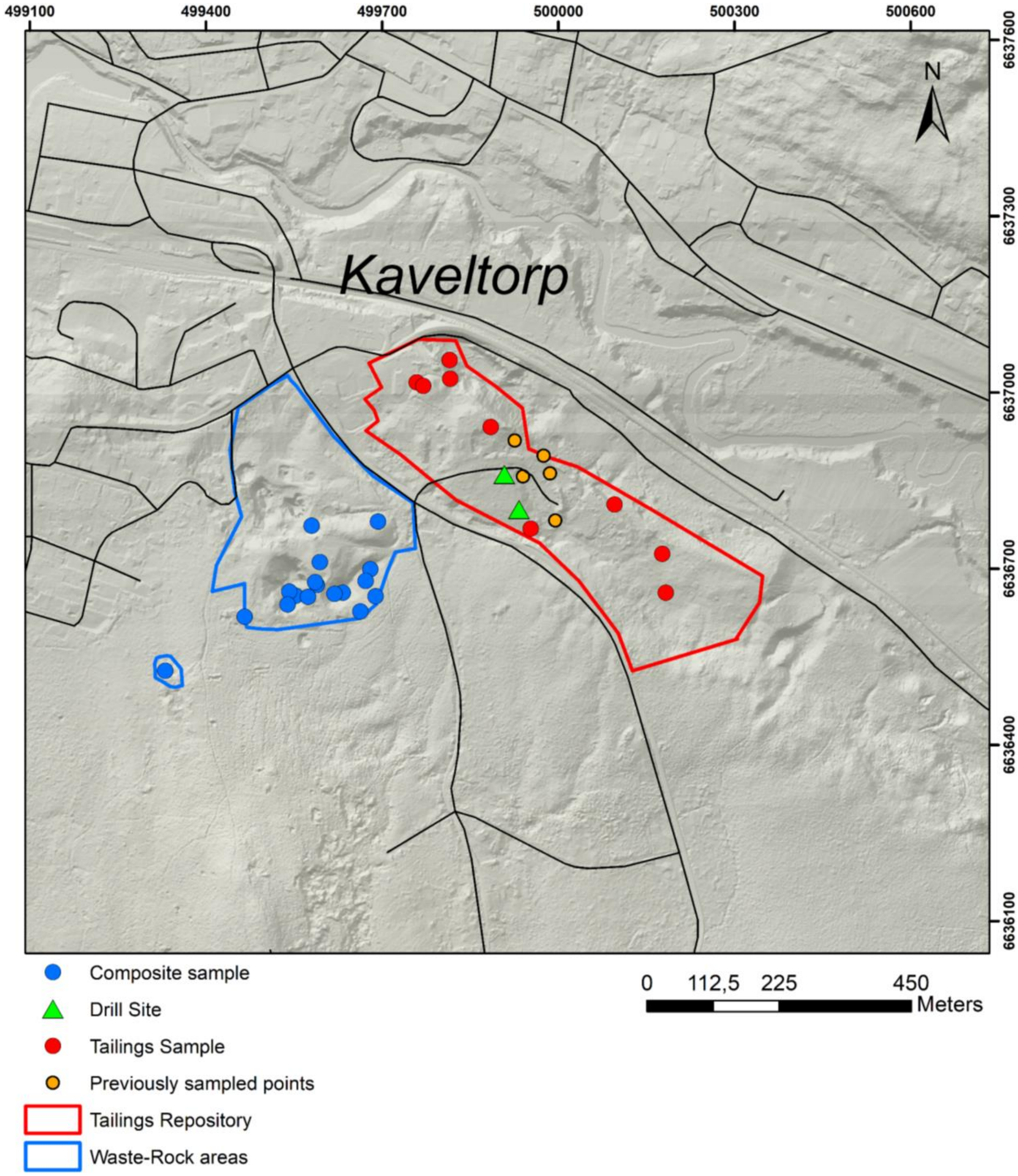

Figure 124. LiDAR image of the Kaveltorp mines and the Kaveltorp tailings dam.

Table 45. Production statistics from Kaveltorp.

	Total (Mt)	Zn (%)	Pb (%)	Cu (%)	Ag (ppm)	Au (ppm)
Mined Ore	0.92	5.1	3.6	0.34	44.7	0.32
Processed in dressing plant	0.63					
Tailings	0.52					
Waste rock	0.23					

Sampling of waste rock at Kaveltorp

A total of 17 composite samples were collected at Kaveltorp. Skarn and meta-rhyolite were the dominant components among the chips collected for the composite samples, with limited amounts of mineralised chips and granite chips collected. The volcanic rock showed varying levels of alteration, often showing foliated biotite layers. Occasionally extremely magnesian altered felsic volcanic rock was observed which was pure white, demonstrating the leaching of most elements from hydrothermally altered rock. The composition of the skarn varied, with amphibole-biotite skarn and calc-skarn occurring, with the silicate skarn dominating most observed chips. Much of the amphibole skarn was dominated by actinolite-tremolite-wollastonite occurring as fibrous masses. Calc-skarn of the ophicalcite variety occurred often and is rich in humite (var. chondrodite) occurring as orange-brown crystals.

The composite waste rock samples (table 46) showed high levels of Pb, Cu, Zn, with Pb exceeding detection limit even in ore grade analyses. Also strongly enriched was Bi, averaging 131 ppm, with one sample containing 594 ppm. Silver and Au were slightly elevated in the composite samples, with 15 and 0.15 ppm, respectively, and enriched 274 ppm Ag, 0.15 ppm Au in the richly mineralised sample. Cadmium was highly elevated in the ore sample at 338 ppm, and slightly elevated above background at 38.9 ppm in the composite samples. Sulphur was elevated at 4%.

Thin section analysis (fig. 125) showed sphalerite and galena as the dominant sulphides with minor chalcopyrite. EDS analysis enabled a clearer picture of trace metal mineralogy. Native Bi was found as inclusions in galena. Acanthite (Ag_2S) was somewhat common, as well as rare petrovskaite (AuAgS) grains. Rare bastnäsite and allanite were observed.

Table 46. Results of sampling of waste rock at Kaveltorp.

Data		Fe (%)	Zn (%)	Pb (%)	Bi (ppm)	Ag (ppm)	Cu (%)
Mineralised sample		7.09	22.1	>20.0	798	274	0.12
Composite Samples (n=17)	Average	6.24	2.24	1.56	131	15.6	0.27
	Max	8.74	6.24	5.84	594	54.9	0.54
	Min	4.23	0.05	0.05	2.58	0.92	0.045

Figure 125. Thin section image in reflected light showing typical mineralisation at Kaveltorp. Bright grey: galena, medium grey, sphalerite, brown: pyrrhotite, yellow: chalcopyrite. Dark grey minerals are silicates. Micrograph: Patrick Casey.

Sampling of tailings at Kaveltorp

Ore from Kaveltorp was processed at a dressing plant on site from 1901 to 1947 and tailings were deposited in a dry dam to the east of the mine. In total 0.52 Mt of ore was processed in the plant. A total of 9 surface samples were analysed of the tailings and two boreholes were drilled. Drilling occurred within the shallower, southwestern side of the tailings. The thickest part of the tailings, totalling 20 metres in depth, proved to be impossible to drill due to the compact, dry nature of the tailings.

Large amounts of mica were observed in the tailings, and high levels of Mg were noted in the analyses, averaging 20%, indicating a predominance of skarn minerals in the tailings. In surface sampling Zn and Pb averaged between 0.8 and 0.9 % in the tailings, with approximately 0.11% Cu. Silver was slightly elevated at 6.2 ppm.

XRD analysis of the tailings from Kaveltorp was used to establish the gangue mineralogy. The dominant minerals present were tremolite, actinolite, diopside, clinochrysotile, quartz, biotite, talc, gypsum and clinochlore. The large amount of skarn minerals provides corroboration for the high Mg levels in the tailings. The presence of gypsum is likely evidence of sulphide weathering occurring within the tailings without the buffering of carbonate.

Figure 126 shows an exposed section of the tailings at Kaveltorp that demonstrates the various sedimentary processes that occur during release of tailings including sedimentary layering, grainsize sorting and crossbedding.

Figure 126. Exposed section of Kaveltorps tailings showing sedimentary layering. Photo: Patrick Casey

Three boreholes were attempted at Kaveltorp. The thickest part of the tailings was impossible to drill through due to the dry, compact character leading the screw to becoming stuck at the 3-metre level. The first two samples from the thickest part of the tailings were analysed, and returned results consistent with regular sand, which indicates a thick layer of sand was placed over the tailings in an attempt to sanitise the area.

The two complete boreholes were drilled in the western side of the tailings repository. Here the sand was much thinner, indicating the bulk of the tailings are in the northwest end of the tailings dam, and thin out to the southeast. Vegetation was dense pine with a thick layer of moss. The tailings in both holes were fine to medium sand with silt layers up to 10 cm in thickness. The tailings showed a large mica component. The total depth of the boreholes was around 5–6 metres. Below the tailings a layer of glaciofluvial sand was encountered.

Borehole BH2_KVT (6636835/499889) was drilled approximately 120 metres form the exposed eastern slope of the tailings. The depth of the tailings was 6 metres with 2 metres of glaciofluvial sand underneath. The tailings were fine to medium, dark grey sand with bands of light grey silt.

Borehole BH3_KVT (SWEREF 6636800/499933) was drilled within dense pine forest near the western wall of the tailings dam. The depth to glaciofluvial sand was approximately 5 meters. The tailings at this drill site were similar to those at BH2_KVT, with mica rich medium to fine sand with occasional bands of silt between 2–4 centimetres thick.

Results from the drill core samples were in broad agreement with the surface sampling, with 0.14% Cu in the tailings, 0.72% Pb and 0.97 % Zn (table 47). Silver showed an average concentration of 6.4 ppm within the drilled samples. The highest levels of Zn and Pb were observed in the lowest level of the tailings, indicating poor recovery in the early phases of mineral concentration. No significant variations were seen in distribution of sulphide contents along depth in the boreholes (fig. 127).

A heavy mineral separate of the Kaveltorp tailings was analysed using SEM-EDS (fig 128). Galena and sphalerite dominated the sample, with lesser chalcopyrite, pyrite, and pyrrhotite. Occasional grains of gahnite were observed. Ore minerals typically showed poor liberation from the gangue minerals, indicating inefficiencies within the crushing and separation processes.

Table 47. Analytical results of Kaveltorp tailings

Data	**Fe_2O_3 (%)**	**Zn (%)**	**Pb (%)**	**Bi (ppm)**	**Ag (ppm)**	**Cu (%)**
Surface samples (n=10)	6.4	0.87	0.81	19.0	6.2	0.11
	8.2	2.24	2.14	50.3	18.3	0.18
	4.1	0.34	0.33	8.0	2.1	0.056
Drilled samples (n=11)	6.2	0.97	0.71	26.2	6.4	0.14
	9.2	1.85	1.25	49.2	11.3	0.21
	2.1	0.53	0.46	11	3.46	0.087

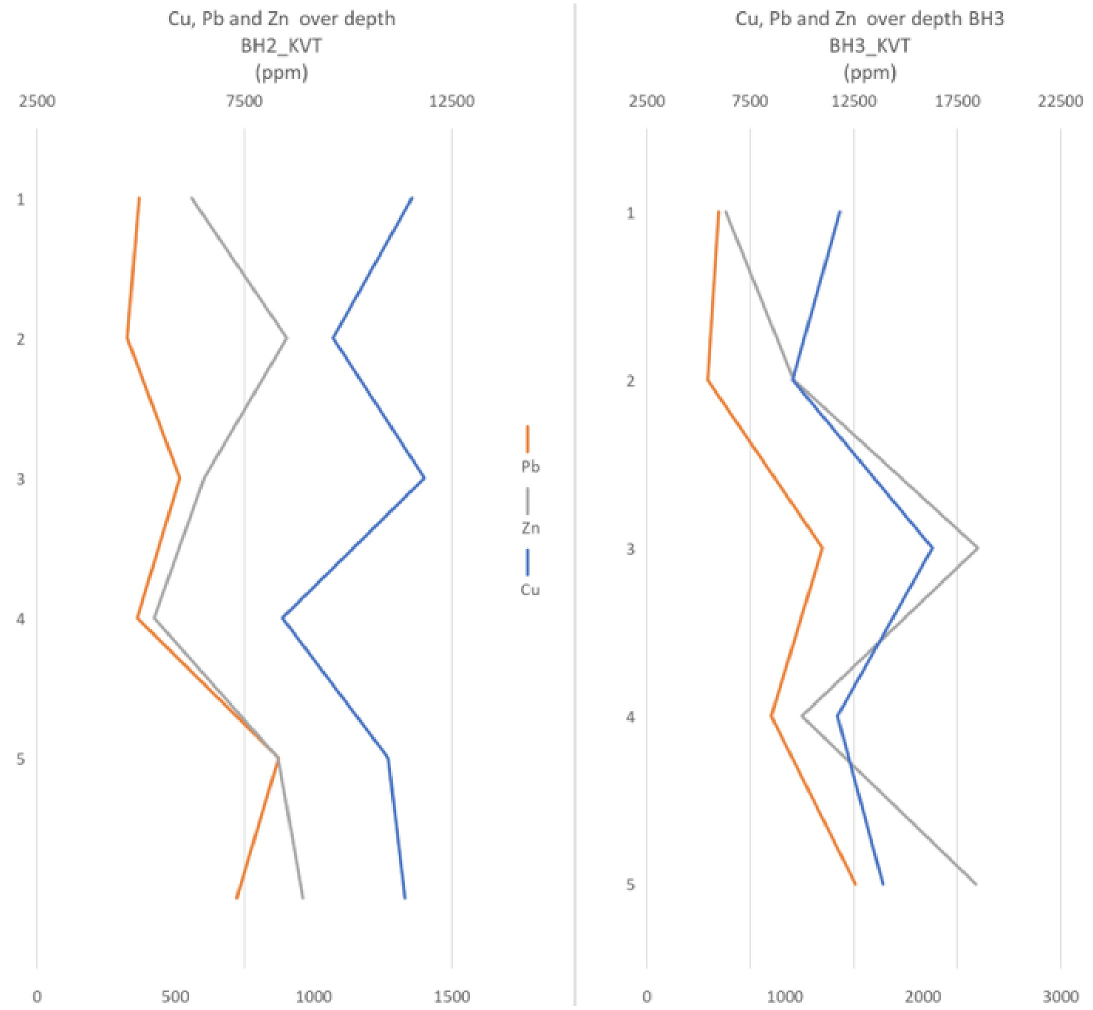

Figure 127. Concentrations of Cu, Pb and Zn over depth in the Kaveltorp boreholes. Cu is plotted along the secondary bottom x-axis.

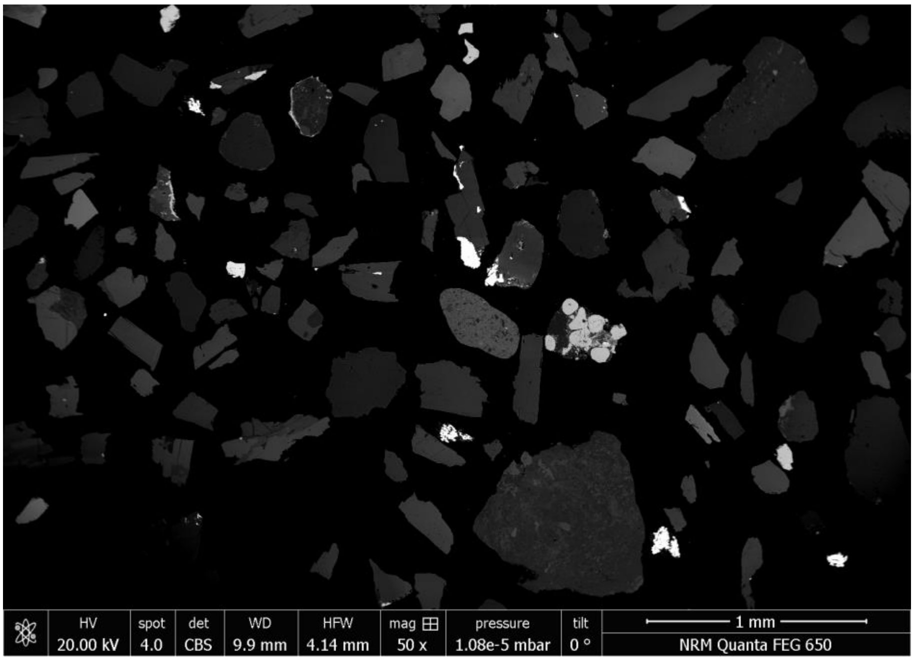

Figure 128. Backscatter electron image of tailings from Kaveltorp showing poor separation of galena (white) from gangue. Chalcopyrite (medium grey) shows distinctly better separation from gangue minerals and demonstrates poor recovery. Micrograph: Patrick Casey.

Potential resources at Kaveltorp

Potential resources from waste rock at Kaveltorp is calculated from tonnage reported in MALMdb. Waste rock at Kaveltorp potentially contains 5,000 tonnes Zn, 3,500 tonnes Pb, 600 tonnes Cu, 3 tonnes Bi, 3.6 tonnes Ag and 300 kg Au.

Potential resources in the tailings at Kaveltorp are calculated from the data reported in MALMdb. The tailings potentially contain 4 700 tonnes Zn, 4 000 tonnes Pb, 630 tonnes Cu, 11 tonnes Bi, and 3.3 tonnes Ag.

Ljusnarsbergs Ore Field

Background

Ljusnarsbergs ore field (fig. 129) is located directly on the edge of the village of Kopparberg (Sweref 6637891/499291). The ore bodies at Ljusnarsberg occur in Zn-Pb-Cu (Ag) and Fe-rich skarn altered carbonate lenses. Numerous small mines and test shafts dot the area. Mining began in small scale after the 1654 discovery of ore, exploiting near to the surface Cu ores, which provided Kopparberg with its name. Cu ore was locally rich, with grades over 4% Cu. Zn, Pb and Fe were also mined here Mining operations ceased in the 1970s when Boliden Mineral AB shut down operations.

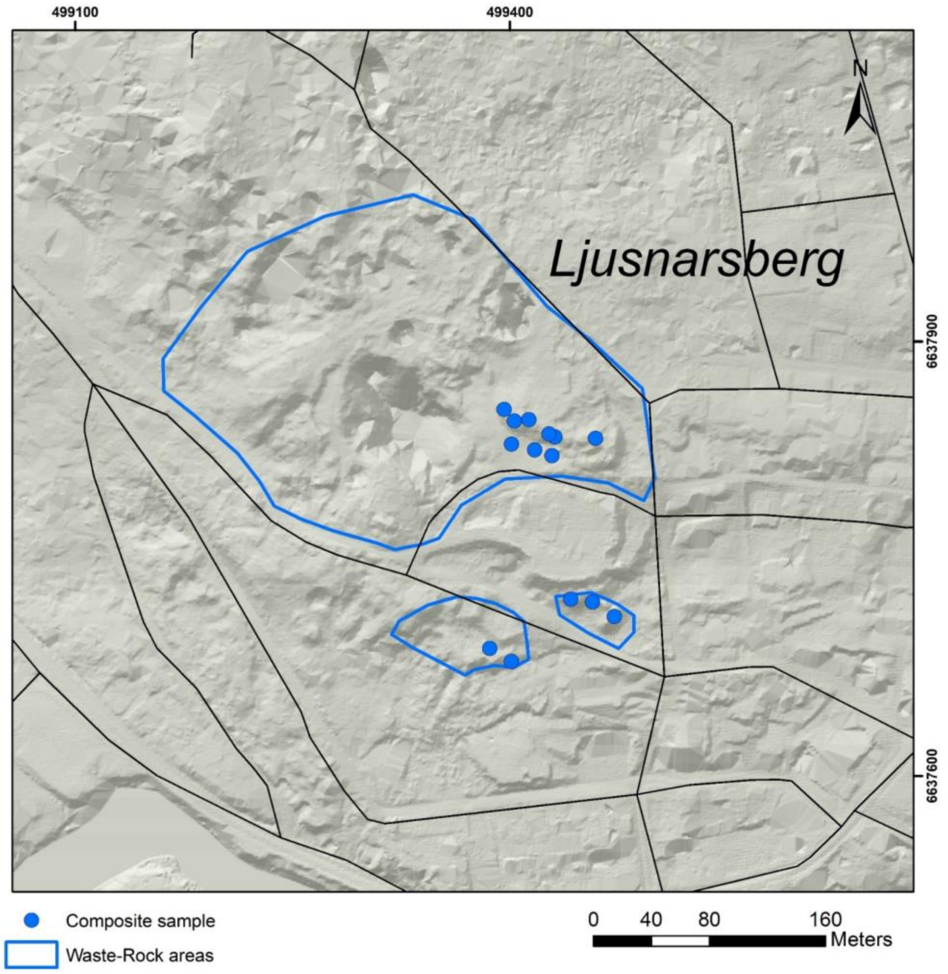

Figure 129. LiDAR map of the Ljusnarsberg ore field with composite sampling points marked.

The dominant mineralogy at Ljusnarsberg is sphalerite, galena, and chalcopyrite, along with magnetite. Subordinate pyrite and pyrrhotite comprise the uneconomical proportions of the sulphides in the ore. Total production at Ljusnarsberg according to MALMdb was 0.73 Mt of ore with 0.12 Mt of waste rock (table 48).

The waste rock at Ljusnarsberg has been well studied as a potential environmental hazard (Bäckström and Sädbom, 2008) due to its proximity to residential areas in Kopparberg. The waste rock shows strong weathering due to the high metal sulphide contents of the ore (fig 130). Compared to other waste rock heaps in western Bergslagen sampled during this study, little vegetation grows in the vicinity, and a strong smell of sulphur is noticeable. Several waste heaps of sorted material were observed at Ljusnarsberg. This material was typically below the size required for composite sampling, and bulk samples were collected by shovel from approximately 30 cm below the surface of the pile.

Table 48. Production statistics from Ljusnarsberg.

	Total (Mt)	Fe (%)	Zn (%)	Pb (%)	Cu (%)	Ag (ppm)	Au (ppm)
Mined Ore	0.92	21.53	2.0	1.46	1.23	13.73	0.26
Waste rock	0.23						

Figure 130. Waste rock heap at Ljusnarsberg showing strong weathering. Photo: Patrick Casey

Sampling of waste rock at Ljusnarsberg

Results of the analyses of waste rock samples showed high concentrations of Fe, Cu, Zn, and Pb as well as high levels of sulphur (table 49). Other elements of interest in the waste rock are Bi and Te, each showing somewhat elevated levels. W is slightly elevated in most samples. Galena and sphalerite are the dominant ore minerals observed in thin section. Magnetite is abundant, and typically contains elevated levels of Ti.

Fe levels were noticeably higher in the samples from Ljusnarsberg when compared with its neighbour Kaveltorp. Kaveltorp showed low concentrations of Fe, averaging around 5% in composite samples, while at Ljusnarsberg composite samples showed an average of 27% Fe. This is noted within the magnetic surveys discussed in a previous section.

High levels of S were noted, as were some higher levels of Cd. Higher levels of Cd appear to correlate to Zn, similar to the observations made by Bäckström and Sädbom (2008). As levels were very low and of little concern. Sulphide weathering is the dominant concern, with Pb being the dominant contaminant that can affect the local watershed. Sulphur contents averaged over 3% in composite samples, while the mineralised sample showed 21% sulphur. The high weathering grade of most of the waste rock was noted, and remining of the waste is a possible solution to reduce any further contamination from release of elements such as Zn, Pb and Cd from the mine waste.

Table 49. Analytical results from Ljusnarsberg.

Data	Object	Fe (%)	Zn (%)	Pb (%)	Cu (%)	S (%)	Bi (ppm)
Ore Sample	Ljusnarsberg	46.1	0.036	0.005	0.56	21.1	12
Composite samples (n=16)	Ljusnarsberg	27.2	0.24	0.08	0.25	3.3	60

Potential resources at Ljusnarsberg

The potential resources in the waste rock at Ljusnarsberg ore field should be considered a very rough estimate. The exposure of only sulphur rich material may have influenced the sampling due to the avoidance of material that was covered by vegetation. Based on the composite samples and the estimated waste rock from MALMdb Ljusnarsberg potentially holds 288 tonnes Zn, 96 tonnes Pb, 300 tonnes Cu, 7.2 tonnes Bi and 0.39 tonnes Ag.

Stollberg

Background

The mines at Stollberg are located approximately 5 km northeast of Ludvika, Dalarna (Sweref 6671508/515263). Mining at Stollberg likely started during the Middle Ages with a focus on silver extracted from lead ore. Ore mineralisation at Stollberg occurs along the eastern edge of the Stollberg syncline, where carbonate bodies in the local volcanic host rock have been replaced by skarn Fe-Mn and sulphide ore bodies. Geochemical analysis of the ores at Stollberg shows evidence of hydrothermal-exhalative mineralisation as evidenced by strong positive Eu anomalies, which are uncommon in sulphide ore bodies in Bergslagen (Jansson et al., 2013). The general trend of the syncline can be seen in figure 131 where the trace of Fe mineralisation (green points) runs along the limestone skarn bodies that have been folded in the syncline.

In the 19th century mining for Zn began, in addition to Fe and, to a lesser extent, Mn. Enrichment of ore began in the late 19th century, expanding shortly after the turn of the century (Tegengren et al., 1924). Large scale mining occurred at Stollberg from 1869–1982, before the mines were shut down due to unprofitability. Over the course of their lifetime the Stollberg fields produced over 3.5 Mt of ore and produced 3 Mt of tailings (table 50) most of which are deposited in the Gårdmyren tailings dam (also referred to as Brusmalmen) approximately 1 km south-west of the mines. Some tailings were deposited by the lake Staren to the east of Silfhyttan. These tailings were sampled by Hallberg and Reginiussen (2020) and showed high levels of Pb, Zn and As. The dam lies next to the dressing plant still visible today that was operated by AB Statsgruvor from 1945 to 1982.

This site has been covered by several studies focused on the environmental risk (e.g. Envipro miljöteknik, 2004) and is still under surveillance. From them and SGU's investigations (Hallberg and Reginiussen, 2020) it is known that most of the material lies above the groundwater level.

The tailings were laid in the north-western flank of a small valley. According to the geological map made prior to the deposition of tailings (Lundqvist & Hjelmqvist, 1937) it was originally covered by peat lying on till, which formed over felsic metavolcanic rock. As can be seen on historical aerial photographs, the tailings dam was built progressively and internally contained by dam walls later extending to the west.

Table 50. Production statistics from Stollberg.

	Total (Mt)	Zn (%)	Pb (%)	Cu (%)	Ag (ppm)
Mined Ore	4.94	4.47	3.40	0.07	80.83
Processed in dressing plant	3.79				
Tailings	3.01				
Waste rock	0.85				

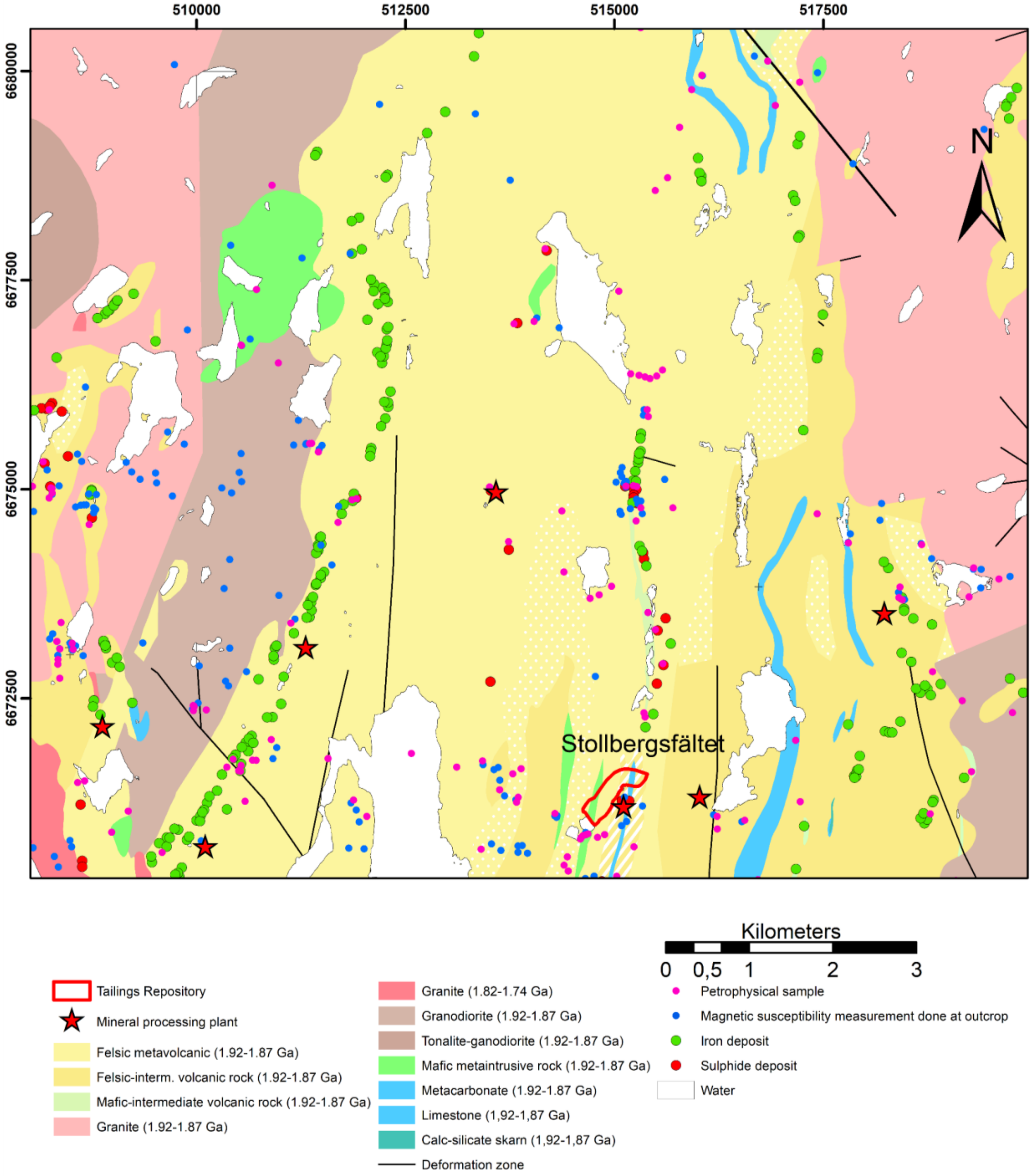

Figure 131. Bedrock map over the Stollberg syncline and mine fields.

Geophysical measurements and estimation of the volume of the tailings

In early May 2022, five ERT-IP profiles and one RMT profile were measured on the Stollberg (Gårdmyren) tailings dam (Fig. 132). It was not possible to use more surface-covering methods due to the dense vegetation. Georadar profiling had been done previously (Hallberg and Reginiussen, 2020) but could only give some indication on the layering and could not reach the bottom of the tailings.

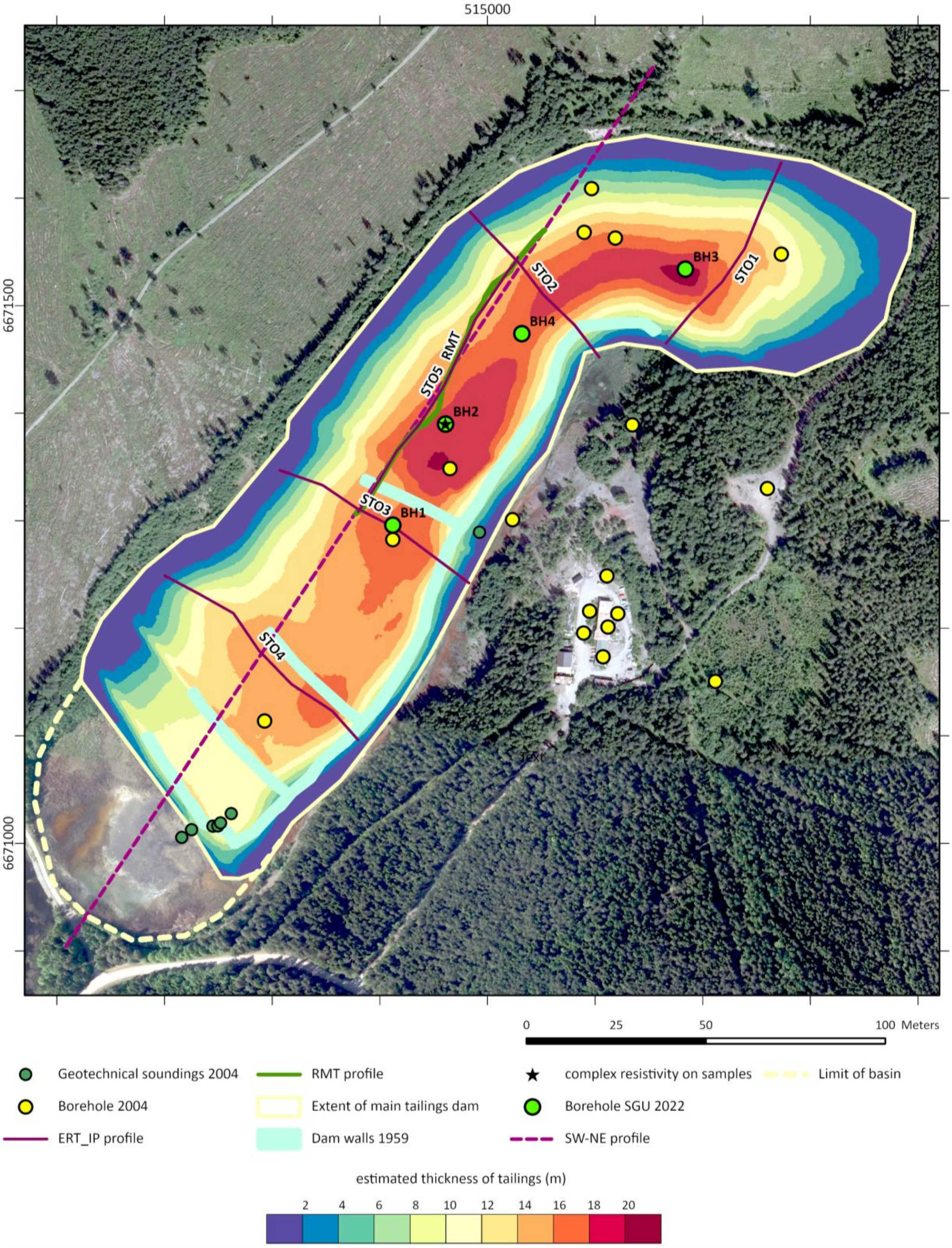

Figure 132. Contoured depth map if tailings at Brusmalmen with location of boreholes and geophysical profiles.

On both RMT (Fig. 133) and ERT results (Fig. 134) the tailings appear as conductive and contrast with the resistive moraine and underlying bedrock. These results are in overall agreement with the boreholes from 2022 and those reported by Envipro miljöteknik, (2004). The soil was frozen at the time of the measurements.

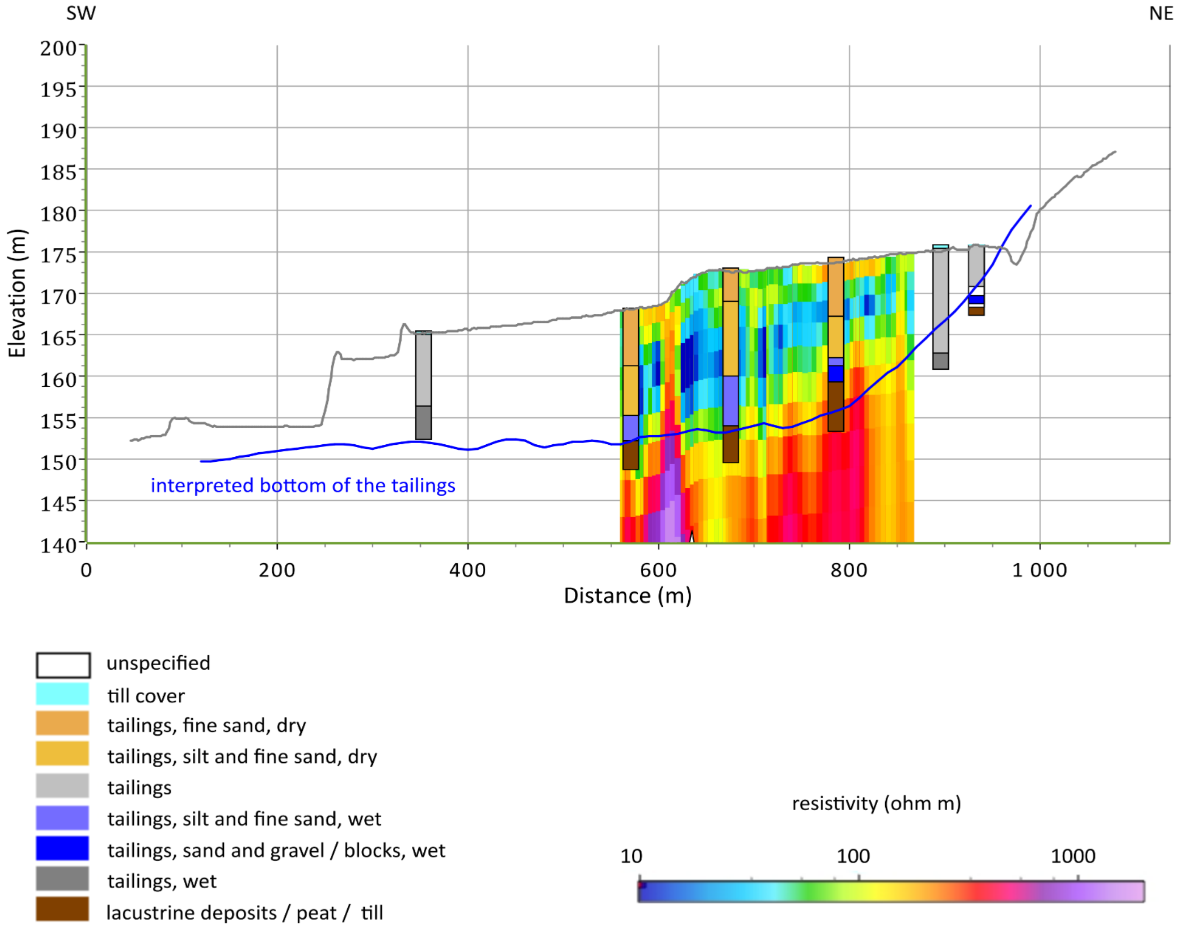

Figure 133. SW_NE section with RMT results and boreholes showing how geophysical results, drilling results and topography were combined in the interpretation.

Even though the contact resistance could be kept low (under 1000 ohm) the ERT results are affected by the resulting near-surface high resistivity. The effect of the frost on near-surface resistivity is less evident on the RMT results which clearly show the bottom of the tailings. Both methods consistently show what is most probably the resistive bedrock. On the ERT sections (see example on figure 134) a clear contrast is seen between tailings above and below the groundwater level, whereas the transition to underlying quaternary sediments is unclear. The groundwater level does not appear on the RMT results, possibly because of a slightly coarser resolution. The RMT results show few internal variations in the tailings. Despite some uncertainty the geophysical results confirm the previous representation of slowly dipping limits to the north and to the east. It is difficult to relate variations of resistivity to mineral content at this site.

Spectral IP measurements were taken on two samples at the same location but at 4–5 metres and 15–16 metres depth respectively (Fig. 132). They show an increased conductivity at depth probably explained by increased water content and to some extent increase in the metal content (Pb and Zn mainly at that location). The polarizability is weak and its peak is at high-frequency, close to 6 kHz. (These results are exposed in detail in Martin, 2022, included in Bastani et al. 2024, in prep.). It can, at least partly, explain why no significant IP effect could be retrieved from the inversion of ERT-IP field data. Another explanation is that the resistivity of the tailings is relatively low, leading to weaker IP signal levels.

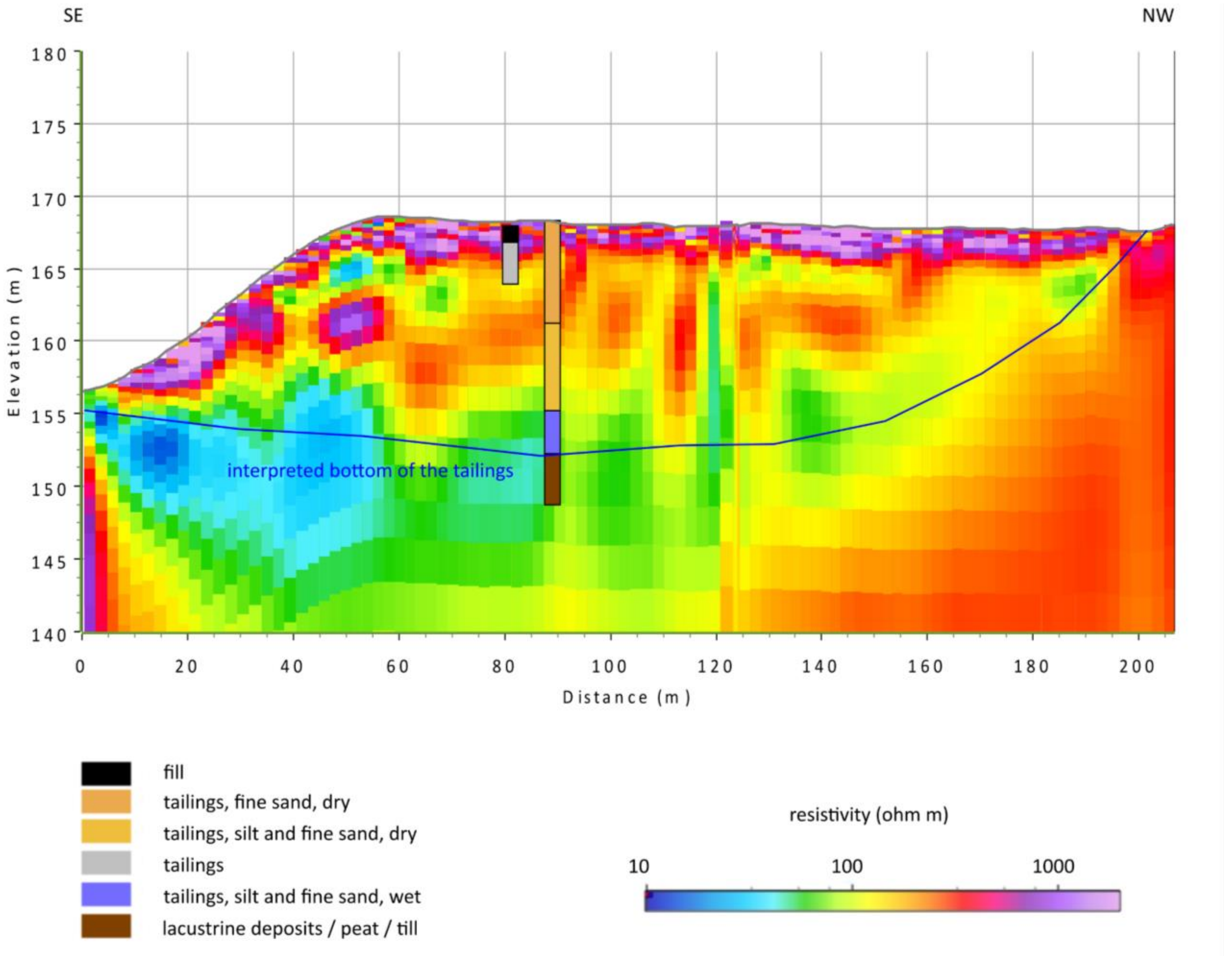

Figure 134. ERT results on line 3 showing how drillings, geophysics and topography were combined in the interpretation.

Using information from the 2004 and 2022 boreholes, the indications from geophysical results and inference from the surrounding it was possible to construct a rough 3-dimensional model and estimate the volume of the tailings to around 1.7 million m^3. This figure does not take the southwestern basin into account, which could add another 53 000 m^3 fine-grained materials of unknown concentrations. It is probably a slight underestimation. Assuming a volume density of 1.6 t/m^3 it yields approximately 2.8 million tons of tailings (+/- 20%)

The Stollberg ore field is a culturally protected site, and no sampling of waste rock was conducted during this study. Details of prior studies of waste rock and surface sampling of tailings at Stollberg can be found in Hallberg and Reginiussen (2020). All samples conducted within this study were of tailings sampled by drilling. Access for the drilling rig to the tailings dam was limited by tight forest. Therefore, sampling was carried out along a limited extent of the tailings dam that had been cleared during placement of groundwater monitoring pipes.

A total of 4 drill holes were sampled and 64 samples taken. As previously noted the tailings dam is tightly vegetated by pine trees (Fig. 135). The surface of the tailings was typically dry, and the water table was reached after 16–18 metres. Of the 4 boreholes drilled, only two succeeded in reaching the bottom of the tailings, while two were hindered by a stony layer at approximately 12 metres below the surface. Sounding of these holes went to the bottom of the tailings, while the sampler was unable to pass through these layers. It is suggested from aerial photographs that certain sections of the dam were covered with layers of waste rock to prevent the tailings from blowing away, and this may be the material that hindered sampling. Tailings at the top of each borehole were typically medium to fine sand with a minor silt fraction, becoming increasingly siltier with depth, likely due to distal transport of the finer sediments from the discharge point.

Analysis of the tailings from Stollberg (table 51) showed elevated levels of Zn (0.48%) and Pb 0.34%, as well as Fe_2O_3 (10%) and MnO (4.7%). The highest Pb and Zn were at the top and bottom of the tailings (Figs. 136 and 137). Silver levels were low, at with an average of 10 ppm, though occasional samples showed concentrations over 20 ppm. Other trace elements with elevated levels include Sb (14 ppm) and Ga (18 ppm). As was highly elevated in most samples with an average concentration of 0.15%. The REE profile of the tailings samples showed the typical positive Eu anomaly typical to the Stollberg ores (Fig. 138).

SEM-EDS analysis was conducted on mineralised samples collected by Magnus Ripa over the course of prior studies of Stollberg. Magnetite was the dominant Fe mineral, with approximately 2% Mn. Sphalerite was observed often in relation to pyrrhotite. Analysis of sphalerite showed no detectable quantities of trace elements such as Cd. Arsenopyrite was abundant in most samples, as was the Fe-As mineral löllingite.

Potential resources at Stollberg

Based on geophysical measurements the total amount of tailings at Brusmalmen tailings dam total 2.8 Mt. Under the assumption that the collected samples are representative for the whole tailings dam, the tailings potentially contain around 299 kt Fe, 13600 tonnes Zn, 8.5 tonnes Pb, 443 tonnes Cu, 39 tonnes of Sb, 40 tonnes Ga and 24.8 tonnes of Ag.

Figure 135. A view of the Stollberg tailings dam taken at the site of BH2_STO. The tight growth of the trees typical to the tailings dam is seen (6671534/515184). Photo: Patrick Casey

Table 51. Results of drilling at Stollberg.

Data	Fe (%)	Zn (%)	Pb (%)	Ag (ppm)	Ga (ppm)	Sb (ppm)
Drilled tailings (n=64)	15.2	0.48	0.31	8.9	18.8	14.2

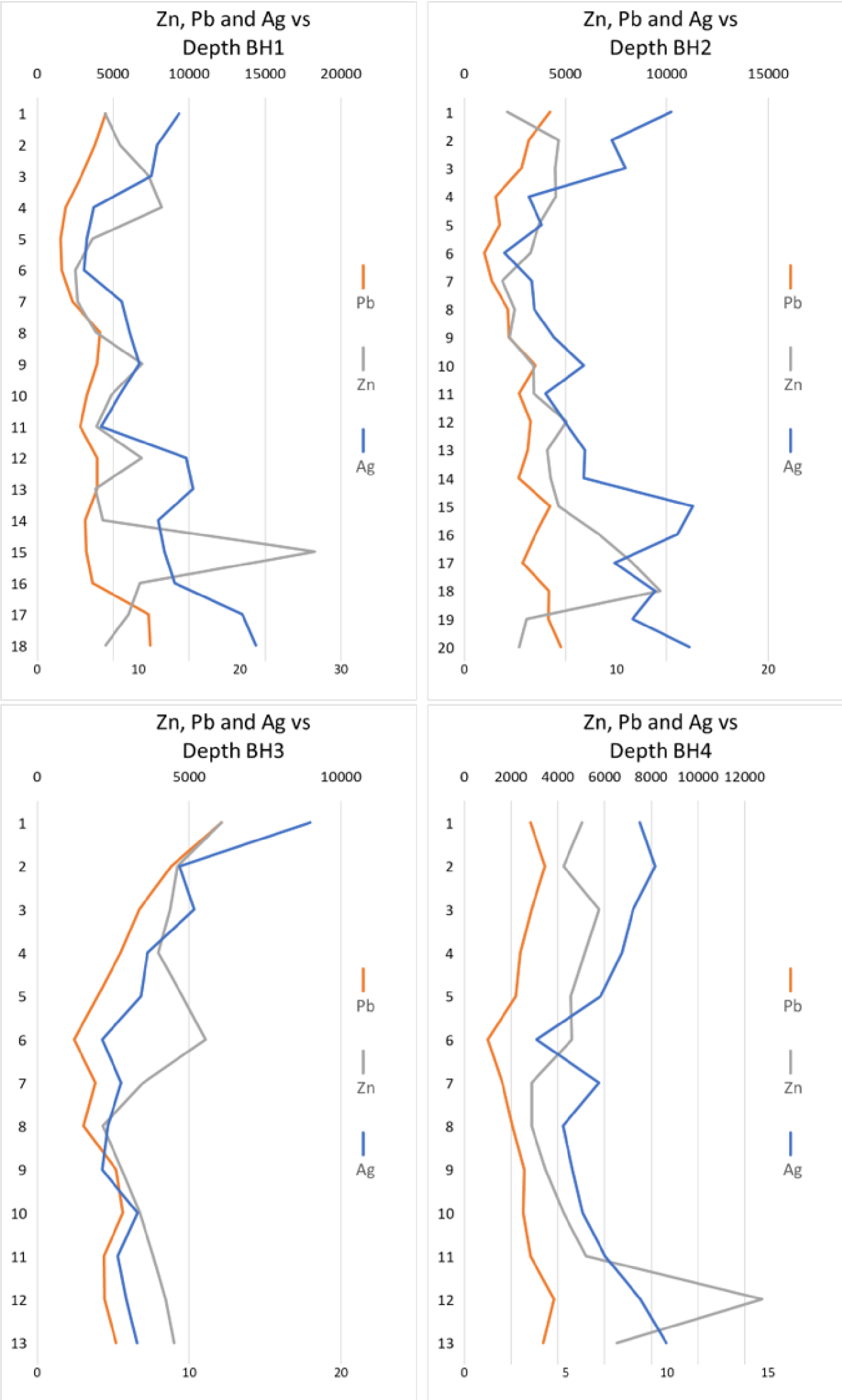

Figure 136. Line plots showing the concentrations of Zn, Pb and Ag over depth in the drilled boreholes. Silver concentrations are plotted on a secondary axis with values shown on the lower x-axis.

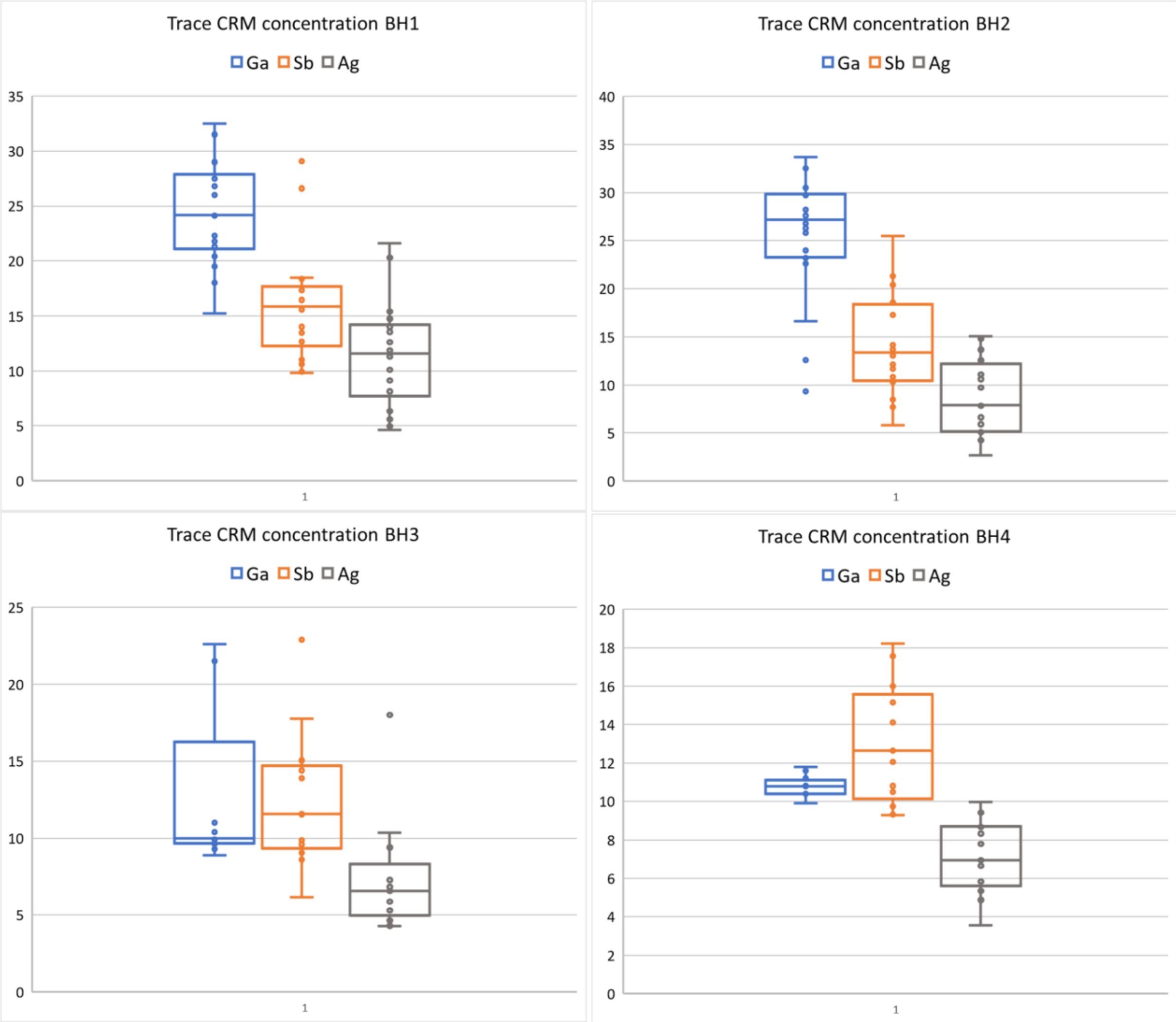

Figure 137. Box and whisker plots showing concentrations of trace CRM in ppm in the Stollberg boreholes.

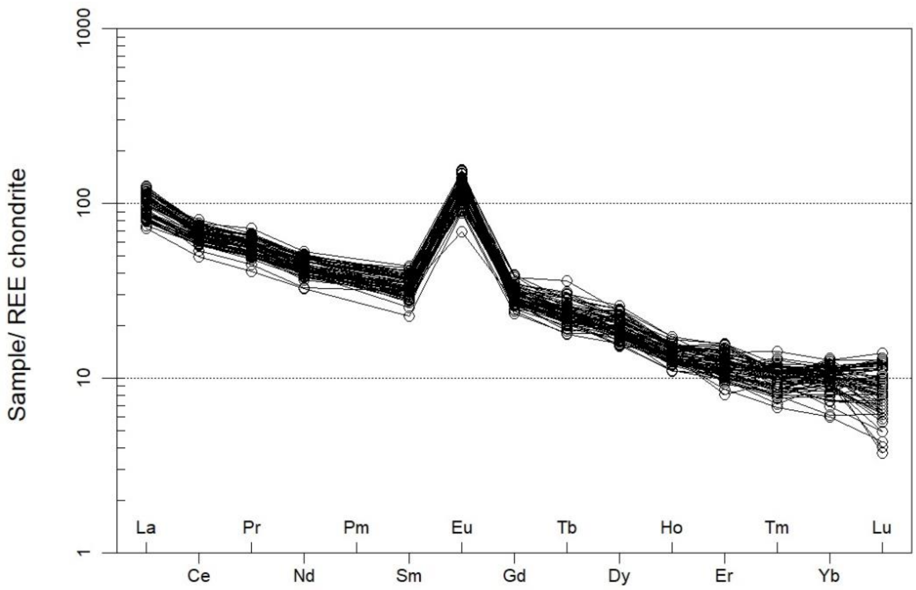

Figure 138. Chondrite normalised REE plot of tailings from samples showing the strong positive Eu anomaly. Chondrite values from Boynton (1984)

Saxberget

Background

Långfallsgruvan at Saxberget (Sweref 6667099/496736) was a Cu-Pb-Ag mine that operated through 1988, exploiting a stratabound sulphide body in a calc-skarn horizon (fig 139). The deposit was discovered in 1848 by a young boy who noticed anomalies in his compass readings and returned to the area to better constrain the location of the ore body. Mining at Saxberget did not begin until 1882, and operated during the years 1884, 1886–1891, 1893, 1895–1905, 1907–1988. A total of 8,2 Mt of ore was mined, which contained 6.3% Zn, 2.6% Pb, 12% Fe, 10% S, 0.81% Cu, 46.3 ppm Ag and 0.38 ppm Au. Refining took place at a dressing plant just north of the mine producing 5.62 Mt of tailings, filling up nearly the entirety of Vattfallsgropsbäcken, a valley just north of the dressing plant (Envipro, 2000).

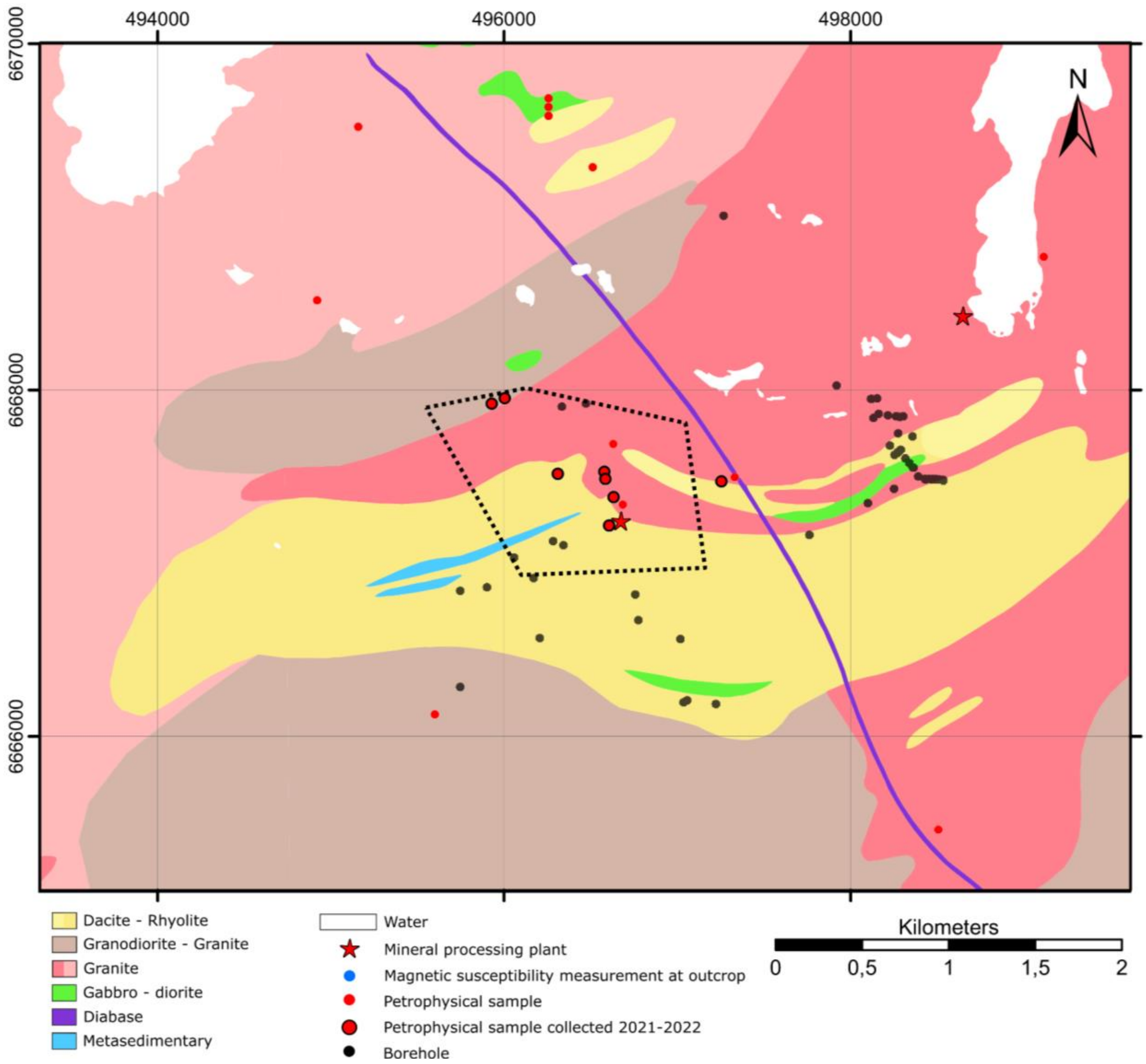

Figure 139. Map of the bedrock geology, petrophysical and borehole data for the area around Saxberget. The Saxberget mapping area is shown as a polygon with a thick black dashed line.


Figure 140. Sanitized area of the former mine dump at Saxberget. Photo: Patrick Casey

In the late 1990s, Boliden Mineral AB and the county of Dalarna sanitized the area (fig 140), using the waste rock as backfilling in the mine, as well as levelling waste rock piles, covering the rock with a layer of till approximately 1 metre thick. The same process was carried out at the tailings repository, and as such there were no composite waste rock or tailings samples taken on site. One richly mineralised block was found exposed in the sanitised area, and this rock was sampled for whole rock analysis.

Mapping was carried out in the area to better constrain the geology of the area. Saxberget and its surroundings have very poor exposure of bedrock. The dominant bedrock exposed are intermediate to felsic intrusives to the north, with limited exposure of the supracrustal volcanic rock. The exposed volcanics however provide a great amount of information of the geologic history of Saxberget. Here the volcanics show a clear banding/stratigraphy evidencing repeated volcanic eruptions. The presence of lava flows intercalated with the pyroclastic ash flows suggest a shallow water environment that was vent proximal.

Available geophysical data

Airborne data (magnetic, VLF, gamma spectrometry)

As part of this project an area around the Saxberget mine was identified for additional bedrock mapping work, with the objective of improving the understanding of the source mineralisation associated with the mining waste. This area is shown in figure 141 as a dashed black line and will be referred to later in the report as the Saxberget mapping area.

The oldest airborne geophysical measurements from the Saxberget area were collected by SGU in 1972 where natural gamma and magnetic measurements were conducted. In 2016 and 2019, additional airborne measurements were performed by SGU using a more modern measurement system, where natural gamma, magnetic and VLF (2 transmitters) measurements were collected. For the more recent measurements a nominal flight height of 60 m and line separation of 200 m was utilized. The airborne data collected in the area around Saxberget is summarised in table 52.

Figure 141 shows a map of the residual magnetic field around the Saxberget area. The largest magnetic anomaly which can be observed on the map is associated with the mineralisation at the Saxberget mine. The mineralisation at Saxberget is stratabound with an approximate east-west strike and dips between 30 and 47º to the south (Prospecting report *BRAP83766*, 1950; Vivallo and Rickard, 1990). The Zn-Pb-Cu mineralisation occurs mainly as massive and disseminated ores associated with a calc-silicate horizon (skarn). Magnetite and pyrrhotite are documented to occur within the mineralisation at Saxberget which most likely lead to the relatively strong magnetic response observed (Prospecting report *BRAP83766*, 1950; Vivallo and Rickard, 1990). To the far north of the map is a small magnetic anomaly, most likely associated with Fe mineralisation documented at the same location. South of the Saxberget mine is a small circular magnetic anomaly. A borehole protocol from the immediate vicinity of this anomaly describes layers rich in biotite as well as sulphide mineralisation (Zn and Cu) which could be associated with this anomaly. About 1 km north of the Saxberget mine an approximately west-east striking magnetic anomaly can be observed. No outcrops appear to occur along this anomaly, and it has been mapped as granitic rocks. However, due to the anomaly it is likely that some heterogeneity exists at this location, for example intrusive mafic rocks or mineralisation.

Figure 142 shows a map of the apparent resistivity over the Saxberget area, calculated from VLF measurements. Several regions of low resistivity can be observed. To the south of the Saxberget mine a broad conductive zone which strikes approximately east west can be observed. Locally, the form of this anomaly does not conform to topography or mapped wetlands or streams. Therefore, it is possible that this anomaly corresponds to a more conductive zone in the bedrock and is perhaps partly associated with mineralisation within the felsic metavolcanic sequence. To the north of the Saxberget mine an additional conductive east west anomaly exists, however this corresponds to a topographic low so can be related to soil moisture. To the far east of figure 141 anomalies associated with power lines can be observed.

Ground-based electromagnetic and magnetic measurements

Table 52 shows a list of the ground-based geophysical data which is available in SGU's database for the area around Saxberget. The numbers in the table correspond to the numbered polygons shown in figures 141 and 142.

Prior to this project the only ground geophysical measurements available for this area were collected by Boliden Mineral AB over the Saxberget mine and to the south of it, using a EM34 instrument (Fig. 142). As part of this project ground-based magnetic and VLF data were collected over the area around the Saxberget mine. The objective of this data acquisition was to support bedrock mapping efforts around the mine and to provide a basis for geophysical modelling of the deposit. The magnetic and VLF measurements were collected using a GEM GSMV-19 instrument. The magnetic data were collected continuously at 1s intervals whilst walking along survey lines with a line spacing of 50 m. The VLF measurements were made with a frequency of 19.6 kHz and point and line spacing of about 40 m and 100 m, respectively. All VLF measurements were made facing an azimuth of 340º.

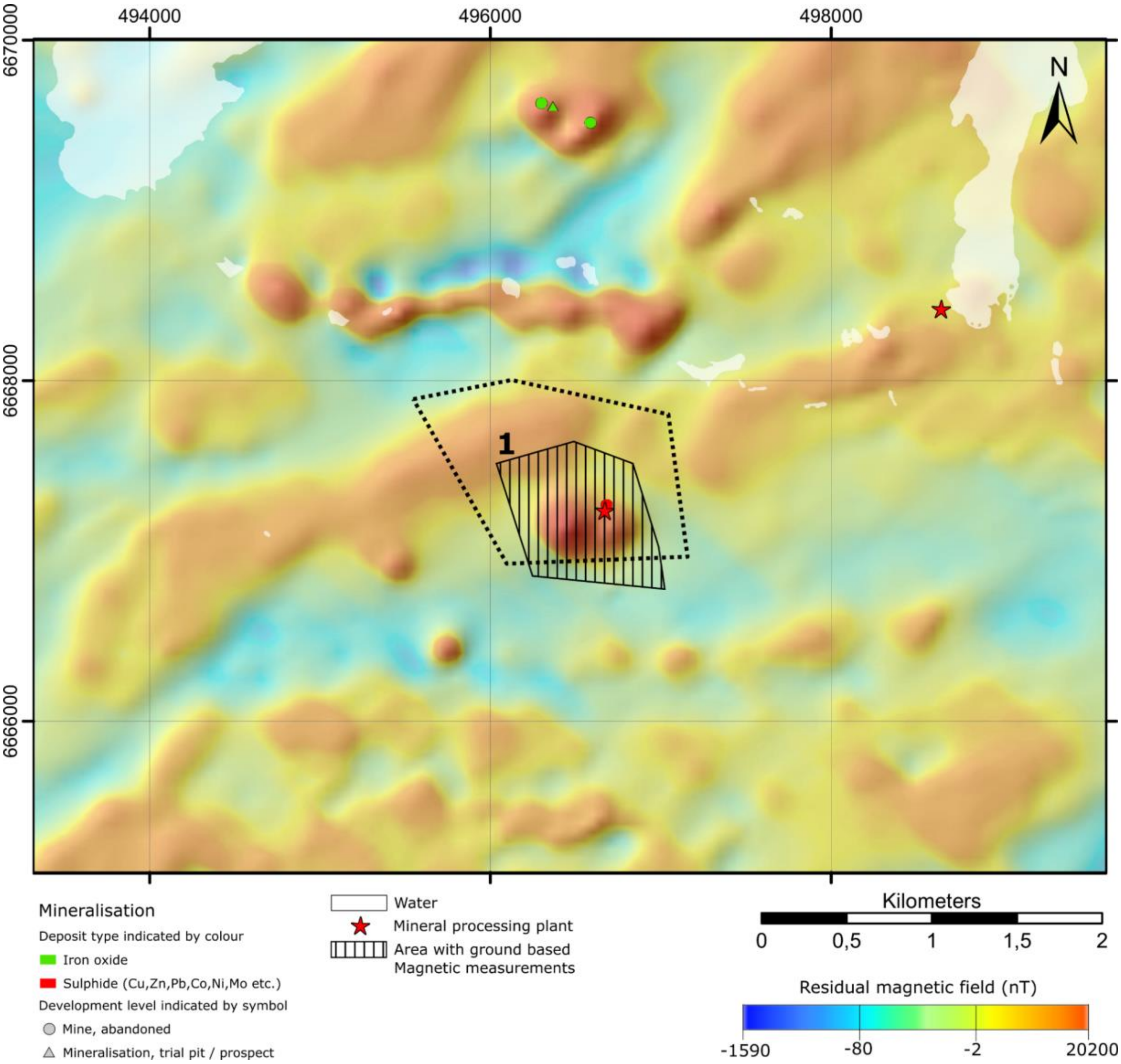

Figure 141. Map of residual magnetic field for the area around Saxberget. The Saxberget mapping area is shown as a polygon with a thick black dashed line. The location of ground-based magnetic measurements, listed in table 52 is shown.

Table 52. Complete list of the airborne geophysical surveys collected over part or all of the area shown in the map in figure 141, i.e., the area around Saxberget. Unless otherwise stated all data are collected using a small, manned aeroplane.

Year	Organisation	Geophysical methods used	Area (SGU map sheet)	Flight direction (degrees)	Flight line separation (m)	Flight altitude (m)
1972*	SGU	Magnetics, gamma spectrometry	Part of 12E and 12F	East–west (90°)	200	30
2016	SGU	Magnetics, gamma spectrometry, VLF (2 transmitters)	Part of 13F,13G, 12E, 12F, 12G, 12H, 11E, 11F, 11G and 11H	Northwest – southeast (130°)	200	60
2019	SGU	Magnetics, gamma spectrometry, VLF (2 transmitters)	Part of 12E	East–west (90°)	200	60

* Not used for producing maps in this report

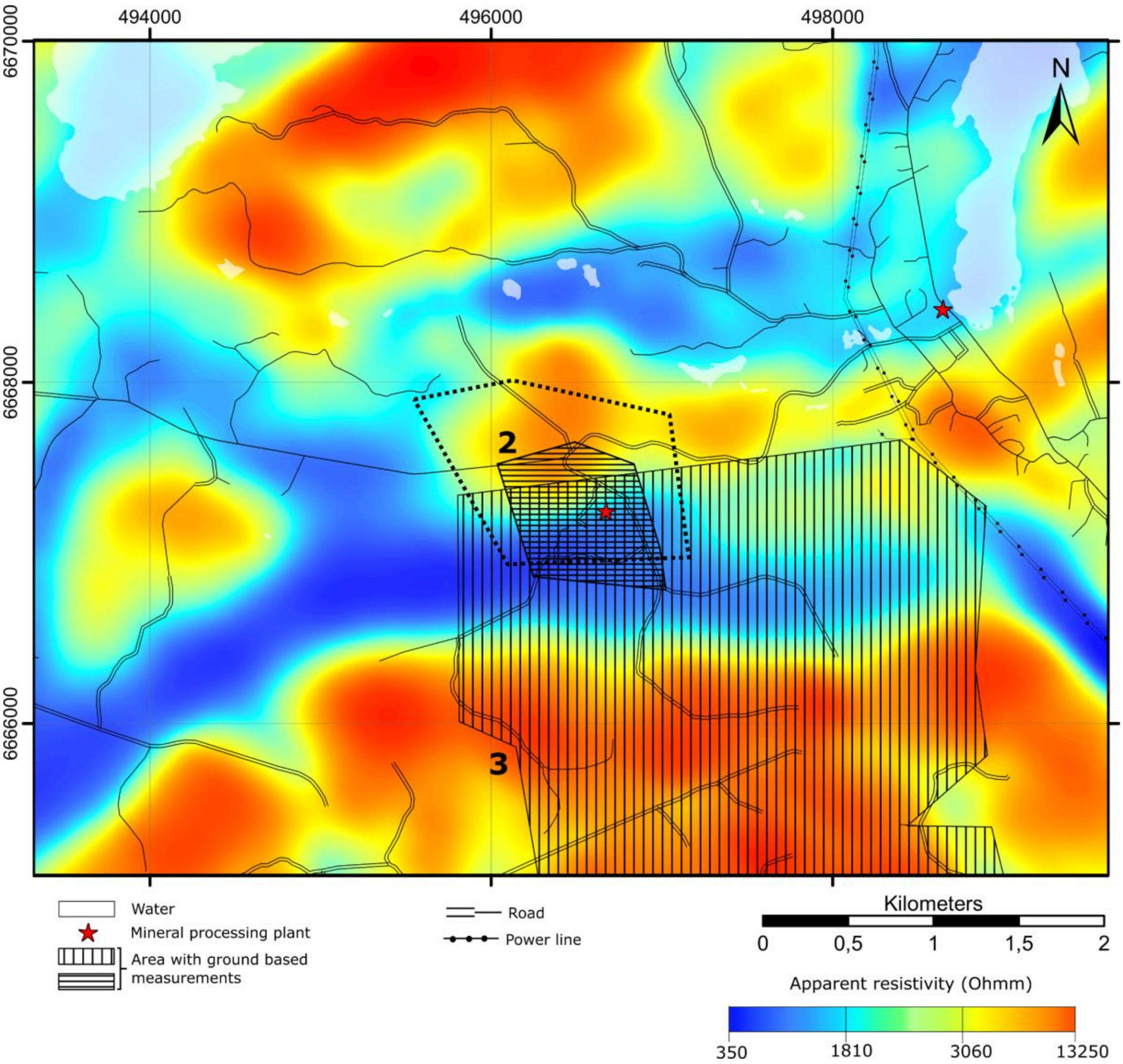

Figure 142. Map of apparent resistivity derived from airborne VLF data collected between 2016 and 2019 for the area around Saxberget. The Saxberget mapping area is shown as a polygon with a thick black dashed line. The location of ground-based electromagnetic measurements, listed in table 53 is shown.

Table 53. Ground-based magnetic and electromagnetic measurements for the area around Saxberget. Numbers correspond to the numbered polygons/lines shown in figures 141 and 142.

Polygon/Line number and name	Method	Year acquired	Responsible	Comments
1. MP21DSR0014 – MP21DSR0019	Magnetic	2021	SGU	Data acquired over an area with nominal profile spacing of 50 m
2. VP21DSR0023 – VP21DSR0027	VLF (19.6 kHz)	2021	SGU	Data acquired over an area with nominal profile spacing of 100 m
3. Saxberget nr 1004	EM34	2012	Boliden Mineral AB	Profile spacing of 100 m.

Ground-based gravity

Prior to this project some ground-based gravity data were available for the area around Saxberget, however, these data were relatively sparse, with an average point spacing of 1–2 km. As part of this project 117 additional ground-based gravity measurements were collected in 2021. This reduced the average spacing between points across the entire Saxberget mapping area to about 200–500 m. While along roads the average spacing was reduced to between 50 and 100 m. A map of the residual gravity anomaly and measurement points for the Saxberget area are shown in figure 143.

A small positive anomaly is present in the residual gravity anomaly map in the southwestern part of the Saxberget mapping area. This could potentially be associated with the presence of carbonate rocks within the felsic volcanic sequence or even, potentially the presence of mineralisation. To the south of the Saxberget mapping area an east-west striking gravity anomaly is present. This anomaly could be associated with mafic rocks, which have been mapped in this area. Borehole protocols from this area document thin layers of amphibolite but also thin layers of sulphide mineralisation (Zn and Cu). Hence, this anomaly may also be partially associated with sulphide mineralisation. To the north of the Saxberget mapping area several small positive gravity anomalies can be observed, these are likely associated with mafic rocks and Fe mineralisation which have been mapped in this area.

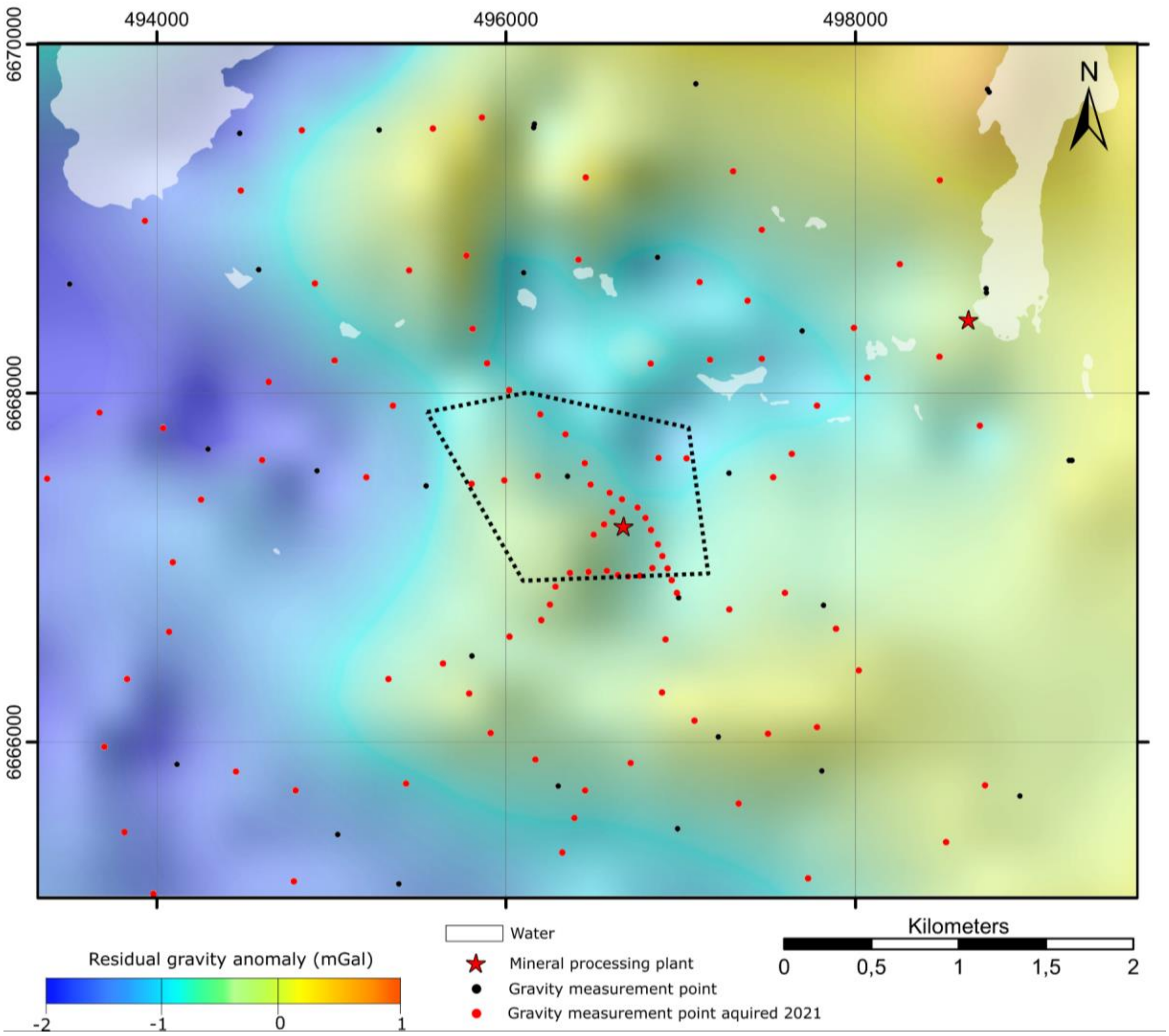

Figure 143. Map of the residual gravity anomaly for the area around Saxberget. The Saxberget mapping area is shown as a polygon with a thick black dashed line. Gravity measurement points are shown as black and red dots.

Petrophysical and borehole data

Figure 139 shows a map of the available petrophysical and borehole data from the area around the Saxberget mine, superimposed on a map of the bedrock geology. Prior to this project there was relatively little petrophysical data available for the area. This is most likely due to the lack of outcrops in the area which limits the possibilities to collect samples or take measurements at outcrop. As part of this project additional petrophysical data were collected in and around the Saxberget mapping area, with the aim of supporting the interpretation of the geology and geophysical data (Fig. 139). The new petrophysical data collected as part of this project are summarised in table 54. Most of the new samples were collected from granodiorite and granite rock types, which have a typical density of around 2600 kg/m^3. A single sample of sulphide mineralisation was taken from waste rock in the vicinity of the Saxberget mine, which exhibits a relatively high magnetic susceptibility and density. However, it should be noted that material from other mines was processed at the Saxberget facility, therefore it cannot be guaranteed that this sample is from Saxberget.

59 boreholes are documented within SGUs borehole database in and around the Saxberget mapping area and are annotated in figure 139. These wells were primarily drilled between 1973 and 1981 by Boliden. Borehole protocols are available for a number of these wells. Several of these wells intersect zones with Cu-Zn-Pb mineralisation.

Table 54. Table summarising the petrophysical results collected as part of this project from the Saxberget mapping area.

Sample ID	Easting (m)	Northing (m)	Description	Density (kg/m3)	Magnetic susceptibility (10-6 SI)	J (mA/m)
DSR210030A	496604	6667226	Sulphide mineralising	3332	760041	511664
DSR210031A	496631	6667390	Granite	2590	388	62
DSR210032A	496308	6667525	Granite	2612	2653	20
DSR210033A	496577	6667538	Granite	2582	41	37
DSR210034A	496583	6667496	Granite	2563	-15	66
PCY210164A	497252	6667481	Granodiorite	2580	38	78
PCY210166A	495927	6667930	Granodiorite	2608	7891	468
PCY210167A	496001	6667962	Granodiorite	2618	92	27

Interpretation of the new ground-based geophysical data

Figure 144 shows a map of the total magnetic field intensity and apparent resistivity (calculated from VLF measurements) derived from the new ground-based measurements collected in 2021 (described in figure 141 and table 54). A clear approximately east-west striking magnetic anomaly is observed at the Saxberget deposit, which is consistent with the previous documentation of the deposit (Prospecting report *BRAP83766*, 1950; Vivallo and Rickard, 1990). The form of the magnetic anomaly is also consistent with a sheet like deposit dipping to the south. The magnetic anomaly associated with the deposit appears to be split up into two parts where the westernmost part has the stronger of the two anomalies. In the apparent resistivity data an east west zone of low resistivity exists at the same location of the magnetic anomaly. This anomaly appears to be largest in the western part of the deposit.

Apart from at the Saxberget deposit, no strong magnetic anomalies can be observed within the surveyed area. Hence, it is unlikely that additional mineralisation of this type (i.e. sulphide mineralisation with magnetite) is present within the survey area, close to the surface.

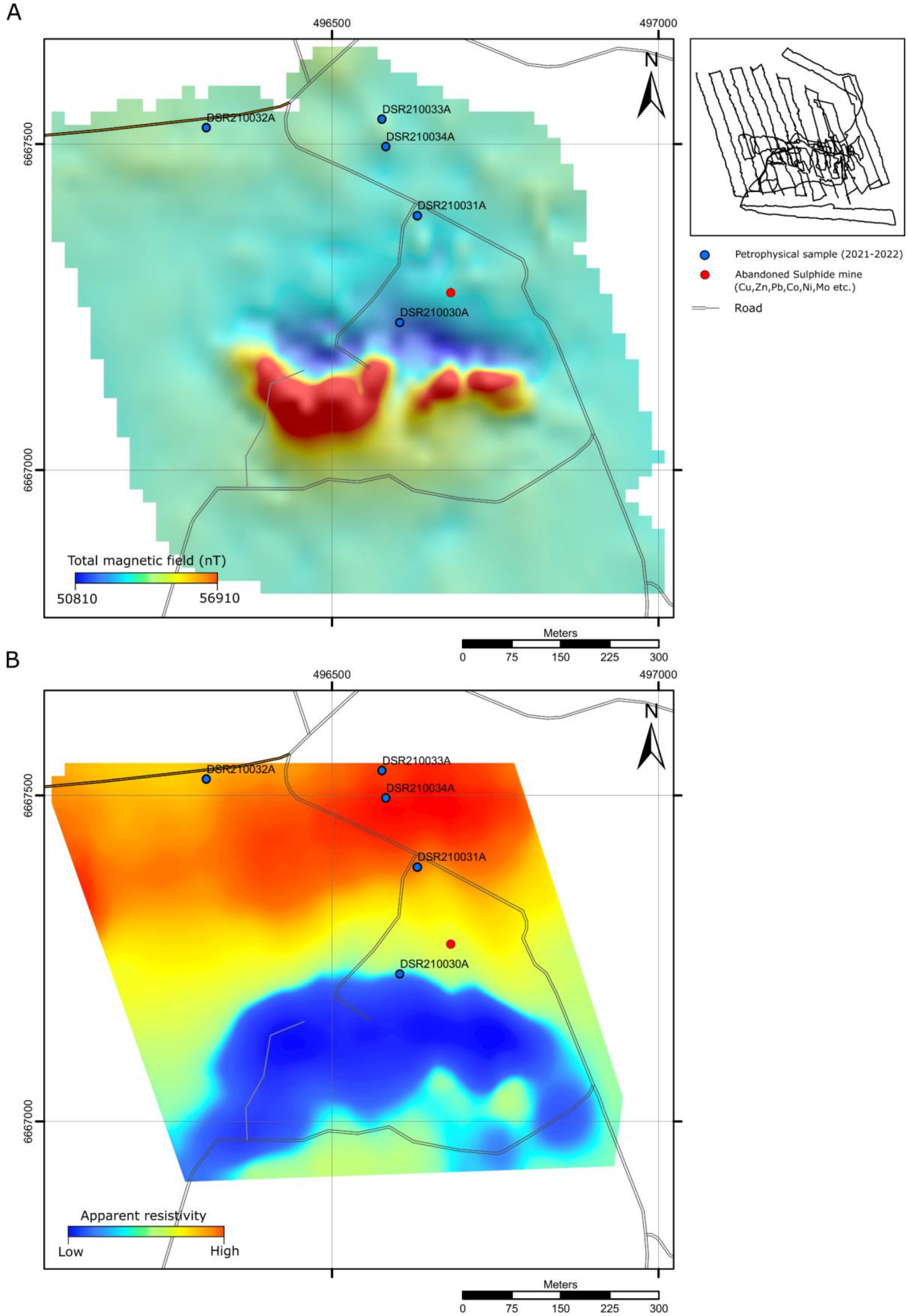

Figure 144. Map showing the ground geophysical measurements collected around the Saxberget mine. **A.** The total magnetic anomaly from ground measurements. **B.** The Apparent resistivity calculated from VLF measurements (19.6 kHz). Mineralisation from SGUs database as well as new petrophysical samples collected between 2021 and 2022 are shown. The inset map in the top right corner shows the measurement points used to generate the map. The extent of the inset map is the same as the main maps.

Geochemical sampling results

A single large block of sulphide ore was sampled from Saxberget. In the hand sample pyrrhotite, chalcopyrite, and amphibole dominate, and they are crosscut by veins of purple fluorite. Thin section analysis (fig. 145) showed pyrrhotite, sphalerite and chalcopyrite were the primary ore minerals, with minor galena. SEM-EDS analysis found native silver and acanthite as the primary silver minerals.

Geochemical analysis showed elevated levels of Cu, Zn, Ag, Au and Pb, as well as minor enrichment in In (Table 55).

Figure 145. Thin section of mineralised sample from Saxberget in reflected light showing pyrrhotite and chalcopyrite with phyllosilicates. Micrograph: Patrick Casey

Table 55. Geochemical analysis of mineralised sample from Saxberget

Sample	Fe_2O_3 (%)	Cu (%)	Zn (%)	Pb (ppm)	Ag (ppm)	Au (ppm)	In (ppm)
Mineralised sample	34.3	6.93	0.96	713	161	0.93	0.86

Bedrock mapping of the Saxberget area

Outcrop exposure in the area surrounding Saxberget is limited and is shown in the grey polygons in figure 146. The largest number of exposed outcrops lie to the north of the mine. These outcrops were mapped previously by SGU as felsic to intermediate subvolcanic intrusive rocks, and observations made during this study confirmed these prior observations. Thin section analysis of these rocks showed quartz and microcline dominating with diffuse grains of hematite and magnetite, as well as pyrite observed within the intrusives. The rocks have undergone Mg alteration, and much of the plagioclase has been altered to sericite, while microcline appears to be more resistant to alteration.

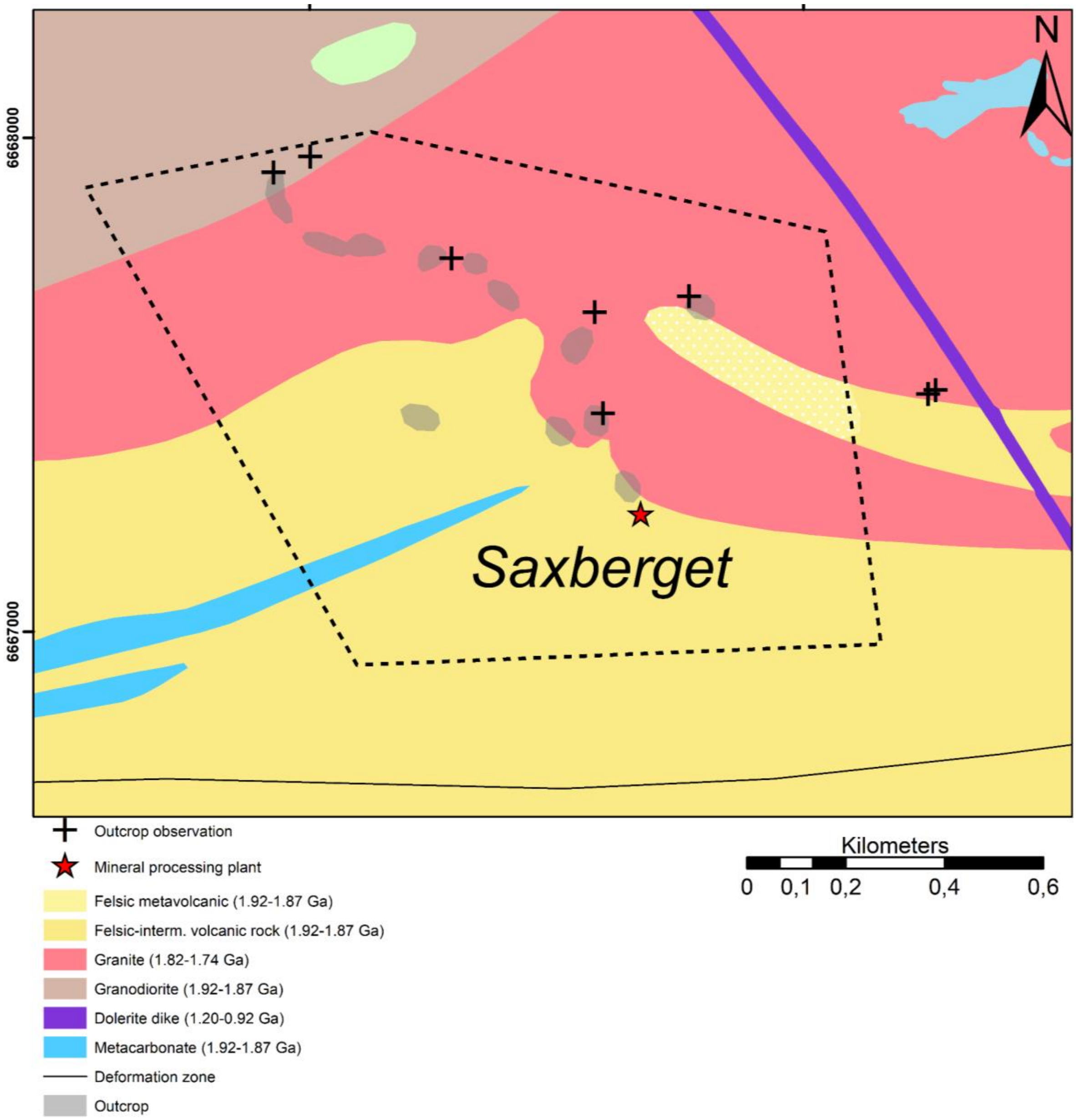

Figure 146. Bedrock map of the Saxberget mapping area. New observations are marked with crosses.

A previously unstudied outcrop was found 600 metres to the west of Saxberget where recent harvesting of trees has left an outcrop of supracrustal felsic metavolcanic rock exposed. Here fine sedimentary layering is apparent with sharp erosive boundaries shown in figure 147. The rock has been folded, with the fold axis striking 260˚. The volcanic sedimentary layers are capped by an extrusive meta-intermediate lava that has been metamorphosed to amphibolite facies. The meta-intermediate lava is quartz poor, and dominated by amphibole and sericitised feldspars. The supracrustal rocks of the outcrop were intruded by a granite body.

Figure 147. A. Typical granite from Saxberget (6667756/496287). **B**. Banding in the layered outcrop of meta-rhyolite (6667482/497252) **C**. Sample taken of the layered outcrop showing the folding and the lava layer at the top. **D.** Polished slab of sample seen in **C** showing layering and with a thin granitic vein cutting parallel to the layering at ~7 cm. Photographs: Patrick Casey

Diffuse sulphide and Fe-oxide grains are present within the ash layers, as well as abundant fluorite. Later alteration during fluid flow that formed the Saxberg deposit led to the formation of these small sulphide and Fe-oxide grains, as well as the formation of fluorite. Fluorite crystals typically contain inclusions of amphibole (fig. 148).

The limited exposure of outcrops within the Saxberget area hinders mapping, and much of the information regarding the local bedrock comes from drill cores taken during the course of mining. Mapping in the course of this project confirms the interpretation of the intrusives as felsic to intermediate as presented in the SGU bedrock maps, and indicated that small extrusive vents were erupting proximal to the mineralised areas.

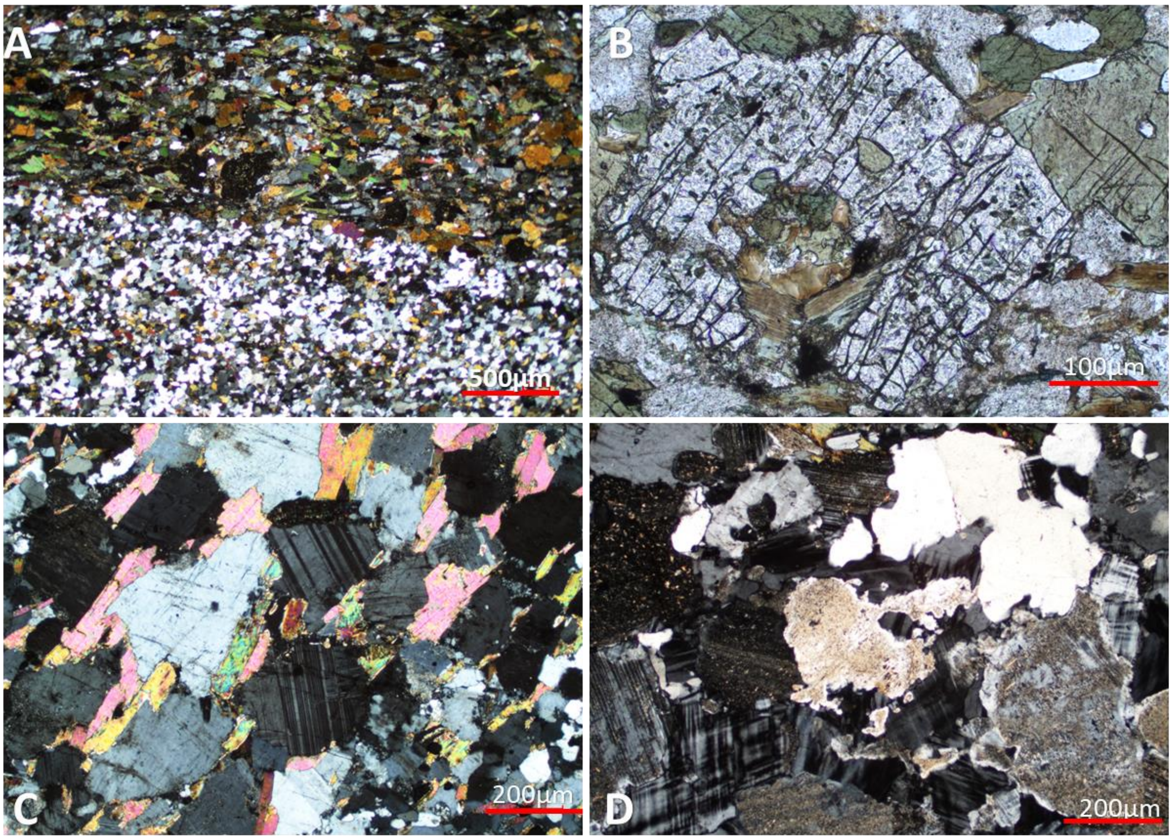

Figure 148. Thin section images from Saxberget. A. Contact between basic extrusive lava (top) and pyroclastic meta-rhyolite (bottom). **B**. Fluorite crystal with inclusions of amphibole and chlorite from the layered outcrop. **C**. Thin granitic vein in layered outcrop. **D**. Granite from outcrop north of the mine showing sericite alteration of plagioclase and relative resistance of K-feldspar to seriticisation. Micrographs: Patrick Casey

CONCLUDING REMARKS

In general, the results of this study show that there are appreciable levels of CRM in mine waste in western Bergslagen. A clear hinderance is seen in calculating the potential total of CRM of waste rock when using data provided from SGU's MALMdb. These production numbers do not take into account how the waste rock was managed after it was extracted. At Blötberget we see based on aerial images that the open pit of the mine was used to dump the remaining waste rock. At Grängesberg a large portion of waste rock has been taken for use as aggregate. Further resource estimates would be needed that include detailed surveys of the remaining waste rock.

The data from MALMdb for tailings appears to be a more accurate estimation of the mass of material available. Geophysical data, as well as data from geochemical analyses and drilling have shown that these data can be used in the future work out a resource estimate.

The drilling campaign has shown that for smaller tailings repositories, up to approximately 2 Mt, surface sampling can provide a reliable estimate of average concentrations on CRM within the site. Larger tailings repositories, especially those that were from mines producing over several decades, can exhibit wide variations in concentrations, for example as observed in this study at Grängesberg Hötjärnen. Hence, sampling from boreholes as well as at the surface is recommended for characterisation of these larger, more complex repositories. Further work is needed to better estimate the uncertainties involved with estimations of resources contained in mine waste.

While the potential resources calculated within this report are not near the levels that are needed by industry in Europe, the availability of these materials for extraction can supplement primary production and also offer opportunities for remediation of former mining sites.

REFERENCES

Allen, R. L., Lundstrom, I., Ripa, M., & Christofferson, H., 1996: Facies analysis of a 1.9 Ga, continental margin, back-arc, felsic caldera province with diverse Zn-Pb-Ag-(Cu-Au) sulfide and Fe oxide deposits, Bergslagen region, Sweden. *Economic Geology*, *91*(6), 979–1008.

Allen, R., Jansson, N. & Ripa, M., 2013: *Bergslagen: Geology of the volcanic- and limestone hosted base metal and Fe oxide deposits.* Excursion Guidebook SWE4, 12th Biennial SGA Meeting 12–15 August 2013, Uppsala, Sweden.

Almqvist, B, S, G., Björk, A., Mattsson, H, B., Hedlund, D., Gunnarsson, K., Malehmir, A., Högdahl, K., Bäckström, E & Marsden, P., 2019: Magnetic characterisation of magnetite and hematite from the Blötberget apatite – Fe oxide deposits (Bergslagen), south-central Sweden. *Canadian Journal of Earth Sciences 56(9)*, 948–957.

Andersson, L.G., Edberg, L., Jonuks, R. & Linder, T., 1986: Prospektering i Yxsjöbergsområdet. Stödetapp II. Slutrapport B-8610, LKAB. *Sveriges geologiska undersökning B-8610*, 15 p.

Bastani, M., Leroux, V., Brolin, C., & Persson, L., 2024: Characterisation of mine tailings in Bergslagen using geophysical and electromagnetic methods. [in preparation] SGU-rapport 2024:XX, Sveriges geologiska undersökning.

Bergman, S., Lynch, E., Berggren, R., 2020: Styrning av W-Mo-mineralisering i granitpegmatit-svitens intrusioner i Bergslagen. *SGU-rapport 2020:07*, Sveriges geologiska undersökning.

Envipro Miljöteknik AB, 2000: Saxbergsprojektet: En dokumentation av projektets genomgång. Linköping.

Envipro Miljöteknik AB, 2004: Efterbehandling av sandmagasin i Stollbergsområdet, huvudstudie. Effekter av äldre silver, bly och zinkbrytning i Smedjebackens kommun. Linköping.

European Commission, Directorate-General for Internal Market, Industry, Entrepreneurship and SMEs, Grohol, M., Veeh, C., 2023, *Study on the critical raw materials for the EU 2023 – Final report*, Publications Office of the European Union.

Grängesberg Fe AB, 2014: Grängesberg Technical report_2014, Grängesberg Fe AB.

Hallberg, A. & Reginiussen, H., 2018 Kartläggning av innovationskritiska metaller och mineral. Slutrapportering av regeringsuppdrag. RR 2018:05, Sveriges geologiska undersökning, 1–90.

Hällström, L.P.B., Alakangas, L. & Martinsson, O., 2018: Geochemical characterization of W, Cu and F skarn tailings at Yxsjöberg, Sweden. *Journal of Geochemical Exploration 194*, 266–279.

Hällström, L. P., Salifu, M., Alakangas, L., & Martinsson, O., 2020: The geochemical behaviour of Be and F in historical mine tailings of Yxsjöberg, Sweden. *Journal of Geochemical Exploration, 218, 106610.*

Janoušek, V., Farrow, C. M., & Erban, V., 2006: Interpretation of whole-rock geochemical data in igneous geochemistry: introducing Geochemical Data Toolkit (GCDkit). *Journal of Petrology*, *47*(6), 1255–1259.

Jansson, N. F., Erismann, F., Lundstam, E., Allen, R. L., 2013: Evolution of the Paleoproterozoic Volcanic-Limestone-Hydrothermal Sediment Succession and Zn-Pb-Ag and Fe Oxide Deposits at Stollberg, Bergslagen Region, Sweden. *Economic Geology 108*, 309–335.

Lewerentz, A. & Brolin, C., 2022: Kartering i området Grängesberg-Idkerberget – fältarbeten 2021. *SGU-rapport 2022:03*, Sveriges geologiska undersökning.

Lindholm T., 2021: Jan-Matts tailings dam Grängesberg, Scoping Study. GeoVista AB, GVR21032, 1–71.

Lundqvist, G., & Hjelmqvist, S., 1937: Geologiska kartbladet Smedjebacken. *Sveriges geologiska undersökning Aa 181*.

Magnusson, N, H., Lundqvist, G., 1933: Beskrivning till kartbladet Grängesberg. *Sveriges geologiska undersökning Aa177*.

Magnusson, N, H., 1940: Ljusnarsbergs malmtrakt: Berggrund and malmfyndigheter. *Sveriges geologiska undersökning Ca 30*, 188 p.

Malehmir, A., Gisselø, P., Socco, L.V., Carvalho, J., Marsden, P., Onar Verboon, A., Loska, M., 2020: New ways of exploring the subsurface with Smart Exploration solutions. *First Break 38, 77*, doi.org/10.3997/1365-2397.fb20200f1

Malehmir, A., Markovic, M., Marsden, P., Gil, A., Buske, S., Sito, L., Bäckström, E., Sadeghi, M., Luth, S., 2021: Sparse 3D reflection seismic survey for deep-targeting Fe oxide deposits and their host rocks, Ludvika Mines, Sweden. *Solid Earth 12*, 483–502.

Majka, J., Jonsson, E., Högdahl, K., Troll, V.R., Harlov, D.E. & Nilsson, K.P., 2013: Textural relations and mineral chemistry of REE in the Grängesberg apatite-Fe oxide deposit, Sweden: the role of fluids. *In*: Jonsson, E. et al. (ed.), 2013: *Mineral deposit research for a high-tech world*, Proceedings of the 12th Biennial SGA Meeting, 12–15 August 2013, Uppsala, Sweden, ISBN 978-91-7403-207-9, 1728–1731.

Markovic, M., Maries, G., Malehmir, A., Ketelhodt, J., Bäckström, E., Schön, M., Marsden, P., 2020: Deep reflection seismic imaging of Fe-oxide deposits in the Ludvika mining area of central Sweden. *Geophysical Prospecting 68*, 7–23.

Maries, G., Malehmir, A., Bäckström, E., Schön, M., Marsden, P., 2017: Downhole physical property logging for Fe-oxide exploration, rock quality, and mining: An example from central Sweden. *Ore Geology Reviews 90*, 1–13.

Mulenshi, J., Khavari, P., Chehreh Chelgani, S., & Rosenkranz, J. (2019). Characterization and beneficiation options for W recovery from Yxsjöberg historical ore tailings. *Processes, 7(12)*, 895.

Ohlsson, L. & Olsson, G., 1980: Zn-, Pb- och Ag-halter i Stollbergs avfallsdamm. *Prospekterings-rapport Grb 198*, Sveriges geologiska undersökning, 2 p.

Ohlsson, C. & Olsson, G., 1985: Regional gravimetri i Yxsjöbergsområdet. *Prospekteringsrapport B 8518,* 38 p.

Opijnen, M. V., & Oldenziel, J., 2010: Responsible supply chain management. Potential success factors and challenges for addressing prevailing human rights and other CSR issues in supply chains of EU-based companies.

Prospecting report - *BRAP83766*., 1950: Saxbergets Gruvor. BRAP83766, 1-7.

Ripa, M., 1988: Geochemistry of wall-rock alteration and of mixed volcanic-exhalative facies at the Proterozoic Stollberg Fe-Pb-Zn-Mn (-Ag) deposit, Bergslagen, Sweden. *Geologie en Mijnbouw 67,* 443–456.

Ripa, M. & Lundin, I, A., Relationen mellan Mo-mineraliserad GP-granit och scheelitförande exoskarn i Pingstaberg. *SGU-rapport 2020:10*, Sveriges geologiska undersökning.

Ripa, M. & Brolin, C., 2022: Malmnära profilkartering i området Ställdalen-Kopparberg under 2021. *SGU-rapport 2022:02*, Sveriges geologiska undersökning.

Romer, R. L., & Öhlander, B., 1994: U-Pb age of the Yxsjöberg W-skarn deposit, Sweden. *Gff, 116(3)*, 161–166.

Rothelius, E., 1957: Swedish Mineral Dressing Mills, Short descriptions and flowsheets. International Mineral Dressing Congress Stockholm, 1–9.

Sädbom, S. & Bäckström, M., 2018: Sampling of mining waste – historical background, experiences and suggested methods. BKBAB 18-109 Rep, Bergskraft Bergslagen AB, 1–71.

Sundis, N., Parwel, A., Rajandi, B., 1966: The minerals of the silver mines of Hällefors. *Sveriges geologiska undersökning C614.* Årsbok 60 nr 9., 21 p

Vivallo, W. & Rickard, D., 1990: Genesis of an Early Proterozoic Zn Deposit in High-Grade Metamorphic Terrane, Saxberget, Central Sweden. *Economic Geology 85*, 714–736.

Stephens, M. B., Ripa, M., Lundström, I., Bergman, T. & Persson, L., 2009: Synthesis of the bedrock geology in the Bergslagen region, Fennoscandian Shield, south-central Sweden. *Sveriges geologiska undersökning Ba 58*.

Stephens, M. B., & Jansson, N. F., 2020: Paleoproterozoic (1.9–1.8 Ga) syn-orogenic magmatism, sedimentation and mineralization in the Bergslagen lithotectonic unit, Svecokarelian orogen. *Geological Society, London, Memoirs, 50(1*), 155–206.

Tegengren, F.R. m.fl., 1924: Sveriges ädlare malmer och bergverk. *Sveriges geologiska undersökning Ca 17,* 1–406.

Wagner, T., Jonsson, E., & Boyce, A. J., 2005: Metamorphic ore remobilization in the Hällefors district, Bergslagen, Sweden: constraints from mineralogical and small-scale sulphur isotope studies. *Mineralium Deposita, 40(1),* 100–114.

Weis, F., Troll, V. R., Jonsson, E., Högdahl, K., Harris, C., Sun, W., Nilsson, K & Dahrén, B., 2022: Absence of hydrothermal oxygen isotope variations in host rocks supports magmatic origin of the giant Grängesberg Fe oxide–apatite (IOA) deposit, Central Sweden. *International Journal of Earth Sciences, 111(2)*, 425–437.

APPENDIX 1. ANALYTICAL METHODS PER ELEMENT

Analytical method	Description[1]	Elements analysed by preferred SGU method[2]
ME-ICP06	Fused bead, acid digestion and ICP-AES. LOI by furnace or TGA	SiO_2, Al_2O_3, Fe_2O_3, CaO, MgO, Na_2O, K_2O, TiO_2, MnO, P_2O_5
ME-MES81	Lithium borate fusion, acid digestion and ICP-MS	Ba, Ce, Cr, Cs, Dy, Er, Eu, Ga, Gd, Hf, Ho, La, Lu, Nb, Nd, Pr, Rb, Sm, Sr, Ta, Tb, Th, Tm, U, V, Y, Yb, Zr, W, Sn
ME-MS41	Aqua regia digestion with ICP-MS	Bi, Hg, Sb, Se, Te, **Ag**, As, B, Be, Cd, **Mo**, **Pb**, Ge
ME-4ACD8	Lithium borate fusion with 4 acid digestion with ICP-MS for base metals	Co, **Cu**, Li, Ni, Sc, **Zn**
ME-MS42	Single element aqua regia analysis by ICP-MS	In, Re, Tl
PGM-ICP23	Lead oxide collection fire assay and ICP-MS analysis	Au, Pt, Pd
S-IR08	Total sulphur by induction furnace/IR	S
C-IR07	Total carbon by induction furnace/IR	C

[1]Description from ALS.
[2]Bolded elements can be analysed using ore grade methodologies if concentrations exceed 10000 ppm (Mo, Pb, Zn, Cu) or 100 ppm (Ag).